SAIMM

JOURNAL OF THE SOUTHERN AFRICAN INSTITUTE OF MINING AND METALLURGY

CAPACI OCCASIO

FOUNDED 1894

VOLUME 115 NO. 1 JANUARY 2015

Danie Krige Commemorative Edition—Volume III

Weir Minerals...
Expertise where it counts.

Weir Minerals is the world leader in the design and manufacture of pumps, valves, hydrocyclones and wear resistant linings, including WARMAN® centrifugal slurry pumps, ENVIROTECH® dewatering pumps and LINATEX® rubber products for the global mining and minerals processing industries. Our reputation is based on engineering excellence applied to innovative, customer focused solutions for processing minerals and aggressive materials.

In line with our customer driven focus, Weir Minerals Africa also offers a pump rental concept as an attractive alternative to an outright purchase.

For more information contact us on
+27 (0)11 9292600
www.weirminerals.com

Excellent
Minerals
Solutions

WEIR
MINERALS

Wealth Unearthed

Our diverse range of robust electronic delay detonators are designed to cope with the most challenging mining environments

Advancing, constantly evolving and defining the future of electronic initiation technology in the global mining industry

AEL Mining Services

Tel: +27 11 606 0000
Adress: 1 Platinum Drive, Longmeadow Business Estate North,
Modderfontein, 1645
www.aelminingservices.com

AEL Mining Services

The Southern African Institute of Mining and Metallurgy

OFFICE BEARERS AND COUNCIL FOR THE 2014/2015 SESSION

Honorary President
Mike Teke
President, Chamber of Mines of South Africa

Honorary Vice-Presidents
Ngoako Ramatlhodi
Minister of Mineral Resources, South Africa

Rob Davies
Minister of Trade and Industry, South Africa

Naledi Pando
Minister of Science and Technology, South Africa

President
J.L. Porter

President Elect
R.T. Jones

Vice-Presidents
C. Musingwini
S. Ndlovu

Immediate Past President
M. Dworzanowski

Honorary Treasurer
C. Musingwini

Ordinary Members on Council

V.G. Duke
M.F. Handley
A.S. Macfarlane
M. Motuku
M. Mthenjane
D.D. Munro
G. Njowa
T. Pegram
S. Rupprecht
N. Searle
A.G. Smith
M.H. Solomon
D. Tudor
D.J. van Niekerk

Past Presidents Serving on Council

N.A. Barcza
R.D. Beck
J.A. Cruise
J.R. Dixon
F.M.G. Egerton
G.V.R. Landman
R.P. Mohring
J.C. Ngoma
S.J. Ramokgopa
M.H. Rogers
G.L. Smith
J.N. van der Merwe
W.H. van Niekerk

Branch Chairmen

DRC	S. Maleba
Johannesburg	I. Ashmole
Namibia	N. Namate
Pretoria	N. Naude
Western Cape	C. Dorfling
Zambia	H. Zimba
Zimbabwe	E. Matinde
Zululand	C. Mienie

Corresponding Members of Council

Australia:	I.J. Corrans, R.J. Dippenaar, A. Croll, C. Workman-Davies
Austria:	H. Wagner
Botswana:	S.D. Williams
Brazil:	F.M.C. da Cruz Vieira
China:	R. Oppermann
United Kingdom:	J.J.L. Cilliers, N.A. Barcza, H. Potgieter
USA:	J-M.M. Rendu, P.C. Pistorius
Zambia:	J.A. van Huyssteen

PAST PRESIDENTS

*Deceased

* W. Bettel (1894–1895)
* A.F. Crosse (1895–1896)
* W.R. Feldtmann (1896–1897)
* C. Butters (1897–1898)
* J. Loevy (1898–1899)
* J.R. Williams (1899–1903)
* S.H. Pearce (1903–1904)
* W.A. Caldecott (1904–1905)
* W. Cullen (1905–1906)
* E.H. Johnson (1906–1907)
* J. Yates (1907–1908)
* R.G. Bevington (1908–1909)
* A. McA. Johnston (1909–1910)
* J. Moir (1910–1911)
* C.B. Saner (1911–1912)
* W.R. Dowling (1912–1913)
* A. Richardson (1913–1914)
* G.H. Stanley (1914–1915)
* J.E. Thomas (1915–1916)
* J.A. Wilkinson (1916–1917)
* G. Hildick-Smith (1917–1918)
* H.S. Meyer (1918–1919)
* J. Gray (1919–1920)
* J. Chilton (1920–1921)
* F. Wartenweiler (1921–1922)
* G.A. Watermeyer (1922–1923)
* F.W. Watson (1923–1924)
* C.J. Gray (1924–1925)
* H.A. White (1925–1926)
* H.R. Adam (1926–1927)
* Sir Robert Kotze (1927–1928)
* J.A. Woodburn (1928–1929)
* H. Pirow (1929–1930)
* J. Henderson (1930–1931)
* A. King (1931–1932)
* V. Nimmo-Dewar (1932–1933)
* P.N. Lategan (1933–1934)
* E.C. Ranson (1934–1935)
* R.A. Flugge-De-Smidt (1935–1936)
* T.K. Prentice (1936–1937)
* R.S.G. Stokes (1937–1938)
* P.E. Hall (1938–1939)
* E.H.A. Joseph (1939–1940)
* J.H. Dobson (1940–1941)
* Theo Meyer (1941–1942)
* John V. Muller (1942–1943)
* C. Biccard Jeppe (1943–1944)
* P.J. Louis Bok (1944–1945)
* J.T. McIntyre (1945–1946)
* M. Falcon (1946–1947)
* A. Clemens (1947–1948)
* F.G. Hill (1948–1949)
* O.A.E. Jackson (1949–1950)
* W.E. Gooday (1950–1951)
* C.J. Irving (1951–1952)
* D.D. Stitt (1952–1953)
* M.C.G. Meyer (1953–1954)
* L.A. Bushell (1954–1955)
* H. Britten (1955–1956)
* Wm. Bleloch (1956–1957)
* H. Simon (1957–1958)
* M. Barcza (1958–1959)
* R.J. Adamson (1959–1960)
* W.S. Findlay (1960–1961)
D.G. Maxwell (1961–1962)
* J. de V. Lambrechts (1962–1963)
* J.F. Reid (1963–1964)
* D.M. Jamieson (1964–1965)
* H.E. Cross (1965–1966)
* D. Gordon Jones (1966–1967)
* P. Lambooy (1967–1968)
* R.C.J. Goode (1968–1969)
* J.K.E. Douglas (1969–1970)
* V.C. Robinson (1970–1971)
* D.D. Howat (1971–1972)
J.P. Hugo (1972–1973)
* P.W.J. van Rensburg (1973–1974)
* R.P. Plewman (1974–1975)
R.E. Robinson (1975–1976)
* M.D.G. Salamon (1976–1977)
* P.A. Von Wielligh (1977–1978)
* M.G. Atmore (1978–1979)
* D.A. Viljoen (1979–1980)
* P.R. Jochens (1980–1981)
G.Y. Nisbet (1981–1982)
A.N. Brown (1982–1983)
* R.P. King (1983–1984)
J.D. Austin (1984–1985)
H.E. James (1985–1986)
H. Wagner (1986–1987)
* B.C. Alberts (1987–1988)
C.E. Fivaz (1988–1989)
O.K.H. Steffen (1989–1990)
* H.G. Mosenthal (1990–1991)
R.D. Beck (1991–1992)
J.P. Hoffman (1992–1993)
* H. Scott-Russell (1993–1994)
J.A. Cruise (1994–1995)
D.A.J. Ross-Watt (1995–1996)
N.A. Barcza (1996–1997)
R.P. Mohring (1997–1998)
J.R. Dixon (1998–1999)
M.H. Rogers (1999–2000)
L.A. Cramer (2000–2001)
* A.A.B. Douglas (2001–2002)
S.J. Ramokgopa (2002-2003)
T.R. Stacey (2003–2004)
F.M.G. Egerton (2004–2005)
W.H. van Niekerk (2005–2006)
R.P.H. Willis (2006–2007)
R.G.B. Pickering (2007–2008)
A.M. Garbers-Craig (2008–2009)
J.C. Ngoma (2009–2010)
G.V.R. Landman (2010–2011)
J.N. van der Merwe (2011–2012)
G.L. Smith (2012–2013)
M. Dworzanowski (2013–2014)

Honorary Legal Advisers
Van Hulsteyns Attorneys

Auditors
Messrs R.H. Kitching

Secretaries

The Southern African Institute of Mining and Metallurgy
Fifth Floor, Chamber of Mines Building
5 Hollard Street, Johannesburg 2001
P.O. Box 61127, Marshalltown 2107
Telephone (011) 834-1273/7
Fax (011) 838-5923 or (011) 833-8156
E-mail: journal@saimm.co.za

Typeset and Published by
The Southern African Institute of Mining and Metallurgy
P.O. Box 61127
Marshalltown 2107
Telephone (011) 834-1273/7
Fax (011) 838-5923
E-mail: journal@saimm.co.za

Printed by
Camera Press, Johannesburg

Advertising Representative
Barbara Spence
Avenue Advertising
Telephone (011) 463-7940
E-mail: barbara@avenue.co.za

The Secretariat
The Southern African Institute of Mining and Metallurgy

ISSN 2225-6253 (print)
ISSN 2411-9717 (online)

SAIMM
JOURNAL OF THE SOUTHERN AFRICAN INSTITUTE OF MINING AND METALLURGY

VOLUME 115 NO. 1 JANUARY 2015

Contents

Danie Krige Commemorative Edition—Volume III

Foreword

Danie Krige

Through his work and exposure to the data and information received while working for the Government Mining Engineer's office in the early 1950s, as well as his methods of comparing sampling information and derived block values by means of regression, Danie Krige became a leader in the field of mineral resource estimation, out of which the science and methods of geostatistics were developed. The *Danie Krige Commemorative Volume* was designed to attract contributions from local and international geostatisticians, practitioners, researchers, and academia in the field of geostatistics with the intention of honouring Danie Krige, who passed away in March 2013, for his work and the impetus it provided in stimulating the creation of new knowledge and improved mineral extraction.

The Southern African Institute of Mining and Metallurgy (SAIMM) has now published three issues of their *Journal* that carry research papers and case studies covering a wide range of topics in the discipline of geostatistics. The first call for papers went out in mid-May 2013, with the first issue containing twelve research papers being published in March 2014, and the second issue, in August 2014, containing fourteen papers. This, the third issue contains eight papers. In total there are 35 papers in the three issues, submitted by 83 authors representing 17 countries including Australia, Brazil, Canada, Chile, China, France, Germany, Ghana, Ireland, Namibia, Peru, Poland, Russia, Scotland, South Africa, Spain, and the USA. This is a remarkable response, for which the Southern African Institute of Mining and Metallurgy and the organizers of the Commemorative Volume are truly grateful.

The foreword to the first and second issues of the *Danie Krige Commemorative Volume* was designed to emphasize the growth and development of the science of geostatistics in the period 1945 to 2005 by numbering the publications of Danie Krige and Georges Matheron. It is not certain that 'number of publications' is an acceptable metric by which to measure the growth of a science or discipline, but is a useful, easy-to-do exercise if the information is readily available. This investigation leaned heavily on a document prepared by Patricia Sheahan (1988) in which she lists 315 publications in the field of geostatistics in the period 1951 to 1988. Within this period Matheron and Kleingeld (1987) identified three phases in the development of aspects of geostatistics, the first being the period 1945–1965, when linear geostatistics was developed, and the second being the period 1966–1974, when interest in nonlinear geostatistics grew. They also describe how and when the terms 'géostatistique' and 'kriging' for 'the mathematical process of assigning grade to individual points or mining blocks' was introduced. The third period, from 1975 onwards, was characterized by the development of more complex geostatistical techniques. The last record by Sheahan (1988) is 133 publications in 1987, but beyond this date it is difficult to quantify the growth and development of the discipline of geostatistics in terms of geostatistically related publications. Global interest in geostatistics and the numbers of publications around the discipline grew exponentially after 1987, and without considerable effort it would be impossible to fairly and comprehensively name the most influential contributors and practitioners.

Although many theoreticians and practitioners of geostatistics have worked across multiple generations, the changes in the discipline from generation to generation are noteworthy. The first generation, including Krige and Matheron and others, launched the characterization of regionalized variables with sound theory and practice. They clearly understood the rich and infinite complexity of geological processes at all scales. The combination of this complexity and widely spaced drilling leads to inevitable uncertainty and defies precise calculation, yet they saw the potential value that could be achieved by a rigorous mathematical statistical approach applied within a sound conceptual geological model. There

Foreword

Danie Krige

was appreciation for the partly structured and partly random nature of mineral deposits. Krige and Matheron pioneered the quantification of spatial correlation, the calculation of optimal local estimates, and an appreciation for the influence of scale/support of different data types and of different mining methods.

For the most part, the second generation was a hardy and strong-minded group. They took the theory of geostatistics around the world and vigorously developed novel solutions to a wide variety of practical applications. They saw the inevitable rise of computing machinery and the potential for more than simply mimicking what we could do by hand. The computation of optimum local estimates with variograms was understood as the foundation of geostatistics, but computationally challenging applications, including simulation and multivariate approaches, were developed.

The third generation is irreverent in many respects. They pay little attention to old debates and schools of thought. There are few that believe in a universal random function approach; this generation will readily develop and adopt custom tools for different deposit types. There is little argument for an absolute best. Debates over conditional bias and other issues have lost momentum as we appreciate there can be no single best estimate suited to all purposes. The absolute belief in a richly complex geological reality frozen in time and space has not diminished, but there is a greater maturity about the inevitable uncertainty and the acceptability of different modelling approaches and models.

Future generations will surely appreciate the rich complexity of geology and the interaction with mining resource and reserve calculations. Krige and Matheron adapted core mathematical principles to these calculations. Significant efforts are being devoted to 'big data', data mining, and predictive analytics. Future generations of geostatisticians will adapt some of the most sophisticated techniques to our problems. It is also likely that, finally, a truly probabilistic view will be adopted where uncertainty is always quantified and always carried through the decision-making process. Massively multivariate modelling of intrinsic grade variables, geomechanical rock properties, and metallurgical properties will become commonplace for the real-time optimization of mining activities. Danie Krige would not even recognize much of what is done, but he would rest easy when he recognized the best practice application of kriging at the heart of many of the techniques.

The importance of the three issues of the SAIMM Journal that together constitute the *Danie Krige Commemorative Volume* is that they document the important strides made in improving and optimizing the determination of available grades and tonnages in deposits and the evaluation of mineral resources and recoverable reserves. This in turn translates into improved quality and optimized evaluation of the metal and mineral content of ore deposits, reduced risk for mining investments, quantification of the risks associated with the evaluations, and generally improved extraction of the Earth's natural resources. The combined outcome is improved 'geovalue', the returns to mining companies and shareholders. For this reason the forthcoming Danie Krige Geostatistical Conference, due to be held in South Africa in August 2015, has the title '*Geostatistical Geovalue — Rewards and Returns for Spatial Modelling*'

R.C.A. Minnitt
C.V. Deutsch

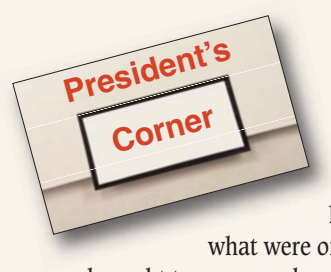

Welcome to 2015. On behalf of all at the SAIMM may I wish our members and readers an abundance of health and safety, at work and at home, in the year that lies ahead. With the global events currently unfolding in terms of geopolitics and economic activity, 2015 is likely to be a year that will continue in much the same way as 2014. It implies that we all need to keep abreast of current affairs as what were once remote events (in time, space, and personal impact) are brought to our own doorsteps through the compressive lens of social networking and by the response of the mining industry to this very dynamic environment. It will be an important objective of the work of the SAIMM Technical Programme Committees (TPC) to ensure that we continue to produce conferences and events that include content that reflect the implications of current affairs as well as future implications. On the inside cover of the back page to this Journal you will find the schedule of upcoming SAIMM events. As I mentioned last month, our Technical Committees continue to offer exceptional value. Their challenge is to make sure that the SAIMM continues to deliver this value to our membership. Should any member have an idea for a conference topic of current interest, please feel free to send me your suggestion and I will ensure that it is passed through to the appropriate TPC Chairman.

This edition of the Journal includes the third and final volume commemorating the lifetime contribution of Professor Danie Krige to the statistical estimation and evaluation of mineral resources. It has been an absorbing three volumes, showcasing a series of papers which clearly demonstrate that scientific research, evolution of methodology, and practical application of the methodologies continues apace and is a core component of how modern mining manages its resources and reserves. Furthermore, South Africa continues to be an important intellectual contributor in this field.

It is with considerable sadness that we also note the passing of an outstanding South African mining engineer, Professor Alex Budavari, on 30 December 2014. Professor Budavari dedicated much of his career to research and teaching in the field of Rock Mechanics. As a result we can be sure that there are many still in the industry whose lives he touched and who continue to add to our knowledge as the industry strives for greater safety performance at improved levels of extraction.

As we move into 2015 it is important to reflect on the great privilege that we all have to be able to stand on the shoulders of such men as these – and there are many that have gone before. No matter how difficult we perceive our current lot, be assured that it would be much more challenging had they not trod the road ahead of us.

J.L. Porter
President, SAIMM

Transactions of the Royal Society of South Africa, 2013
http://dx.doi.org/10.1080/0035919X.2013.826748

UNISA | Taylor & Francis
Taylor & Francis Group

IN MEMORIAM

Professor D.G. Krige FRSSAf

R.C.A. Minnitt[1]* & W. Assibey-Bonsu[2]

[1]*School of Mining Engineering, University of the Witwatersrand, South Africa*
[2]*Group Consultant, Geostatistics and Evaluation, Gold Fields Limited, Perth, Australia*
**Author for correspondence email: Richard.Minnitt@wits.ac.za*

Daniel Gerhardus ("Danie") Krige, whose name is world-renowned in the field of mineral resource estimation and evaluation, passed away peacefully on Sunday morning, 23 March 2013; he was 93 years old. The funeral at Constantia Kloof Dutch Reformed Church on 28 March was attended by more than 200 family members, friends and colleagues from industry and universities, with eulogies by Oscar Steffen, Richard Minnitt and Winfred Assibey-Bonsu. Such was the renown of Daniel Krige that his death is recorded together with that of Margaret Thatcher in Wikipedia (Deaths in April, 2013).

Born in Bothaville, Free State, on the 26 August 1919, Daniel G. Krige grew up in Krugersdorp, matriculating from Monument High School in Krugersdorp in 1934 at the age of 15. He graduated with a BSc(Eng) degree in mining engineering from the University of the Witwatersrand at the end of 1938 (aged 19). In 1938 he joined Anglo Transvaal where he worked on a number of gold mines until 1943, gaining a wide range of valuable practical experience in surveying, sampling and ore valuation. He then joined the Government Mining Engineer's Department where he worked for eight years before returning to industry as Group Financial Engineer of the Anglovaal Group. He held this post until 1981, after which he spent 10 years as Professor of Mineral Economics at the Witwatersrand University. He remained a registered Professional Engineer although his activity as a consultant naturally diminished.

Danie Krige learning the trade, 1939.

HONOURS AND AWARDS

His contributions were recognised by the Witwatersrand University through the award of the DSc(Eng) degree in 1963 and a DIng(HC) degree in 1981 by the University of Pretoria. He received further honorary doctorates from the University of South Africa in April 1996 and from the Moscow State Mining University in September 1997. He received many merit awards from the SA Institute of Mining and Metallurgy, including two gold medals in 1966 and 1980 and two silver medals in 1979 and 1993. In 1984 he received the Institute's highest award, the Brigadier Stokes platinum medal. He was awarded the William Krumbein medal from the International Association of Mathematical Geology in 1984, the Gold Medal for Scientific and Technical Achievements from the Suid Afrikaanse Akademie vir Wetenskap en Kuns in 1982, the Distinguished Achievement Award from the APCOM International Council in 1989 and in the same year the Percy Fox Foundation Award in South Africa. In 1987 he received from the American Society of Mining Engineers one of its highest awards, the Daniel Jackling Award, and in 1988 he was made a 'Distinguished Member'; in both cases he was the first, and to date, the only South African to receive these honours. In 1992 the University of Antofagasta in Chile also honoured him with a special award. The South African State President awarded him with the Order for Meritorious Service Class 1, Gold in 1989. In 1998 The Royal Society of South Africa awarded him the John F. Herschel Medal for outstanding contributions to science in South Africa.

In February 2010 his distinguished contributions to engineering were acknowledged by the United States National Academy of Engineering (NAE) and he was elected a Foreign Associate, Section 11, Earth Resources engineering. Danie was the first South African to ever receive this award from the NAE. In December 2010 he received an Honorary Doctorate from the University of the Witwatersrand, and in 2011 he was awarded the Order of the Baobab (Kremetart Silwer), by President Jacob Zuma.

CAREER ACCOMPLISHMENTS

During his period in government service Danie Krige handled several of the post-war lease applications in the Free State and Klerksdorp goldfields. The fact that decisions on new gold mines of critical importance to the State and the economy as a whole were being taken on a limited number of drillholes, without any scientific analysis of the risks of failure, stimulated him to start basic research into ore evaluation. His approach was based on the application of mathematical statistics to these problems, an approach of which very little was known worldwide at that stage but which had already

been initiated in South Africa by Herbert Sichel via the lognormal frequency distribution model. In Krige's 1951 paper, published in the *Journal of the Chemical, Metallurgical and Mining Society of South Africa*, he covered the statistical explanation of the conditional biases in ore block valuations and stimulated the use by several gold mines of regression corrections for routine ore reserve valuations, a technique which, in effect, was the first use on an elementary basis of what is now known as kriging. This paper introduced, inter alia, the basic geostatistical concepts of 'support.' 'spatial structure,' 'selective mining units' and 'grade-tonnage curves.'

Danie Krige with Herbert Sichel.

As the Anglovaal Group's Financial Engineer, he was responsible for the Group's ore evaluation, mine surveying, financial analyses of mining projects and negotiations, share valuations and technical computing facilities. During the early 1960s he implemented geostatistical kriging procedures on the two large gold mines of the Group. This was the first routine application of the kriging of ore reserves in the world. Apart from ore evaluation, his career led to significant contributions in the fields of investment and financial analysis and mining taxation. This is evidenced by his contributions to the establishments of the original South African uranium contracts, and by a substantial number of local and overseas publications in his field. These include the publication in 1955, in Afrikaans, of what was probably one of the first papers on risk analysis for new mining investments.

As Professor of Mineral Economics in the Mining Engineering Department of the University of the Witwatersrand he was responsible mainly for postgraduate courses in geostatistics and mining economics and supervised many masters and doctoral theses. After retirement from the university he continued his research, lecturing and publication activities and remained active as a consultant in the valuation of resources and reserves of mineral deposits and financial analysis for several of the Mining Houses and various local international mining and consulting companies. He presented courses in geostatistics and/or lectured at local universities (Pretoria, UNISA, RAU and Rhodes) and overseas (Australia, Germany, Taiwan, Chile, Russia and China). He has participated in, and contributed to, many international mining congresses in South Africa, the USA, Canada, Germany, Spain, Chile, Colombia, Slovenia, Australia, the UK, Russia, France and China; in several cases as the keynote speaker.

OUTCOMES

Krige's work led directly, or contributed largely, to the following:

1. His recognition worldwide in mining circles as the principal pioneer in modern statistical methods of ore evaluation, or geostatistics as it is now called.
2. Since the early 1960s his surname has been used to describe the geostatistical techniques of 'kriging.' The term was coined by Georges Matheron and is now applied worldwide mainly in the fields of exploration and ore evaluation, but the environmental, petroleum, hydrology, agriculture and other disciplines.
3. The teaching of geostatistics in graduate and postgraduate mining engineering and other courses at universities worldwide.
4. The establishment of the now world-renowned French school of ore evaluation in Fontainebleau, Le Centre de Géostatistique de l'Ecole des Mines de Paris.

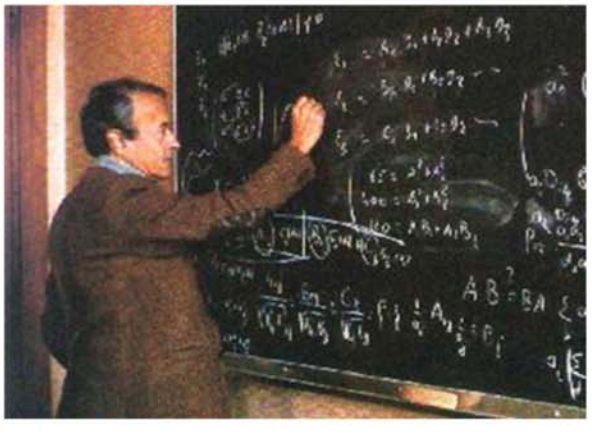

Professor Georges Matheron.

PUBLICATIONS

Danie Krige published some 90 technical papers both locally and overseas, including Russia. His early research papers that had stimulated interest in several mining circles overseas were republished in French in 1955, resulting in a major research effort by French mining engineers in this field. A 1951 paper, based on his MSc(Eng.) thesis submitted to the Department of Mining Engineering to the University of the Witwatersrand, expounded his pioneering work in geostatistics in more detail. His 1978 publication was the first Monograph (Geostatistics) in the monograph series of the SA Institute of Mining and Metallurgy.

A complete record of all Krige's publications is available on a CD disc from the SA Institute of Mining and Metallurgy. They are presented under the following headings:

1. Original basic concepts and developments
2. Routine block kriging on mines
3. Geostatistical techniques, Simple kriging versus Ordinary kriging, Conditional biases
4. Bayesian approach
5. Valuation of new mines from drillholes
6. Reference works
7. Reviews
8. Economic and Financial.

OTHER PROFESSIONAL CONTRIBUTIONS

As a Professional Engineer, Danie Krige served for many years on the mining committee of the Engineering Council of South Africa. For an extensive period he was honorary treasurer on the Council of the SA Institute of Mining and Metallurgy and became an honorary life member. He was also a mining engineering member of the Income Tax Special Court, a founder member of the International Association for Mathematical Geology and of the Geostatistical Association of Southern Africa, a founder-member and honorary life Fellow of the Statistical Association, an honorary life member of the Institute of Mine Surveyors of South Africa and a Fellow of the Royal Society of South Africa. He also served as a director of several mining companies, as well as for the South African Development Trust, the Lebowa Development Corporation, and the Lebowa Mineral Trust.

Danie served on the sub-committee of the Prime Minister's Economic Advisory Council which investigated State Aid for marginal gold mines in 1967/8. He designed the State Aid formula which assisted a large number of gold mines to survive the period of low gold prices. This scheme significantly contributed to the stabilisation and growth of the gold mining industry and the economy as a whole during a difficult time. He also served for many years on various committees of the Chamber of Mines. In 1974 he was a Chamber-nominated member of the Government-Chamber mining mission to Iran which investigated aspects of a closer co-operation on mining matters. More recently, he served as a member of the Marais Committee on mining taxation and on the Melamet Commission of Enquiry into further State aid for the ERPM gold mine; he was also an observer for the State on this mine's Management Committee and Board of Directors until early 1994. He was also a member of the SAMREC Working Committee which developed the South African Code for reporting of Mineral Resources and Reserves as published in 2000.

He was South Africa's representative on the International APCOM Council from its inception and initiated the arrangements for the Symposia held in South Africa in 1972 and in 1987, and he assisted in the preparation of this Symposium in Cape Town in 2003. He served as Chairman of the International Council, the first non-USA member to be elected to this position, from 1990 to 1993.

The outstanding feature of Danie Krige's contributions was his focus on, and dedication to, the basic tenets of geostatistics and the use, wherever practical, of large databases to undertake practical follow-up studies. This style of approach to statistical and geostatistical research became apparent in his initial 1950/2 work and consistently underpinned his research. His rigorous practice of verifying new geostatistical techniques using large data sets, allowed him to test and audit their applicability and interrogate alternative approaches. His high standards of research contributed significantly to the advancement of the science of geostatistics and provided many fruitful avenues for future research. His lasting contributions are a tribute to a lifetime of dedication and he was a worthy leader and an example to all who practice and research in the field of geostatistics.

DANIE KRIGE'S ACKNOWLEDGEMENT OF THE GRACE GIVEN TO HIM

Thoughts from an interview he gave to Richard Minnitt during 2012

With his weight of achievement and a life of distinguished contributions to science and engineering behind him, Professor Danie Krige was a devout Christian who also recognised and acknowledged that he had been the recipient of gifts of grace from the Creator. He drew attention to six specific areas in which he could identify the grace of the Almighty at work in his life and career. The first was a tribute to his parents for the practical application of a godly lifestyle, the establishment of a firm foundation, and a life philosophy that was modelled by them in every area of life. An example of this was that even with the limited resources of a pastor, his parents saw to it that seven of the nine siblings received a tertiary education.

The second of the gifts of grace that Danie acknowledged was the support he had received from his two spouses. He was happily married for 45 years to his first wife (until her death), and for 20 years to Ansie, his second wife.

The third gift of grace was the way in which his career developed, and the various turns in direction that it took as his research unfolded. Having graduated from Wits he was employed in the sampling and survey departments of the Anglovaal Group. In the interview Danie stated that the most important event of his career occurred when an extensive prospecting programme of deep drilling was launched to determine the extent and value of the extensions of the Witwatersrand gold deposits westwards to Klerksdorp and the Orange Free State. Mining companies involved in exploration applied to the Government Mining Engineer for mining leases which led to the opening up of the new goldfields. The GME enrolled additional Mining Engineers to handle this work and he was one of the lucky ones to be chosen. Danie was involved full time in collecting, analysing, and using statistical modelling of the data to determine the underlying patterns of the gold distribution in the widening fields. These patterns proved to be adaptable to modern statistical programmes and these were in turn developed to yield improved grade estimation procedures. This work was successfully submitted for a Master's thesis at the University of the Witwatersrand and a technical paper that was published here and overseas, raised interest. A French team under Professor Georges Matheron in Paris translated the publication and republished it in French. Professor Matheron insisted for the worldwide acceptance of the term KRIGING for this new valuation method, a term for a practice that is now accepted internationally.

Danie and Ansie at Danie's 90th birthday party.

The fourth gift of grace was that when Danie returned to work at Anglovaal, they began to apply these advanced methods of valuation on their mines. Comparisons with later

follow-up values demonstrated the advantages of the new methods. Following the clear demonstration of the validity of the new methods, Anglovaal fully supported the application of Danie's methods on their mines, as well as the publication of these findings, both locally and internationally, particularly at international conferences. In addition, Wits University awarded Danie a DSc(Eng) degree in recognition of this work. This led to the award of two Honorary Doctorate degrees in South Africa, from the University of Pretoria and the University of South Africa (UNISA), and a third from the Moscow State University, in addition to numerous other awards both locally and overseas.

The fifth gift of grace Danie acknowledged was that on retirement from Anglovaal at the age of 60, he accepted the unexpected opportunity of taking up the chair of Professor of Mine Economics at Wits University, which he occupied for the next 10 years. This enabled him to teach and undertake extensive consulting work for mining companies both locally and internationally, and was, in his opinion, a great blessing.

The final gift of grace that Danie recognised was that after his retirement from Wits University he was able to undertake extensive national and international consulting work which he believed kept him occupied and young for the following 20 years. Danie also acknowledged, with deep gratitude, that while the opportunities presented themselves to him, his was the responsibility to make good use of them, and that without these gifts of grace his life's work would not have been possible.

Acknowledgement

This paper which was first published in August 2013 is republished with the permission of the Royal Society of South Africa, http://dx.doi.org/10.1080/0035919X.2013.826748.

Criteria for the Annual Danie Krige Medal Award

Daniel Gerhardus Krige (26 August 1919 – 3 March 2013), one of South Africa's most influential mining engineers and geostatistician of international repute, passed away last year. Danie was a recipient of the Brigadier Stokes award in 1984 – this is the Institute's highest recognition of contribution to the minerals industry.

Following discussions at Office Bearers and Council during 2013 it was agreed to honour his memory and contribution to the mineral industry through three activities:

- The publication of a Danie Krige Commemorative Volume of the Journal. This is planned for March 2014 with a number of papers (37) having been submitted to the publications committee to date
- An annual Danie Krige Memorial Lecture to be facilitated by the School of Mining Engineering at the University of the Witwatersrand
- The annual award of a Danie Krige medal for a qualifying geostatistics paper published by the SAIMM in the previous year.

Selection criteria

The Danie Krige Medal will be awarded annually to the author (or co-authors) of the best geostatistical paper published in the previous calendar year. Accordingly, SAIMM members would be invited to nominate and/or submit papers for consideration on an annual basis.

The following criteria will govern the award:

i. Papers on theoretical or applied geostatistics are eligible
ii. The papers must have been published in the Journal of the SAIMM in the preceding calendar year
iii. Nominations for the award may be made by a member of the SAIMM (who is not an author) or submissions may be made by the author(s)
iv. Nominations and submissions must be submitted by email in pdf format to the SAIMM for attention of the Chairperson of the Danie Krige Medal Committee;
v. An individual may only submit one paper (or be nominated, based on one paper) for the award in any year
vi. No award will be made if none of the papers in a given year meet the minimum standards of the Danie Krige Medal Committee. In evaluating papers, the committee will use the following criteria and apply their professional judgement:
    a. The impact and contribution to knowledge of the paper in its specific field
    b. How innovative are the ideas or techniques described in the paper
    c. The relevance of the problem being addressed
    d. How well the paper is written (language, structure, supporting figure etc.)
vii. Only one paper, or one series of papers on a topic by the same author, per year will qualify for the award
viii. The decision of the Danie Krige Medal Committee on the award of the medal will be final
ix. Award of a Danie Krige Medal excludes the winning paper from consideration for any other SAIMM publications awards i.e. the SAIMM Gold and Silver medals for Journal papers.

The Danie Krige medal will comprise a 38 mm diameter medal in 9 carat gold in an engraved rosewood case and carry an impression of Danie Krige on one side and the SAIMM logo on the other.

G.L. Smith
Past President, SAIMM

Memories of Danie Krige

Geostatistician Extraordinaire

Ansie, Danie´s first wife

Let me start the story in 1969, when I was a final-year mining engineering student at the University of Chile. At that time, Andre Journel, a young man from the Paris School of Mines (Fontainebleau), came to Chile to teach a two or three months-long seminar on geostatistics. If I am not mistaken, that was the very start of geostatistics in Chile. This effort was continued in the early 70's by Andre´s colleague Alain Merechal. In those days, geostatistics was highly mathematical and theoretical, as commercial software did not exist and enthusiastic users had to write their own code. It is not surprising that geostatistics in Chile had a distinct French flavor and Kriging was referred to as 'Krigeage'. In my ignorance, I grew up thinking that Daniel Krige was a very clever Frenchman.

I had no further contact with geostatistics until 1975. At that time, I was working for Anglo American Corporation in Welkom, South Africa, in the Management Sciences Department, developing mixed integer programming models for mine planning. Of course, the gold grades assigned to the different mining areas had a large impact on the sequencing, as well as on the expected profits. My esteemed friends, the geologists, had the almost impossible task of predicting the gold and uranium grades of large blocks, based on perhaps half a dozen boreholes covering an area as large as 50 km^2. On the other hand, closely spaced underground sampling showed large variability and intricate grade patterns. Grade predictions based on a very limited number of drill hole results seemed almost impossible. This is what started my interest in the subject.

Danie with Prof. Wilke and his wife

At that time, publications were few - many of them in French, with at least 50 integrals per page. It was not easy! I admit I was battling to get to grips with the subject. One fine day, my boss said 'Why don't you go and see Danie Krige, perhaps he can give you a hand'. Immediately I replied 'Great, I´m off to France'. 'I'm afraid not, Danie works for Anglovaal in Johannesburg, so just get in your car', came the reply.

I visited Danie every three or four months. He introduced me to his co-worker, Jean-Michel Rendu. They were extremely helpful and shared their knowledge, papers and lots of advice. During one visit, Danie explained that he was rather sad since Jean-Michel had accepted and offer as Professor at a prestigious University in the USA. Before returning to Welkom that evening, I walked into Danie's office and said to him 'What about the job, then?' I thought to myself that I was being rather cheeky. To my great surprise Danie said 'If you want the job, it is all yours'. I was delighted and could not wait to get home and tell my wife Patricia the great news.

D.M. Hawkins, H.S. Sichel, D.G. Krige and P. Brooker

I joined Anglovaal in 1976 and worked with Danie for 10 years. Danie was a patient boss and explained the famous log-normal regression model – the first steps towards kriging - on more than one occasion.

In the early 80's, we gave four one-week courses at the University of Clausthal-Zellerfeld in Germany. On one of these occasions, our wives Ansie and Patricia accompanied us. We stayed in the silver-mining medieval town of Goslar, in Lower Saxony, close to the beautiful Harz Mountains. The hotel was close to the central square, housed in a thousand year-old building. In the evenings, after classes, we would sit in a quaint little coffee shop on the square, enjoying coffee with wonderful pastries and listening to the Town Hall 'glockenspiel'.

Danie with a group of Professors from the University of the Witwatersrand

For a weekend, we visited Berlin and took a bus tour to East Berlin. We crossed the wall at Check Point Charlie. A uniformed lady, who looked and acted as if she were a member of the Gestapo, boarded the bus, checked all the passports and returned them to each passenger, except Danie´s and mine. She took our passports into an office and stayed there for about 20 minutes. The other passengers were all muttering in German and looking at us. We had a quiet chat with Danie: 'We are going to be famous; you coming from the land of apartheid and me from General Pinochet´s dictatorship. We might be here for a long, long time'. In the end the police woman came back, gave us our passports with a dour look and the tour continued normally.

Patricia, Danie & Ansie

Memories of Danie Krige

Danie & Ansie at Villarica

Unfortunately, Ansie suffered from severe asthma and passed away in 1989. We remember her as a very kind and loving person. Some years later, Danie married a wonderful lady, co-incidentally also named Ansie.

South Africa has produced a number of great statisticians. On one occasion, we had lunch at the Johannesburg Club with Danie, D.M. Hawkins, H.S. Sichel and Peter Brooker from the UK. In my modest opinion, having had the honour and the pleasure of working with some of these great minds, they all seemed to have something in common: they are all unassuming, approachable, helpful and always willing to share their knowledge. It seems to be the mark of truly great people.

Patricia, Ansie & Danie with my university students

I remember those 10 years I worked at Anglovaal with Danie as very happy, friendly and productive. The company and Danie were very special and encouraged research, conferences, publications and teaching part time at the Mining Engineering Department of the University of the Witwatersrand. We developed a fine working relationship with my favorite clients and lifelong friends, the geologists; in particular with Jan Mostert.

Bruno Behen, Danie (drinking Pisco Sour) and myself

In 1986, due mainly to family pressures, we moved back to Chile, where I have been working as a part time Professor at the University of Chile and as a mining consultant in geostatistics and sampling ever since. Over the years in Chile, our working relationship with Danie continued and we presented some short courses together, met at conferences and seminars and completed ore resource calculation reviews for several large Chilean copper mines. On one occasion, Danie was accompanied by Ansie and we went on holiday to the beautiful Chilean Lake District, some 900 km south of Santiago. On the way south, I got a speeding fine. A few kilometers further, another policeman stopped me for yet another traffic offence. Ansie could not bear it, got out of the car and gave the policeman a dressing-down in English. To our great surprise, he let us go, remarking that my driving was not at all brilliant that day.

At the APCOM 2007 Dinner

Some years ago, I was teaching the undergraduate course on linear geostatistics to the mining engineering students. We had covered the estimation variance material and had still to continue with Kriging. By coincidence, Danie was in Chile and I asked him if he would be so kind as to give the Kriging lecture himself. Typical of Danie, he immediately accepted. As we walked into the class, there was silence. I told the students that the next topic was Kriging and the best person to present the subject was none other than Professor Krige himself. You should have seen the look on their faces ..... That evening, the students came to our home to socialize and enjoy a few drinks with Danie. They took many photos and had a wonderful time with Ansie and Danie.

In 2007, I chaired APCOM in Chile. Danie very kindly delivered the opening keynote address with Clayton Deutsch on 'The Origins and Future of Geostatistics'. The conference went very well and many people almost queued to have their pictures taken with Danie. As a keepsake, I still have a bottle of good Chilean wine with Danie´s signature on the label.

In July 2007, we went on safari to Tanzania with our dear friends Jeanne and Jan Mostert. On our return to Johannesburg, Ansie and Danie invited us for dinner at their home. We had a very pleasant, friendly evening. That was the last time we saw Danie.

Through the years, I lost track of the number of well-deserved Honorary Doctorates and distinctions that Danie received. A concept that was started off by comparing estimated block values against follow up mining values (true block values) in the South African Gold Mines has developed into a global industry with perhaps thousands of users in mining and other applications, by software developers and researchers all around the world. Danie´s seed idea was picked up by research centers such as Fontainebleau, Stanford, Alberta, at various centers in South Africa and more recently in Chile, and numerous new applications are continually being proposed and developed. An aspect perhaps less known was Danie´s extensive knowledge and ability in subjects such as taxation and financial evaluation of mining projects. In fact, his company designation was that of Financial Engineer.

While travelling through Patagonia in early March, 2013, we received a message from Oskar Steffen saying that after an illness, Danie had passed away on Saturday March 2. It was a long, sad day.

Danie was my friend, my mentor. We remember him with great fondness and respect.

E. Magri

Zibulo Colliery named runner-up in Nedbank Capital Sustainable Business Awards

Anglo American Coal's Zibulo Colliery was named the runner-up in the Resources and Non-Renewable Energy category at the prestigious 2014 Nedbank Capital Sustainable Business Awards held in Johannesburg recently. Zibulo was recognized for what it has achieved through its Phola sanitation and waste management initiative.

The awards honour companies that are able to balance economic profitability with truly sustainable business practices. This competition has become a vehicle to challenge African companies operating across all major industries to ensure they deliver sustainable value, in all its forms, to their stakeholders.

Zibulo colliery operates an opencast pit near the town of Ogies in Mpumalanga, which incorporates the Phola township. Even before operations began at the mine in 2011, Zibulo management recognized the dire need for sanitation and waste management interventions in the local community. Two separate projects were initiated as part of the mine's social and labour plan to improve the safety and health of residents and to mitigate the adverse environmental impacts. The two projects were informed by the needs of the local municipality and have become part of its integrated development planning process.

The sewerage infrastructure project has upgraded the Phola township's entire sewerage network and doubled its existing capacity in anticipation of the area's future growth needs. The project involved increasing the existing capacity of the Ogies outfall sewer line, the complete refurbishment of the pump station and treatment works, expansion of the treatment works to cater for an increase in wastewater flow, implementation of mechanisms to ensure the efficient operation and maintenance of the system, as well as provision of ongoing monitoring and evaluation.

The refuse removal project began with the clearing of more than 20 informal dumping grounds, after which 32 refuse containers were placed at strategic sites across the township. To provide a sustainable solution to the eMalahleni Local Municipality's transport constraints, the Zibulo team acquired two refuse collection trucks that will be transferred to local government once the transfer of skills is complete.

The Phola sanitation and waste management initiative also involved capacity-building and employment creation, successfully creating nearly 40 jobs for full-time project employees and 'Enviro teams' to run refuse collection activities.

'As we are not in the business of managing waste, it was vital that a partnership-based approach be taken to initiate the project and to ensure that the municipality will ultimately be able to run these services independently, making use of the improved infrastructure and skills imparted through the venture,' says Themba Mkhwanazi, CEO of Anglo American Coal South Africa. 'We're also committed to ensuring that both projects extend beyond the life of the operation and that community members continue to benefit from these essential services once operations have ceased.

'We're proud that this initiative has significantly enhanced the quality of life of the township's 37 000 residents, who now benefit from a safe and efficient sewerage system and refuse collection services. The project also succeeded in strengthening the mine's partnership with the municipality.

'An exciting spin-off has emerged from the leadership role we assumed in identifying a range of challenges around municipal capacity, which has prompted other mining houses in the area to invest in similar institutional capacity projects.'

M. Mofokeng

http://dx.doi.org/10.17159/2411-9717/2015/v115n1a1

Self-similarity and multiplicative cascade models

by F. Agterberg*

Synopsis

In his 1978 monograph 'Lognormal-de Wijsian Geostatistics for Ore Evaluation', Professor Danie Krige emphasized the scale-independence of gold and uranium determinations in the Witwatersrand goldfields. It was later established in nonlinear process theory that the original model of de Wijs used by Krige was the earliest example of a multifractal generated by a multiplicative cascade process. Its end product is an assemblage of chemical element concentration values for blocks that are both lognormally distributed and spatially correlated. Variants of de Wijsian geostatistics had already been used by Professor Georges Matheron to explain Krige's original formula for the relationship between the block variances as well as permanence of frequency distributions for element concentration in blocks of different sizes. Further extensions of this basic approach are concerned with modelling the three-parameter lognormal distribution, the 'sampling error', as well as the 'nugget effect' and 'range' in variogram modelling. This paper is mainly a review of recent multifractal theory, which throws new light on the original findings by Professor Krige on self-similarity of gold and uranium patterns at different scales for blocks of ore by (a) generalizing the original model of de Wijs to account for random cuts; (b) using an accelerated dispersion model to explain the appearance of a third parameter in the lognormal distribution of Witwatersrand gold determinations; and (c) considering that Krige's sampling error is caused by shape differences between single ore sections and reef areas.

Keywords

lognormal-de Wijsian geostatistics, self-similarity, multifractals, nugget effect, Witwatersrand goldfields.

Introduction

Professor Danie Krige has played, and continues to play, an important role in the historical development of mathematical statistics and the mathematical geosciences. His MSc thesis (Krige, 1951a) contained new ideas including the use of regression analysis to extrapolate from known gold assays to estimate mining block averages. This was the first application of 'kriging', which is a translation of the term '*Krigeage*' originally coined by Georges Matheron, who remarked in 1962 that use of this word was sanctioned by the [French] Commissariat à l'Energie Atomique to honour work by Krige on the bias affecting estimation of mining block grades from sampling in their surroundings, and on the correction coefficients that should be applied to avoid this bias (Matheron, 1962, p. 149). Later, Matheron (1967) urged the English-speaking community to adopt the term 'kriging', which now is used worldwide.

Krige (1951b) also published his original ideas on the use of mathematical statistics in economic geology in a well-known paper in the *Journal of the South African Institute of Mining and Metallurgy*, which was translated into French (Krige, 1955) in a special issue of *Annales des Mines*. It was followed by a paper by Matheron (1955), who emphasized the 'permanence' of lognormality in that gold assays from smaller and larger blocks all have lognormal frequency distributions with variances decreasing with increasing block size. Matheron discusses 'Krige's formula' for the propagation of variances of logarithmically transformed mining assays, which states that the variance for small blocks within a large block is equal to the variance for the small blocks within intermediate-size blocks plus the variance of the intermediate-size blocks within the large block. This empirical formula could not be reconciled with simple applications of mathematical statistics to blocks of ore, according to which the variance of mean block metal content is inversely proportional to block volume. However, it constitutes a characteristic feature in a spatial model of orebodies previously developed by the Dutch mining engineer de Hans de Wijs (1948, 1951), whose approach helped Matheron (1962) to formulate the idea of 'regionalized random variable'. Also in South Africa, the mathematical statistician Herbert Sichel 1952) had introduced a maximum likelihood technique for efficiently estimating mean and variance from small samples of lognormally-distributed, stochastically independent

* *Geological Survey of Canada, Ottawa, Ontario, Canada.*

(uncorrelated) gold assays. Later, Krige (1960) discovered that a small but significant improvement of this approach could be obtained by using a three-parameter lognormal distribution.

Rather than using autocorrelation coefficients, as were generally employed in time series analysis under the assumption of existence of a mean and finite variance, Matheron (1962) introduced the variogram as a basic tool for structural analysis of spatial continuity of element concentration values. This is because the variogram allows for the possibility of infinitely large variance, as would result from the de Wijsian model for indefinitely increasing distances between sampling points. Aspects of this model were adopted by Krige (1978) in his monograph 'Lognormal-de Wijsian Geostatistics for Ore Evaluation' summarizing earlier studies including his successful application for characterizing self-similar gold and uranium distribution patterns in the Klerksdorp goldfield (Krige, 1966a).

Personally, I have had the privilege of knowing Danie Krige as a friend and esteemed colleague for more than 50 years. As a graduate student at the University of Utrecht I had studied Krige's MSc thesis on microfilm at the library in preparation of an economic geology seminar on the skew frequency distribution of mining assays. This resulted in a paper (Agterberg, 1961) that was read by Danie, who wrote me a letter about it. After I had joined the Geological Survey of Canada (GSC) in 1962, he visited me in Ottawa with his wife and a colleague on the way to the 3rd APCOM meeting held at Stanford University in 1963. APCOM is the acronym of *Applications of Computers and Operations Research in the Mineral Industries*. Before the birth of the International Association for Mathematical Geology, APCOMs provided the most important forum for mathematical geoscientists. Danie persuaded GSC management that I should attend the 4th APCOM, hosted by the Colorado School of Mines in 1964. I also participated in discussions of two of Danie's SAIMM papers (Krige and Ueckermann, 1963; Krige, 1966b) on value contours and improved regression techniques and two-dimensional weighted moving average trend surfaces for ore evaluation (Agterberg, 1963; 1966). I visited Danie and his family three times in Johannesburg. His great hospitality included joint visits to the Kruger National Park and the wildlife reserve in Krugersdorp, in addition to descents into deep Witwatersrand gold mines.

In the following sections, the model of de Wijs will be discussed with its application by Danie Krige to the Witwatersrand goldfields. Another application is to worldwide uranium resources. First, frequency distributions and spatial correlation of element concentration values in rocks and orebodies will be considered, and this discussion will be followed by a review of multifractal theory and singularity analysis. Finally, block-variance relations of element concentration values are briefly reviewed from the perspective of permanence of block frequency distributions. The objectives of this paper are (1) to draw increased attention to recent developments in developments of multifractal theory, (2) to highlight various generalizations of the original model of de Wijs and approaches commonly taken in geostatistics as applied to ore reserve estimation, and (3) to illustrate how singularity analysis can be used to help determine the nature of nugget effects and sampling errors.

The model of de Wijs

The model of de Wijs (1948, 1951) is based on the simple assumption that when a block of rock with an element concentration value x is divided into two halves, the element concentration values of the two halves are $(1+d)\cdot x$ and $(1-d)\cdot x$ regardless of the size of the block. The coefficient $d > 1$ is the index of dispersion. The ratio $(1+d)/(1-d)$ can be written as $\eta > 1$. The process of starting with one block that is divided into halves, dividing the halves into quarters, and continuing the process of dividing the smaller blocks repeatedly into halves results in a log-binomial frequency distribution of the element concentration values. This model has the property of self-similarity or scale-independence. It can be readily generalized in two ways:

- In practical applications, there is generally a lower limit to the size of blocks with the same index of dispersion as larger blocks. Below this limit, d usually decreases rapidly to zero; this limitation is accommodated in the three-parameter model of de Wijs (Agterberg, 2007a) that has an effective maximum number of subdivisions beyond which the hypothesis of a constant index of dispersion does not apply
- The idea of cutting any block into halves with constant value of d is not realistic on a local scale (*e.g.*, d does not stay exactly the same when halves become quarters). However, this problem is eliminated in the random-cut model for which the coefficient d is replaced by a random variable D with variance that is independent of block size (Agterberg, 2007a). The end products of constant dispersion and random-cut models are similar.

The log-binomial frequency distribution of element concentration values (x) resulting from the model of de Wijs has logarithmic variance:

$$\sigma^2 (\ln x) = n\cdot(\ln \eta)^2/4 \qquad [1]$$

where n represents the number of subdivisions of blocks. This is the original variance equation of de Wijs (1951). Frequency density values in the upper and lower tails of the log-binomial distribution are less than those of the lognormal. The log-binomial would become lognormal only if n were increased indefinitely. Paradoxically, its variance then also would become infinitely large. In practical applications, it is usually seen that the upper tail of a frequency density function of element concentration values is not thinner, but thicker, and extending further than a lognormal tail. Later in this paper, models that generate thicker-than-lognormal upper tails will be considered.

Matheron (1962) generalized the original model of de Wijs by introducing the concept of 'absolute dispersion' here written as $A = (\ln \eta)^2 / \ln 16$. It leads to the more general equation

$$\sigma^2 (\ln x) = A \cdot \ln \{V/v\} \qquad [2]$$

where $\sigma^2 (\ln x)$ represents logarithmic variance of element concentration values x in smaller blocks with volume v contained within a larger block of rock with volume V. Equation [2] was used by Krige (1966a, 1978), as will be illustrated in the next section.

Self-similarity and multiplicative cascade models

The Witwatersrand goldfields

Figure 1 is a classic example of the relationship between logarithmic variance and block size for Witwatersrand gold values as derived by Krige (1966a). The gold occurs in relatively thin sedimentary layers called 'reefs'. Average gold concentration value is multiplied by length of sample cut across reef, and the unit of gold assay values is expressed as inch-pennyweight in Figure 1 (1 inch-pennyweight = 3.95 cm-g). Three straight-line relationships for smaller blocks within larger blocks are indicated. Size of reef area ranged from 0.1 to 1 000 million square feet. Consequently, in Krige's application, scale-independence applies to areal domains with side lengths extending over five orders of magnitude. Clearly, the logarithmic variance increase is approximately in accordance with Equation [2]. In this paper, discussions will be restricted to the top line in Figure1, which applies to the distribution of original assay values within larger blocks. Variance-size relations for the other two lines in Figure 1 are discussed by Krige (1966a).

There are two minor departures from the simple model of Equation [2]. The first of these departures is that a small constant term (+20 inch-pennyweights) was added to all gold values. This reflects the fact that, in general, the three-parameter lognormal model provides a better fit than the two-parameter lognormal (Krige, 1960). As will be discussed in more detail later in this paper, this departure corresponds to a narrow secondary peak near the origin of the normal Gaussian frequency density curve for logarithmically transformed gold assay values, and can be explained by adopting an accelerated dispersion model. The second departure consists of the occurrence of constant terms that are contained in the observed logarithmic variances plotted in Figure 1. These additive terms are related to shape differences of the blocks with volumes v and V, as will also be discussed later in this paper.

Worldwide uranium resources

A second example of application of the model of de Wijs is as follows. The log-binomial frequency distribution model was used in mineral resource evaluation studies by Brinck (1971, 1974). A comprehensive review of Brinck's approach can be found in Harris (1984). The original discrete model of de Wijs was assumed to apply to a chemical element in a very large block consisting of the upper part of the Earth's crust with known average concentration value ξ, commonly set equal to the element's crustal abundance or 'Clarke'.

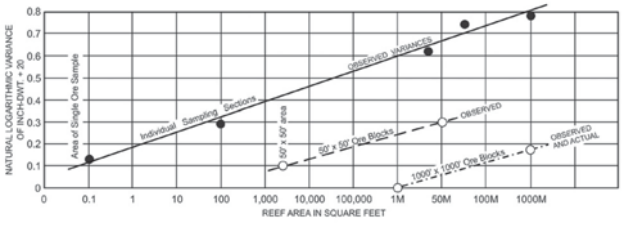

Figure 1—Logarithmic variance of gold values as a function of reef area sampled. The variance increases linearly with area if the area for gold values is kept constant. The relationship satisfies the model of de Wijs (based on Krige, 1966a)

Chemical analysis is applied to blocks of rock that are very small in comparison to the large block targeted for study. Let $n = N$ represent the maximum number of subdivisions of this very large block. Suppose that the element concentration values available for study: (1) constitute a random sample from the population of 2^N small blocks within the large block, and (2) show an approximate straight line pattern on their lognormal Q-Q plot. The slope of this line then provides an estimate of σ from which η (and d) can be derived by means of the original variance formula of de Wijs. Brinck (1974) set 2^N equal to average weight of the small block used for chemical analysis divided by total weight of the environment targeted for study.

Figure 2 (modified from Brinck, 1974) is a worldwide synthetic diagram for uranium with average crustal abundance value set equal to 3 ppm and dispersion index $d = 0.2003$. This diagram is equivalent to a cumulative frequency distribution plot with two logarithmic scales. Value (ppm U) is plotted in the vertical direction and weight (tons U) is plotted in the horizontal direction. All weight values are based on cumulative frequencies calculated for the log-binomial distribution and are fully determined by the mean and coefficient of dispersion. The diagram shows curved lines of equal metal content. In 1971 it was, on the whole, profitable to mine uranium if the cost of exploitation was less than US$6.00 per pound U_3O_8. Individual orebodies can be plotted as points in Figure 2. In 1971 such deposits would have been mineable if their point fell within the elliptical contour labeled $6.00. The other elliptical contours are for uranium deposits that would have been more expensive to mine.

Frequency distributions and spatial statistics

Multiplicative cascade processes that generate spatial frequency distributions of chemical concentration were preceded by generating process models, as will be discussed next.

Theory of proportionate effect

The theory of proportionate effect was originally formulated by Kapteyn (1903) and later in a more rigorous manner by Kolmogorov (1941). It can be regarded as another type of

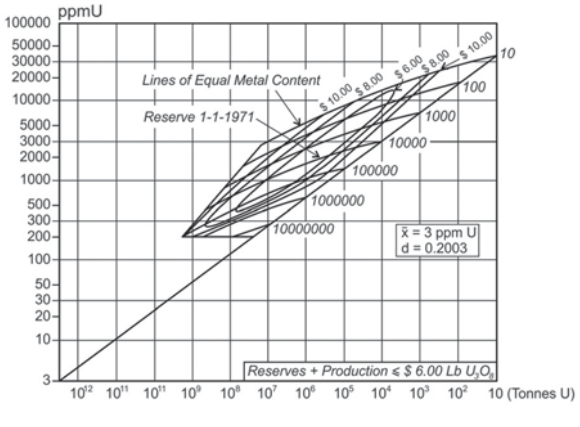

Figure 2—Uranium resources and inferred potential reserves as estimated by the program MIMIC (Brinck, 1974). Numbers along diagonal refer to largest possible deposits for given values of $\bar{x}$ and d. Dollar values refer to estimated average exploitation costs

application of the central limit theorem of mathematical statistics. Suppose that a random variable X was generated stepwise by means of a process that started from a constant value X_0. At the i-th step of this process ($i = 1, 2, \ldots, n$) the variable was subject to a random change that was a proportion of some function $g(X_{i-1})$, or $X_i - X_{i-1} = \varepsilon_i \cdot g(X_{i-1})$. Two special cases are $g(X_{i-1}) = 1$ and $g(X_{i-1}) = X_{i-1}$. If g remains constant, X becomes normal (Gaussian) because of the central limit theorem. In the second case, it follows that:

$$\sum_{i=1}^{n} \frac{X_i - X_{i-1}}{X_{i-1}} = \sum_{i=1}^{n} \varepsilon_i \approx \int_{X_0}^{X_n} \frac{dx}{x} = \log_e X_n - \log_e X_0 \quad [3]$$

This generating process has the lognormal distribution as its end product. There is an obvious similarity between generating processes and the multiplicative cascade processes to be discussed later in this paper in the context of fractals and multifractals.

The starting point of the preceding discussion of the generating process also can be written as $dX_i = g(X_i) \cdot \varepsilon_i$, where dX_i represents the difference $X_i - X_{i-1}$ in infinitesimal form. Often an observed frequency distribution can be reduced to normal (Gaussian) form. In Figure 3 a lognormal curve is plotted on normal probability paper. An auxiliary variable z is plotted along the horizontal axis. It has the same arithmetic scale as x, which is plotted in the vertical direction. The variable x is a function of z or $x = G(z)$. The slope of $G(z)$ is measured at a number of points giving the angle ϕ. For example, if $z = x = 20$ in Figure 3A, $\phi = \phi_1$, and:

$$\frac{dG(z)}{dZ} = \tan \varphi \quad [4]$$

If, in a new diagram (Figure 3B), tan ϕ is plotted against x, we obtain a function $F(x)$ that represents $g(X_i)$ except for a multiplicative constant which remains unknown. This procedure is based on the general solution of the generating process that can be formulated as:

$$Z = \int_0^{\infty} \frac{dX_1}{g(X_i)} = \sum_0^{\infty} \varepsilon_i \quad [5]$$

under the assumption that Z is normally distributed.

The function $g(X_i)$ derived in Figure 3B for the lognormal curve of Figure 3A is simply a straight line through the origin. This result is in accordance with the origin theory of proportional effect. However, the method can produce interesting results in situations where the frequency distribution is not lognormal. Two examples are given in Figure 4. The original curves for these two examples (Figure 3) are on logarithmic probability paper. They are for a set of 1000 Merriespruit gold values from Krige (1960), and a set of 84 copper concentration values for sulphide deposits that surround the Muskox intrusion, District of Mackenzie, northern Canada (Agterberg, 1974) as a rim. The results obtained by the graphical method are shown in Figure 4B.

The generating function $g(X_i)$ for Merriespruit is according to a straight line, the extension of which would intersect the X-axis at a point with negative abscissa $\alpha = \approx 55$. This is equal to the constant added to pennyweight values by Krige (1960). Addition of this small constant term (55 inch-dwt) to all Merriespruit gold assays has the effect that the straight line in Figure 4B passes through the origin. The departure from lognormality is restricted to the occurrence of a small secondary peak near the origin. The second example (Muskox sulphides) gives a function $g(X_i)$ that resembles a broken line. It would suggest a rather abrupt change in the generating process for copper concentration after the value $X_i = \approx$ 0.5%. The influence of X_i on dX_i may have decreased with increasing X_i.

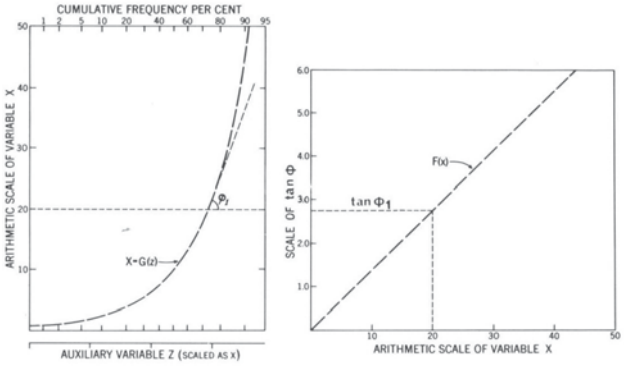

Figure 3—Graphical construction of *F*(*x*), which is proportional to the tangent of the slope of *x* = *G*(*z*) representing the theoretical lognormal distribution plotted on arithmetic probability paper (Agterberg, 1974, Figure 33)

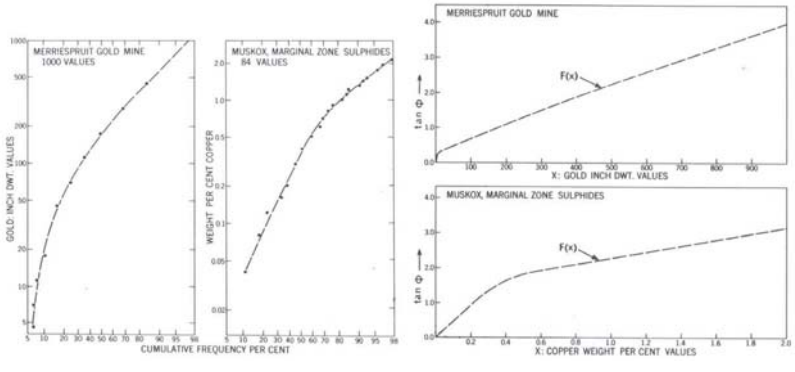

Figure 4—Left side. Two frequency distributions that depart from the lognormal model plotted on logarithmic probability paper. Example of 1000 gold values from Merriespruit gold mine is after Krige (1960; see also Sichel, 1961), and 84 copper values from the Muskox intrusion (Agterberg, 1974). Right side. Method of Equation [5] resulted in two types of *F*(*x*): the one for the Merriespruit mine is approximately a straight line that would intersect the *x*-axis at a point with abscissa of about -55 (value used in Krige, 1960, for the same data-set). Function *F*(*x*) for Muskox copper values would suggest a change in the generating process after 0.5% Cu (Agterberg, 1974, Figure 34)

The usefulness of a graphical method of this type is limited, in particular because random fluctuations in the original frequency histograms cannot be considered carefully. However, the method is rapid and offers suggestions with respect to the physicochemical processes that may underlie a frequency distribution of observed element concentration values.

Accelerated dispersion model

The model of de Wijs has the property of self-similarity or scale-independence. In his application of this model to gold in the Klerksdorp goldfield, Krige (1966a) worked with approximately 75 000 gold determinations for very small blocks. In Figure 1 it was illustrated that there are approximate straight line relationships between logarithmic variance and logarithmically transformed size of reef area for gold. Validity of the concept of self-similarity was also illustrated by means of moving-average gold value contour maps for square areas measuring 500 ft and 10 000 ft on a side. The contours of moving-average values obtained by Krige (1966a) for these squares show similar patterns of gold concentration contours in both areas, although one area is 400 times as large as the other.

The original assay values satisfy a three-parameter lognormal distribution, because of which a small value was added to all assays to obtain approximate (two-parameter) lognormality. Originally, the following variant of the model of de Wijs was developed (Agterberg, 2007b) because, in a number of applications of the lognormal in resource studies, the high-value tail of the frequency distribution was found to be thicker and longer than log-binomial and lognormal tails. Suppose that the coefficient of dispersion (d) in the model of de Wijs increases as follows with block concentration value (x):

$$d = d_0 \cdot \exp(-b \cdot x) \qquad [6]$$

where d_0 represents the initial dispersion index at the beginning of the process, and b is a constant. This accelerated dispersion model produces thicker and longer tails than the lognormal frequency distribution (Agterberg, 2007b). Additionally, it yields more very small values, thus producing a secondary peak near the origin of the frequency density function similar to Merriespruit.

Figure 5 is the result of a two-dimensional computer simulation experiment with $d_0 = 0.4$, $n = 14$, and $p = 0.01$. In total, $2^{14} = 16\,384$ values were generated on a 128 × 128 grid. The generating process commenced with a single square with element concentration value set equal to 1. This square was divided into four quadrants of equal size with values $(1+d)^2$, $(1+d)(1-d)$, $(1-d)(1+d)$, and $(1-d)^2$ in a random configuration (Agterberg, 2001). The process was repeated for each square until the pattern of Figure 5 was obtained. Because p is small, most element concentration values after 14 iterations are nearly equal to values that satisfy the original model of de Wijs. Exceptions are that the largest values, which include $(1+d)^{14} = 316$, significantly exceed values that would be generated by the original model, which include $(1+d_0)^{14} = 111$ (*cf.* Agterberg, 2007b, Figure 6). Likewise, the frequencies of very small values that are generated exceed those generated by the ordinary model of de Wijs.

Sill and nugget effect

Geostatistical studies are commonly based on a semivariogram fitted to element concentration values from a larger neighbourhood. Generally, these models assume the existence of a 'nugget effect' at the origin, and a 'range' of significant spatial autocorrelation with a 'sill' that corresponds to the variance with respect to regional mean concentration value (see *e.g.* Journel and Huijbregts, 1978, or Cressie, 1991). It is well known that the 'nugget effect' is generally much larger than chemical determination errors or microscopic randomness associated with ore grain boundaries. This second source of randomness arises because chemical elements are generally confined to crystals with boundaries that introduce randomness at very small scales. In general, the preceding two sources of local randomness have effects that rapidly decline with distance.

Suppose $\gamma(h)$ represents the semivariogram, which is half the variance of the difference between values separated by lag distance h. Semivariogram values normally increase when h is increased until a sill is reached for large distances. If element concentration values are subject to second-order stationarity, $\gamma(h) = \sigma^2 \cdot (1 - \rho_h)$ where σ^2 represents variance and ρ_h is the autocorrelation function. The sill is reached when there is no spatial autocorrelation or $\gamma(h) = \sigma^2$. If regional trends can be separately fitted to element concentration values, the residuals from the resulting regional, systematic variation may become second-order stationary because the overall mean in the study area then is artificially set equal to zero. In most rock types such as granite or sandstone, randomness of chemical concentration is largely restricted to the microscopic scale and sills for compositional data are reached over very short distances. The nugget effect occurs when extrapolation of $\gamma(h)$ towards the origin ($h \rightarrow 0$) from observed element concentration values yields estimates with $\gamma(h) > 0$ (or $\rho_h < 1$). Often, what seems to be a nugget effect arises when there is strong local autocorrelation that cannot be detected because the locations of samples subjected to chemical analysis are too far apart to describe local continuity.

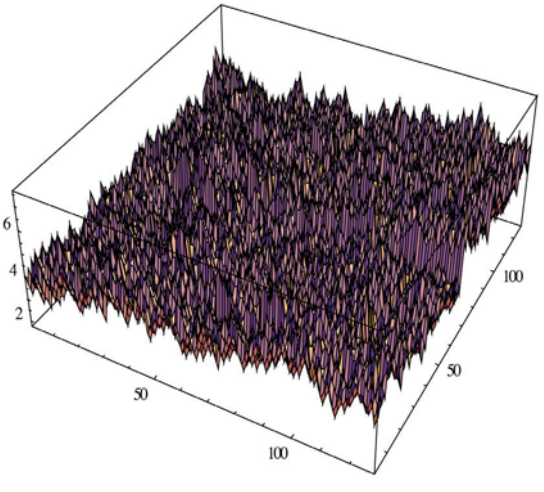

Figure 5—Realization of accelerated dispersion model for $d_0 = 0.4$, $N = 14$, and $p = 0.01$. Vertical scale is for 4 + log10 (value) (Agterberg, 2007b, Figure 5)

Self-similarity and multiplicative cascade models

Matheron (1989) has pointed out that in rock sampling there are two possible infinities if the number of samples is increased indefinitely: either the sampling interval is kept constant so that more rock is covered, or the size of the study area is kept constant whereby sampling interval is decreased. These two possible sampling schemes provide additional information on sample neighbourhood, for sill and nugget effect respectively. In practice, the exact form of the nugget effect usually remains unknown, because extensive sampling would be needed at a scale that exceeds microscopic scale but is less than scale of sampling space commonly used for ore deposits or other geological bodies.

If the model of de Wijs would remain applicable for $n \rightarrow \infty$, the variance would not exist and it would not be possible to estimate the spatial covariance function. This was the main reason that Matheron (1962, 1989) originally advocated using the variogram, because this tool is based on differences between values that are distance h apart and the existence of a finite variance is not required. Independent of Matheron, Jowett (1955) also advocated use of the variogram instead of the correlogram. Recently, Serra (2014) has calculated the rather strong bias that could result from estimating the spatial covariance from data for which the variance does not exist. Such an approach differs from statistical applications of time series analysis, in which the existence of mean and variance is normally taken for granted. If the variance σ^2 of spatial observations exists, it follows immediately that the semivariogram satisfies $\gamma_h = \sigma^2 - \sigma_h$ where σ_h is the covariance of values that are distance h apart. On the other hand, Matheron (1962) originally assumed $\gamma_h = 3A \cdot \ln h$ for logarithmically transformed element concentration values for infinitesimally small volumes, and his approach was in accordance with the model of de Wijs.

De Wijs (1951) used a series of 118 zinc assays for channel samples taken at 2 m intervals along a drift in the Pulacayo Mine, Bolivia, as an example to illustrate his original model. Matheron (1962) analysed this data-set as well, constructing a semivariogram for the channel samples based on the $\gamma_h = 3A \cdot \ln h$ model with $\gamma_0 = 0$ and $\sigma^2 = \infty$. The original zinc assays for this example are shown in Figure 6. In Agterberg (1974), a standard time series approach was taken in which mean and variance were assumed to exist. The model used for smoothing the 118 zinc values was that each zinc value is the sum of a 'signal' value and small-scale 'noise' with autocorrelation function $\rho_h = c \cdot \exp(-ah)$, where c represents the small-scale noise variance and the parameter a controls the decreasing influence of observed values on their surroundings. The two parameters were estimated to be $c = 0.5157$ and $a = 0.1892$. Signal+noise models of this type are well known in several branches of science (*cf.* Yaglom, 1962). Filtering out the noise component produces the signal shown in Figure 6. Various other statistical methods such as ordinary kriging can be used to produce similar smoothed patterns.

If the logarithmic variance of element concentration values is relatively large, it may not be easy to obtain reliable estimates of statistics such as mean, variance, autocorrelation function, and semivariogram by using untransformed element concentration values. This is a good reason for using logarithmically transformed values instead of original values in such situations. Approximate lognormality for the frequency distribution of element concentration values can often be assumed. If the coefficient of variation, which is equal to the standard deviation divided by the mean, is relatively small (< 0.5), the lognormal distribution can be approximated by a normal (Gaussian) distribution and statistics such as the autocorrelation function can be based on original data without use of a logarithmic transformation. Agterberg (2012a) showed that the estimated and theoretical autocorrelation coefficients for the 118 zinc values from the Pulacayo orebody are almost exactly the same whether or not a logarithmic transformation is used. Consequently, the original data can be used in subsequent statistical calculations for this example.

Multifractals

Fractals are objects or features characterized by a fractal dimension that is either greater than or less than the integer Euclidean dimension of the space in which the fractal is embedded. The term 'fractal' was coined by Mandelbrot (1975). On the one hand, fractals are often closely associated with the random variables studied in mathematical statistics; on the other hand, they are connected with the concept of 'chaos' that is an outcome of some types of nonlinear processes. Evertsz and Mandelbrot (1992) explain that fractals are phenomena measured in terms of their presence or absence in cells or boxes belonging to arrays superimposed on the one-, two-, or three-dimensional domain of study, whereas multifractals apply to 'measures' of how much of a feature is present within the cells. Multifractals are either spatially intertwined fractals (*cf.* Stanley and Meakin, 1988) or mixtures of fractals in spatially distinct line segments, areas, or volumes that are combined with one another. Fractals and multifractals often indicate the existence of self-similarity that normally results in power-law relations (Korvin, 1992; Agterberg, 1995), which plot as straight lines on log-log paper.

Brinck's (1974) model constituted an early application of the model of de Wijs. Estimation of parameters in this model, including d, could be improved by adopting a multifractal modelling approach (Agterberg, 2007a). At first glance, the Brinck approach seems to run counter to the fact that mineral deposits are of many different types and result from different

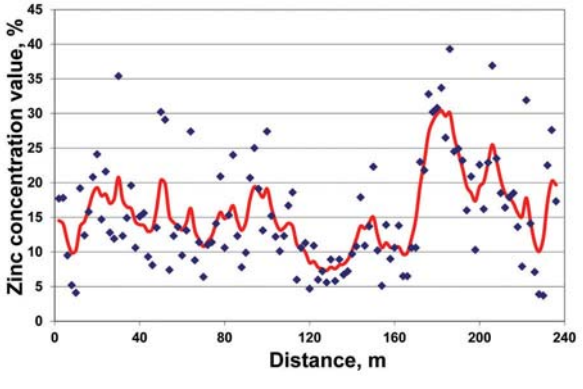

Figure 6—Pulacayo Mine zinc concentration values for 118 channel samples along horizontal drift samples (original data from De Wijs, 1951). Sampling interval is 2 m. 'Signal' retained after filtering out 'noise' (Agterberg, 2012a, Figure 1)

genetic processes. However, Mandelbrot (1983) has shown that, for example, mountainous landscapes can be modeled as fractals. Smoothed contours of elevation on such maps continue to exhibit similar shapes when the scale is enlarged, as in Krige's (1966a) example for Klerksdorp gold contours. Lovejoy and Schertzer (2007) argued convincingly that the Earth's topography can be modelled as a multifractal, both on continents and ocean floors, in accordance with power-law relations originally established by Vening Meinesz (1964). These broad-scale approaches to the nature of topography also seem to run counter to the fact that landscapes are of many different types and result from different genetic processes. In this paper it is assumed that chemical elements within the Earth's crust or within smaller, better-defined environments like the Witwatersrand goldfields can be modeled as multifractals.

The model of de Wijs is a simple example of a binomial multiplicative cascade (*cf.* Mandelbrot, 1989). Cascade theory has been developed extensively over the past 25 years; for example, by Lovejoy and Schertzer (1991) and other geophysicists (Lovejoy *et al.*, 2010), particularly in connection with cloud formation and rainfall (Schertzer and Lovejoy, 1987; Veneziano and Langousis, 2005). More recently, multifractal modelling of solid Earth processes, including the genesis of ore deposits, has been advanced by Cheng and others (Cheng, 1994, 2008, 2012; Cheng and Agterberg, 1996). In applications concerned with turbulence, the original binomial model of de Wijs became widely known as the binomial/*p* model (Schertzer *et al.*, 1997). With respect to the problem that in various applications observed frequency distribution tails are thicker than log-binomial or lognormal, it is noted here that several advanced cascade models in meteorology (Veneziano and Langousis, 2005) result in frequency distributions that resemble the lognormal but have thicker tails.

Binomial/p model

The theory of the binomial/*p* model is clearly presented in textbooks, including Feder (1988), Evertsz and Mandelbrot (1992), Mandelbrot (1989), and Falconer (2003). There have been numerous successful applications of this relatively simple model, including many for solving solid Earth problems (*e.g.* Cheng, 1994; Cheng and Agterberg, 1996; Agterberg, 2007a,b; Cheng, 2008). Although various departures from the model have also been described in these papers and elsewhere, the binomial/*p* model remains useful. Basically, it is characterized by a single parameter. In the original model of de Wijs (1951), this parameter is the dispersion index *d*. When the parameter *p* of the binomial/*p* model is used, $p = 0.5(1\text{-}dh)$.

Evertsz and Mandelbrot (1992) defined the 'coarse' Hölder exponent α as:

$$\alpha = \frac{\log_e \mu\{B_x(\epsilon)\}}{\log_e \epsilon} \quad [7]$$

where μ represents a quantity measured for a cell with volume B_x ($\in$) around a point x, and $\in$ is a line segment, *e.g.* the edge of cubical cells used to partition the domain of study in a three-dimensional application. In most applications by physicists and chemists, α is called the 'singularity'. The mass-partition function χ_q ($\in$) is defined as:

$$\chi_q(\epsilon) = \sum_{N(\epsilon)} \mu_i^q = \int N_\epsilon(\alpha)(\epsilon^\alpha)^q \, d\alpha \quad [8]$$

where q is a real number ($-\infty \le q \le \infty$), $N(\in)$ is total number of cells, and $N\in(a) = \in^{-f(a)}$; $f(a)$ represents the fractal dimension for all cells with singularity α. It follows that

$$\lim_{\epsilon \to 0} \chi_q(\epsilon) = \int \epsilon^{q\alpha - f(\alpha)} d\alpha \quad [9]$$

At the extremum, for any 'moment' q: $\frac{\partial\{qa - f(a)\}}{\partial a} = 0$ and $\frac{\delta f(a)}{\delta q}|_{\ddot{a}=\ddot{a}(q)} = q$ (*cf.* Evertsz and Mandelbrot, 1992, Equation B.14). Mass exponents $\tau(q)$ are defined as:

$$\tau(q) = q\alpha - f(\alpha), \quad [10]$$

It follows that $\frac{\delta\tau(q)}{\delta a} = q$, and the so-called multifractal spectrum satisfies:

$$f(\alpha) = q\alpha - \tau(q) \quad [11]$$

The preceding derivation is used in the method of moments to construct a multifractal spectrum in practice. This spectrum shows the fractal dimension $f(\alpha)$ as a function of the singularity a and has its maximum $f(\alpha) \le 1$ at $\alpha = 1$, and $f(\alpha) = 0$ at two points along the α -axis with:

$$\alpha_{\min} = -\log_2(1 - p); \alpha_{\max} = -\log_2 p \quad [12]$$

A one-dimensional example of a multifractal is as follows. Suppose that $\mu = x\cdot \in$ represents the total amount of a metal for a rod-shaped sample that can be approximated by a line segment of length $\in$, and x is the metal's concentration value. In the multifractal model it is assumed that (1) $\mu \propto \in^\propto$ where $\propto$ denotes proportionality and α is the singularity exponent corresponding to element concentration value x; and (2) $N_\alpha(\in) \propto \in^{-f(\alpha)}$ represents the total number of line segments of length $\in$ with concentration value x, while $f(\alpha)$ is the fractal dimension of these line segments.

The binomial/*p* model can be characterized by the second-order mass exponent $\tau(2)$ with

$$\tau(2) = -\log_2 \{p^2 + (1\text{-}p)^2\} \quad [13]$$

If the binomial/*p* model is satisfied, any one of the parameters p, d, $\tau(2)$, $\alpha_{\min}$, $\alpha_{\max}$, or σ^2 (ln X) can be used for its characterization. Using different parameters can be helpful for checking goodness of fit for the model or finding significant departures from model validity. The mass-partition function and multifractal spectrum of the Pulacayo zinc values were derived by Cheng (1994; also see Cheng and Agterberg, 1996, Figure 2). The line for the second-order moment $q = 2$ is shown in Figure 7. This line was fitted by least-squares. Its slope provides the fairly precise estimate $\tau(2) = 0.979 \pm 0.038$. The degree of fit in Figure 7 is slightly better than can be obtained by semivariogram or correlogram modelling applied to the same data. From this estimate of $\tau(2)$ it would follow that $d = 0.121$.

Estimates of $\alpha_{\min}$ and $\alpha_{\max}$ derived for the Pulacayo zinc deposit in Chen *et al.* (2007) by a technique called 'local singularity analysis' (see later) were 0.532 and 1.697, respectively. Using a slightly different method, Agterberg (2012a) obtained 0.523 and 1.719. These results, which correspond to $d = 0.392$ Agterberg, 2012b), differ greatly from the estimates based on the binomial/*p* model with $d =$

0.121. Clearly, the binomial/*p* model has a limited range of applicability, although it shows well-defined linear patterns for different moments (q) on the log-log plot of partition function versus $\in$ (see *e.g.* Figure 7).

This discrepancy can be explained By using more flexible models with additional parameters, such as the accelerated dispersion model of Equation [6]. The multifractal spectrum resulting from an accelerated dispersion model would be approximately equal to that for the binomial/*p* model except at the largest (and smallest) concentration values. Because these extreme values occur rarely in practical applications, it follows that the smallest (and largest) singularities that correspond to the extremes cannot be determined by means of the method of moments, which requires relatively large sample sizes. Local singularity analysis has the advantage that it operates on all values from within relatively small neighbourhoods in the immediate vicinity of the extreme values. Another approach resulting in thicker tails is provided by the 'universal multifractal model' initially developed during the late 1990s by Schertzer and Lovejoy (1991). These authors have successfully applied their model to the Pulacayo zinc deposit (Lovejoy and Schertzer, 2007). A basic tool in their approach is the 'first-order structure function', which can be regarded as a generalization of the semivariogram, because differences between spatially separated element concentration values are not only raised to the power 2 but to any positive real number.

Multifractal spatial correlation

Cheng (1994) (also see Cheng and Agterberg, 1996) derived general equations for the semivariogram, spatial covariance, and correlogram of any scale-independent multifractal including the model of de Wijs. Cheng's model is applicable to sequences of adjoining blocks along a line. Experimentally, the resulting semivariogram resembles Matheron's semivariogram for infinitesimally small blocks. In both approaches, extrapolation of the spatial covariance function to infinitesimally small blocks yields infinitely large variance when h approaches zero. The autocorrelation function along a line through a multifractal is:

$$\rho_k(\in) = \frac{C\varepsilon^{\tau(2)-2}}{2\sigma^2(\varepsilon)}\left[(k+1)^{\tau(2)+1} - 2k^{\tau(2)+1} + (k-1)^{\tau(2)+1}\right] - \frac{\xi^2}{\sigma^2(\varepsilon)} \quad [14]$$

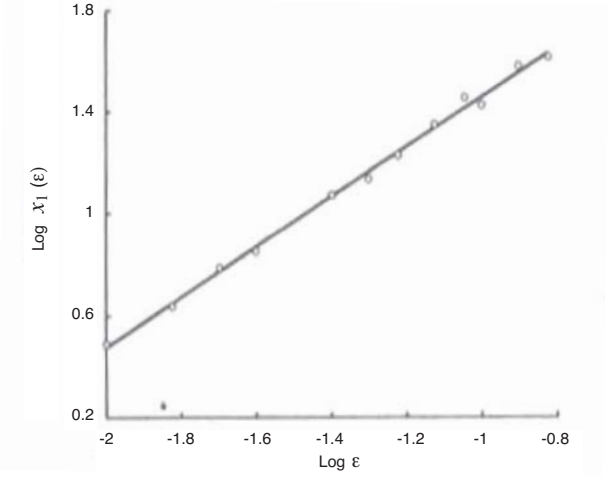

Figure 7—Log-log plot for relationship between $\chi_2(\in)$ and $\in$; logarithms base 10 (Cheng and Agterberg, 1994, Figure 3)

where C is a constant, $\in$ represents the length of line segment for which the measured zinc concentration value is assumed to be representative, $\tau(2)$ is the second-order mass exponent, ξ represents overall mean concentration value, and $\sigma^2(\in)$ is the variance of the zinc concentration values. The unit interval $\in$ is measured in the same direction as the lag distance h. The index k is an integer value that can be transformed into a measure of distance by setting $k = ½h$. Estimation for the 118 Pulacayo zinc values using an ordinary least-squares model after setting $\tau(2) = 0.979$ gave:

$$\hat{\rho}_k = 4.37\left[(k+1)^{1.979} - 2k^{1.979} + (k-1)^{1.979}\right] - 8.00 \quad [15]$$

The first 15 values ($k \geq 1$) resulting from this equation are nearly the same as the best-fitting semi-exponential (broken line in Figure 8). This semi-exponential function was used for the filtering in Figure 6. The heavy line in Figure 8 is based on the assumption of scale-independence over shorter distances ($h < 2$m). It represents a multifractal autocorrelation function.

This model can be used for extrapolation toward the origin by replacing the second-order difference on the right side of Equation [15] by the second derivative (*cf.* Agterberg, 2012a, Equation 9):

$$\left[(k+1)^{\tau(2)-1} - 2k^{\tau(2)-1} + (k-1)^{\tau(2)-1}\right] \cong \{\tau(2)+1\}\tau(2)k^{\tau(2)-1} \quad [16]$$

The theoretical autocovariance function shown as a solid line in Figure 8 was derived by application of this method to lag distances with 2 m > $h \geq 0.014$ m. It is approximately in accordance with Matheron's original semivariogram for the Pulacayo zinc assays. For integer values ($1 \leq k \leq 15$), the curve of Figure 7 (solid line) reproduces the estimated autocorrelation coefficients obtained by the original multifractal model using Equation [15]. This method cannot be used when the lag distance becomes very small ($h < 0.07$ in Figure 8), so that the white noise variance at the origin ($h = 0$) cannot be estimated by this method. However, as will be illustrated in the next section, white noise as estimated by local singularity mapping represents only about 2% of the total variability of the zinc values (Agterberg, 2012a). This

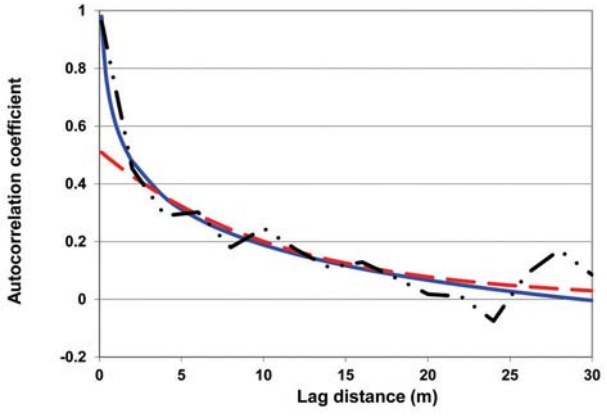

Figure 8—Estimated autocorrelation coefficients (connected by partly broken line) for 118 zinc concentration values of Figure 6. Broken line represents best-fitting semi-exponential function used to extract 'signal' in Figure 6. Solid line is based on multifractal model that assumes continuance of self-similarity over distances less than the sampling interval (Agterberg, 2012b, Figure 3)

white noise would represent measurement error and strong decorrelation at microscopic scale.

Singularity analysis

Cheng (1999, 2005) proposed a new model for incorporating spatial association and singularity in interpolation of exploratory data. In his approach, geochemical or other data collected at sampling points within a study area is subjected to two treatments. The first of these is the construction of a contour map by any of the methods, such as kriging or inverse distance weighting techniques, generally used for this purpose. Secondly, the same data is subjected to local singularity mapping. The local singularity α is then used to enhance the contour map by multiplication of the contour value by the factor $\in^{\alpha-2}$ where $\in < 1$ represents a length measure. In Cheng's (2005) approach to predictive mapping, the factor $\in^{\alpha-2}$ is greater than 2 in places where there has been local element enrichment, or by less than 2 where there has been local depletion. Local singularity mapping can be useful for the detection of geochemical anomalies characterized by local enrichment (*cf.* Cheng, 2007, Cheng and Agterberg, 2009).

According to Chen *et al.* (2007), local scaling behaviour follows the following power-law relationship:

$$\rho[B_x(\in)] = \frac{\mu[B_x(\in)]}{\in^E} = c(x)\cdot \in^{\alpha(x)-E} \qquad [17]$$

where $\rho\{B_x(\in)\}$ represents the element concentration value determined on a neighbourhood size measure B_x at point x, $\mu\{B_x(\in)\}$ represents the amount of metal, and E is the Euclidean dimension of the sampling space. For our 1-dimensional Pulacayo example, $E = 1$; and, for $\in = 1$, B_x extends $\in /2 = 1$ m in two directions from each of the 118 points along the line parallel to the mining drift. Suppose that average concentration values $\rho\{B_x(\in)\}$ are also obtained for $\in = 3$, 5, 7, and 9, by enlarging B_x on both sides. The yardsticks $\in$ can be normalized by dividing the average concentration values by their largest length (= 9). Reflection of the series of 118 points around its first and last points can be performed to acquire approximate average values of $\rho\{B_x(\in)\}$ at the first and last four points of the series. Provided that the model of Equation [17] is valid, a straight line fitted by least squares to the five values of ln $\mu\{B_x(\in)\}$ against $\alpha(x)\cdot$ln $\in$ then provides estimates of both ln $c(x)$ and $\alpha(x)$ at each point. Chen *et al.* (2007) proposed an iterative algorithm to obtain improved estimates. Their rationale for this was as follows.

In general, $\rho\{B_x(\varepsilon)\}$ is an average value of element concentration values for smaller B values at points near x with different local singularities. Consequently, use of Equation [17} would produce biased estimates of $c(x)$ and $\alpha(x)$. How could we obtain estimates of $c(x)$ that are non-singular in that they are not affected by the differences between local singularities within B_x? Chen *et al.* (2007) proposed to replace Equation. [17] by:

$$\rho(x) = c^*(x) \in^{\alpha^*(x)-E} \qquad [18]$$

where $\alpha^*(x)$ and $c^*(x)$ are the optimum singularity index and local element concentration coefficient, respectively. The initial crude estimate $c(x)$ obtained by Equation [17] at step $k = 1$ is refined repeatedly by using the iterative procedure:

$$c_{k-1}(x) = c_k(x) \in^{\alpha_k(x)-E} \qquad [19]$$

In their application to the 118 zinc values from the Pulacayo orebody, Chen *et al.* (2007) selected $\alpha^*(x) = \alpha_4(x)$ because at this point the rate of convergence has slowed considerably. Agterberg (2012a) duplicated their results and continued the algorithm until full convergence was reached at approximately $k = 1000$. A bias may arise due to the fact that, at each step of the iterative process, straight-line fitting is being applied to logarithmically transformed variables and results are converted back to the original data scale. This bias can be avoided by forcing the mean to remain equal to 15.61% Zn during all steps of the iterative process. After convergence, all c_k became approximately equal to the average zinc value (= 15.61%). For increasing value of k, c_k represents element concentration values of increasingly large volumes. On the other hand, the corresponding $\alpha_k(x)$ values are singularities for increasingly small volumes around the points x.

The end product of this application consisted of 118 singularities that are related to the original zinc values according to a logarithmic relationship (Figure 9). It can be assumed that every original zinc value (shown as a cross in Figure 6) is the sum of a true zinc concentration value and an uncorrelated random variable. The latter is a white noise component that would represent both measurement error and strictly local decorrelation because of granularity at the microscopic level. In Figure 9 it is represented by the deviations between the logarithmically transformed measured zinc concentration values and the final singularities obtained at the end of the iterative process. The white noise variance (2.08% of total variance of Zn values) is much smaller than the nugget effect previously used for filtering, which had 48.43% of the total variance.

Relations between variances for blocks of different sizes and shapes

The following argument is summarized from Agterberg (1984), where further discussions can be found. It is relevant because it is based on the assumption of permanence of shape of frequency distributions of measures on blocks of different sizes. Suppose that a rock or geological environment

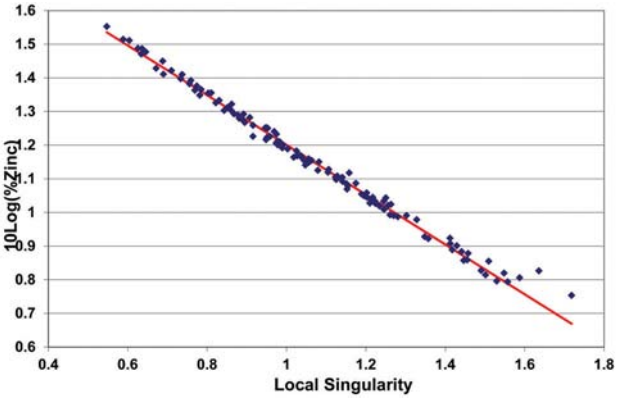

Figure 9—Relationship between final singularity and zinc concentration value is logarithmic. Plotted values (diamonds) are for $k = 1000$. Straight line was fitted by least squares (Agterberg, 2012a, Figure 21)

is sampled by randomly superimposing on it a large block with average value X_2, and that a small block with value X_1 is sampled at random from within the large block. Then the expected value of X_1 is X_2, or $E(X_1 \mid X_2) = X_2$. Let $f(x_1)$ and $f(x_2)$ represent the frequency density functions of the random variables X_1 and X_2, respectively. Suppose that X_1 can be transformed into Z_1 and X_2 into Z_2 so that the random variables Z_1 with marginal density function $f(z_1)$, and Z_2 with $f(z_2)$ satisfy a bivariate density function of the type

$$f(z_1, z_2) = f_1(z_1) \cdot f_2(z_2) [1 + \sum_{j=1}^{\infty} \rho^j Q_j(z_1) S_j(z_2) / h_{1j} h_{2j}] \quad [20]$$

In this equation, ρ represents the product-moment correlation coefficient of Z_1 and Z_2. $Q_j(z_1)$ and $S_j(z_2)$ are orthogonal polynomials with $f_1(z_1)$ and $f_2(z_2)$ as weighting functions, and with norms h_{1j} and h_{2j} respectively. Equation [20] implies

$$E[Q_j(Z_1) \mid Z_2] = \rho^j S_j(z_2) h_{1j} / h_{2j} \quad [21]$$

In most applications, $f(z_1, z_2)$ is symmetric with $f_1(z_i) = f_2(z_i)$ for $f = 1, 2$. For example, if $f_1(z_1)$ and $f_2(z_2)$ are standard normal, $Q_j(z_1) = Q_j(z_1)$ and $S_j(z_2) = H_j(z_2)$ are Hermite polynomials. Then Equation [20] is the Mehler identity, which is well known in mathematics.

When $f(x_1)$ is known, $f(x_2)$ can be derived from Equation [20] in combination with $E(X_1 \mid X_2) = X_2$. If $f(x_1)$, and $f(x_2)$ are of the same type, their frequency distribution is called 'permanent'. Six types of permanent frequency distributions are listed in Agterberg (1984). His Type 2 (logarithmic transformation) includes the lognormal and log-binomial distributions. Permanence of these two distributions was first established by Matheron (1974). It means that blocks of different sizes have the same type of frequency distribution; for example, all can be lognormal with the same mean but different logarithmic variances.

It is noted that $E(X_1 \mid X_2) = X_2$, which can be called the 'regression' of X_1 on X_2, results in the following two relations between block variances:

$$\sigma^2(X_1) = \sigma^2(X_1 - X_2) + \sigma^2(X_2); \sigma^2(X_2) = \rho_x^2 \sigma^2(X_1) \quad [22]$$

with $\rho_x > 0$ representing the product-moment correlation coefficient of X_1 and X_2. The first part of Equation [7] can be rewritten as $\sigma^2(v, V) = \sigma^2(v) + \sigma^2(V)$. Suppose that v is contained within a larger volume v' that, in turn, is contained within V. Then: $\sigma^2(v, V) = \sigma^2(v, v') + \sigma^2(v', V)$. Equations [20]–[22] are general in that they do not apply only to original element concentration, but also to transformed concentration values; for example, $E(\ln X_1 \mid \ln X_2) = \ln X_2$.

As mentioned before, Matheron (1962) showed that the semivariogram $\gamma(h)$ in his extension of the model of de Wijs satisfies $\gamma(h) = 3A \cdot \ln h$ where A is absolute dispersion. This result applies to element concentration values of infinitesimally small blocks at points that are distance h apart. Extending this to volumes v and V by integration yields $\sigma^2(\ln x) = A \cdot \ln V/v$. Suppose that $\sigma^2(v, V) = \sigma^2(v, v') + \sigma^2(v', V)$ applies to volumes v that differ in shape from the volumes v' and V, which have similar shapes. Then Matheron's extension of the model of de Wijs yields: $\sigma^2(v, v') = A \cdot \ln (v'/v) + C$ where C is a constant (*cf.* Matheron, 1962, Equation IV-57, p. 76). In the application to Witwatersrand gold values there is a distinct shape difference between the linear samples used for assaying and the larger plate-shaped volumes on which the average values were based. This shape difference probably accounts for a constant term included in the observed variances for samples plotted. This constant term (called the 'sampling error' by Krige, 1966a), which equals 0.10 units along the vertical scale in Figure 1) is independent of the size of the area.

Concluding remarks

In this paper, Krige's formula for the propagation of metal concentration variances in blocks with different volumes, as well as his demonstration of approximate scale independence of gold assays in the Klerksdorp goldfield, were viewed in the context of multifractal theory. The original model of de Wijs used by Krige and Matheron was the first example of a multiplicative cascade. Various new modifications of this model were discussed to explain inconsistencies that may arise in applications. It was shown that singularity analysis provides useful new information on element concentration variability over distances that are shorter than the sampling intervals used in practice. These new developments reinforce the practical usefulness of Krige's original ideas on self-similarity and scale-independence of patterns of block averages for gold and uranium values in the Witwatersrand goldfields. This paper was mainly a review of recent multifractal theory, which throws new light on the original findings by Professor Danie Krige on self-similarity of gold and uranium patterns at different scales for blocks of ore by (a) generalizing the original model of de Wijs; (b) using the accelerated dispersion model to explain the appearance of a third parameter in the lognormal distribution of Witwatersrand gold determinations; and (c) considering that Krige's sampling error is caused by geometrical differences between single ore sections and reef areas.

Acknowledgement

Thanks are due to Dr Zhijun Cheng and two anonymous reviewers for helpful comments that improved the paper.

References

Agterberg, F.P. 1961. The skew frequency curve of some ore minerals. *Geologie en Mijnbouw*, vol. 40. pp.149–162.

Agterberg, F.P. 1963. Value contours and improved regression techniques for ore reserve calculation. *Journal of the South African Institute of Mining and Metallurgy*, vol. 64. pp. 108–117.

Agterberg, F.P. 1966. Two-dimensional weighted moving average trend surfaces for ore evaluation. *Proceedings of the Symposium on Mathematical Statistics and Computer Applications in Ore Valuation*, 7–8 March 1966. South African Institute of Mining and Metallurgy, Johannesburg. pp. 39–45.

Agterberg, F.P. 1974. Geomathematics. Elsevier, Amsterdam.

Agterberg, F.P. 1984. Use of spatial analysis in mineral resource estimation. *Mathematical Geology*, vol. 16, no. 6. pp. 144–158.

Agterberg, F.P. 1995. Multifractal modeling of the sizes and grades of giant and supergiant deposits. *International Geological Reviews*, vol. 37. pp. 1–8.

Agterberg, F.P. 2001. Multifractal simulation of geochemical map patterns. *Geologic Modeling and Simulation: Sedimentary Systems*. Merriam, D.F. and Davis, J.C. (eds.). Kluwer, New York. pp. 327–346.

Agterberg, F.P. 2007a. New applications of the model of de Wijs in regional geochemistry. *Mathematical Geology*, vol. 39, no. 1. pp. 1–26.

AGTERBERG, F.P. 2007b. Mixtures of multiplicative cascade models in geochemistry. *Nonlinear Processes in Geophysics*, vol. 14. pp. 201–209.

AGTERBERG, F.P. 2012a. Sampling and analysis of element concentration distribution in rock units and orebodies. *Nonlinear Processes in Geophysics*, vol. 19. pp. 23–44.

AGTERBERG, F.P. 2012b. Multifractals and geostatistics. *Journal of Geochemical Exploration*, vol. 122. pp. 113–122.

BRINCK, J.W. 1971. MIMIC, the prediction of mineral resources and long-term price trends in the non-ferrous metal mining industry is no longer Utopian. *Eurospectra,* vol. 10. pp. 46–56.

BRINCK, J.W. 1974. The geochemical distribution of uranium as a primary criterion for the formation of ore deposits. *Chemical and Physical Mechanisms in the Formation of Uranium Mineralization, Geochronology, Isotope Geology, and Mineralization*. IAEA Proceedings Series STI/PUB/374. pp. 21-32.

CHEN, Z., CHENG, Q., CHEN, J., and XIE, S. 2007. A novel iterative approach for mapping local singularities from geochemical data. *Nonlinear Processes in Geophysics*, vol. 14. pp. 317–324.

CHENG, Q. 1994. Multifractal modeling and spatial analysis with GIS: gold mineral potential estimation in the Mitchell-Sulphurets area, northwestern British Columbia. Doctoral dissertation, University of Ottawa.

CHENG, Q. 1999. Multifractality and spatial statistics. *Computers and Geosciences*, vol. 25. pp. 949–961.

CHENG, Q. 2005. A new model for incorporating spatial association and singularity in interpolation of exploratory data. *Geostatistics Banff 2004*. Leuangthong, D. and Deutsch, C.V. (eds.). Springer, Dordrecht, The Netherlands. pp. 1017–1025.

CHENG, Q. 2007. Mapping singularities with stream sediment geochemical data for prediction of undiscovered mineral deposits in Gejiu, Yunnan Province, China. *Ore Geology Reviews*, vol. 32. pp. 314–324.

CHENG, Q. 2008. Non-linear theory and power-law models for information integration and mineral resources quantitative assessments. *Progress in Geomathematics*. Bonham-Carter, G. and Cheng, Q. (eds.). Springer, Heidelberg. pp. 195–225.

CHENG, Q. 2012. Multiplicative cascade processes and information integration for predictive mapping. *Nonlinear Processes in Geophysics*, vol. 19. pp. 1–12.

CHENG, Q. and AGTERBERG, F.P. 1996. Multifractal modelling and spatial statistics. *Mathematical Geology*, vol. 28, no. 1. pp.1–16.

CHENG, Q. and AGTERBERG, F.P. 2009. Singularity analysis of ore-mineral and toxic trace elements in stream sediments. *Computers and Geosciences*, vol. 35. pp. 234–244.

CRESSIE, N.A.C. 1991. Statistics for Spatial Data. Wiley, New York.

DE WIJS, H.J. 1948. Statistische methods toegepast op de schatting van ertsreserven. *Jaarboek der Mijnbouwkundige Vereniging te Delft*, 1947-1948. pp. 53–80.

DE WIJS, H.J. 1951. Statistics of ore distribution. *Geologie en Mijnbouw*, vol. 30. pp. 365–375.

EVERTSZ, C.J.G. and MANDELBROT, B.B. 1992. Multifractal measures. Chaos and Fractals. Peitgen, H.-O., Jurgens, H., and Saupe, D. (eds.). Springer-Verlag, New York.

FALCONER, K. 2003. *Fractal Geometry*. 2nd edn. Wiley, Chichester.

FEDER, J. 1988. Fractals. Plenum, New York.

HARRIS, D.P. 1984. *Mineral Resources Appraisal*. Clarendon Press, Oxford.

JOURNEL, A.G. and HUIJBREGTS, C.J. 1978. *Mining Geostatistics*. Academic Press, New York.

JOWETT, G.H. 1955. Least-squares regression analysis for trend reduced time series. *Journal of the Royal Statistical Society*, Series B, vol. 17. pp. 91–104.

KAPTEYN, J.C. 1903. Skew Frequency Curves in Biology and Statistics. Noordhoff, Groningen.

Kolmogorov, A.N. 1941. On the logarithmic normal distribution law for the sizes of splitting particles. *Doklady Akademia Nauk SSSR*, vol. 31. pp. 99–100.

KORVIN, G. 1992. Fractal Models in the Earth Sciences. Elsevier, Amsterdam.

KRIGE, D.G. 1951a. A statistical approach to some mine valuation and allied problems on the Wtwatersrand. MSc thesis, University of the Witwatersrand, Johannesburg.

KRIGE, D.G. 1951b. A statistical approach to some basic valuation problems on the Witwatersrand. *Journal of the South African Institute of Mining and Metallurgy*, vol. 52. pp. 119–139.

KRIGE, D.G. 1955. Emploi statistique mathématique dans les problèmes poses par l'évaluation des gisements. *Annales des Mines*, Décembre.

KRIGE, D.G. 1960. On the departure of ore value distributions from the lognormal model in South African gold mines. *Journal of the South African Institute of Mining and Metallurgy*, vol. 61. pp. 231–244.

KRIGE, D.G. 1966a. A study of gold and uranium distribution pattern in the Klerksdorp goldfield. *Geoexploration*, vol. 4. pp. 43–53.

KRIGE, D.G. 1966b. Two-dimensional weighted moving average trend surfaces for ore valuation. *Proceedings of the Symposium on Mathematical Statistics and Computer Applications in Ore Valuation*, 7–8 March, 1966. South African Institute of Mining and Metallurgy, Johannesburg. pp. 13–38.

KRIGE, D.G. 1978. Lognormal-de Wijsian Geostatistics for Ore Evaluation. Monograph Series, vol.1. South African Institute of Mining and Metallurgy, Johannesburg.

KRIGE, D.G. and UECKERMANN, H.J. 1963. Value contours and improved regression techniques for ore reserve valuations. *Journal of the South African Institute of Mining and Metallurgy*, vol. 63. pp. 429–452.

LOVEJOY, S. and SCHERTZER, D. 1991. Multifractal analysis techniques and the rain and cloud fields from 10–3 to 106 m. Non-linear Variability in Geophysics. Schertzer, D. and Lovejoy, S. (eds.). Kluwer, Dordrecht. pp. 111–144.

LOVEJOY, S. and SCHERTZER, D. 2007. Scaling and multifractal fields in the solid earth and topography. *Nonlinear Processes in Geophysics*, vol. 14. pp. 465–502.

LOVEJOY, S., AGTERBERG, F., CARSTEANU, A., CHENG, Q., DAVIDSEN, J., GAONAC'H, H., GUPTA, V., L'HEUREUX, I., LIU, W., MORRIS, S.W., SHARMA, S., SHCHERBAKOV, R., TARQUIS, A., TURCOTTE, D., and URITSKY, V. 2010. Nonlinear geophysics: why we need it. *EOS*, vol. 90, no. 48. pp. 455–456.

MANDELBROT, B.B. 1975. Les Objects Fractals: Forme, Hazard et Dimension. Flammarion, Paris.

MANDELBROT, B.B. 1983. The Fractal Geometry of Nature. Freeman, San Francisco.

MANDELBROT, B.B. 1989. Multifractal measures, especially for the geophysicist. *Pure and Applied Geophysics*, vol. 131. pp. 5–42.

MATHERON, G. 1955. Application des methods statistiques à l'évaluation des gisements. *Annales des Mines*, Décembre.

MATHERON, G. 1962. Traité de géostatistique appliquée. Mémoires de BRGM, 14. Paris.

MATHERON, G. 1967. Kriging or polynomial interpolation procedures? *Transactions of the Canadian Institute of Mining and Metallurgy*, vol. 70. pp. 240–242.

MATHERON, G. 1974. Les fonctions de transfert des petits panneaux. Note Géostatistique 127. Centre de Morphologie Mathématique, Fontainebleau, France.

MATHERON, G. 1989. Estimating and choosing, an essay on probability in practice. Hasover, A.M. (trans.). Springer, Heidelberg.

SCHERTZER, D. AND LOVEJOY, S. 1987. Physical modeling and analysis of rain and clouds by anisotropic scaling of multiplicative processes. *Journal of Geophysical Research*, vol. 92. pp. 9693–9714.

SCHERTZER, D. and LOVEJOY, S. (eds.). 1991. Non-linear Variability in Geophysics. Kluwer, Dordrecht.

SCHERTZER, D., LOVEJOY, S., SCHMITT, F., CHIGIRINSKAYA, Y. and MARSAN, D. 1997. Multifractal cascade dynamics and turbulent intermittency. *Fractals*, vol. 5. pp. 427–471.

SERRA, J. 2014 Revisiting 'Estimating and Choosing'. *Mathematics of Planet Earth*. Pardo-Igúzquiza, E., Guardiola-Albert, C., Heredia, J., Moreno-Merino, L., Durán, J.J., and Vargas-Guzmán, J.A. (ed.). Springer, Heidelberg. pp. 57–60.

SICHEL, H.S. 1952. New methods in the statistical evaluation of mine sampling data. *Journal of the South African Institute of Mining and Metallurgy*, vol. 61. pp. 261–288.

SICHEL, H.S. 1961. On the departure of ore value distributions from the lognormal model in South African gold mines. *Journal of the South African Institute of Mining and Metallurgy*, vol. 62. pp. 333–338.

STANLEY, H. and MEAKIN, P. 1988. Multifractal phenomena in physics and chemistry. *Nature*, vol. 335. pp. 405–409.

VENEZIANO, D. and LANGOUSIS, A. 2005. The maximum of multifractal cascades: exact distribution and approximations. *Fractals*, vol. 13, no. 4. pp. 311–324.

VENING MEINESZ, F.A. 1964. The Earth's Crust and Mantle. Elsevier, Amsterdam.

YAGLOM, A.M. 1962. An Introduction to the Theory of Stationary Random Functions. Prentice-Hall, Englewood Cliffs, NJ. ◆

SUSTAINABLE USE OF EARTH'S NATURAL RESOURCES

Outotec provides leading technologies and services for the sustainable use of Earth's natural resources. As the global leader in minerals and metals processing technology, we have developed many breakthrough technologies over the decades for our customers in metals and mining industry. We also provide innovative solutions for industrial water treatment, the utilization of alternative energy sources and the chemical industry.
www.outotec.com

For the whole story, please visit our YouTube channel.

Sustainable use of Earth's natural resources

Outotec

http://dx.doi.org/10.17159/2411-9717/2015/v115n1a2

Improving processing by adaption to conditional geostatistical simulation of block compositions

by R. Tolosana-Delgado*, U. Mueller†, K.G. van den Boogaart*‡, C. Ward**, and J. Gutzmer*‡

Synopsis

Exploitation of an ore deposit can be optimized by adapting the beneficiation processes to the properties of individual ore blocks. This can involve switching in and out certain treatment steps, or setting their controlling parameters. Optimizing this set of decisions requires the full conditional distribution of all relevant physical parameters and chemical attributes of the feed, including concentration of value elements and abundance of penalty elements. As a first step towards adaptive processing, the mapping of adaptive decisions is explored based on the composition, in value and penalty elements, of the selective mining units.

Conditional distributions at block support are derived from cokriging and geostatistical simulation of log-ratios. A one-to-one log-ratio transformation is applied to the data, followed by modelling via classical multivariate geostatistical tools, and subsequent back-transforming of predictions and simulations. Back-transformed point-support simulations can then be averaged to obtain block averages that are fed into the process chain model.

The approach is illustrated with a 'toy' example where a four-component system (a value element, two penalty elements, and some liberable material) is beneficiated through a chain of technical processes. The results show that a gain function based on full distributions outperforms the more traditional approach of using unbiased estimates.

Keywords

adaptive processing, change of suppport, compositions, geometallurgy, stochastic optimization.

Introduction

One of the key usages of geostatistics has long been the prediction of the spatial structure of orebodies. This is used for the evaluation of resources and/or reserves and for further planning of the mining and beneficiation process schedule. For most applications, and until quite recently, metal grade has been regarded as the central property of study and the main objective has been to distinguish between ore and waste. However, recently other properties have come into focus through better analytical methods, such as automated mineralogy (see *e.g.* Fandrich *et al.* 2007), and new geostatistical methods considering more complex information, such as kriging of compositions (Pawlowsky-Glahn and Olea, 2004). Two ores with the same chemical composition can have totally different mineralogies and microfabrics, which will result in different recoveries, energy requirements, or reagent consumptions, thus yielding very different mass streams. An ore is thus no longer understood as represented by a single value element, but through a complex microfabric (Hagni, 2008). This perspective allows quantitative insight into relevant properties of different ore and gangue minerals (Sutherland and Gottlieb, 1991), potentially containing poison elements or phases (*e.g.* Houot, 1983) that modify the efficiency of downstream processing steps or require additional treatment.

Accordingly, processing choices have become more complex. Grade-based studies allow a mere 'beneficiate-or-dump' decision. With the advent of these analytical and methodological advances, it is possible to better adapt processing to the ore mined due to a more profound understanding of the processing required. For instance, good knowledge of microfabric properties can reduce energy consumption, if overgrinding is avoided, which also results in improved recovery by avoiding losses due to poor liberation (Wills and Napier-Munn, 2006). Similarly, accurate information on mineral composition may permit the specification of a cut-off in any separation technique (magnetic, electrostatic, or density-based), optimally weighting recovery and further processing costs. Or depending on the proportion of fines generated during milling, desliming might or might not be necessary. Finally, different concentrations of chemicals might be needed for an optimal flotation process as a function of the composition of the concentrate. These

* *Helmholtz Zentrum Dresden-Rossendorf, Helmholtz Institute Freiberg for Resource Technology, Germany.*

† *Edith Cowan University, Perth, Australia.*

† *Technical University Bergakademie Freiberg, Germany.*

** *Cliffs NR, Perth, Australia.*

are simple examples of the possible adaptive choices that could be implemented in several steps of the process chain, if the necessary ore feed properties were known. Actually, the complexity of the interactions between the several processes is such that the best processing stream might not be an intuitive one, requiring the solution of large combinatorial problems. Such considerations will become a requirement in the near future, due to the lower margins imposed by a globalized economy.

In most current mining operations, ore is blended to a homogeneous quality based on geostatistical prediction, to ensure optimal performance of a beneficiation route that has been empirically optimized, but that remains mostly constant throughout the mine life. Geometallurgy (Jackson *et al.*, 2011) aims to produce higher overall gains by adapting the processing to the predicted ore quality of the block currently being processed.

The aim of this paper is to demonstrate the use of geostatistics in such a complex processing situation, with particular regard to the following key issues.

- The relevant microfabric information is not captured by a single real number, but typically involves nonlinear and multivariate scales. This is illustrated by analysing compositional data, where a direct application of standard geostatistics can lead to artefacts, including negative concentrations and dependence of predictions on irrelevant components. For example, a non-compositional cokriging of a mineral composition applied to a system that includes both value and waste minerals cannot be transformed in a simple way into an optimal unbiased prediction of the subcomposition of value minerals only (Tolosana-Delgado, 2006), so that waste components separated in the first processing steps have a lasting influence all along the processing chain. These problems are analogous to the well-known order relation problems of indicator kriging (Deutsch and Journel, 1992; Carle and Fogg, 1996)
- The prediction is used for a nonlinear decision problem, involving geological uncertainty and a processing model. In this context, a decision based on unbiased estimates of the relevant properties is no longer optimal.

To illustrate how geostatistics must be applied in such a situation, an example from a mined-out iron ore orebody is used. Since no systematic adaptive processing has been applied during the exploitation of the mine, a 'toy' example will be used to illustrate possible classes of processing choices and their effect in the geostatistical treatment. A simple processing decision set is presented here, to keep the discussion focused on the methodological geostatistical aspects. Readers should be aware that realistic decision sets will be much more complex.

Interpolation of geometallurgical data

Kinds of geometallurgical data

Several kinds of data may be collected to characterize the materials to be mined and beneficiated. Each of these kinds of data has its own scale, that is, a way to compare different values. Typical geometallurgical scales are the following:

- *Positive quantities*, such as the volume of an individual crystal or particle, or its density, its hardness, or the area or major length of a given section
- *Distributions*, which describe the relative frequency of any possible value of a certain property in the material. The most common property is size: grain size or particle size distributions, either of the bulk material or of certain phases are the typical cases
- *Compositional data*, formed by a set of variables that describe the importance or abundance of some parts forming a total. These variables can be identified because their sum is bounded by a constant, or by their dimensionless relative units (proportions, ppm, percentage, *etc.*). Typical compositions include geochemistry, mineral composition, chemical compositions of certain phases, and elemental deportment in several phases. If the composition of many particles/crystals of a body is available, one can also obtain its *compositional distribution*. A systematic account of compositions can be found in Aitchison (1986) and van den Boogaart and Tolosana-Delgado (2013).
- *Texture data*, representing crystallographic orientations and their distributions, for instance the concentration (*i.e.* inverse of spread) of the major axis orientation distribution of a schist
- More *complex data structures* can be generated by mixing the preceding types, for example a mean chemical composition can be characterized for each grain-size fraction, or a preferred orientation can be derived from each mineral type.

All these scales require a specific geostatistical treatment. For instance, classical cokriging of a composition seen as a real vector leads to singular covariance matrices (Pawlowsky-Glahn and Olea, 2004), and even if corrected for this problem, predictions can easily have negative components in minerals with highly variable overall abundances. Putting such predictions into processing models is not sensible. Therefore, *ad-hoc* geostatistical methods honouring the special properties of each of these scales have been developed. Geostatistics for positive data (Dowd, 1982; Rivoirard, 1990) is well established. Textural data-sets have been studied by van den Boogaart and Schaeben (2002), while one-dimensional distributional data-sets were treated by Delicado *et al.* (2008) and Menafoglio *et al.* (2014). Compositional data geostatistics was studied in depth by Pawlowsky-Glahn and Olea (2004) and Tolosana-Delgado (2006), and is applied here.

Some of these kinds of data are not additive, in the sense that the average property of a mining block is not the integral over the property within the block. For instance, the arithmetic mean of mass composition within a block is not the average composition of a block if the density varies within the block, or when some components are not considered, a problem known as *subcompositional incoherence* (Aitchison, 1986). The lack of additivity is particularly important for spatial predictions of the properties of mining blocks or selective mining units (SMUs). The proposed method will require only that the property – or more precisely its effect through processing – is computable from a simulation of a random function describing the variation of the property within the block.

An additional difficulty to be considered in a general framework of geometallurgical optimization is stereological degradation. Many kinds of data available are measured from 2D sections by automated mineralogy systems (Mineral Liberation Analyser (MLA), QUEMSCAN, EBSD, EMP, *etc.)*, while the relevant target properties are actually their 3D counterparts. Some of these 2D data types are nevertheless unbiased estimates of their 3D properties. Modal mineralogy will belong to this category if it is computed from proportions of grain area of each mineral type with respect to the total area translated into volume ratios of that mineral with respect to the total volume. For many other properties, one should consider the possible 3D to 2D stereological degradation effects, in addition to all other considerations presented in this work.

To avoid introducing the extra complexity derived from stereological reconstruction, this paper focuses on the use of compositional information for geometallurgical characterization, that is, modal mineralogy and chemical composition. Due to the lack of a reference deposit with mineralogical data at a sufficiently fine spatial resolution, the mineralogy was reconstructed from the chemical data. However, in future projects where adaptive processing is planned, it is likely that automated mineralogy will be routinely applied and direct measurements of mineralogy are expected to be the rule, not the exception.

Compositional data

Compositional data consists of vectors $\mathbf{x} = [x_1, x_2, \ldots, x_D]$ of positive components that describe the relative importance of D parts forming a total. Compositions are characterized by the fact that their total sum is either an artefact of the sampling procedure, or it can be considered irrelevant. Because of this irrelevance, it is legitimate to apply the closure operation

$$\mathrm{C}[\mathbf{x}] = \frac{100\%}{\sum_{i=1}^{D} x_i}\mathbf{x} \qquad [1]$$

to allow for comparison between compositions.

The most typical compositions in geometallurgy are chemical composition and mineral composition. These compositions can be defined on the same body, and one might require transforming one into the other. If the chemical and mineralogical compositions of a block are assumed to be represented by $\mathbf{x}^c$ and $\mathbf{x}^m$, having D^c and D^m components respectively, and each of the minerals is assumed to have a known stoichiometry in the chemical components considered, then the stoichiometry can be realized as a matrix transformation. If the stoichiometry is placed in the columns of a $D^c \times D^m$ matrix $\mathbf{T}$, then $\mathbf{T}$ maps any mineralogical composition to a chemical composition:

$$\mathbf{x}^c = \mathbf{T} \cdot \mathbf{x}^m \qquad [2]$$

Inverting this equation is called *unmixing*, and is a part of the broader class of end-member problems (Weltje, 1997). The relation in Equation [2] can be inverted only in the case when $D^c = D^c$ and no chemically possible reactions exist within the system of minerals under consideration (*i.e.*, $\mathbf{T}$ is a square matrix and its columns are linearly independent vectors). For $D^c > D^m$, Equation [2] may not have an exact solution, and one must resort to a least-squares estimate, $\hat{\mathbf{x}}^m = (\mathbf{T}^t \cdot \mathbf{T})^{-1}\, \mathbf{T}^t \cdot \mathbf{x}^c$, to find the $\hat{\mathbf{x}}^m$ that best approximates $\mathbf{x}^m$. When $D^c < D^m$, the system will have infinitely many solutions and not all of these will be mineralogically meaningful. Note that these cases do not ensure that the recast composition has positive components. Tolosana-Delgado *et al.* (2011b) present an algorithm for estimating mineral compositions compatible with observed chemical compositions in all three cases, an algorithm that can also account for varying mineral stoichiometry and ensures that results are positive. For the purpose of this paper, we consider the same number of chemical components as end-members, related through the transfer matrices specified in the section 'Geochemical data and mineral calculations'. Note that in the case $D^c = D^m$, results can be strongly dependent on the stoichiometry assumed, in which case it could become safer to further treat the geochemical information. On the other hand, the advent of automated mineralogy systems may soon render these calculations unnecessary.

The end-member formalism applies a multivariate analysis framework prone to some fundamental problems of compositions, such as the so-called spurious correlation (Chayes, 1960) induced by the closure operation (Equation [1]). Aitchison (1982, 1986) analysed this difficulty systematically and proposed a strategy for the statistical treatment of compositional data-sets based on log-ratio transformations. The idea is transform the available compositions to log-ratios, for instance through the additive log-ratio transformation (alr):

$$\boldsymbol{\xi} = \mathrm{alr}[\mathbf{x}] = \left[\ln\left(\frac{x_1}{x_D}\right), \ln\left(\frac{x_2}{x_D}\right), \ldots, \ln\left(\frac{x_{D-1}}{x_D}\right)\right] \qquad [3]$$

and apply any desired method to the transformed scores Those results that admit an interpretation as a composition (for instance, predicted scores) can be back-transformed with the additive generalized logistic function (agl). The agl is applied to a vector of $D - 1$ scores, $\xi = [\xi_1, \xi_2, \ldots, \xi_{D-1}]$, and delivers a D-part composition:

$$\mathrm{agl}[\boldsymbol{\xi}] = \mathrm{C}\left[\left[\exp(\xi_1), \exp(\xi_2), \ldots, \exp(\xi_{D-1}), 1\right]\right] \qquad [4]$$

where the closure operation C from Equation [1] is used. This strategy has the advantage of capturing the information about the relative abundance (*i.e.* abundance of one component with respect to another, their ratio) in a natural way (Aitchison, 1997, van den Boogaart and Tolosana-Delgado, 2013). Another advantage of working on the alr-transformed scores is that, without any need of further constraints, all results represent valid compositions. This was not the case with Weltje's (1997) end-member algorithms, where the final results might present negative components. On the side of the disadvantages, the log-ratio methodology cannot deal directly with components of zero or below the detection limit, and some missing data techniques must be applied, prior to or within the end-member unmixing or (geo) statistical treatment (Tjelmeland and Lund, 2003; Hron *et al.*, 2010; Martín-Fernández *et al.*, 2012). It is often proposed to impute the zeroes by some reasonable values, often a constant fraction of the detection limit. However, for geomet-

allurgical optimization purposes, this imputation by a constant value should be avoided, because it leads to reduced uncertainty scenarios; multiple imputation offers a much better framework accounting for that extra uncertainty (Tjelmeland and Lund, 2003).

Using the log-ratio approach it is possible to define a multivariate normal distribution for compositions (Aitchison, 1986; Mateu-Figueras *et al.*, 2003), with density

$$f_{\mathbf{X}}(\mathbf{x}) = ((2\pi)^{D-1}|\boldsymbol{\Sigma}|)^{-\frac{1}{2}} \times \exp\left(-\frac{1}{2}(\mathrm{alr}(\mathbf{x}) - \boldsymbol{\mu})^t \cdot \boldsymbol{\Sigma}^{-1} \cdot (\mathrm{alr}(\mathbf{x}) - \boldsymbol{\mu})\right) \quad [5]$$

where $\boldsymbol{\mu}$ and $\sum$ are the mean vector and covariance matrix of the alr-transformed random composition $\mathbf{X}$ (uppercase indicates the random vector, and lowercase a particular realization). Given a compositional sample $\{\mathbf{x}_1, \mathbf{x}_2,\ldots,\mathbf{x}_N\}$, unbiased estimates of these parameters are provided by the classical formulae applied to the log-ratio transformed scores:

$$\hat{\boldsymbol{\mu}} = \frac{1}{N}\sum_{n=1}^{N} \mathrm{alr}(\mathbf{x}_n) \quad [6]$$

and

$$\hat{\boldsymbol{\Sigma}} = \frac{1}{N-1}\sum_{n=1}^{N} (\mathrm{alr}(\mathbf{x}_n) - \hat{\boldsymbol{\mu}}) \cdot (\mathrm{alr}(\mathbf{x}_n) - \hat{\boldsymbol{\mu}})^t$$

The mean vector estimate can be back-transformed to the *compositional centre*, $\mathrm{cen}[\mathbf{X}]=\mathrm{agl}(\hat{\boldsymbol{\mu}})$, which is an intrinsic property of $\mathbf{X}$, not depending on the alr transformation used to calculate it (taking a different denominator would produce the same compositional centre).

Regionalized compositions

Following the principle of working on alr-transformed scores, the classical multivariate geostatistical framework can be applied to compositions (Pawlowsky-Glahn and Olea, 2004; Tolosana-Delgado, 2006; Boezio *et al.*, 2011, 2012; Ward and Mueller, 2012; Rossi and Deutsch, 2014). In this section the relevant notation is introduced and several particularities are clarified that arise from the nature of compositional data. Assume that an isotopic compositional sample is available $\{\mathbf{x}(s_1), \mathbf{x}(s_2),\ldots, \mathbf{x}(s_N)\}$ at each of a set of locations $\{s_1, s_2,\ldots, s_N\}$ within a domain E, and for each location s_α denote by $\xi(s_\alpha) = \mathrm{alr}(\mathbf{x}(s_\alpha))$ the corresponding alr-transformed composition. Then as with the covariance in Equation [6], experimental matrix-valued alr-variograms can be estimated by conventional routines as semivariances of increments of log-ratio-transformed data.

A linear model of coregionalization $\boldsymbol{\Gamma}(h)$ (Journel and Huijbregts, 1978; Wackernagel, 2003) is fitted to the experimental alr variogram, expressed as

$$\boldsymbol{\Gamma}(h) = \sum_{k=1}^{K} \mathbf{B}_k\, g_k(h) \quad [7]$$

where K denotes the number of structures. For each structure k, $1 \le k \le K$, the function g_k is an allowable semivariogram model function and the matrix $\mathbf{B}_k$ is its associated positive semi-definite covariance matrix. Alternative ways exist for estimating the LMC and ensuring its validity without using any specific alr transformation (Tolosana-Delgado *et al.*, 2011a; Tolosana-Delgado and van den Boogaart, 2013). As usual, a covariance model $\mathbf{C}$ can be linked to the variogram through $\mathbf{C}(h) = \mathbf{C}(0) - \boldsymbol{\Gamma}(h)$ (Cressie, 1993), assuming second-order stationarity of the log-ratios.

Once a valid LMC for the alr variables is available, kriging estimates can be computed. As in the case of classical multivariate geostatistics, estimates of the alr variables can be made at unsampled locations using the covariance structure defined in Equation [7]. For example, the local neighbourhood simple cokriging estimate $\xi^*_{\mathbf{SK}}(s_0)$ at location s_0 is given by

$$\boldsymbol{\xi}^*_{\mathbf{SK}}(s_0) = \hat{\boldsymbol{\mu}} + \sum_{\alpha=1}^{n(s_0)} \boldsymbol{W}_\alpha(s_0)\,(\boldsymbol{\xi}(s_\alpha) - \hat{\boldsymbol{\mu}}) \quad [8]$$

where $\hat{\boldsymbol{\mu}}$ is the mean of the alr-transformed data, $\mathbf{W}_\alpha(s_0)$ is the matrix of weights derived from the simple cokriging system (*e.g.*, Myers, 1982), and $n(s_0)$ is the number of data locations forming the local neighbourhood relevant to predicting $\mathbf{x}(s_0)$. The kriging estimates $\xi^*(s_\alpha)$ need to be back-transformed to a composition. A simple approach for doing so is to use the agl transformation, which provides a slightly biased back-transform of the results; an alternative method is to apply Gauss-Hermite quadrature to compute an estimate of the expected value of the composition, assuming that it has a normal distribution (Equation [5]) specified by the cokriging predictor and its cokriging variance. In estimation procedures, that option would be preferable, and the interested reader is referred to Pawlowsky-Glahn and Olea (2004) or Ward and Mueller (2012) for details. However, simulation is more relevant for the goals of this paper, as it allows at the same time an upscaling of the output to block estimates.

In what follows it is assumed that the compositional data does not show gross departures from joint additive logistic normality (Equation [5]). In practice, this happens to be more restrictive than one would think, and a transformation to normal scores is required prior to simulation. The current accepted geostatistical workflow includes applying a normal-score transform to each variable separately (in this case, to each alr-transformed score). Although this guarantees only marginal normality and not joint normality, until recently there were no practical alternative methods that deliver a multivariate jointly normal data-set. Stepwise conditional transformation (Leuangthong and Deutsch, 2003) is not practical for high-dimensional data-sets, and the projection pursuit multivariate transform (Barnett *et al.*, 2014), a recent approach that promises to remedy this shortfall, could not be implemented here as it appeared only during the review process.

For simulation, the turning bands algorithm (Matheron, 1973; Emery, 2008; Lantuéjoul, 2002) is particularly efficient in a multivariate setting as it can be realized as a set of univariate unconditional simulations based on the LMC fitted to the alr or normal-score transformed data and only a single cokriging step is required.

Assuming that the LMC for the data is given by Equation [7], each structure is simulated separately making use of the spectral decomposition of the corresponding coefficient matrix $\mathbf{B}_k = \mathbf{A}_k\mathbf{A}_k^t$ of the LMC. A Gaussian random field can be simulated by putting

$$\mathbf{Y}(s) = \sum_{k=1}^{K} \mathbf{A}_k \mathbf{U}_k(s) \quad [9]$$

where $\mathbf{U}_k$ is a vector random field with D–1 independent components for each k, $1 \le k \le K$. Because of the independence of the components, the simulation of the random field $\mathbf{Y}$ reduces to the simulation of K univariate Gaussian random fields, $\mathbf{U}_k$, $1 \le k \le K$. These are simulated separately using the turning bands algorithm and then re-correlated via Equation [9]. This produces at each location s and at each data location a simulated vector $\mathbf{y}(s)$ with the specified spatial correlation structure. Then, simple cokriging (Equation [8]) of the residuals $\boldsymbol{\varepsilon}(s_n) = \mathbf{y}(s_n) - \boldsymbol{\xi}(s_n)$ at the sample locations s_n, $1 \le n \le N$, is used to condition the realizations through $\boldsymbol{\xi}(s_0) = \mathbf{y}(s_0) + \boldsymbol{\varepsilon}^*(s_0)$ for each location s_0 of the simulation grid. Finally, an agl (and/or a Gaussian anamorphosis) transformation is applied to back-transform the conditioned vectors to compositional space, $\mathbf{x}(s_0) = \text{agl}(\boldsymbol{\xi}(s_0))$.

Monte Carlo approximation to compositional block cokriging

A common problem of geostatistics applied to any extensive variable with a non-additive scale is the lack of a universal model of change of support – that is, a way to infer the properties of a large block from much smaller samples. For positive data, for instance, Dowd (1982) and Rivoirard (1990) offer methods for estimating the average grade value within a block, mostly assuming a certain preservation of lognormality between the samples and the blocks. For the other geometallurgical scales, geostatistical simulation offers a general computationally-intensive solution, albeit not an impossible one with modern computers and parallel code. This is illustrated here again for a compositional random function.

Assuming that the random function $\mathbf{X}(s)$ can be defined at any differential block du, its average within a block v centred at the position s is

$$\mathbf{X}_v(s) = \frac{1}{|v|}\int_v \mathbf{X}(u)du = \frac{1}{|v|}\int_v \text{agl}\big(\Xi(u)\big)du$$

with $|v|$ denoting the block volume, and $\Xi(s) = \text{alr}(\mathbf{X}(s))$ the alr-transformed random function. Block cokriging would deliver an estimate of $\frac{1}{|v|}\int_v \Xi(u)du$, which is not a good stimate of $\mathbf{X}_v(s)$ due to the nonlinearity of the alr-transformation. Instead of block cokriging, the block is discretized into M equal-volume units, and the corresponding point-support random function is simulated at their centres. If there are J realizations, then for each j, where $1 \le j \le J$, averaging over the units within the block results in an estimate

$$\mathbf{X}_v^{(j)}(s) = \frac{1}{M}\sum_{m=1}^{M} \text{agl}\left(\boldsymbol{\xi}^{(j)}(u_m)\right) \quad [10]$$

where $\xi^{(j)}(u_m)$ denotes the alr vector at location $u_m \in v$, $1 \le m \le M$ drawn in the j-th simulation. This approach has the further advantage of also delivering information about the distribution of $\mathbf{x}_v(s)$, not just an estimate of its central value,

$$\mathbf{X}_v^*(s) = \frac{1}{J}\sum_{m=1}^{J} \mathbf{X}_v^{(j)}(s) \quad [11]$$

Tolosana-Delgado *et al.* (2014) propose to simulate these alr vectors using the LU decomposition method (Davis, 1987), which is able to produce a large number of replications with minimal cost (large J), but can handle only a limited number of locations (small $N + M$). This is convenient for obtaining independent estimates of each block, as only simulation within it is needed. Alternatively, if the block estimates are intended to guide global choices, as is the case here, the use of a global simulation like the turning bands algorithm is preferable.

Modelling optimization problem

Processing model

Within the framework of Coward *et al.* (2009) distinguishing between primary variables (intrinsic properties of the natural materials) and response variables (results of human manipulations of the material), the block mean composition $\mathbf{X}_v(s)$ can be understood as a primary variable, while the *benefit* or *gain* $G(\mathbf{X}_v(s), C(s))$ is the ultimate response variable, a function of the primary properties of the block s and of all choices $C(s)$ taken during its processing. From this point on, the block support taken will be assumed to correspond to the processing unit, *i.e.* that volume that may be assumed to behave additively as a homogeneous mass through the process chain. Moreover, the true primary properties are usually not available, because they were interpolated/extrapolated from nearby information or because they are not measurable at all (like size distribution information, affected by stereological distortion). In these cases, one has only estimates, nearby observations, or even indirect or proxy measurements of the target primary properties, jointly denoted as $\mathbf{Z}$. Many of the kinds of geometallurgical data discussed earlier are direct proxies for primary variables, with the notable exception of data on particle properties (which already depend on which kind of breakage was applied, and are therefore response variables). The choice $C(s)$ may denote a complete decision tree, with a complex combination of multiple sub-choices. As such, it might encode the processing sequence (like whether or not to include an extra flotation step) and operational parameters (like the cut-off density selected for density separation), but it can also be a simple on/off choice of processing the material or dumping it as waste.

Once the processing options have been determined for a block v centred at location s, the option yielding the largest gain must be found. A typical approach would be to replace the true material property $\mathbf{X}_v(s)$ in the gain function by its unbiased estimate $\mathbf{X}_v^*(s|\mathbf{Z})$ based on the available data $\mathbf{Z}$, *i.e.* the estimate with $E[\mathbf{X}_v^*(s|\mathbf{Z}) - \mathbf{X}_v(s)] = 0$. This has been shown to be a poor decision rule (van den Boogaart *et al.*, 2011). Given that $\mathbf{X}_v(s)$ is uncertain, that naïve approximation would be equivalent to assuming

$$\text{E}[G\big(\mathbf{X}_v(s), C(s)\big)|\mathbf{Z}] = G(\mathbf{X}_v^*(s|\mathbf{Z}), C(s))$$

which is identically true only if either $\mathbf{X}_v(s)$ is a known constant, or the gain $G(\mathbf{X}_v(s), C(s))$ is a linear function of $\mathbf{X}_v(s)$. Given that the gain function is usually piecewise defined (see the 'Illustration example' section) and that recovery portions are bounded by 0 and 1, one cannot expect linearity to hold.

Maximizing the expected gain

According to van den Boogaart *et al.* (2013), the best choice $C_Z(s)$ for processing the block at location s given the data $\mathbf{Z}$ is computed by maximizing the expected gain with respect to the available decisions conditional on the data:

$$C_{\mathbf{Z}}(s) := \underset{C(s)}{\operatorname{argmax}}\, \mathrm{E}[G(\mathbf{X}_v(s), C(s))|\mathbf{Z}] \qquad [12]$$

This requires computing the conditional expectation of the gain given the data for each possible choice, readily available from J conditional simulations $\{\mathbf{X}_v^{(j)}(s),\ 1 \le j \le J\}$ obtained from Equation [10], through a Monte Carlo approximation:

$$\hat{G}(C(s)|\mathbf{Z}) = \frac{1}{J}\sum_{j=1}^{J} G\left(\mathbf{X}_v^{(j)}(s), C(s)\right) \qquad [13]$$

Having computed the gain for each choice, one can then select the choice yielding the largest gain.

Decision-making in mining is rarely based exclusively on the properties of the individual blocks. Rather, many choices are global decisions, *i.e.* non-adaptive choices that affect the entire domain E. This requires maximizing

$$C_{\mathbf{Z}} := \underset{C}{\operatorname{argmax}} \int_E \mathrm{E}[G(\mathbf{X}_v(s), C)|\mathbf{Z}]dv$$

which can also be estimated within the same framework by Monte Carlo approximation of the gain

$$\hat{G}(C|\mathbf{Z}) = \frac{1}{JB}\sum_{j=1}^{J}\sum_{b=1}^{B} G\left(\mathbf{X}_v^{(j)}(s_b), C(s_b)\right)$$

with the domain $E = \cup_{b=1}^{B} v(s_b)$ discretized into B blocks, each centred at a location s_b, $1 \le b \le B$. This category of global choices includes the setting of quality thresholds, blending strategies, design throughput, or the block extraction sequence. These aspects are not treated in this paper.

Illustration example

Geological description

The data-set used comes from a high-grade iron ore deposit (K-pit deposit, see description by Angerer and Hagemann, 2010) hosted by banded iron formations of the Archean Koolyanobbing Greenstone Belt, Western Australia, located 360 km east of Perth in the Southern Cross Province of the Yilgarn Craton. The greenstone belt strikes northwest and is approximately 35 km long and 8 km wide. It is composed of a folded sequence of amphibolites, meta-komatiites, and intercalated metamorphosed banded iron formation (BIF; Griffin, 1981). The K-deposit occurs where the main BIF horizon, striking 300° and dipping 70° NE, is offset by younger NNE-striking faults (Angerer and Hagemann, 2010). The resource of the K-deposit consists of different mineralogical and textural ore types, including hard high-grade (>55% Fe) magnetite, haematite, and goethite ores and medium-grade fault-controlled haematite-quartz breccia (45-58% Fe) and haematite-magnetite BIF (45-55% Fe).

Three domains, 202 (west main domain), 203 (east main domain), and 300 (haematite hangingwall) were selected as they can be considered reasonably homogeneous from a mineralogical point of view: the iron-rich facies is dominated by haematite in all of them, with minor contributions from magnetite or goethite/limonite.

Geochemical data and mineral calculations

Six parameters were considered for analysis: Fe, LOI, Mn, SiO_2, P, and Al_2O_3, as well as the residual to 100% not accounted for by these. The residual should be considered equal to the mass contribution of the remaining elements not reported here: for example, oxygen from the various Fe and Mn oxides, or OH and Ca from apatite. Thus, the number of original components is D^c =7. Table I summarizes the main characteristics of this data-set.

The chemical compositions were converted to mass proportions of the following D^m = 7 mineralogical-petrological reference material types as end-members (amalgamated then in four types):

- Haematite (*Hm*), taking all the Fe in the chemical composition, and as much of the residual as required for haematite (Fe_2O_3)
- Deleterious (*Dl*), adding up two contributions:
  - Mn oxides, whose mass proportion was computed using all Mn and the necessary oxygen from the residual in a molar proportion of 1:4 (giving a mass proportion of 1:0.0751)
  - Apatite, with an ideal composition $Ca_5(PO_4)_3(OH)$, where again the mass proportion of P was increased by removing the necessary mass from the residual (to account for Ca, O, and OH)
- Shales (*Sh*), again with two contributions:
  - The whole LOI mass contribution (because goethite/limonite contribution to Fe is negligible in the chosen domains), and
  - All Al_2O_3, together with a 1:1 mass proportion of SiO_2 (equivalent to 10:6 in molar proportion, i.e. an Al-rich material type)
- Silica (*Qz*), equal to the residual SiO_2 not attached to shales
- Residual, equal to the remaining residual not attributed to any of the preceding classes. This can be disregarded, because it is assumed to be inert and it represents an irrelevant small mass input to the system.

Table II summarizes the transfer matrix from material types to geochemistry. The proportions of the four types can be computed from the (generalized) inverse of the transfer matrix. None of the resulting four main components was negative, and the residual disregarded component always dropped to zero (accepting an error of ±2%). Material type proportions obtained are shown in Figure 1, and Table II summarizes their statistics also.

Table I

Statistics of the geochemical variables and of the reconstructed mineral/material type composition, globally and by domains. All statistics in %

Variable	Count	Min.	Q25	Q50	Q75	Max.	Mean	Std. Dev.
Al_2O_3	2209	0.023	0.263	0.483	0.87	25	0.8788	1.711
Fe	2209	18.04	60.333	62.793	64.667	69.521	61.8764	4.6289
LOI	2209	0.005	3.837	5.187	7.33	23.747	5.7004	2.5098
Mn	2209	0.001	0.019	0.033	0.063	1.694	0.0557	0.0936
P	2209	0.003	0.075	0.109	0.156	0.663	0.1217	0.0656
SiO_2	2209	0.17	0.97	1.757	3.897	46.58	3.5668	4.8294
Variable	**Domain**	**Min.**	**Q25**	**Q50**	**Q75**	**Max.**	**Mean**	**Std. Dev.**
Al_2O_3	202	0.027	0.22	0.367	0.623	23.46	0.6897	1.5897
Fe	202	27.68	60.7	62.947	64.478	68.9	62.0145	4.255
LOI	202	0.005	3.88	5.253	6.92	23.747	5.5312	2.2218
Mn	202	0.003	0.02	0.03	0.053	0.75	0.0442	0.0516
P	202	0.006	0.088	0.12	0.165	1.097	0.1339	0.0747
SiO_2	202	0.1	1	2.1035	5.7	46.58	4.4162	5.6017
Al_2O_3	203	0.023	0.263	0.5225	0.903	25	0.988	1.9535
Fe	203	11.3	60.943	63.5365	65.413	69.521	62.2792	5.5877
LOI	203	0.197	3.6485	4.877	6.7685	20.837	5.3836	2.4268
Mn	203	0.001	0.015	0.027	0.053	1.694	0.0576	0.1212
P	203	0.002	0.061	0.095	0.14	0.418	0.1083	0.0632
SiO_2	203	0.17	0.783	1.41	2.787	36.678	2.8725	4.1914
Al_2O_3	300	0.283	0.63	0.862	1.19	10.3	1.1215	1.0714
Fe	300	33.81	59.023	60.356	62.377	68.3	60.5123	3.0431
LOI	300	1.1	6.3815	8.889	10.4435	12.393	8.27	2.6539
Mn	300	0.008	0.047	0.073	0.107	0.253	0.0795	0.0439
P	300	0.029	0.092	0.1385	0.1965	0.382	0.1491	0.0728
SiO_2	300	0.6	1.5	1.853	2.55	27.09	2.4992	2.379
Variable	**Count**	**Min.**	**Q25**	**Q50**	**Q75**	**Max.**	**Mean**	**Std. Dev.**
Haematite	2209	0.3066	0.8292	0.872	0.9073	0.9805	0.8586	0.0763
Quartz	2209	0.0002	0.0091	0.0179	0.0455	0.5501	0.0411	0.0595
Shale	2209	0.0018	0.0628	0.0864	0.123	0.5776	0.0978	0.0539
Deleterious	2209	0.0002	0.0014	0.0021	0.0031	0.0243	0.0025	0.0017

Variable	Dom	Count	Min.	Q25	Q50	Q75	Max.	Mean	Std. Dev.
Haematite	202	969	0.3225	0.8322	0.8724	0.9021	0.9625	0.8554	0.0753
Quartz	202	969	0.0002	0.0103	0.0267	0.0753	0.5501	0.0562	0.0719
Shale	202	969	0.0018	0.0587	0.0777	0.1035	0.5267	0.0861	0.0457
Deleterious	202	969	0.0002	0.0015	0.0022	0.003	0.014	0.0024	0.0013
Hematite	203	954	0.0002	0.0012	0.0018	0.0028	0.0243	0.0023	0.0021
Quartz	203	954	0.3066	0.8405	0.8899	0.9192	0.9805	0.8691	0.0812
Shale	203	954	0.0006	0.0072	0.0133	0.0295	0.4558	0.0312	0.0487
Deleterious	203	954	0.0118	0.062	0.0842	0.1189	0.5776	0.0973	0.0583
Haematite	300	286	0.0007	0.002	0.0031	0.0041	0.0066	0.0031	0.0013
Quartz	300	286	0.4178	0.8106	0.8314	0.8617	0.9695	0.8343	0.052
Shale	300	286	0.005	0.0136	0.0175	0.0237	0.2584	0.0232	0.0225
Deleterious	300	286	0.0247	0.1139	0.1432	0.1633	0.3222	0.1394	0.0423

Table II

Conversion tables from material type to geochemistry considering D^c=D^m= 7 classes (top) and from geochemistry to material type amalgamating and removing non-relevant classes (bottom). Zeroes are kept as empty cells for clarity

	Haematite	Deleterious		Shale		Silica	Rest
		MnO_2	Apatite	Type 1	Type 2		
Al_2O_3				1.000			
Fe	1.000						
LOI					1.000		
Mn		1.000					
SiO_2				0.589		1.000	
P			1.000				
Rest	0.430	0.075	2.291				1.000
		Al_2O_3	Fe	LOI	Mn	SiO_2	P
	Haematite		1.000				
	Deleterious				1.000		1.000
	Shale	1.589		1.000		– 0.589	
	Silica					1.000	

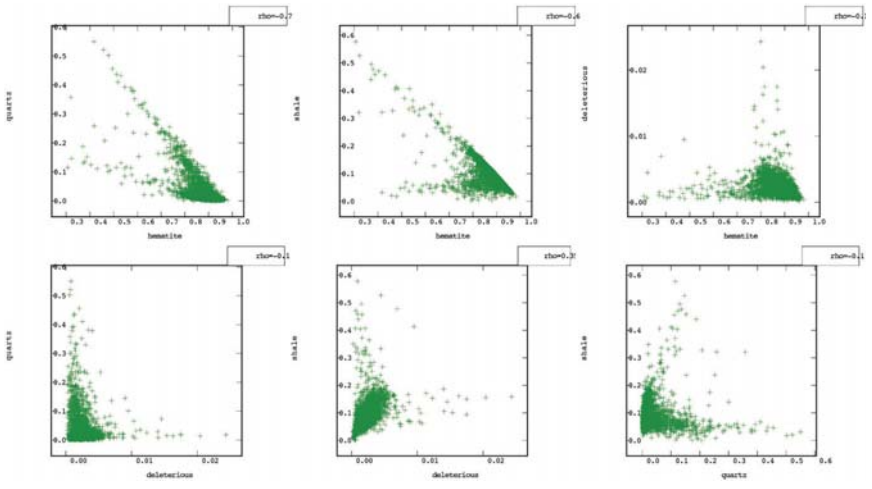

Figure 1 – Scatterplot diagrams of calculated mineral proportions of deleterious, haematite, quartz, and shale

Devised toy processing

Although the K-deposit was exploited without any processing beyond crushing and (eventually) screening, in this contribution a reasonable selection of processing choices was assumed for BIF-hosted iron ores (Houot, 1983; Krishnan and Iwasaki, 1984), with the aim of illustrating what can be expected from the proposed geostatistical method of geometallurgical adaption.

Selective mining units (SMUs) are considered to be volumes of 12×12×6 m³. If an SMU is considered economically interesting, it is processed as follows (Figure 2). First, the SMU is extracted, transported, and crushed by a primary crusher. This represents fixed costs of Q_0. Here it is assumed that all material containing more than 88% haematite will be a lump product, *i.e.* particle size greater than 6.3 mm and less than 31.5 mm. An SMU with an average haematite content greater than 88% (*i.e.* more than 60% Fe), is considered to be in this lump category. Otherwise, the product is sent for further grinding (costing an extra Q_f), and will be considered as fines. Usually, the definition of lump depends on other geometallurgical properties (hardness and grain size), but for the sake of simplicity this has not been taken into account here.

Material that is not considered to be lump can be processed through a desliming process, depending on the proportion of shale. If desliming is switched in, the amount of shale is assumed to be reduced by 15%, with the rest of the components unchanged. Desliming costs are Q_d monetary units per volume washed, independent of the actual amount of shale. Thirdly, the product is fed to a separation process (for instance, flotation), devised to remove quartz: 100% of the quartz, together with 10% of shale and 30% of haematite and deleterious components, is sent to the tailings. Separation costs per unit of material recovered are denoted as Q_s. The product must then be classified into high-grade fines (more than T_h = 85% haematite in the product), low-grade fines (haematite with T_l = 80% or more), or waste. The different products are sold at different prices: I_0 for lump, I_h for high-grade fines, I_l for low-grade fines, and zero for waste.

Table III summarizes the quantities used for these monetary values. The prices and the partition coefficients considered for each phase through desliming and separation were chosen to enhance the contrast between the proposed methodology and the classical one. The calculations proposed here can be adapted to current market prices by changing these constants.

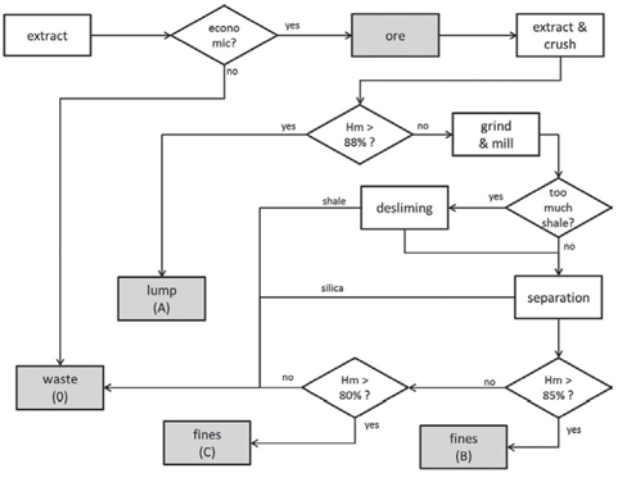

Figure 2—Chosen processing scheme. Note that although the choices appear to be sequential in this diagram, actually the route taken by each block mass is pre-established from the beginning

Table III

Costs of each processing stage and selling prices of the products

	Process	Cost	Units
Q_0	Extraction and crushing	70	$/t (of block)
Q_f	Grinding and milling	25	$/t (of feed)
Q_d	Desliming	0.05	$/m³ (of feed)
Q_s	Separation	0.02	$/ton (of feed)
	Product	**Price**	**Units**
I_0	Lump (Hm>88%)	150	$/t (of product)
I_h	Fines (Hm>85%)	140	$/t (of product)
I_l	Fines (Hm>80%)	130	$/t (of product)

The first choice is to process or dump the block. If processed, the following costs will be incurred. Denoting the original block composition in terms of the four components [*Hm*, *Dl*, *Sh*, *Qz*] by $\mathbf{X}_v$ (the spatial dependence is dropped here for the sake of simplicity), and considering ideal densities of each of these materials respectively as $\rho_{Hm} = \rho_{Dl}$ = 3.5 t/m³ and $\rho_{Sh} = \rho_{Qz}$ = 2.5 t/m³ within a vector $\boldsymbol{\rho} = [\rho_{Hm}, \rho_{Dl}, \rho_{Sh}, \rho_{Qz}]$, the cost of crushing and transporting a block of unit volume is $Q_0\, \mathbf{X}_v \cdot \boldsymbol{\rho}^t$, using the dot product notation for product of matrices. Note that the result is in this case a scalar value. The second choice is to sell the processed block as the category 'lump' or further process it. Selling as lump produces an income of $I_0\, \mathbf{X}_v \cdot \boldsymbol{\rho}^t$ if the material fulfils the quality requirements. The gain of selling it as lump is thus

$$G(\boldsymbol{X}_v, \text{"lump"}) = \begin{cases} (I_0 - Q_0)\, \mathbf{X}_v \cdot \boldsymbol{\rho}^t, & \mathbf{X}_v Hm \geq 88\%, \\ -Q_0\, \mathbf{X}_v \cdot \boldsymbol{\rho}^t, & \mathbf{X}_v Hm < 88\%. \end{cases} \quad [14]$$

If the product is not sold as lump, it must be further ground, which represents a cost of $Q_f\, \mathbf{X}_v \cdot \boldsymbol{\rho}^t$. The following choice is to apply a desliming process, which costs Q_d. Its effect is to modify the mass proportions to $\mathbf{X}_d = \mathbf{X}_v * [1, 1, 1, 0.85]$, where $*$ denotes the direct product (*i.e.* component-wise product of the two vectors). Note that this is analogous to a filter, *i.e.* a process where the partial output concentration is obtained by keeping a known different portion of each input component. Then, a separation process is applied, which represents a similar filter to a vector of masses $\mathbf{X}_s = \mathbf{X}_v * [0.7, 0.7, 0, 0.9]$ with cost $Q_s\, \mathbf{X}_v \cdot \boldsymbol{\rho}^t$ if no desliming was applied, or to $\mathbf{X}_{ds} = \mathbf{X}_d * [0.7, 0.7, 0, 0.9]$ costing $Q_s\, \mathbf{X}_s \cdot \boldsymbol{\rho}^t$ if desliming was switched in. Finally, one must choose the quality at which the product is desired to be sold, choosing between high ($\mathbf{X}_s Hm \geq T_h$ =85%) and low qualities (T_l = 80% ≤ $\mathbf{X}_s Hm < T_h$ = 85%). If no desliming was applied, this produces four options:

$$G(\boldsymbol{X}_v, \text{"high"}) = \begin{cases} I_h\, \mathbf{X}_s \cdot \boldsymbol{\rho}^t - Q_{sep}, & \mathbf{X}_s Hm \geq T_h \\ -Q_{sep}, & \mathbf{X}_s Hm < T_h \end{cases} \quad [15]$$

$$G(\boldsymbol{X}_v, \text{"low"}) = \begin{cases} I_l\, \mathbf{X}_s \cdot \boldsymbol{\rho}^t - Q_{sep}, & \mathbf{X}_s Hm \geq T_l \\ -Q_{sep}, & \mathbf{X}_s Hm < T_l \end{cases} \quad [16]$$

being $Q_{sep} = (Q_0 + Q_f + Q_s)\, \mathbf{X}_v \cdot \boldsymbol{\rho}^t$; or if desliming was necessary

$$G(\boldsymbol{X}_v, \text{"high, desl"}) = \begin{cases} I_h\, \mathbf{X}_{ds} \cdot \boldsymbol{\rho}^t - Q_{sepdesl}, & \mathbf{X}_{ds} Hm \geq T_h \\ -Q_{sepdesl}, & \mathbf{X}_{ds} Hm < T_h \end{cases} \quad [17]$$

$$G(\boldsymbol{X}_v, \text{"low, desl"}) = \begin{cases} I_l\, \mathbf{X}_{ds} \cdot \boldsymbol{\rho}^t - Q_{sepdesl}, & \mathbf{X}_{ds} Hm \geq T_l \\ -Q_{sepdesl}, & \mathbf{X}_{ds} Hm < T_l \end{cases} \quad [18]$$

where $Q_{sepdesl} = (Q_0 + Q_f)\, \mathbf{X}_v \cdot \boldsymbol{\rho}^t + Q_d + Q_s\, \mathbf{X}_s \cdot \boldsymbol{\rho}^t$. Note that all these costs, incomes, and gains are expressed for blocks of unit volume, so that they should be multiplied by 12 · 12 · 6 m³ if one wishes to refer them to an SMU.

Results

Following the geostatistical procedure for compositions outlined before, the alr transformation was applied (Equation [3]) to the material composition Dl-Hm-Qz-Sh, taking shale as common denominator. To better approach the required normality in simulation algorithms, alr variables were converted to normal scores via a normal scores transform, and the variograms of the resulting scores were estimated (Figure 3) and modelled with an LMC (Equation [7]) consisting of a nugget and two spherical structures, *i.e.* using a unit variogram

$$g_2(h) = g_3(h) = \begin{cases} \dfrac{3h}{2a} - \dfrac{h^3}{2a^3} & h < a \\ 1 & h \geq a \end{cases}$$

with the first range a = 52 m in the plane (and an anisotropy ratio vertical/horizontal of 23/52) and the second range a = 248 m in the plane (and an anisotropy ratio

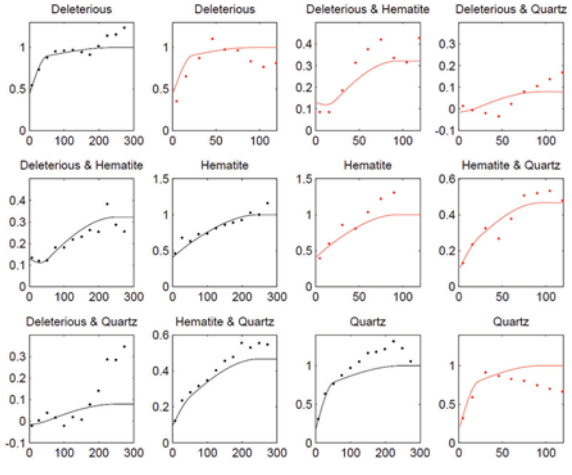

Figure 3—Variograms (experimental as dots, models as thick solid line) of the normal scores of alr-transformed mineral composition, taking Shale as common denominator. Upper triangle of diagrams show the downhole direction, lower triangle of diagrams show the isotropic variogram on the horizontal plane (after a global rotation _+Z 160° +Y -10° +X 45°)

vertical/horizontal of 94/248). Table IV reports the sill matrices $\mathbf{B}_1$ (linked to the nugget), $\mathbf{B}_2$, and $\mathbf{B}_3$ of this model. Note that a global rotation along +Z 160° –Y 10° +X 45° (mathematical convention) was applied.

An SMU grid was constructed such that no block was more than 50 m away from a sample location. Each of the resulting 33 118 blocks was discretized into 4 × 4 × 2 = 32 points, oriented along the natural easting-northing-depth directions. The SMU grid and the underlying point grid are described in Table V. Using a turning bands algorithm, 100 non-conditional simulations were obtained and conditioned via simple cokriging. The conditioning step was succeeded by the application of the Gaussian anamorphosis and the agl transformation (Equation [4]) to obtain values for the four-material composition, which were then averaged in accordance with Equation [10]. This provided 100 realizations of the average composition for each block. Figure 4 shows the scatter plots of mean values of block averages of these simulations after applying Equation [11]. A comparison with the spread of the original data (Figure 1) shows a satisfactory agreement of both sets, and that the obtained block average estimates show similar constraints as the original data.

Two methods for decision-making are compared in what follows. First, for each block Equations [14]–[18] were applied using the block averages $\mathbf{X}^{*}_{v}(s|\mathbf{Z})$ computed previously. Then, each block was treated with the choice that produces the largest gain out of the five options available. Figure 5 (right) shows a selection of ZY sections of the domain, where the colour of each block depends on the treatment chosen according to this average unbiased

Table IV

Sill matrices of the variogram model used

B1	**alr(Dl)**	**alr(Hm)**	**alr(Qz)**
alr(Dl)	0.4300	0.1292	–0.0166
alr(Hm)	0.1292	0.4035	0.0950
alr(Qz)	–0.0166	0.0950	0.1704
B2	**alr(Dl)**	**alr(Hm)**	**alr(Qz)**
alr(Dl)	0.4204	–0.0898	–0.0154
alr(Hm)	–0.0898	0.0281	0.0711
alr(Qz)	–0.0154	0.0711	0.5184
B3	**alr(Dl)**	**alr(Hm)**	**alr(Qz)**
alr(Dl)	0.1496	0.2824	0.1113
alr(Hm)	0.2824	0.5684	0.3000
alr(Qz)	0.1113	0.3000	0.3112

Table V

Prediction grid used

Locations	**Easting**	**Northing**	**Depth**
min	740520.5	6590057.5	126.5
Δ	3	3	3
nodes	197	131	102
blocks	**Easting**	**Northing**	**Depth**
Δ	12	12	6
nodes	57	40	56

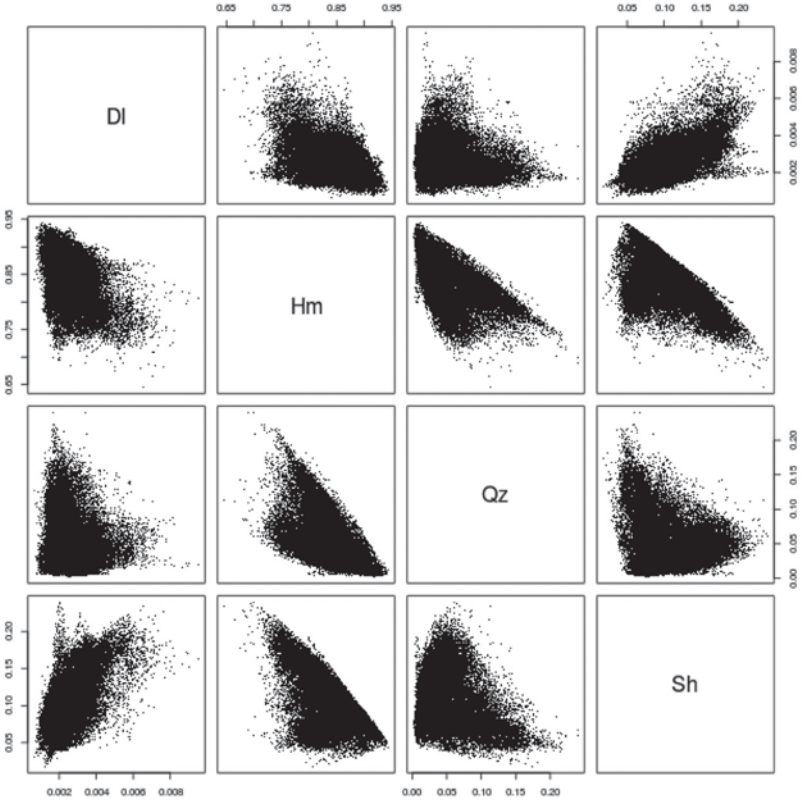

Figure 4—Scatterplot diagrams of interpolated block proportions of deleterious, haematite, quartz, and shale

estimate. This represents the approach of choosing the treatment on the basis of the best available unbiased estimate of the primary properties.

Secondly, the gain was calculated for each simulation and then averaged via Equation [13]. For each block, the option yielding the largest average gain was chosen. This represents the proposed approach of maximizing the conditionally expected gain. Figure 5 (left) shows also the same sections of the domain, using the same set of colours but now defined according to the proposed criterion. Table VI summarizes the two choices for each block (after the unbiased estimate and after the proposed criterion). From Figure 5 and Table VI, it is immediately obvious that the proposed criterion promotes a much more thorough exploitation of the deposit, prescribing more treatment and suggesting selling part of it at lower prices.

Finally, for each of the 100 simulations, the gains for the entire domain were computed using both approaches. These are compared in Figure 6, where it is clear that the proposed criterion always delivers a larger gain than the unbiased estimator criterion. Figure 6 also shows histograms of the gain (and loss) contribution of each individual block for three selected ranked simulations (representing a poor deposit, an average deposit, and a rich deposit, all three scenarios compatible with the available data). These histograms show that the individual gains are very different, typically: a large gain (around $2.5 \cdot 10^5$), a minimal gain (>0), a minimal loss (<0), and moderate-large losses (two subgroups, around $-2 \cdot 10^5$ and $-3 \cdot 10^5$). The histograms show that, with respect to the unbiased estimator choice, the best choice primarily reduces the large losses (increasing slightly the minimal losses) and slightly increases the large gains.

Discussion

The results suggest that mean block unbiased estimates deliver poor choices because of the asymmetry of the gain function. A synthetic example might explain why this happens. If one considers all blocks for which the *estimated* haematite average content is slightly above the lump

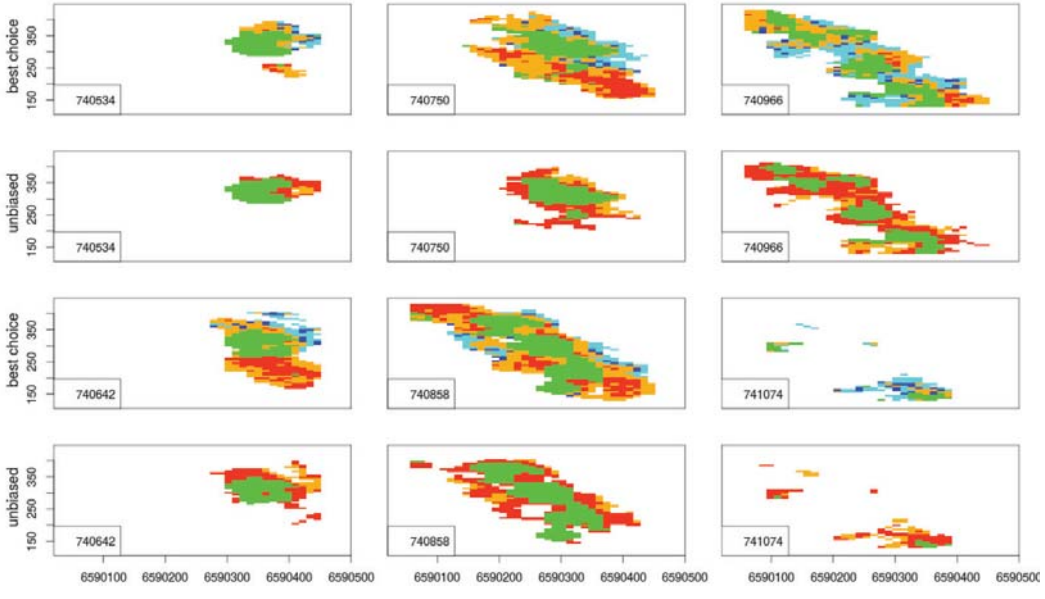

Figure 5—Selected ZY sections of the orebody with estimated unbiased and best choices for each block: sell as lump (green); sell as high quality, without (red) and with (orange) previous desliming; and sell as low quality, without (blue) and with (cyan) previous desliming

Table VI

Number of blocks showing each possible combination of choices, according to the unbiased estimator or according to the best choice proposed; 'nothing' is the choice taken when all other five options yield a negative gain

	Unbiased choice				
Best choice	**Nothing**	**Lump**	**High**	**High deslime**	**Total**
Nothing	8280	1	75	379	8735
Lump	250	6717	791	2	7760
High	2832	44	640	0	3516
High deslime	3866	115	3659	123	7763
Low	204	0	629	331	1164
Low deslime	1362	1	949	1868	4180
Total	16794	6878	6743	2703	33118

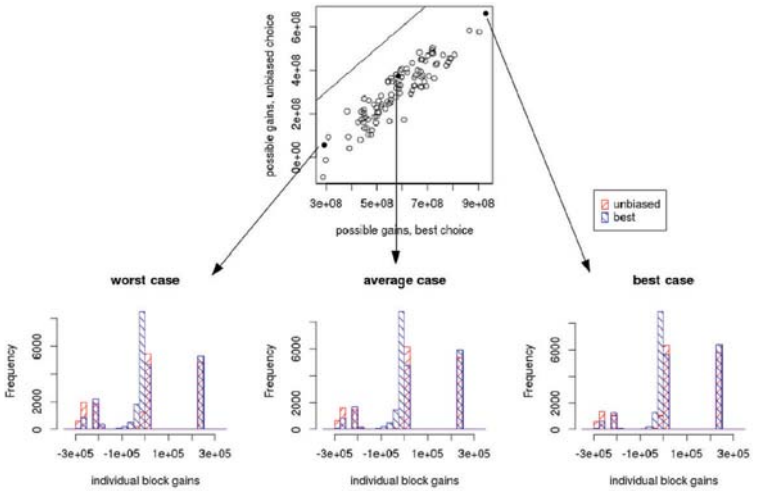

Figure 6—(Upper plot) Scatterplot of the real gains that might be obtained applying the best choice proposed here against a choice based on unbiased estimates of the block properties; reference diagonal line shows equal gains with both options; (lower plots) individual gains for each processed block according to the two criteria, for three particular simulations (marked as filled circles on the scatterplot)

threshold (*Hm*>88%), then the unbiased choice would immediately consider all of them as lump, but each could be sold only if its *real* haematite content was greater than 88 wt%. This means that, depending on the uncertainty on the real haematite content, some of the blocks will actually fall below the threshold, and cannot be sold at the expected price (thus incurring non-realized gains). In contrast, if all blocks are considered whose estimated haematite content is slightly below the threshold, then all of them will be sold at the 'high-quality' price, and those whose real haematite content would qualify them as 'lump' will be sold at this lower price. In other words, the effects of these two errors ('high quality' taken as 'lump', and 'lump' taken as 'high quality') do not compensate one another, and the result is a net loss with respect to that predicted by plugging the unbiased estimate into the gain function. With more thresholds and more decisions this effect accumulates, producing systematic losses in each classification step.

The proposed criterion essentially minimizes the loss, often by reducing the threshold at which the product is considered economic. In that way, though more 'high quality' is classified as 'lump' and extracted but not sold (thus resulting in some loss), also more 'lump' is properly classified and sold at the higher price, (more than just compensating the potential losses). The same can be seen in the prediction of low-quality blocks: the optimal criterion proposes to process many blocks for which the estimated average haematite content is slightly below the threshold of minimal quality (*Hm*>80%), because those of them that are above the threshold will pay for the extra costs of processing those that are actually below the defined threshold. In real applications, this concept would be used for the whole deposit, in order to look for those quality thresholds (fixed to 88%, 85%, and 80% here) that after blending each quality class would maximize the global gain. This global optimization was left for further research, to keep the discussion simpler, but readers should be aware that optimizing blending is one of the most important choices in terms of global impact on the gain.

The modification of the threshold can also operate in the other direction, as it depends on the uncertainty attached to each estimate, and the differences between gains and losses for each misclassification. This can be inferred from two aspects seen in Figure 5. First, desliming a block that according to its average value would not require desliming is considered by the unbiased criterion as a waste of money, thus almost no block is deslimed here; on the other hand, the proposed criterion switches in desliming if its expected cost is less than the expected increment of gain that we will obtain by reducing the chances of a bad classification. The net result is that desliming is much more frequently prescribed by the best criterion than by the unbiased choice. Secondly, several blocks are considered of high quality by the unbiased choice, while the optimal choice classifies them as low quality; these blocks typically lie far from the central part of the orebody (*i.e.* far from the data). Their actual composition is thus highly uncertain. In both cases, the optimal choice takes a conservative decision, preferring a lower but more certain income since this promises a higher overall gain.

A thorough uncertainty characterization is thus the key to proper adaptive processing. In other words, 'second-order reasoning' – so typical of linear geostatistical applications – does not suffice: having a kriging estimate and a kriging variance might be sufficient to describe the uncertainty around the mean value, but it does not provide a good characterization of the whole distribution. According to van den Boogaart *et al.* (2013), the optimization based on the conditional expectation can be proven to be optimal, but a correct prediction of this conditional expectation by Monte Carlo simulation requires correct modelling of the conditional distribution. The key to good adaptive processing is thus a good geostatistical model for the primary geometallurgical properties of the ore and a correct processing model.

Conclusions

To properly select the best option for adaptive processing of each SMU block, the use of unbiased estimates of the average block properties is not a suitable criterion. This criterion always overestimates the real gain that can be obtained from

the block, because high-quality products that are classified as low quality are sold at the lower prices, and low-quality products classified as high quality cannot be sold at the higher price that was predicted. This is analogous to the well-known conditional bias.

To determine the best processing options for each block, it is necessary to calculate the conditional expectation of the gain of processing the block with each option, and then to choose the option that maximizes that expectation. This criterion takes into account the uncertainty on the real values of the material primary properties of each block around the estimated values of these properties, given all the available data. The final adaptive rules obtained tend to have slightly lower thresholds than the pre-established quality thresholds. The idea is to take all really high-quality products as such and compensate with the losses produced by misclassified lower quality products.

In a geostatistical framework, conventional geostatistical simulation can be used to provide the required calculations of the expected gain. A particularly important condition here is that the distribution of the block primary properties is properly estimated on their whole sample space, because the strong nonlinearity of the gain functions places high importance on parts of the distributions far from the central value. For this reason, an in-depth assessment of the scale of the primary properties, inclusion of all relevant co-dependence between variables available, and ensuring quasi-normality of the analysed scores are necessary.

In summary, *geometallurgy* (understood as adaptively processing the ore based on a geostatistical prediction) requires all aspects of geostatistics: attention to nonconventional scales, nonlinear transforms, change of support, and geostatistical (co)simulation. The key is a geostatistical model that takes into account the particular scale of each microfabric property or group of properties, and all cross-dependencies between them. These aspects often require some assessment on the natural scale of each parameter considered, and the use of co-regionalization, cokriging, or cosimulation to adequately capture the spatial co-dependence between all variables.

Finally, it is worth stressing that the task is not to estimate the primary properties themselves, but the expected gain of processing each block through each geometallurgical option available given the whole uncertainty on the true value of the primary properties. This is a stochastic, nonlinear, change-of-support problem, which is solved by averaging the gains over Monte Carlo geostatistical simulations of the primary geometallurgical variables.

Acknowledgements

This work was funded through the base funding of the Helmholtz Institute Freiberg for Resource Technology by the German Federal Ministry for Research and Education and the Free State of Saxony. We would like to thank three anonymous reviewers for their exhaustive revisions and suggestions for improvement.

References

Aitchison, J. 1982. The statistical analysis of compositional data. *Journal of the Royal Statistical Society*, Series B (Applied Statistics), vol. 44, no. 2. pp. 139–177.

Aitchison, J. 1986. The Statistical Analysis of Compositional Data. Chapman and Hall, London.

Aitchison, J. 1997. The one-hour course in compositional data analysis or compositional data analysis is simple. *Proceedings of IAMG 1997*, Technical University of Catalunya, Barcelona, Spain. Pawlowsky-Glahn, V. (ed.). pp. 3–35.

Angerer, T. and Hagemann, S. 2010. The BIF-hosted high-grade iron ore deposits in the Archean Koolyanobbing Greenstone Belt, Western Australia: Structural control on synorogenic- and weathering-related magnetite-, hematite- and goethite-rich iron ore. *Economic Geology*, vol. 105. pp. 917–945.

Barnett, R.M., Manchuk, J.G., and Deutsch, C.V. 2014. Projection pursuit multivariate transform. *Mathematical Geosciences*, vol. 46, no. 3. pp. 337–359.

Boezio, M., Costa, J., and Koppe, J. 2011. Ordinary cokriging of additive log-ratios for estimating grades in iron ore deposits. *Proceedings of CoDaWork 2011*, Sant Feliu de Guixols, Girona, Spain, 9–13 May 2011. Egozcue, J., Tolosana Delgado, R., and Ortego, M.I. (eds.).

Boezio, M., Abicheque, L.A., and Costa, J.F.C.L. 2012. MAF decomposition of compositional data to estimate grades in iron ore deposits. *Ninth International Geostatistics Congress*, Oslo, Norway, 11–15 June 2012. Abrahamsen, P., Hauge, R., and Kolbjørnsen, O. (eds.). Springer, Dordrecht.

Carle, S.F. and Fogg, G.E. 1996. Transition probability-based indicator geostatistics. *Mathematical Geology*, vol, 28, no. 4. pp. 453–476.

Chayes, F. 1960. On correlation between variables of constant sum. *Journal of Geophysical Research*, vol. 65. pp. 4185–4193.

Coward, S, Vann, J., Dunham, S., and Stewart, M. 2009. The Primary-Response framework for geometallurgical variables. *7th International Mining Geology Conference*, Perth, Australia, 17–19 August 2009. Australasian Institute of Mining and Metallurgy, Melbourne. pp. 109–113.

Cressie, N.A. 1993. Statistics for Spatial Data. Wiley, New York.

Davis, M.W. 1987. Production of conditional simulations via the LU triangular decomposition of the covariance matrix. *Mathematical Geology*, vol. 19, no. 2. pp. 91–98.

Delicado, P., Giraldo, R., and Mateu, J. 2008. Point-wise kriging for spatial prediction of functional data. *Functional and Operatoriall Statistics.* Dabo-Niang, S, and Ferraty, F. (eds.). Springer, Heidelberg. pp. 135–141.

Deutsch, C. and Journel, A.G. 1992. GSLIB: Geostatistical Software Library and User's Guide. Oxford University Press, New York. 340 pp.

Dowd, P. 1982. Lognormal kriging – the general case. *Mathematical Geology*, vol. 14, no. 5. pp. 475–499.

Emery, X. 2008. A turning bands program for conditional cosimulation of cross-correlated Gaussian random fields. *Computers and Geosciences*, vol. 34. pp. 1850–1862.

Fandrich, R., Gu, Y., Burrows, D., and Moeller, K. 2007. Modern SEM-based mineral liberation analysis. *International Journal of Mineral Processing*, vol. 84, no. 1. pp. 310–320.

Griffin, A.C. 1981. Structure and Iron Ore deposition in the Archaean Koolyanobbing Greenstone belt, Western Australia. Special Publication 7, Geological Society of Australia. pp. 429–438.

Hagni, A.M. 2008. Phase identification, phase quantification, and phase association determinations utilizing automated mineralogy technology. *Journal of the Minerals, Metals and Materials Society*, vol. 60, no. 4. pp. 33–37.

Houot, R. 1983. Beneficiation of iron ore by flotation– Review of industrial and potential applications. *International Journal of Mineral Processing*, vol. 10. pp. 183–204.

Hron, K., Templ, M., and Filzmoser, P. 2010. Imputation of missing values for compositional data using classical and robust methods. *Computational Statistics and Data Analysis*, vol. 54, no. 12. pp. 3095–3107.

Jackson, J., McFarlane, A.J., and Olson Hoal, K. 2011. Geometallurgy – back to the future: scoping and communicating Geomet programs. *Geomet 2011*, Brisbane, Australia, 5–7 September 2011. Australasian Institute of Mining and Metallurgy. Melbourne. pp. 125–131.

Journel, A., and Huijbregts, Cjh. 1978. Mining Geostatistics, Academic Press, London. 600 pp.

Krishnan, S.V. and Iwasaki, I. 1984. Pulp dispersion in selective desliming of iron ores. *International Journal of Mineral Processing*, vol. 12. pp. 1–13.

Lantuéjoul, C. 2002. Geostatistical Simulation: Models and Algorithms. Springer, Berlin.

Leuangthong, O., and Deutsch, C.V. 2003. Stepwise conditional transformation for simulation of multiple variables. *Mathematical Geology*, vol. 35, no. 2. pp 155–173.

Martín-Fernández, J.A., Hron, K., Templ, M., Filzmoser, P., and Palarea-Albadalejo, J. 2012. Model-based replacement of rounded zeros in compositional data: classical and robust approaches. *Computational Statistics and Data Analysis*, vol. 56, no. 9. pp. 2688–2704.

Mateu-Figueras, G., Pawlowsky-Glahn, V., and Barceló-Vidal, C. 2003. Distributions on the simplex. *Proceedings of CoDaWork '03, Universitat de Girona*, Girona, Spain. Martín-Fernández, J.A. and Thió-Henestrosa, S. (eds.).

Matheron, G. 1973. The intrinsic random functions and their applications. *Advances in Applied Probability*, vol. 5, no. 3. pp. 439–468.

Menafoglio, A., Guadagnini, A., and Secchi, P. 2014. A kriging approach based on Aitchison geometry for the characterization of particle-size curves in heterogeneous aquifers. *Stochastic Environmental Research and Risk Assessment*, vol. 28, no. 7. pp. 1835–1851.

Myers, D.E. 1982, Matrix formulation of co-kriging. *Mathematical Geology*, vol. 14, no. 3. pp. 249–257.

Pawlowsky-Glahn, V. and Olea, R.A. 2004. Geostatistical Analysis of Compositional Data. Oxford University Press.

Rivoirard, J. 1990. A review of lognormal estimators for in situ reserves (teacher's aid). *Mathematical Geology*, vol. 22, no. 2. pp 213–221.

Rossi, M.E. and Deutsch, C.V. 2014. Mineral Resource Estimation. Springer, Heidelberg. 332 pp.

Sutherland, D.N. and Gottlieb, P. 1991. Application of automated quantitative mineralogy in mineral processing. *Minerals Engineering*, vol. 4, no. 7. pp. 753–762.

Tjelmeland, H. and Lund, K.V. 2003. Bayesian modelling of spatial compositional data. *Journal of Applied Statistics*, vol. 30, no. 1. pp. 87–100.

Tolosana-Delgado, R. 2006. Geostatistics for constrained variables: positive data, compositions and probabilities. Application to environmental hazard monitoring. PhD thesis. University of Girona, Spain.

Tolosana-Delgado, R., Van den Boogaart, K.G., and Pawlowsky-Glahn, V. 2011a. Geostatistics for compositions. *Compositional Data Analysis at the Beginning of the XXI Century*. Pawlowsky-Glahn, V. and Buccianti, A. (eds.). John Wiley and Sons, London. pp. 73–86.

Tolosana-Delgado, R., Von Eynatten, H., and Karius, V. 2011b. Constructing modal mineralogy from geochemical composition: a geometric-Bayesian approach. *Computers and Geosciences*, vol. 37, no. 5. pp. 677–691.

Tolosana-Delgado, R., Mueller, U., Van den Boogaart, K.G., and Ward, C. 2014. Compositional block cokriging. *Proceedings of the 15th Annual Conference of the International Association for Mathematical Geosciences*. Pardo-Igúzquiza, E., Guardiola-Albert, C., Heredia, J., Moreno-Merino, L., Durán, J.J., and Vargas-Guzmán, J.A. (eds.). Lectures Notes in Earth System Sciences, Springer, Heidelberg. pp. 713–716.

Tolosana-Delgado, R. and Van den Boogaart, K.G. 2013. Joint consistent mapping of high dimensional geochemical surveys. *Mathematical Geosciences*, vol. 45, no. 8. pp. 983–1004.

Van den Boogaart, K.G. and Schaeben, H. 2002. Kriging of regionalized directions, axes, and orientations II: Orientations. *Mathematical Geology*, vol. 34, no. 6. pp. 671–677.

Van den Boogaart, K.G., Weißflog, C., and Gutzmer, J. 2011. The value of adaptive mineral processing based on spatially varying ore fabric parameters, *Proceedings of IAMG 2011*, Salzburg, Austria, 5–9 September 2011. University of Salzburg.

Van den Boogaart, K.G., Konsulke, S., and Tolosana-Delgado, R. 2013. Nonlinear geostatistics for geometallurgical optimisation. *Proceedings of Geomet 2011 Brisbane,* Australia, 30 September–2 November 2013. Australasian Institute of Mining and Metallurgy, Melbourne. pp. 125–131.

Van den Boogaart, K.G. and Tolosana-Delgado, R. 2013. Analyzing compositional data with R. Springer, Heidelberg.

Wackernagel, H. 2003. Multivariate Geostatistics. Springer, Berlin.

Ward, C. and Mueller, U. 2012. Multivariate estimation using log-ratios: a worked alternative. *Geostatistics Oslo 2012*. Abrahamsen, P., Hauge, R., and Kolbjørnsen, O. (eds.). Springer, Dordrecht. pp. 333–344.

Weltje, G.J. 1997. End-member modeling of compositional data: numerical-statistical algorithms for solving the explicit mixing problem. *Mathematical Geology*, vol. 29, no. 4. pp. 503–549.

Wills, B.A. and Napier-Munn, T. 2006. Wills' Mineral Processing Technology: an Introduction to the Practical Aspects of Ore Treatment and Mineral Recovery. Elsevier Butterworth, Oxford. ◆

http://dx.doi.org/10.17159/2411-9717/2015/v115n1a3

Dealing with high-grade data in resource estimation

by O. Leuangthong* and M. Nowak†

Synopsis

The impact of high-grade data on resource estimation has been a long-standing topic of interest in the mining industry. Concerns related to possible over-estimation of resources in such cases have led many investigators to develop possible solutions to limit the influence of high-grade data. It is interesting to note that the risk associated with including high-grade data in estimation appears to be one of the most broadly appreciated concepts understood by the general public, and not only professionals in the resource modelling sector. Many consider grade capping or cutting as the primary approach to dealing with high-grade data; however, other methods and potentially better solutions have been proposed for different stages throughout the resource modelling workflow.

This paper reviews the various methods that geomodellers have used to mitigate the impact of high-grade data on resource estimation. In particular, the methods are organized into three categories depending on the stage of the estimation workflow when they may be invoked: (1) domain determination; (2) grade capping; and (3) estimation methods and implementation. It will be emphasized in this paper that any treatment of high-grade data should not lead to undue lowering of the estimated grades, and that limiting the influence of high grades by grade capping should be considered as a last resort. A much better approach is related to domain design or invoking a proper estimation methodology. An example data-set from a gold deposit in Ontario, Canada is used to illustrate the impact of controlling high-grade data in each phase of a study. We note that the case study is by no means comprehensive; it is used to illustrate the place of each method and the manner in which it is possible to mitigate the impact of high-grade data at various stages in resource estimation.

Keywords
grade domaining, capping, cutting, restricted kriging.

Introduction

A mineral deposit is defined as a concentration of material in or on the Earth's crust that is of possible economic interest. This generic definition is generally consistent across international reporting guidelines, including the South African Code for Reporting of Exploration Results, Mineral Resources and Mineral Reserves (SAMREC Code), Canadian Securities Administrators' National Instrument 43-101 (NI 43-101), and the Australasian Code for Reporting of Exploration Results, Mineral Resources and Ore Reserves (2012), published by the Joint Ore Reserves Committee (the JORC Code). Relative to its surroundings, we can consider that a mineral deposit is itself an *outlier*, as it is characterized by an anomalously high concentration of some mineral and/or metal. This presents an obvious potential for economic benefit, and in general, the higher the concentration of mineral and/or metal, the greater the potential for financial gain.

Indeed, many mining exploration and development companies, particularly junior companies, will publicly announce borehole drilling results, especially when high-grade intervals are intersected. This may generate public and/or private investor interest that may be used for project financing. Yet, it is interesting that these high-grade intercepts that spell promise for a mineral deposit present a challenge to resource modellers in the determination of a resource that will adequately describe ultimately unknown *in-situ* tons and grade.

Resource estimation in the mining industry is sometimes considered an arcane art, using old methodologies. It relies on well-established estimation methods that have seen few advancements in the actual technology used, and it is heavily dependent on the tradecraft developed over decades of application. Unlike in other resource sectors, drilling data is often readily available due to the accessibility of prospective projects and the affordability of sample collection. As such, the 'cost' of information is often low and the relative abundance of data translates to reduced uncertainty about the project's geology and resource quality and quantity. It is in this context that more advanced geostatistical developments, such as conditional simulation (see Chiles and Delfiner (2012) for a good

* *SRK Consulting (Canada) Inc., Toronto, ON, Canada.*

† *SRK Consulting (Canada) Inc., Vancouver, BC, Canada.*

summary of the methods) and multiple point geostatistics (Guardiano and Srivastava, 1992; Strebelle and Journel, 2000; Strebelle, 2002), have struggled to gain a stronghold as practical tools for mineral resource evaluation.

So we are left with limited number of estimation methods that are the accepted industry standards for resource modelling. However, grade estimation is fundamentally a synonym for grade averaging, and in this instance, it is an averaging of mineral/metal grades in a spatial context. Averaging necessarily means that available data is accounted for by a weighting scheme. This, in itself, is not an issue nor is it normally a problem, unless extreme values are encountered. This paper focuses on extreme high values, though similar issues may arise for extreme low values, particularly if deleterious minerals or metals are to be modelled. High-grade intercepts are problematic if they receive (1) too much weight and lead to a possible over-estimation, or if kriging is the method of choice, (2) a negative weight, which may lead to an unrealistic negative estimate (Sinclair and Blackwell, 2002). A further problem that is posed by extreme values lies in the inference of first- and second-order statistics, such as the mean, variance, and the variogram for grade continuity assessment. Krige and Magri (1982) showed that presence of extreme values may mask continuity structures in the variogram.

This is not a new problem. It has received much attention from geologists, geostatisticians, mining engineers, financiers, and investors from both the public and private sectors. It continues to draw attention across a broad spectrum of media ranging from discussion forums hosted by professional organizations (*e.g.* as recently as in 2012 by the Toronto Geologic Discussion Group) and online professional network sites (*e.g.* LinkedIn.com). Over the last 50 years, many geologists and geostatisticians have devised solutions to deal with these potential problems arising from high-grade samples.

This paper reviews the various methods that geomodellers have used or proposed to mitigate the impact of high-grade data on resource estimation. In particular, the methods are organized into three categories depending on the stage of the estimation workflow when they may be invoked: (1) domain determination; (2) grade capping; and (3) estimation methods and implementation. Each of these stages is reviewed, and the various approaches are discussed. It should be stressed that dealing with the impact of high-grade data should not lead to undue lowering of estimated grades. Very often it is the high-grade data that underpins the economic viability of a project.

Two examples are presented, using data from gold deposits in South America and West Africa, to illustrate the impact of controlling high-grade data in different phases of a study. We note that the review and examples are by no means comprehensive; they are presented to illustrate the place of each method and the manner in which it is possible to mitigate the impact of high-grade data at various stages in resource estimation.

What constitutes a problematic high-grade sample?

Let us first identify which high-grade sample(s) may be problematic. Interestingly, this is also the section where the word *outlier* is normally associated with a 'problematic' high-grade sample. The term outlier has been generally defined by various authors (Hawkins, 1980; Barnett and Lewis, 1994; Johnson and Wichern, 2007) as an observation that deviates from other observations in the same grouping. Many researchers have also documented methods to identify outliers.

Parker (1991) suggested the use of a cumulative coefficient of variation (CV), after ordering the data in descending order. The quantile at which there is a pronounced increase in the CV is the quantile at which the grade distribution is separated into a lower grade, well-behaved distribution and a higher grade, outlier-influenced distribution. He proposes an estimation of these two parts of the distribution, which will be discussed in the third stage of dealing with high-grade data in this manuscript.

Srivastava (2001) outlined a procedure to identify an outlier, including the use of simple statistical tools such as probability plots, scatter plots, and spatial visualization, and to determine whether an outlier can be discarded from a database. The context of these guidelines was for environmental remediation; however, these practical steps are applicable to virtually any resource sector.

The identification of spatial outliers, wherein the local neighbourhood of samples is considered, is also an area of much research. Cerioli and Riani (1999) suggested a forward search algorithm that identifies masked multiple outliers in a spatial context, and provides a spatial ordering of the data to facilitate graphical displays to detect spatial outliers. Using census data for the USA, Lu *et al.* (2003, 2004) have documented and proposed various algorithms for spatial outlier detection, including the mean, median, and iterative r (ratio) and iterative z algorithms. Liu *et al.* (2010) devised an approach for large, irregularly spaced data-sets using a locally adaptive and robust statistical analysis approach to detect multiple outliers for GIS applications.

In general, many authors agree that the first task in dealing with extreme values is to determine the validity of the data, that is, to confirm that the assay values are free of errors related to sample preparation, handling, and measurement. If the sample is found to be erroneous, then the drill core interval should be re-sampled or the sample should be removed from the assay database. Representativeness of the sample selection may also be confirmed if the interval is re-sampled; this is particularly relevant to coarse gold and diamond projects. If the sample is deemed to be free of errors (excluding inherent sample error), then it should remain in the resource database and subsequent treatment of this data may be warranted.

Stages of high-grade treatment

Once all suspicious high-grade samples are examined and deemed to be correct, such that they remain part of the resource database, we now concern ourselves with how this data should be treated in subsequent modelling. For this, we consider that there are three particular phases of the resource workflow wherein the impact of high-grade samples can be explicitly addressed. Specifically, these three stages are:

1. Domaining to constrain the spatial impact of high grade samples
2. Grade capping or cutting to reduce the values of high-grade samples

3. Restricting the spatial influence of high-grade samples during estimation.

The first stage of domaining addresses the stationarity of the data-set, and whether geological and/or grade domaining can assist in properly grouping the grade samples into some reasonable grouping of data. This may dampen the degree by which the sample(s) is considered high; perhaps, relative to similarly high-grade samples, any one sample appears as part of this population and is no longer considered an anomaly.

The second phase is that which many resource modellers consider a necessary part of the workflow: grade capping or cutting. This is not necessarily so; in fact, some geostatisticians are adamant that capping should never be done, that it represents a 'band-aid' solution and masks the real problem, which is likely linked to stationarity decisions and/or an unsuitable estimation method.

The third phase, where the influence of a high-grade sample may be contained, is during the actual estimation phase. In general, this can occur in one of two ways: (1) as an implementation option that may be available in some commercial general mining packages (GMPs); or (2) a non-conventional estimation approach is considered that focuses on controlling the impact of high-grade samples.

The following sections discuss the various approaches that may be considered in each of these three stages of addressing high-grade samples. We note that these three stages of treating high grades are not necessarily mutually exclusive. For instance, grade domaining into a higher grade zone does not pre-empt the use of grade capping prior to resource estimation. In fact, most mineral resource models employ at least one or some combination of the three stages in resource evaluation.

Stage 1: Domaining high-grade data

Resource modelling almost always begins with geological modelling or domaining. This initial stage of the model focuses on developing a comprehensive geological and structural interpretation that accounts for the available drill-hole information and an understanding of the local geology and the structural influence on grade distribution. It is common to generate a three-dimensional model of this interpretation, which is then used to facilitate resource estimation. In many instances, these geological domains may be used directly to constrain grade estimation to only those geological units that may be mineralized.

It is also quite common during this first stage of the modelling process to design grade domains to further control the distribution of grades during resource estimation. One of the objectives of grade domaining is to prevent smearing of high grades into low-grade regions and *vice versa*. The definition of these domains should be based on an understanding of grade continuity and the recognition that the continuity of low-grade intervals may differ from that of higher grade intervals (Guibal, 2001; Stegman, 2001).

Often, a visual display of the database should help determine if a high-grade sample comprises part of a subdomain within the larger, encompassing geological domain. If subdomain(s) can be inferred, then the extreme value may be reasonable within the context of that subpopulation.

Grade domains may be constructed via a spectrum of approaches, ranging from the more time-consuming sectional method to the fast, semi-automatic boundary or volume function modelling methods (Figure 1). The difference between these two extremes has also been termed explicit *versus* implicit modelling, respectively (Cowan *et al.*, 2002; 2003; 2011). Of course, with today's technology, the former approach is no longer truly 'manual' but commonly involves the use of some commercial general mine planning package to generate a series of sections, upon which polylines are digitized to delineate the grade domain. These digitized polylines are then linked from section to section, and a 3D triangulated surface can then be generated. This process can still take weeks, but allows the geologist to have the most control on interpretation. The other end of the spectrum involves the use of a fast boundary modelling approach that is based on the use of radial basis functions (RBFs) to create isograde surfaces (Carr *et al.*, 2001, Cowan *et al.*, 2002; 2003; 2011). RBF methods, along with other linear approaches, are sensitive to extreme values during grade shell generation, and often some nonlinear transform may be required. With commercial software such as Leapfrog, it can take as little as a few hours to create grade shells. In between these two extremes, Leuangthong and Srivastava (2012) suggested an alternate approach that uses multigaussian kriging to generate isoprobability shells corresponding to different grade thresholds. This permits uncertainty assessment in the grade shell that may be used as a grade domain.

In practice, it is quite common that some semi-automatic approach and a manual approach are used in series to generate reasonable grade domains. A boundary modelling method is first applied to quickly generate grade shells, which are then imported into the manual wireframing approach and used, in conjunction with the projected drill-hole data, to guide the digitization of grade domains.

Stegman (2001) used case studies from Australian gold deposits to demonstrate the importance of grade domains, and highlights several practical problems with the definition of these domains, including incorrect direction of grade continuity, too broad (or tight) domains, and inconsistency in data included/excluded from domain envelopes. Emery and Ortiz (2005) highlighted two primary concerns related to grade domains: (1) the implicit uncertainty in the domain definition and associated boundaries, and (2) that spatial dependency between adjacent domains is unaccounted for. They proposed a stochastic approach to model the grade domains and the use of cokriging of data across domains to estimate grades.

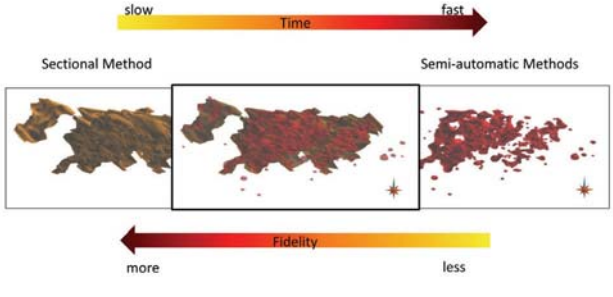

Figure 1—Spectrum of methods for grade domaining: from pure explicit modelling (right) to pure implicit modelling (left)

Stage 2: Capping high-grade samples

In the event that grade domaining is not viable and/or insufficient to control the influence of one or more high-grade samples, then more explicit action may be warranted in order to achieve a realistic resource estimate. In these instances, grade capping or cutting to some level is a common practice in mineral resource modelling. This procedure is also sometimes referred to as 'top cut', 'balancing cut', or a 'cutting value'. It generally involves reducing those grade values that are deemed to be outliers or extreme erratic values to some lower grade for the purposes of resource evaluation. Note that this practice should never involve deletion of the high-grade sample(s) from the database.

Two primary reasons for capping high-grade samples are: (1) there is suspicion that uncapped grades may overstate the true average grade of a deposit; and (2) there is potential to overestimate block grades in the vicinity of these high-grade samples. Whyte (2012) presented a regulator's perspective on grade capping in mineral resource evaluation, and suggested that the prevention of overestimation is good motivation to consider grade capping. For these reasons, capping has become a 'better-safe-than-sorry' practice in the mining industry, and grade capping is done on almost all mineral resource models (Nowak *et al.*, 2013).

Given the prevalence of this approach in mining, it is no surprise that there are a multitude of tools available to help a modeller determine what grade value is an appropriate threshold to cap. These include, but are not limited to, the use of probability plots, decile analysis (Parrish, 1997), metal-at-risk analysis, cutting curves (Roscoe, 1996), and cutting statistics plots. Nowak *et al.* (2013) compared four of these approaches in an application to a West African gold deposit (Figure 2).

Probability plots are likely the most commonly used tool, due to their simplicity and the availability of software to perform this type of analysis. Inflection points and/or gaps in the distribution are often targeted as possible capping values (Figure 2a). In some instances, legacy practice at a particular mine site may dictate that capping is performed at some threshold, *e.g.* the 95th percentile of the distribution. In these cases, the initial decision to cap at the 95th percentile may well have been reasonable and defensible; however, this choice should be revisited and reviewed every time the database and/or domains are updated.

Parrish (1997) introduced decile analysis, which assesses the metal content within deciles of the assay distribution. Total metal content for each decile and percentage of the overall metal content are calculated. Parrish suggested that if the top decile contains more than 40% of the metal, or if it contains more than twice the metal content of the 80% to 90% decile, then capping may be warranted (Figure 2b). Analysis then proceeds to split the top decile into percentiles. If the highest percentiles have more than 10% of the total metal content, a capping threshold is chosen. The threshold is selected by reducing all assays from the high metal content percentiles to the percentile below which the metal content does not exceed 10% of the total.

The metal-at-risk procedure, developed by H. Parker and presented in some NI 43-101 technical reports, *e.g.* (Neff *et al.*, 2012), uses a method based on Monte Carlo simulation. The objective of the process is to establish the amount of metal which is at risk, *i.e.*, potentially not present in a domain for which resources will be estimated. The procedure assumes that the high-grade data can occur anywhere in space, *i.e.*, there is no preferential location of the high-grade data in a studied domain. The assay distribution can be sampled at random a number of times with a number of drawn samples representing roughly one year's production. For each set of drawn assays a metal content represented by high-grade composites can be calculated. The process is repeated many times, and the 20th percentile of the high-grade metal content is applied as the risk-adjusted amount of metal. Any additional metal is removed from the estimation process either by capping or by restriction of the high-grade assays.

Cutting curves (Roscoe, 1996) were introduced as a means to assess the sensitivity of the average grade to the capped grade threshold. The premise is that the average grade should stabilize at some plateau. The cap value should be chosen as near the inflection point prior to the plateau (Figure 2c), and should be based on a minimum of 500 to 1000 samples.

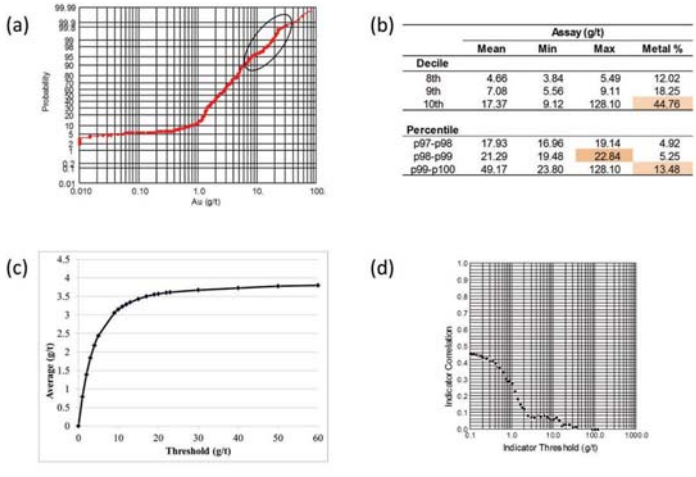

Figure 2—Example of grade capping approaches to a West African gold deposit using (a) probability plot, (b) decile analysis, (c) cutting curves, and (d) cutting statistics plot (Nowak *et al.*, 2013)

Cutting statistics plots, developed by R.M. Srivastava and presented in some internal technical reports for a mining company in the early 1990s, consider the degradation in the spatial correlation of the grades at various thresholds using an indicator approach (personal communication, 1994). The capping values are chosen by establishing a correlation between indicators of assays in the same drill-holes via downhole variograms, at different grade thresholds. Assays are capped at the threshold for which correlation approaches zero (Figure 2d).

Across the four approaches illustrated in Figure 2, the proposed capping value ranges from approximately 15 g/t to 20 g/t gold, depending on the method. While the final selection is often in the hands of the Qualified Person, a value in this proposed range can generally be supported and confirmed by these multiple methods. In any case, the chosen cap value should ensure a balance between the loss in metal and loss in tonnage.

Stage 3: Estimating with high-grade data

Once we have 'stabilized' the average grade from assay data, we can now focus further on how spatial location of very high-grade assays, potentially already capped, affects estimated block grades. The risk of overstating estimated block grades is particularly relevant in small domains with fewer assay values and/or where only a small number of data points are used in the estimation. The first step in reviewing estimated block grades is to visually assess, on section or in plan view, the impact of high-grade composites on the surrounding block grades. Swath plots may also be useful to assess any 'smearing' of high grades. This commonly applied, simple, and effective approach is part of the good practice recommended in best-practice guidelines, and can be supplemented by additional statistical analysis. The statistical analysis may be particularly useful if a project is large with many estimation domains.

One simple way to test for potential of overestimation in local areas could be a comparison of cumulative frequency plots from data and from estimated block grades. Let us consider two domains, a larger Domain D, and amuch smaller Domain E, both with positively skewed distributions which are typically encountered in precious metal deposits. A typical case, presented in Figure 3(a) for Domain D, shows that for thresholds higher than average grade, the proportion of estimated block grades above the thresholds is lower than the proportion of high-grade data. This is a typical result from smoothing the estimates. On the other hand, in Domain E, we see that the proportion of high-grade blocks above the overall average is higher than the proportion from the data (Figure 3b). We can consider this as a warning sign that those unusual results could potentially be influenced by very high-grade assays that have undue effect on the overall estimates.

Cutting curve plots can be also quite helpful; however, in this instance we are not focused on identifying a capping threshold, but rather the impact of high-grade blocks on the overall average block grade. Figure 4 shows the average estimated block grades below a set of thresholds in domains D and E. In Domain D (Figure 4a) there is a gradual increase in average grades for increasing thresholds, eventually stabilizing at 2. 7 g/t Au. On the other hand, in Domain E (Figure 4b) there is a very abrupt increase in average grade for very similar high-grade block estimates. This indicates a relatively large area(s) with block estimates higher than 6 g/t.

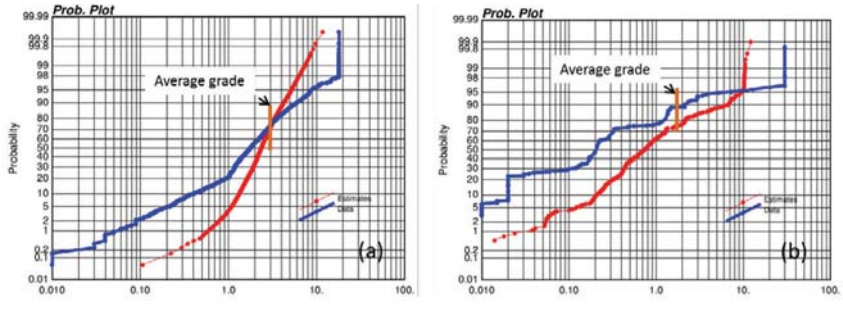

Figure 3—Cumulative frequency plots for original data and estimated block grades in (a) Domain D, (b) Domain E

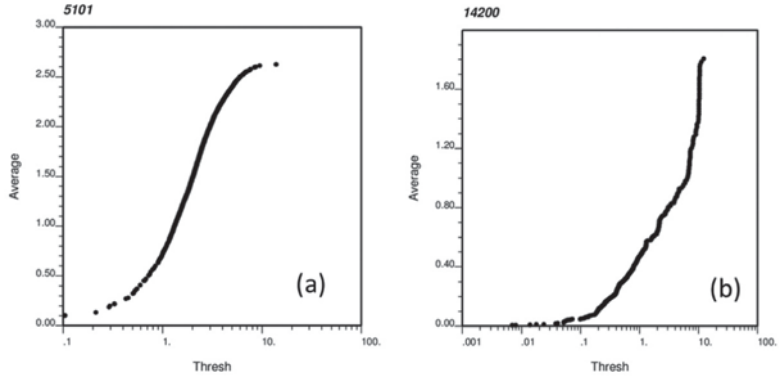

Figure 4—Extreme value plots from estimated block grades in (a) Domain D, (b) Domain E

Limiting spatial influence of high-grade samples

If the result of these early estimation validation steps reveals that high-grade composites may be causing over-estimation of the resource, then we may wish to consider alternative implementation options in the estimation that may be available within software. Currently, a few commercial general mining packages offer the option to restrict the influence of high-grade samples. That influence is specified by the design of a search ellipsoid with dimensions smaller than that applied for grade estimation.

Typically the choice of the high-grade search ellipsoid dimensions is based on an educated guess. This is based on a notion that the size of the high-grade search ellipsoid should not extent beyond the high-grade continuity. There are, however, two approaches that the authors are aware of that are potentially better ways to assess high-grade continuity.

The first approach involves assessing the grade continuity via indicator variograms. The modeller simply calculates the indicator variograms for various grade thresholds. As the focus is on the high-grade samples, the grade thresholds should correspond to higher quantiles, likely above the 75th percentile. A visual comparison of the indicator variograms at these different thresholds may reveal a grade threshold above which the indicator variogram noticeably degrades. This may be a reasonable threshold to choose to determine which samples will be spatially restricted. The range of the indicator variogram at that threshold can also be used to determine appropriate search radii to limit higher grade samples.

The second approach is also quantitative, and relies on a *p*-gram analysis developed by R.M. Srivastava (personal communication, 2004). The *p*-gram was developed in the petroleum industry to optimize spacing for production wells. To construct *p*-grams, assay composites are coded with an indicator at a threshold for high-grade population. Using a process similar to that for indicator variography, the data is paired over a series of lag distances. Unlike the conventional variogram, the *p*-gram considers only the paired data in which the tail of the pairs is above the high-grade threshold. The actual *p*-gram value is then calculated as the ratio of pairs where both the head and tail are above the threshold to the number of pairs where the tail of the pair is above the threshold. Pairs at shorter lag distances are given more emphasis by applying an inverse distance weighting scheme to the lag distance. Figure 5 shows an example of a *p*-gram analysis for a series of high-grade thresholds. The curves represent average probability that two samples separated by a particular distance will both be above the threshold, given that one is already above the threshold. In this specific example, up to a threshold of 15 g/t gold, the range of continuity, *i.e.*, the distance at which the curve levels off, is 30 m. This distance can be applied as search ellipsoid radius to limit high-grade assays.

Alternative estimation approaches for high-grade mitigation

While the above methods work within the confines of a traditional estimation framework for resource estimation, there are alternative, lesser known estimation methods that were proposed specifically to deal with controlling the influence of high-grade samples. Journel and Arik (1988) proposed an indicator approach to dealing with outliers, wherein the high grade falls within the last class of indicators and the mean of this class is calculated as the arithmetic average of samples in the class. Parker (1991) pointed out that using the arithmetic average for this last class of indicators may be inefficient or inaccurate. Instead, Parker (1991) proposed a procedure that first identifies which threshold should be chosen to separate the high grades from the rest of the sample population (discussed earlier), and secondly proposes an estimation method that combines an indicator probability and the fitting of a lognormal model to the samples above the threshold to calculate the average grade for this class of data, Z_h^*. A block grade is then obtained by combining estimates of both the lower and higher grade portions of the sample data: $Z^* = I^* Z_l^* + (1-I^*) Z_h^*$, where the superscript * denotes an estimate, I^* is the probability of occurrence of lower grades below the threshold, and Z_l^* is the kriged estimate of the block using only those samples below the threshold. The implicit assumption is that there is no correlation between the probability and grade estimates.

Arik (1992) proposed a two-step kriging approach called 'outlier restricted kriging' (ORK). The first step consists of assigning to each block at location X the probability or the proportion $\Phi(X, Z_c)$ of the high-grade data above a predefined cut-off Z_c. Arik determines this probability based on indicator kriging at cut-off grade Zc. The second step involves the assignment of the weights to data within a search ellipsoid. These weights are assigned in such a way that the sum of the weights for the high-grade data is equal to the assigned probability $\Phi(x, Z_c)$ from the first step. The weights for the other data are constrained to add up to 1 - $\Phi(X, Z_c)$. This is similar to Parker's approach in the fact that indicator probabilities are used to differentiate the weights that should be assigned to higher grade samples and lower grade samples.

Costa (2003) revisited the use of a method called robust kriging (RoK), which had been introduced earlier by Hawkins and Cressie (1984). Costa showed the practical implementation of RoK for resource estimation in presence of outliers of highly skewed distributions, particularly if an erroneous sample value was accepted as part of the assay database. It is interesting to note that where all other approaches discussed

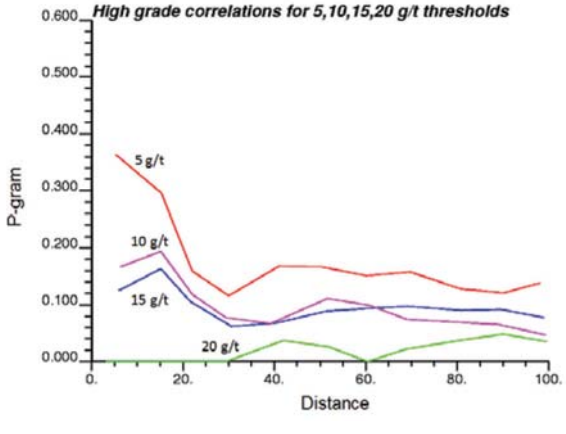

Figure 5—*p*-grams for different data thresholds

previously were concerned with the weighting of higher grade samples, RoK focuses on directly editing the sample value based on how different it is from its neighbours. The degree of change of a sample value is controlled by a user-specified *c* parameter and the kriging standard deviation obtained from kriging at that data location using only the surrounding data. For samples that are clearly part of the population, *i.e.* not considered an outlier or an extreme value, then the original value is left unchanged. For samples that fall within the extreme tail of the grade distribution, RoK yields an edited value that brings that sample value closer to the centre of the grade distribution.

More recently, Rivoirard *et al.* (2012) proposed a mathematical framework called the top-cut model, wherein the estimated grade is decomposed into three parts: a truncated grade estimated using samples below the top-cut grade, a weighted indicator above the top-cut grade, and an independent residual component. They demonstrated the application of this top-cut model to blast-hole data from a gold deposit and also to a synthetic example.

Impact of various treatments – examples

Two examples are presented to illustrate the impact of high-grade samples on grade estimation, and the impact of the various approaches to dealing with high-grade data. In both cases, data from real gold deposits is used to illustrate the results from different treatments.

Example 1: West African gold deposit

This example compares the estimation of gold grades from a West African gold deposit. Three different estimations were considered: (1) ordinary kriging with uncapped data; (2) ordinary kriging with capped data; and (3) Arik's ORK method with uncapped data. Table I shows an example of estimated block grades and percentage of block grades above a series of cut-offs in a mineralized domain from this deposit. At no cut-off, the average estimated grade from capped data (2.0 g/t) is almost identical to the average estimated grades from the ORK method (2.04 g/t). On the other hand, the coefficient of variation CV is much higher from the ORK method, indicating much higher estimated block grade variability. This result is most likely closer to actually recoverable resources than the over-smoothed estimates from ordinary kriging. Once we apply a cut-off to the estimated block grades, the ORK method returns a higher grade and fewer recoverable tons, which is in line with typical results during mining when either blast-hole or underground channel samples are available.

It is interesting to note that locally the estimated block grades can be quite different. Figure 6 shows the estimated high-grade area obtained from the three estimation methods. Not surprisingly, ordinary kriging estimates from uncapped data result in a relatively large area with estimated block grades higher than 3 g/t (Figure 6a). Capping results in the absence of estimated block grades higher than 5 g/t (Figure 6b). On the other hand, estimation from uncapped data with the ORK method results in block estimated grades located somewhere between the potentially too-optimistic (uncapped) and too-pessimistic (capped) ordinary kriged estimates (Figure 6c).

Example 2: South American gold deposit

This second example compares five different approaches to grade estimation on one primary mineralized domain from a South American gold deposit. This one domain is considered to generally be medium grade; however, an interior, continuous high-grade domain was identified, modelled, and considered for resource estimation.

The first three methods consider a single grade domain, while the last two cases consist of two grade domains: the initial medium-grade shell with an interior high-grade shell. Therefore, the last two cases make use of grade domaining as another means to control high-grade influence. Specifically, the five cases considered for comparison are:

Table I

Example 1. Estimated block grades and tonnes for three estimation methods

Cut-off	Block grade estimates								
	Uncapped			Capped			ORK method with uncapped data		
	Grade	Tons (%)	CV	Grade	Tons (%)	CV	Grade	Tons (%)	CV
0	2.44	100	0.66	2	100	0.52	2.04	100	0.85
0.5	2.77	87	0.53	2.25	87	0.38	2.55	79	0.63
1	2.95	80	0.47	2.41	79	0.3	2.77	70	0.56

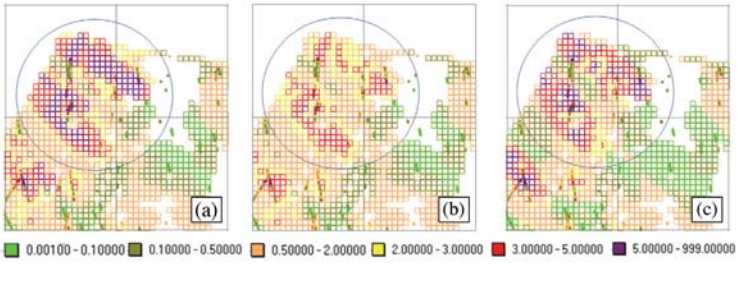

Figure 6—Estimated block grades from (a) uncapped data, (b) capped data, (c) uncapped data and ORK method

(a) One grade domain, uncapped composites
(b) One grade domain, capped composites
(c) One grade domain, capped composites with limited radii imposed on higher grade values
(d) Two grade domains, uncapped data with a hard boundary
(e) Two grade domains, capped data with a hard boundary.

In all cases, estimation is performed using ordinary kriging. Case (a) is referred to as the base case and is effectively a do-nothing scenario. Case (b) considers only the application of grade capping to control high-grade influence. Case (c) considers a two-phase treatment of high-grade data, namely capping grades and also limiting the influence of those that are still considered to be high-grade samples but remain below the cap value. The limiting radii and threshold were chosen based on a preliminary assessment of indicator variograms for various grade thresholds. The last two cases introduce Phase 1 treatment via domaining as another possible solution, with uncapped and capped composites, respectively.

Table II shows a comparison of the relative tons for this mineralized domain as a percentage of the total tons, the average grade of the block estimates, and the relative metal content shown as a percentage of the total ounces relative to the base case, at various cut-off grades. At no cut-off and when only a single grade domain is considered (*i.e.* cases (a) to (c)), we see that capping has only a 4% impact in reducing the average grade and consequently ounces, while limiting the influence of high grade with capping reduces the average grade and ounces by 15%. Results from cases (d) to (e) show that the impact of the grade domain is somewhere between that of using capped data and limiting the influence of the high-grade data. At cut-off grades of 1.0 g/t gold and higher, cases (d) and (e) show a significant drop in tonnage accompanied by much higher grades than the single domain case. In ounces, however, the high-grade domain yields global results similar to the high-grade limited radii option.

To compare the local distribution of grades, a cross-section is chosen to visualize the different cases considered (Figure 7). Notice the magnified region in which a composite gold grade of 44.98 g/t is found surrounded by much lower gold grades. Figures 7a to 7c correspond to the single grade domain, while Figures 7d and 7e correspond to high-grade treatment via domaining, where the interior high-grade domain is shown as a thin polyline. From the base case (Figure 7a), it is easy to see that this single high-grade sample results in a string of estimated block grades higher than 3 g/t. Using capped samples (Figure 7b) has minimal impact on the number of higher grade blocks. Interestingly, limiting the high-grade influence (Figure 7c) has a similar impact to high-grade domaining (Figures 7d and 7e) in that same region. However, the high-grade domain definition has a larger impact on the upper limb of that same domain, where a single block is estimated at 3 g/t or higher, with the majority of the blocks surrounding the high-grade domain showing grades below 1 g/t.

In this particular example, the main issue lies in the over-arching influence of some high-grade composites. Capping accounted for a reduction of the mean grade of approximately 7%; however, it is the local impact of the high grade that is of primary concern. A high-grade domain with generally good continuity was reliably inferred. As such, this more controlled, explicit delineation of a high-grade region is preferred over the more dynamic approach of limiting high-grade influence.

Table II

Example 2. Comparison of HG treatment scenarios

Cutoff grade (g/t)	Tons (% of total)				
	Single grade domain			Medium- and high-grade domain	
	(a) Uncapped	(b) Capped	(c) Limited HG influence, capped	(d) Hard boundary, uncapped	(e) Hard boundary, capped
0.0	100%	100%	100%	100%	100%
0.5	98%	98%	97%	95%	95%
1.0	74%	74%	71%	57%	57%
1.5	46%	46%	41%	36%	36%
Cutoff grade (g/t)	**Average block grade estimates (g/t)**				
	Single grade domain			Medium- and high-grade domain	
	(a) Uncapped	(b) Capped	(c) Limited HG influence, capped	(d) Hard boundary, uncapped	(e) Hard boundary, capped
0.0	1.79	1.71	1.53	1.67	1.61
0.5	1.83	1.74	1.55	1.74	1.67
1.0	2.17	2.06	1.84	2.40	2.29
1.5	2.73	2.56	2.29	3.08	2.90
Cut-off grade (g/t)	**Quantity of metal (% of total)**				
	Single grade domain			Medium- and high grade domain	
	(a) Uncapped	(b) Capped	(c) Limited HG influence, capped	(d) Hard boundary, uncapped	(e) Hard boundary, capped
0.0	100%	96%	85%	93%	90%
0.5	99%	95%	84%	92%	88%
1.0	89%	85%	73%	76%	73%
1.5	70%	65%	52%	62%	59%

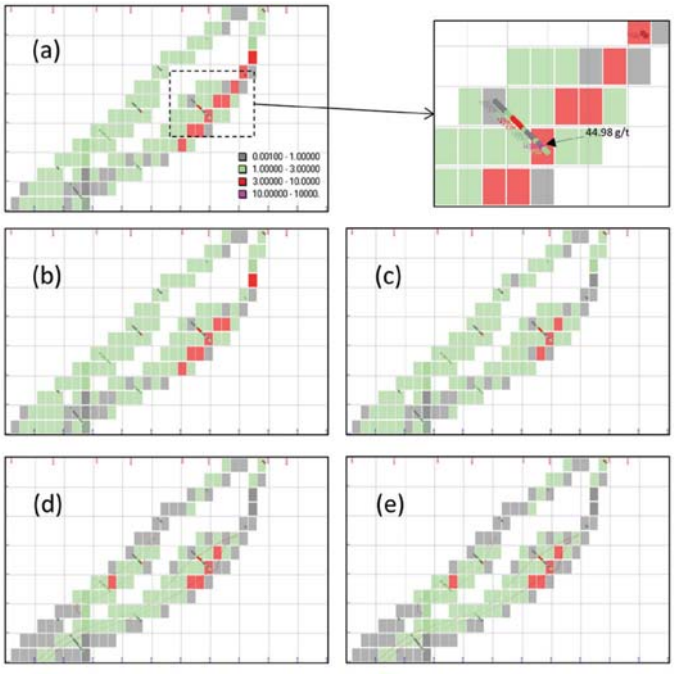

Figure 7—Comparison of high-grade treatment methods: (a) single grade domain, uncapped data; (b) single grade domain, capped data; (c) single grade domain, capped data plus HG limited radii; (d) interior HG domain, uncapped and hard boundaries; and (e) interior HG domain, capped and hard boundaries

Discussion

Many practitioners, geologists, and (geo)statisticians have tackled the impact of high-grade data from many perspectives, broadly ranging from revisiting stationarity decisions to proposals of a mathematical framework to simple, practical tools. The list of methods to deal with high-grade samples in resource estimation in this manuscript is by no means complete. It is a long list, full of good sound ideas that, sadly, many in the industry have likely never heard of. We believe this is due primarily to a combination of software inaccessibility, professional training, and/or time allocated to project tasks.

There remains the long-standing challenging of making these decisions early in pre-production projects, where an element of arbitrariness and/or wariness is almost always present. The goal should be to ensure that the overall contained metal should not be unreasonably lost. Lack of data in early stage projects, however, makes this judgement of representativeness of the data challenging. For later stage projects where production data is available, reconciliation against production should be used to guide these decisions.

This review is intended to remind practitioners and technically-minded investors alike that mitigating the influence of high-grade data is not fully addressed simply by top-cutting or grade capping. For any one deposit, the challenges of dealing with high-grade data may begin with an effort to 'mine' the different methods presented herein and/or lead to other sources whereby a better solution is found that is both appropriate and defensible for that particular project.

Conclusions

It is interesting to note the reaction when high-grade intercepts are discovered during drilling. On the one hand, these high-grade intercepts generate excitement and buzz in the company and potentially the business community if they are publicly announced. This is contrasted with the reaction of the geologist or engineer who is tasked with resource evaluation. He or she generally recognizes that these same intercepts pose challenges in obtaining reliable and accurate resource estimates, including potential overestimation, variogram inference problems, and/or negative estimates if kriging is the method of estimation. Some mitigating measure(s) must be considered during resource evaluation, otherwise the model is likely to be heavily scrutinized for being too optimistic. As such, the relatively straightforward task of top-cutting or grade capping is almost a *de facto* step in constructing most resource models, so much so that many consider it a 'better safe than sorry' task.

This paper reviews different approaches to mitigate the impact of high-grade data on resource evaluation that are applicable at various stages of the resource modelling workflow. In particular, three primary phases are considered: (1) domain design, (2) statistical analysis and application of grade capping, and/or (3) grade estimation. In each stage, various methods and/or tools are discussed for decision-making. Furthermore, applying a tool/method during one phase of the workflow does not preclude the use of other methods in the other two phases of the workflow.

In general, resource evaluation will benefit from an understanding of the controls of high-grade continuity within a geologic framework. Two practical examples are used to illustrate the global and local impact of treating high-grade samples. The conclusion from both examples is that a review of any method must consider both a quantitative and qualitative assessment of the impact of high-grade data prior to acceptance of a resource estimate from any one approach.

Acknowledgments

The authors wish to thank Camila Passos for her assistance with preparation of the examples.

References

ARIK, A. 1992. Outlier restricted kriging: a new kriging algorithm for handling of outlier high grade data in ore reserve estimation. *Proceedings of the 23rd International Symposium on the Application of Computers and Operations Research in the Minerals Industry*. Kim, Y.C. (ed.). Society of Mining Engineers, Littleton, CO. pp. 181–187.

BARNETT, V. and LEWIS, T. 1994. Outliers in Statistical Data. 3rd edn. John Wiley, Chichester, UK.

CARR, J.C., BEATON, R.K., CHERRIE, J.B., MITCHELL, T.J., FRIGHT, W.R., MCCALLUM, B.C., and EVANS, T.R. 2001. Reconstruction and representation of 3D objects with radial basis function. *SIGGRAPH '01 Proceedings of the 28th Annual Conference on Computer Graphics and Interactive Techniques*, Los Angeles, CA, 12-17 August 2001. Association for Computing Machinery, New York. pp. 67–76.

CERIOLI, A. and RIANI, M. 1999. The ordering of spatial data and the detection of multiple outliers. *Journal of Computational and Graphical Statistics*, vol. 8, no. 2. pp. 239–258.

CHILES, J.P. and DELFINER, P. 2012. Geostatistics – Modeling Spatial Uncertainty. 2nd edn. Wiley, New York.

COSTA, J.F. 2003. Reducing the impact of outliers in ore reserves estimation. *Mathematical Geology*, vol. 35, no. 3. pp. 323–345.

COWAN, E.J., BEATSON, R.K., FRIGHT, W.R., MCLENNAN, T.J., and MITCHELL, T.J. 2002. Rapid geological modelling. *Extended abstract: International Symposium on Applied Structural Geology for Mineral Exploration and Mining*, Kalgoorlie, Western Australia, 23–25 September 2002. 9 pp.

COWAN, E.J., BEATSON, R.K., ROSS, H.J., FRIGHT, W.R., MCLENNAN, T.J., EVANS, T.R., CARR, J.C., LANE, R.G., BRIGHT, D.V., GILLMAN, A.J., OSHUST, P.A., and TITLEY, M. 2003. Practical implicit geological modelling. *5th International Mining Geology Conference*, Bendigo, Victoria, November 17–19, 2003. Dominy, S. (ed.). Australasian Institute of Mining and Metallurgy Melbourne. Publication Series no. 8. pp. 89–99.

COWAN, E.J., SPRAGG, K.J., AND EVERITT, M.R. 2011. Wireframe-free geological modelling – an oxymoron or a value proposition? *Eighth International Mining Geology Conference,* Queenstown, New Zealand, 22-24 August 2011. Australasian Institute of Mining and Metallurgy, Melbourne. pp 247–260.

EMERY, X. and ORTIZ, J.M. 2005. Estimation of mineral resources using grade domains: critical analysis and a suggested methodology. *Journal of the South African Institute of Mining and Metallurgy*, vol. 105. pp. 247–256.

GUARDIANO, F. and SRIVASTAVA, R.M. 1993. Multivariate geostatistics: beyond bivariate moments. *Geostatistics Troia*, vol. 1. Soares, A. (ed.). Kluwer Academic, Dordrecht. pp. 133–144.

GUIBAL, D. 2001. Variography – a tool for the resource geologist. *Mineral Resource and Ore Reserve Estimation – The AusIMM Guide to Good Practice*. Edwards, A.C. (ed.). Australasian Institute of Mining and Metallurgy, Melbourne.

HAWKINS, D.M. 1980. Identification of Outliers. Chapman and Hall, London.

HAWKINS, D.M. and CRESSIE, N. 1984. Robust kriging – a proposal. *Mathematical Geology*, vol. 16, no. 1. pp. 3–17.

JOHNSON, R.A. and WICHERN, D.W. 2007. Applied Multivariate Statistical Analysis, 6th edn. Prentice-Hall, New Jersey.

JOURNEL, A.G. and ARIK, A. 1988. Dealing with outlier high grade data in precious metals deposits. *Proceedings of the First Canadian Conference on Computer Applications in the Mineral Industry*, 7–9 March 1988. Fytas, K., Collins, J.L., and Singhal, R.K. (eds.). Balkema, Rotterdam. pp. 45–72.

KRIGE, D.G. and MAGRI, E.J. 1982. Studies of the effects of outliers and data transformation on variogram estimates for a base metal and a gold ore body. *Mathematical Geology*, vol. 14, no. 6. pp. 557–564.

LEUANGTHONG, O. and SRIVASTAVA, R.M. 2012. On the use of multigaussian kriging for grade domaining in mineral resource characterization. *Geostats 2012. Proceedings of the 9th International Geostatistics Congress*, Oslo, Norway, 10–15 June 2012. 14 pp.

LIU, H., JEZEK, K.C., and O'KELLY, M.E. 2001. Detecting outliers in irregularly distributed spatial data sets by locally adaptive and robust statistical analysis and GIS. *International Journal of Geographical Information Science*, vol. 15, no. 8. pp 721–741.

LU, C.T., CHEN, D., and KOU, Y. 2003. Algorithms for spatial outlier detection. *Proceedings of the Third IEEE International Conference on Data Mining (ICDM '03)*, Melbourne, Florida, 19–22 November 2003. DOI 0-7695-1978-4/03. 4 pp.

LU, C.T., CHEN, D., and KOU, Y. 2004. Multivariate spatial outlier detection. *International Journal on Artificial Intelligence Tools*, vol. 13, no. 4. pp 801–811.

NEFF, D.H., DRIELICK, T.L., ORBOCK, E.J.C., and HERTEL, M. 2012. Morelos Gold Project: Guajes and El Limon Open Pit Deposits Updated Mineral Resource Statement Form 43-101F1 Technical Report, Guerrero, Mexico, June 18 2012. http://www.torexgold.com/i/pdf/reports/Morelos-NI-43-101-Resource-Statement_Rev0_COMPLETE.pdf 164 pp.

NOWAK, M., LEUANGTHONG, O., and SRIVASTAVA, R.M. 2013. Suggestions for good capping practices from historical literature. *Proceedings of the 23rd World Mining Congress 2013*, Montreal, Canada, 11–15 August 2013. Canadian Institute of Mining, Metallurgy and Petroleum. 10 pp.

PARKER, H.M. 1991. Statistical treatment of outlier data in epithermal gold deposit reserve estimation. *Mathematical Geology*, vol. 23, no. 2. pp 175–199.

PARRISH, I.S. 1997. Geologist's Gordian knot: to cut or not to cut. *Mining Engineering*, vol. 49. pp 45–49.

RIVOIRARD, J., DEMANGE, C., FREULON, X., LECUREUIL, A., and BELLOT, N. 2012. A top-cut model for deposits with heavy-tailed grade distribution. *Mathematical Geosciences*, vol. 45, no. 8. pp. 967–982.

ROSCOE, W.E. 1996. Cutting curves for grade estimation and grade control in gold mines. *98th Annual General Meeting,* Canadian Institute of Mining, Metallurgy and Petroleum, Edmonton, Alberta, 29 April 1996. 8 pp.

SINCLAIR, A.J. and BLACKWELL, G.H. 2002. Applied Mineral Inventory Estimation.Cambridge University Press, Cambridge.

SRIVASTAVA, R.M. 2001. Outliers – A guide for data analysts and interpreters on how to evaluate unexpected high values. Contaminated Sites Statistical Applications Guidance Document no. 12-8, British Columbia, Canada. 4 pp. http://www.env.gov.bc.ca/epd/remediation/guidance/technical/pdf/12/gd08_all.pdf [Accessed 8 Aug. 2013].

STEGMAN, C.L. 2001. How domain envelopes impact on the resource estimate – case studies from the Cobar Gold Field, NSW, Australia. *Mineral Resource and Ore Reserve Estimation – The AusIMM Guide to Good Practice*. Edwards, A.C. (ed.). Australasian Institute of Mining and Metallurgy. Melbourne.

STREBELLE, S. and JOURNEL, A.G. 2000. Sequential simulation drawing structures from training images. *Proceedings of the 6th International Geostatistics Congress*, Cape Town, South Africa, April 2000. Kleingeld, W.J. and Krige, D.G. (eds.). Geostatistical Association of Southern Africa. pp. 381–392.

STREBELLE, S. 2002. Conditional simulation of complex geological structures using multiple-point statistics. *Mathematical Geology*, vol. 34, no. 1. pp. 1–21.

WHYTE, J. 2012. Why are they cutting my ounces? A regulator's perspective. *Presentation: Workshop and Mini-Symposium on the Complexities of Grade Estimation*, 7 February 2012. Toronto Geologic Discussion Group. http://www.tgdg.net/Resources/Documents/Whyte_Grade%20Capping%20talk.pdf [Accessed 8 Aug. 2013]. ◆

http://dx.doi.org/10.17159/2411-9717/2015/v115n1a4

Robust and resistant semivariogram modelling using a generalized bootstrap

by R.A. Olea*, E. Pardo-Igúzquiza†, and P.A. Dowd ‡

Synopsis

The bootstrap is a computer-intensive resampling method for estimating the uncertainty of complex statistical models. We expand on an application of the bootstrap for inferring semivariogram parameters and their uncertainty. The model fitted to the median of the bootstrap distribution of the experimental semivariogram is proposed as an estimator of the semivariogram. The proposed application is not restricted to normal data and the estimator is resistant to outliers. Improvements are more significant for data-sets with less than 100 observations, which are those for which semivariogram model inference is the most difficult. The application is illustrated by using it to characterize a synthetic random field for which the true semivariogram type and parameters are known.

Keywords
geostatistics, sampling distribution, median, normal score transformation, ordinary least-squares fitting.

Introduction

The semivariogram is a second-order moment used in geostatistics for quantifying spatial correlation. We assume a true underlying semivariogram model, $\gamma(\mathbf{h})$, which quantifies the second-order spatial correlation of the population of all values of a spatial (or regionalized) random variable, $Z(\cdot)$; a semivariogram, $\hat{\gamma}(\mathbf{h})$, can be inferred from a set of data values, $z(\mathbf{u}_i)$, measured at the set of (relatively sparse) locations $\{\mathbf{u}_i\}$. The underlying semivariogram is defined as:

$$\gamma(\mathbf{h}) = \frac{1}{2} \cdot Var\left[Z(\mathbf{u}) - Z(\mathbf{u}+\mathbf{h})\right] \quad [1]$$

where $\mathbf{h}$ is a vector denoting the direction and the Euclidean distance between a pair of locations (*e.g.* Journel and Kyriakidis, 2004). Although several approaches have been proposed to estimate the semivariogram from the available data, the most commonly used is the unbiased estimator:

$$\hat{\gamma}(\mathbf{h}) = \frac{1}{2 \cdot N(\mathbf{h})} \cdot \sum_{i=1}^{N(\mathbf{h})} \left[z(\mathbf{u}_i) - z(\mathbf{u}_i+\mathbf{h})\right]^2 \quad [2]$$

where $N(\mathbf{h})$ is the number of pairs of data values separated by the directional distance $\mathbf{h}$ (*e.g.* Chilès and Delfiner, 2012). This estimator is valid only if the increments (differences) of the regionalized variable are second-order stationary. When the sampling is regular, the calculations are done for multiples of the sampling interval. Otherwise, the distances are grouped into appropriate classes and the effective values of $\mathbf{h}$ are the centroids of these classes. The discrete set of $\hat{\gamma}(\mathbf{h})$ values is called variously the sample, experimental, or empirical semivariogram. Semivariogram is also sometimes shortened to 'variogram' in the literature.

For any distance, the ultimate aim is to infer the underlying (or population) semivariogram from a sample. The traditional solution is to fit an analytical model to a set of $\hat{\gamma}(\mathbf{h})$ values. The type of model is restricted to those that ensure positive definiteness of variance-covariance matrices in subsequent calculations, which ensures that the solution exists and is unique when the matrix is used in kriging equations. Commonly used semivariogram models include the spherical, exponential, and Gaussian (*e.g.* Olea, 2009). To maximize consistency between models and data, model parameters are obtained by fitting the model equations to the experimental points either (a) semi-manually with the assistance of graphical software in which the goodness of fit is decided visually, or (b) automatically by using some sort of optimization method. It is often the case that: (i) there are too few pairs for a given distance, (ii) the empirical semivariogram is noisy, and (iii) the data are not normally distributed.

The objective here is to describe the results of work conducted to overcome some of the problems with the two-step approach of calculating semivariogram values and fitting a

* *US Geological Survey, Reston, USA.*

† *Instituto Geológico y Minero de España (IGME), Madid, Spain.*

† *Faculty of Engineering, Computer and Mathematical Sciences, University of Adelaide, Adelaide, Australia.*

model, in particular, to: (a) minimize discrepancies between the underlying and the modelled semivariograms, (b) propose a method that is resistant to data preparation errors and robust to departures from normality, and (c) quantify the uncertainty of the estimated model parameters. The results are improvements over previous efforts (Pardo-Iguzquiza and Olea, 2012) in the sense that:

- The bootstrap semivariogram is proposed for inferring the semivariogram model (*i.e.* semivariogram parameters)
- A procedure is proposed for building confidence intervals
- The bias, variance, and mean square error for the semivariogram parameters are given for a synthetic random field for which semivariogram parameters are known
- The robustness and resistance of the proposed approach are analysed.

Robustness and resistance

Equation [2] is a quadratic estimator. Consequently, although theoretically unbiased, it shares all the problems of such estimators, including sensitivity to (a) small sample sizes, (b) skewness in the sample distribution, and (c) presence of outliers. We apply three techniques to mitigate the effect of these factors.

Bootstrap

For a given sample size, n, the bootstrap allows the generation of new samples of the same size. This is accomplished by resampling the sample data-set with replacement, producing multiple data-sets of size n. The new data-sets tend to be all different because in any given resampling some values will be sampled more than once and some will not be sampled at all (*e.g.* Efron and Tibshirani, 1994). These new samples – called bootstrap samples or resamples – are intended to mimic the results that would have been obtained from other samples that could have been drawn from the random field.

Given a sample of size n, the bootstrap is a method for predicting the dispersion in results that would occur if all possible samples of the same size n were drawn from the population. The classical bootstrap steps for identically distributed and independent values are:

1. Select at random and with replacement n values from the available sample
2. Use the resample values to calculate any statistic of interest, say, the mean, and store the results
3. Go back to Step 1 and repeat the process a large number of times, at least 1000 times
4. Stop.

The set of values generated in Step 2 is the numerical approximation of the variability in the parameter that would be obtained by actually collecting multiple samples of size n.

If the data are spatially correlated then the bootstrap resamples will not be independent and the assumption will be violated. Therefore the application of the bootstrap to spatially correlated data requires two additional steps. First, the spatial correlation must be removed to satisfy the requirement that the values are independent. Once the resample is obtained, the spatial correlation must be re-introduced (Solow, 1985; Pardo-Igúzquiza and Olea, 2012). The effectiveness of the first step could be tested by the p-values of a decorrelation test of normal scores as described in Pardo-Igúzquiza and Olea (2012). However, this has not been pursued further in the proposed approach.

For samples that include abnormally high values, the bootstrap can produce other more typical resamples. By doing so, the values of the parameter of interest, the semivariogram in our case, will also be less extreme and closer to the underlying value, which is the ultimate objective of any statistical inference. The bootstrap filters extreme values by exclusion.

Normal score transformation

The normal score transformation is a bijection between the sample distribution and a standard normal (Gaussian) distribution (*e.g.* Olea, 2009). Given a sample of size n, it is always possible to rank the values to obtain n quantiles. The bijection is the operation by which the ith measurement in the sample is assigned the value of the standard normal distribution for the same ith quantile. Thus, for example, if 20.8 ranks 50 in a sample of size 200, its normal score transformation is –0.675. Most formulations in statistics are either strictly valid for normal distributions or behave better when the sample is normal. The normal score transformation, for example, minimizes the influence of values in the high tail of a positively skewed distribution by scaling the entire sample distribution. The transform reduces the impact of outliers by rescaling to a normal distribution.

The median

The median is the value that divides a sample into two classes of low and high values, each with the same number of measurements. Thus, the median is completely insensitive to changes in observation ranking that do not result in a move from one class to the other. For example, if the median is 45.5 and an observation of 60.9 is erroneously coded as 609, the error has absolutely no effect on the median. If instead, it is miscoded as 6.09, the median does change, but only slightly, to the nearest value below 45.5, say, 44.8. The resistance of the median to these types of changes or to true abnormally high values contrasts significantly with the sensitivity of quadratic statistics (*e.g.* Cox and Pardo-Igúzquiza, 2001), such as the variance or the semivariogram, particularly to changes in the upper tail of a distribution. Thus, the median buffers the results from outliers.

In a loss function context, the median is the moment that minimizes the sum of absolute errors. In contrast, the mean minimizes the sum of quadratic errors (Klugman *et al.*, 2012).

More than thirty years ago, Armstrong and Delfiner (1980) explored the possibility of estimating the semivariogram in terms of quantiles, but their work has largely been ignored. Other approaches to robust and resistant calculation of semivariograms can be found, *inter alia*, in Cressie and Hawkins (1980), Cressie (1984), and Dowd (1984).

Performing a fitting to the median of squared differences instead of directly to the empirical semivariogram reduces the sensitivity of the semivariogram modelling to erratic fluctuations. We still use Equation [2] to generate values of an

empirical semivariogram as there is no point in using the median for this purpose. The difference here is that the modelling does not stop there. We use the generalized bootstrap to generate multiple empirical semivariograms. The median is used as a measure of central tendency for the set of all bootstrap empirical semivariograms for which the fitting is done.

Algorithm

Conformance of the empirical semivariogram with the underlying semivariogram is a necessary condition for the semivariogram model to follow the underlying semivariogram. The general idea is to post-process (filter) the traditional estimator resulting from the application of Equation [2] to remove all the noise that ordinarily causes the empirical semivariogram to deviate from the underlying semivariogram. In this regard, our proposal differs from that of Armstrong and Delfiner (1980) in which the estimator is replaced by the median and the results are corrected to obtain the mean experimental semivariogram.

The algorithm is iterative in the sense of the Kirkpatrick *et al.* (1983) solution to the classical travelling salesman problem and the simulated annealing of Deutsch and Journel (1998). It comprises two loops, an inner one to generate multiple resamples and an outer one to obtain median semivariograms, as many as necessary to reach convergence. The method stops either when a maximum number of iterations has been reached or the discrepancy between the semivariogram models in the last two iterations is below a threshold. Our approach determines a distance increment to model empirical semivariograms and makes use of two types of analytical models, one for the attribute (B) and another one for its normal scores (A). The iterative steps are:

1. Read in the data
2. Set the number of resamples, the distance interval, the stopping value, and the maximum number of iterations
3. Select the analytical type of the semivariogram model both for the attribute and the normal scores
4. Transform the attribute measurements to normal scores
5. Use a sample of size n to calculate the empirical semivariogram
6. Automatically fit a semivariogram model of type A, which becomes the starting model
7. Use the normal score semivariogram model to calculate the covariance model for all pairs of data locations
8. Apply the Cholesky decomposition to spatially decorrelate the original normal scores to generate a new set of independent normal score values
9. Take a bootstrap resample of the decorrelated values
10. Run a test to check that the normal scores are indeed decorrelated and store the p-value
11. Make the resample spatially correlated by inverting the Cholesky method
12. Calculate the empirical semivariogram for the normal scores and store the results
13. Back-transform the values to their original space
14. Calculate the empirical semivariogram for the resample and store the results
15. Go back to Step 9 if the minimum number of resamples has not been reached. Otherwise, continue to the next step
16. For every distance, take the median value of the estimated semivariogram for the normal scores and for the attribute and then fit corresponding semivariograms of type A and B. If this is the first pass, go back to Step 7. Otherwise, continue
17. If G_i and G_{i+1} are the last two semivariogram models of type B, calculate

$$D(G_i(h), G_{i+1}(h)) = \int_0^\infty [G_i(h) - G_{i+1}(h)]^2 \, dh \qquad [3]$$

and compare it to the stopping value. If the maximum number of iterations has not been reached and the integral is larger than the stopping value, go back to Step 7. Otherwise, stop; G_{i+1} is the semivariogram model for the attribute.

In general, the analytical expression for the semivariogram of the attribute and that of its normal scores may be different and certainly unknown (Stefanou *et al.*, 2004). The algorithm can be simplified for the case when the semivariogram of interest is for the normal scores or for normally distributed values.

The normal scores in Steps 8 and 9 are perfectly decorrelated if, and only if, the semivariogram used to define the correlation matrix is exactly the underlying semivariogram (Hoeksema and Kitanidis, 1985). If the user is interested in investigating the mathematical goodness of alternative semivariogram models, the p-value offers an adequate criterion for comparisons.

Case study

Exhaustive sample

A simulated realization of a Gaussian random field is used as an exhaustive sample at a finite number of experimental locations. The advantage of using a synthetic example is that the underlying semivariogram parameters are known and thus the performance of the estimators can be compared in terms of bias, variance, and mean square error. Furthermore, the simulated realization is guaranteed to follow the imposed model, whereas a natural phenomenon will do so only in an approximate manner. Figure 1 shows a realization of a second-order stationary, zero-mean, Gaussian random field with an exponential semivariogram with range 10 units, nugget variance 0.3, partial sill of 0.7, and thus total variance of 1.0. The realization in Figure 1 comprises a grid of 128 × 128 locations with unit grid sides in the X and Y directions. All 16 384 values on the grid were used to calculate the exhaustive experimental semivariogram for the realization shown in Figure 2, together with the model fitted to it:

$$\gamma(h) = 0.3 + 0.7\mathrm{Exp}(h;10)$$

which is the exact theoretical model used to generate the simulation.

In practice, of course, an exhaustive sampling is not possible and, in most geoscience applications, the total sample volume is significantly less than 1% of the total volume from which the measurements are taken. For example, a quartz-vein hosted gold deposit extending over an area of 900 m × 300 m and a vertical extent of 150 m would

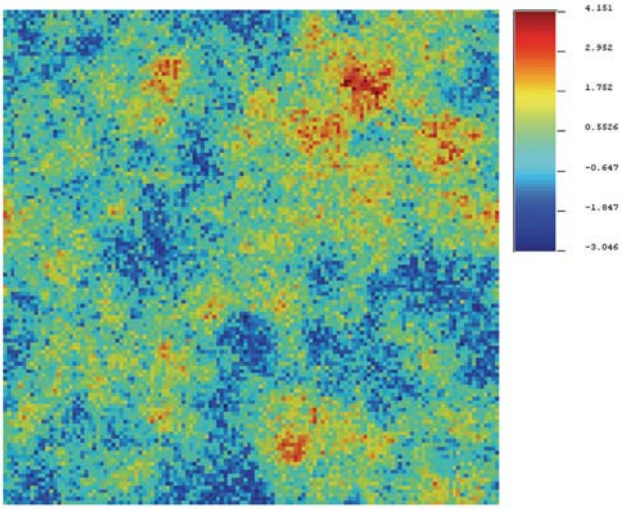

Figure 1—Simulated realization of a Gaussian random field of 128 by 128 nodes with nugget variance of 0.3, total variance of 1.0, and an exponential semivariogram of range 10 units (*i.e.* practical range of 30 units)

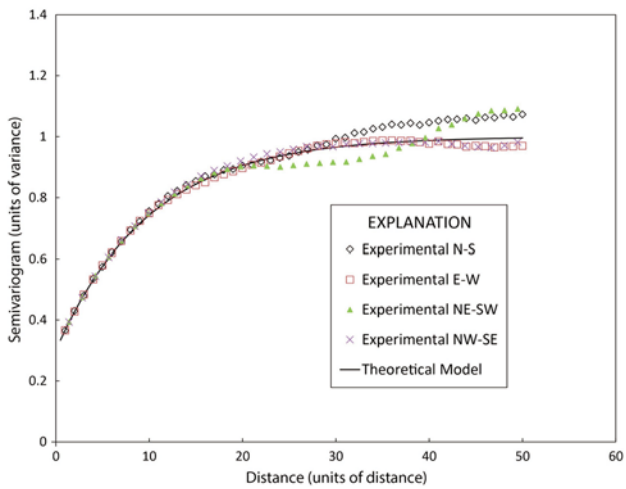

Figure 2—Exhaustive experimental semivariogram of the complete 128×128 data-set for the four main geographical directions. The best fit is obtained with the true values of the underlying model

typically be sampled for reserve estimates on a drilling grid of 30 m (along strike) × 15 m (across strike). Assuming that each drill-hole is 150 m in length and that the diameter of the core is 10 cm, the total sample volume represents 0.002% of the total orebody volume. The proportion of samples does, of course, have to be tempered by the range of spatial correlation and the nugget effect to account just for the independent amount of information in the sample, thus reducing even further the sample representativity. In the synthetic simulated example reported here for demonstration purposes, we have considered primarily samples of size 50, which are: (a) 0.3% of the total possible number of samples that could be taken, and (b) on average, 18 units away from the nearest neighbour, or 60% of the effective range of 30 units. The analysis included samples up to size 200 in some cases.

Assessment of the new estimator

In order to assess the algorithm, a larger number of samples, M, is generated by random sampling from the exhaustive grid of values in Figure 1. For this work we chose 200 ($M = 200$) for the total number of samples, and 50 ($n = 50$) for the size of each sample. We specify the semivariogram model as exponential, and compare a conventional model-fitting method to the bootstrapped fitting method. The traditional procedure is to find the exponential model parameters by fitting the model to the experimental semivariogram. Our method calculates the bootstrapped median semivariogram parameters for the exponential model. We then compare the two methods using measures of bias, variance, and mean square error.

For the ith sample, a given semivariogram model parameter θ is estimated and the estimated value is denoted θ_i^*. The mean and variance of the estimated parameter values are given by:

$$\overline{\theta}^* = \frac{1}{M}\sum_{i=1}^{M}\theta_i^* \qquad [4]$$

$$\sigma^2_{\theta^*} = \frac{1}{M}\sum_{i=1}^{M}\left(\theta_i^* - \theta\right)^2 \qquad [5]$$

The bias (B) and mean square error (MSE) are estimated as:

$$\mathrm{B} = \overline{\theta}^* - \theta \qquad [6]$$

and

$$\mathrm{MSE} = \mathrm{B}^2 + \sigma^2_{\theta^*} \qquad [7]$$

respectively.

Bias, variance, and mean square error are used to assess the performance of the median semivariogram estimator with respect to conventional estimator (ordinary least-squares fitting of the exponential semivariogram model to the experimental variogram) for several situations of interest. We focus on the most usual semivariogram parameters in the so-called basic Matheron representation: range, nugget variance, and total variance.

The results of 1, 5, 10, and 30 iterations for a base case are shown in Tables I–III for the three parameters nugget variance, total variance, and range. The decrease in mean square error is different for the different parameters and it is concluded that most of the gain is obtained from the first iteration.

Resistance to outliers was checked by comparing the results using samples from Figure 1 with the results from a contaminated sample. Two contaminations have been used: (a) 10% contamination from a Gaussian distribution with zero mean and variance 10, and (b) adding a single outlier of fixed value 7, which is seven times the standard deviation from the mean. The results are shown in Tables IV to VI for the three parameters of an exponential semivariogram. For the first contamination the bootstrap estimator produces a reduction in the mean square error with respect to ordinary least squares (OLS) for all three parameters. For the second contamination the reduction is smaller, although the contamination model is somewhat naïve.

Table I

Results for the range parameter for 200 samples of size 50. The true value of the range is 10. Mean, bias, variance, and mean square error (MSE) for the OLS fitting and the fitting to the median of the bootstrap distribution

Range	Mean	Bias	Variance	MSE
Conventional experimental	11.42	1.42	44.396	46.412
Bootstrap 1 iterations	11.89	1.89	29.078	32.678
Bootstrap 5 iterations	10.93	0.93	24.370	25.531
Bootstrap 10 iterations	10.84	0.84	25.623	26.337
Bootstrap 30 iterations	11.72	1.72	26.23	29.206

Table II

Results for the nugget variance parameter for 200 samples of size 50. The true value of the nugget is 0.3. Mean, bias, variance. and mean square error (MSE) for the OLS fitting and the fitting to the median of the bootstrap

Nugget variance	Mean	Bias	Variance	MSE
Conventional experimental	0.25	-0.05	0.085	0.088
Bootstrap 1 iterations	0.16	-0.14	0.030	0.049
Bootstrap 5 iterations	0.15	-0.14	0.037	0.059
Bootstrap 10 iterations	0.13	-0.17	0.028	0.057
Bootstrap 30 iterations	0.15	-0.15	0.028	0.051

Table III

Results for the total variance parameter for 200 samples of size 50. The true value of the total variance is 1.0. Mean, bias, variance, and mean square error (MSE) for the OLS fitting and the fitting to the median of the bootstrap distribution by using one iteration, five iterations, ten iterations, and thirty iterations

Total variance	Mean	Bias	Variance	MSE
Conventional experimental	1.04	0.04	0.054	0.056
Bootstrap 1 iterations	1.00	0.00	0.043	0.043
Bootstrap 5 iterations	0.98	-0.02	0.048	0.049
Bootstrap 10 iterations	0.96	-0.04	0.041	0.043
Bootstrap 30 iterations	1.00	0.00	0.040	0.040

Robustness with respect to departure from the Gaussian distribution was tested by comparing the results obtained when sampling from the Gaussian random field in Figure 1 with those obtained when sampling from the highly skewed chi-squared field resulting from squaring the Gaussian random field. The distribution is skewed as shown in Figure 3, and the range of the exponential covariance is halved so that the new target range is five units of distance. The results are shown in Tables VII to IX, from which it can be seen that the median semivariogram estimator has a mean square error that is smaller than that the OLS estimates, but the improvement is not as great as in the Gaussian case.

Table IV

Results for the range parameter for the OLS and the median bootstrap methods applied to the outlier contaminated data using 200 samples of size 50. The true value of the range is 10. In (1), 10% of the values are drawn from a zero-mean normal distribution with variance 10. In (2), a fixed outlier value of 7 was added to each realization

Range	Mean	Bias	Variance	MSE
(1) Experimental	7.49	-2.51	42.257	48.532
Bootstrap 1 iteration	9.70	-0.30	20.027	20.027
(2) Experimental	8.13	-1.87	46.405	49.902
Bootstrap 1 iteration	12.24	-2.24	18.494	23.512

Table V

Results for the nugget variance parameter for the OLS and the median bootstrap methods applied to the outlier contaminated data using 200 samples of size 50. The true value of the nugget is 0.3. In (1), 10% of the values are drawn from a zero-mean normal distribution with variance 10. In (2), a fixed outlier value of 7 was added to each realization

Nugget variance	Mean	Bias	Variance	MSE
(1) Experimental	0.64	0.34	0.924	1.041
Bootstrap 1 iteration	0.26	-0.04	0.138	0.139
(2) Experimental	0.43	0.13	0.600	0.617
Bootstrap 1 iteration	0.18	-0.12	0.041	0.055

Table VI

Results for the total variance parameter for the OLS and the median bootstrap methods applied to the outlier contaminated data using 200 samples of size 50. The true value of the total variance is 0.3. In (1), 10% of the values are drawn from a zero-mean normal distribution with variance 10. In (2), a fixed outlier value of 7 was added to each realization

Total variance	Mean	Bias	Variance	MSE
(1) Experimental	1.96	0.96	0.528	1.455
Bootstrap 1 iteration	1.77	0.77	0.401	1.003
(2) Experimental	2.07	1.07	0.155	1.313
Bootstrap 1 iteration	1.58	0.58	0.130	0.469

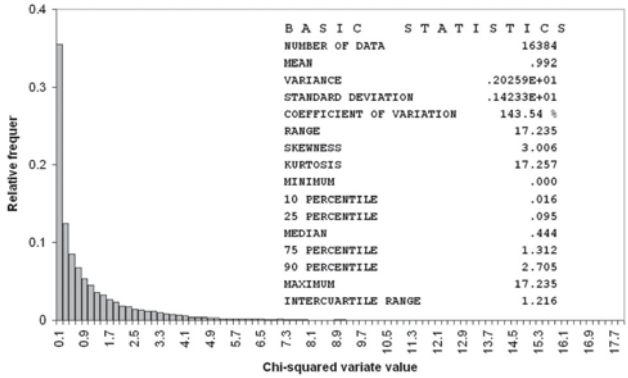

Figure 3—Histogram of the chi-squared field from squaring the realization shown in Figure 1

Table X shows the results of a sensitivity analysis of the type of analytical model. All results were obtained assuming the correct exponential model. The method showed some discrimination power for automatically predicting the model type.

Discussion

Number of samples

For small sample sizes, the new method is an improvement relative to fitting values to $\hat{\gamma}(\mathbf{h})$ from Equation [2], but the improvement declines as the number of samples increases. For 100 data values (or 0.6% of the total possible samples in our case study) the improvement is less than 3% and the results are not significantly different. Nevertheless, there are many important applications that are confined to small datasets (tens of values) and for which the median bootstrap estimator offers significant improvements. In addition, as noted earlier, in most geoscience applications a sample of 0.6% of the total mass to be sampled is, in fact, a relatively large sample. For the gold orebody example cited earlier, a sample proportion of 0.6% would require a drilling grid of 5 m × 2.5 m or 36 times more drill-holes, which would be economically unfeasible.

Comparing different semivariogram parameters for the same model

Equation [3] allows the comparison of semivariogram models by redefining G_i and G_{i+1} as the underlying model and an estimated model. For the case of the exponential model, Table XI shows the results for the same 200 samples used to prepare Tables I–III.

The median bootstrap estimate performs better than the conventional estimate for sample sizes of less than 100. For the 200 samples, the bootstrap models give smaller discrepancies in 116 cases; the total discrepancy is 652.0 against 827.5 for the conventional model fitting and the mean misfit at a distance of half the range (*i.e.* five units of distance) decreases from 0.50 to 0.31. Thus, using the previous criterion, the model fitted by the bootstrap method is significantly better than the model fitted directly to the values obtained from Equation [2].

Robustness

Robustness with respect to departure from normality is perhaps the best property of the new estimator because, when working with true experimental geoscience data,

Table VII

Results for the range with respect to robustness against non-normality using 200 samples of size 50. The true value of the range is 5

Range	Mean	Bias	Variance	MSE
(1) Experimental	6.92	1.92	40.636	44.636
Bootstrap 1 iteration	8.79	3.79	22.020	36.441
Bootstrap 5 iterations	8.43	3.43	20.721	32.503
Bootstrap 10 iterations	8.68	3.68	17.818	31.397
Bootstrap 30 iterations	8.47	3.37	19.171	31.212

Table VIII

Results for nugget with respect to robustness against non-normality using 200 samples of size 50. The true value of the nugget is 1.02

Nugget variance	Mean	Bias	Variance	MSE
(1) Experimental	0.59	-0.01	0.916	0.916
Bootstrap 1 iteration	0.25	-0.35	0.160	0.281
Bootstrap 5 iterations	0.26	-0.76	0.158	0.741
Bootstrap 10 iterations	0.28	-0.73	0.176	0.714
Bootstrap 30 iterations	0.26	-0.76	0.199	0.773

Table IX

Results for total variance with respect to robustness against non-normality using 200 samples of size 50. The true value of total variance is 2.0

Total variance	Mean	Bias	Variance	MSE
(1) Experimental	2.04	0.04	0.897	0.898
Bootstrap 1 iteration	1.82	-0.18	0.718	0.749
Bootstrap 5 iterations	1.79	-0.21	0.758	0.803
Bootstrap 10 iterations	1.75	-0.24	0.635	0.696
Bootstrap 30 iterations	1.79	-0.20	0.705	0.745

Table X

Sensitivity to the type of analytical model. Out of 200 resamples, the number of times discrepancy with underlying semivariogram was best in terms of minimal sum of square errors

Sample size	Exponential	Gaussian	Spherical
50	100	99	1
100	116	61	23

Table XI

Discrepancies according to Equation [3] for the same samples of size 50 in Tables I–III, where h is the lag distance

	Conventional experimental	Bootstrap 1 iteration
Number of times with lowest misfit	84	116
Total misfit	827.522	651.998
Mean misfit for h = 5	0.504	0.314
Mean misfit for h = 4	0.425	0.258
Mean misfit for h = 3	0.338	0.202
Mean misfit for h = 2	0.243	0.143
Mean misfit for h = 1	0.134	0.078

although the underlying probability density function is almost always unknown, the presence of skewed histograms is the norm rather than the exception.

Resistance

The median bootstrap estimator is resistant with respect to contamination (Tables IV–VI). This is a significant practical advantage as abnormally high values are common in geoscience data and particularly in grade values for mineral deposits. Outliers can significantly and adversely affect the method of moments semivariogram estimator and, for this reason, there is reluctance to using it for analyses and estimations (Krige and Magri, 1982).

Uncertainty evaluation

A fundamental objective of any inference method should be to provide the uncertainty of the estimated parameters, especially for small data-sets for which the uncertainty may be large and, consequently, the use of estimated parameters may be meaningless. The most practical way of specifying the uncertainty in an inference problem is by providing probabilistic interval estimates for the parameters. That is, instead of single values, provide an interval containing the true underlying and unknown parameters with a given level of probability. This can be easily obtained from the proposed procedure by fitting a model to each of the 1000 bootstrap samples and then obtaining percentile bootstrap intervals from the bootstrap distribution of the estimated parameters. The median of this bootstrap distribution produces results similar to, but slightly worse than, results from fitting a model to the median semivariogram, and thus this procedure is used only for estimating the uncertainty in the form of percentile confidence intervals. Figure 4 shows the results of an experiment in which the achieved coverage of these confidence intervals was calculated and compared with their nominal coverage. The results show that for low nominal coverage (less than 40%), the achieved coverage is close to the nominal values for the nugget and the range. For high values of the nominal coverage (greater than 65%), the achieved coverage is close the nominal coverage for the total variance parameter and the coverage is overestimated (*i.e.* on the safe side) for the nugget variance and range parameters.

Sensitivity to type of analytical model

All results were obtained by assuming the correct exponential model. In a real case study, however, in general the type of model is unknown. Particularly for small data-sets, the significant scatter of the experimental values provides scope for assuming different analytical models. In addition to estimating the underlying parameters, we tested the capability of the methodology to predict the correct functional form of the semivariogram. The testing was limited to three basic choices: exponential, spherical, and Gaussian. Table X shows the number of times each model produced the best result, defined as the best fit to the set of points defining the resulting median semivariogram. In this case at least, the method showed limited discrimination power, indicating that it was insufficient to rely on an automatic prediction of the model type. This ability, however, improved with the sample size.

Conclusions

A new approach to modelling the semivariogram estimator has been proposed: the median bootstrap semivariogram. The new method is an improvement on the conventional approach of directly fitting a model to a few empirical semivariogram values. According to an evaluation based on a synthetic exhaustive sample, the improvement is significant mainly for small sample sizes (with n less than 100, or 0.6% of the total possible samples, for the demonstration example). The new estimator has proved to be resistant to slight contamination of the sample distribution and significantly robust to departures from normality. Although further research is required on mathematical proofs, the results are encouraging for incorporating the estimator in computer implementations in which a large number of automatic fittings are required as,

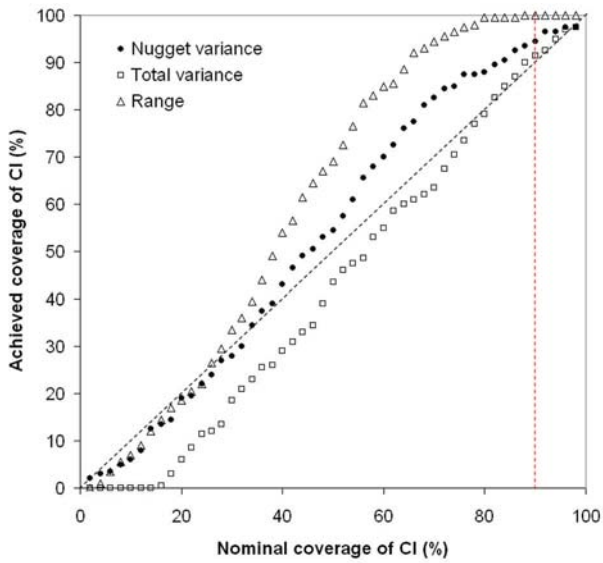

Figure 4—Nominal coverage *versus* the achieved coverage for the confidence intervals calculated by bootstrap. The achieved coverage for a nominal coverage of 90% (vertical dashed red line) is 91.5% for total variance, 94.5% for nugget variance, and 100% for the range. The overestimation of coverage is on the safe side of providing an uncertainty slightly larger than it should be

for example, when applying moving window statistics in remote sensing, contouring, and other global applications of geostatistics.

Acknowledgements

The authors are grateful to Geoffrey Phelps (US Geological Survey) and to Frederik Agterberg (Geological Survey of Canada) for constructive discussion of an earlier version of the manuscript. The work of the second author was supported by the research project KARSTINV CGL2010-15498 from the Ministerio de Economía y Competitividad of Spain. The work of the third author was supported by Australian Research Council Discovery Project grant DP110104766.

References

Armstrong, M. and Delfiner, P. 1980. Toward a more robust variogram. A case study on coal. *Technical Report N-671*, Centre de Géostatistique, Fontainebleau, France.

Chilès, J.-P. and Delfiner, P. 2012. Geostatistics—Modeling Spatial Uncertainty. 2nd edn. John Wiley & Sons, Hoboken, NJ. 699 pp.

Cox, M. and Pardo-Igúzquiza, E. 2001. The total median and its uncertainty. *Advanced Mathematical and Computational Tools in Metrology V*. Ciarlini, O., Cox, M.G., Filipe, E., Pavese, F., and Ritchter, D. (eds.). World Scientific Publishing Company, Singapore. pp. 106–117.

Cressie, N. and Hawkins, D. 1980. Robust estimation of the variogram: I. *Mathematical Geology*, vol. 12, no. 2. pp. 115–125.

Cressie, N. 1984. Towards resistant geostatistics. *Geostatistics for Natural Resources Characterisation*. Veryl, G., David, M., Journel, A.G., and Marechal, A. (eds.). D. Reidel Publishing Company. *Series C: Mathematical and Physical Sciences*, vol. 122, Part 1, pp. 21–44.

Deutsch, C.V. and Journel, A.G. 1998, GSLIB—Geostatistical Software Library and User's Guide. 2nd edn. Oxford University Press, New York. 369 pp. and 1 CD.

Dowd, P.A. 1984. The variogram and kriging: robust and resistant estimators. *Geostatistics for Natural Resources Characterisation*. Verly, G., David, M., Journel, A.G., and Marechal, A. (eds.). D. Reidel Publishing Company. *Series C: Mathematical and Physical Sciences*, vol. 122, Part 1. pp. 91–106.

Efron, B. and Tibshirani, R.J. 1994. An Introduction to the Bootstrap. Chapman & Hall, New York. 456 pp.

Hoeksema, R.J. and Kitanidis, P.K. 1985. Analysis of the spatial structure of properties of selected aquifers. *Water Resources Research*, vol. 21, no. 4. pp. 563–572.

Journel, A.G. and Kyriakidis, P.C. 2004. Evaluations of mineral reserves—a simulation approach. Oxford University Press, New York. 216 pp.

Kirkpatrick, S., Gellat, C.D., J.R., and Vecchi, M.P. 1983. Optimization by simulated annealing. *Science*, vol. 220, no. 4598. pp. 671–680.

Klugman, S.A., Panger, H.H., and Willmot, G.E. 2012. Loss Models: from Data to Decisions. 4th edn. John Wiley & Sons, Hoboken, NJ, 513 pp.

Krige, D.G and Magri, E.J. 1982. Studies of the effects of outliers and data transformation on variogram estimates for a base metal and a gold orebody. *Mathematical Geology*, vol. 14, no. 6. pp. 557–564.

Olea, R.A. 2009. A Practical Primer on Geostatistics. US Geological Survey, Open File Report 2009-1103. 346 pp. http://pubs.usgs.gov/of/2009/1103/

Pardo-Igúzquiza, E. and Olea, R.A. 2012. VARBOOT: a spatial bootstrap program for semi-variogram uncertainty assessment. *Computers and Geosciences*, vol. 41. pp. 188–198.

Solow, A.R. 1985. Bootstrapping correlated data. *Mathematical Geology*, vol. 17, no. 7. pp. 769–775.

Stefanou, G., Lagaros, N.D., and Papadrakakis, M. 2004. An efficient method for the simulation of highly skewed non-Gaussian stochastic fields. *III European Congress on Computational Methods in Applied Sciences and Engineering*. Neittaanmäki, P., Rossi, T., Majava, K. and Pironneau, O. (eds.). Springer, The Netherlands. 15 p., http://www.imamod.ru/~serge/arc/conf/ECCOMAS_2004/ECCOMAS_V1/proceedings/pdf/281.pdf ◆

http://dx.doi.org/10.17159/2411-9717/2015/v115n1a5

Regression revisited (again)

by I. Clark*

Synopsis

One of the seminal pioneering papers in reserve evaluation was published by Danie Krige in 1951. In that paper he introduced the concept of regression techniques in providing better estimates for stope grades and correcting for what later became known as the 'conditional bias'. In South Africa, the development of this approach led to the phenomenon being dubbed the 'regression effect', and regression techniques ultimately formed the basis of simple kriging in Krige's later papers. In the late 1950s and early 1960s, Georges Matheron (1965) formulated the general theory of 'regionalized variables' and included copious discussion on what he termed the 'volume-variance' effect. Matheron defined mathematically the reason for, and quantification of, the difference in variability between estimated values and the actual unknown values. In 1983, this author published a paper that combined these two philosophies so that the 'regression effect' could be quantified before actual mining block values were available. In 1996 and in some earlier presentations, Krige revisited the regression effect in terms of the conditional bias and suggested two measures that might enable a practitioner of geostatistics to assess the 'efficiency' of the kriging estimator in any particular case. In this article, we revisit the trail from 'regression effect' to 'kriging efficiency' in conceptual terms and endeavour to explain exactly what is measured by these parameters and how to use (or abuse) them in practical cases.

Keywords
geostatistics, block estimation, regression effect, conditional bias, kriging efficiency.

Introduction

In recent years, major mining and geostatistical software packages have included additional parameters in block kriging analyses, such as a 'regression' coefficient and a measure of 'kriging efficiency'. Krige (1996) presented a paper at the APCOM conference in Wollongong discussing factors that affect these parameters during resource estimation. These measures were discussed by Snowden (2001) in her section dealing with classification guidelines released by the AusIMM.

While 'kriging efficiency' is a relatively new concept, the 'regression effect' has been in use in southern Africa for over 60 years. In this paper, the basis and development of the regression parameter will be explained in detail and illustrated with an uncomplicated case study. This illustration shows that while a regression correction might correct for the 'conditional bias', it does not necessarily improve the confidence in the estimated value for an individual mining block. The relevance of 'kriging efficiency' in the assessment of confidence in estimated block values, and a simple discriminator between indicated and inferred values, are also discussed.

The aim of this paper is to show that modern practice world-wide is well founded on over a half-century of established practice in southern Africa, pioneered by Krige on the gold mines, by illustration with a simulated example where the geology is continuous and homogeneous, and precise and accurate sampling is carried out on a square grid with grades that are normally distributed.

The case study

The full database of sampling is as close to exhaustive as possible (less than 0.5% of the range of influence). A block size typical for mine planning and grade control is used throughout this paper, although other (larger) block sizes were studied. This block size corresponds to around 10% of the full range of influence on the semivariogram. Around 700 blocks are available for assessment and analysis.

The exhaustive sampling is combined to provide 'actual block averages' from the 625 sample points that lie within each of the blocks in this model. The simplest estimation method – ordinary kriging (OK) – is used throughout this discussion, although similar estimation results could probably be obtained using inverse distance squared.

* *Geostokos Limited, Scotland.*

Varying the sample density

Sampling grids were studied at grid sizes varying from centre of every block (10% of the range of influence) up to centre of every sixth block (60% of the range of influence). For simplicity, we present results here only from grids at three and six times the block size. Expressed another way, the two sampling grids correspond to 30% and 60% of the range of influence respectively.

Quantifying the regression effect

Krige's original discussions (1951) were based on very large data-sets available from Witwatersrand-type gold reefs where chip samples were taken initially in development drives and then, as mining proceeded, on each stope face advance. The average grade of the development samples was used to evaluate the likely average of a stope panel of (say) 30 m by 30 m. As the stoping panel was mined out, face samples were used to evaluate the next advance into the stope. As a result, once the stope is mined out, a dense grid of samples is available to determine what was actually mined from that stope.

Krige found that, even allowing for the lognormal nature of the gold values, there was a discrepancy between the average stope value and the average development value. A simple scatter plot of development *versus* stope averages showed that the relationship between them is neither perfect nor clustered around the 45° line.

In 1972, this author was asked to look into the same question for Geevor Tin Mines Limited in Cornwall, UK. Again, the question was why development averages did not match the stope values found during mining. Again, the obvious approach was to plot development against stope averages to find out where the discrepancy arose.

In this paper we illustrate the approach with a simple example that could be considered as a single bench through an open pit, with drilling on a square grid used to estimate the values within each planned mining block.

Sparse sampling – sampling grid spacing six blocks

OK using an isotropic semivariogram model and search radius at the full range of influence was applied to produce a block model for this illustration. The block size is realistic at 10% of the range of influence, and sampling is relatively sparse at six times the block size. Around 700 blocks were estimated.

A scattergram of the actual block average along the vertical axis and ordinary kriged estimates along the horizontal axis is shown in Figure 1. The 'perfect estimator' is shown as a dashed line with a slope of 1 on this graph. It can be seen clearly that the points on the graph do not lie around this 45° line. The estimated values have a much smaller spread or 'dispersion' around the centre of the graph than do the actual values.

In classical statistics, a 'best fit' line can be fitted through the points to find the slope of the line that 'best' fits the points. In least squares regression (LS), the 'best' line (solid line in Figure 1) is that which minimizes the difference between the true average block value and the value that would be estimated using the regression line. This slope is calculated by:

$$\frac{\text{Covariance between estimated and actual value}}{\text{Variance of estimated values}}$$

and the intercept on the line is determined by making sure that the line passes through the average value of all the points for each variable. According to stated theory, application of these regression factors to the estimates produces a new estimate of the form:

Intercept + slope × kriged estimate

which should 'correct' for the regression effect and produce estimates that lie around the 45° line. However the scattergram of the kriged estimate corrected for the regression effect using the LS approach shown in Figure 2 shows little difference from Figure 1.

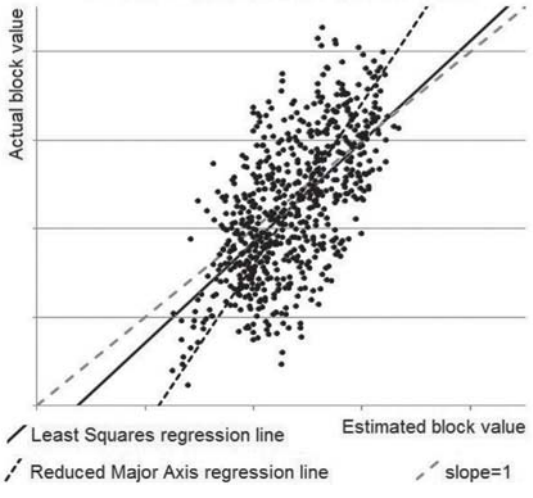

Figure 1—Comparison between actual block values and OK estimates from a sampling grid at six blocks (60% of range of influence) showing LS and RMA regression lines

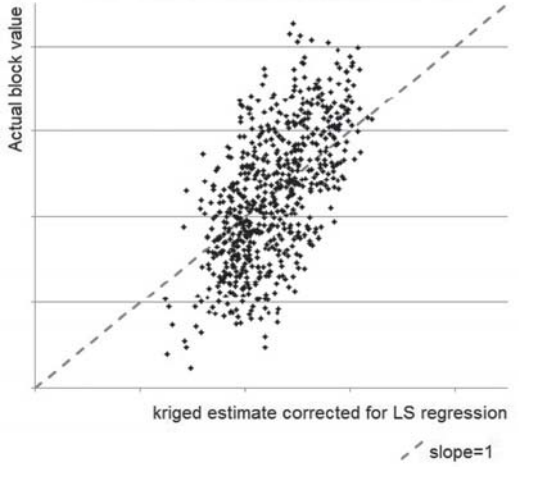

Figure 2—Comparison between actual block values and OK estimates corrected for LS regression from a sampling grid at six blocks (60% of range of influence)

Other types of regression

There are other types of regression lines that can be used to 'correct' the estimated values. One of these is the 'reduced major axis' (RMA) form, which calculates the slope as:

$$\frac{\text{Standard deviation of actual value}}{\text{Standard deviation of estimate}}$$

(*cf.* Till, 1974). This slope simply rescales the estimates to have the same dispersion as the true values. This is a highly simplified version of an 'affine correction'. Figure 1 shows the RMA regression as a dotted line, and Figure 3 shows a plot of the corrected estimates using RMA *versus* the actual block averages. This scatter lies more pleasingly around the 45° line.

It should, perhaps, be noted that the confidence on individual corrected estimates will not be affected by the correction if (and only if) the actual average value over the study area is exactly known. The intercept on the regression line requires the knowledge of the actual block values. In this illustration the true average value is known for every block and for the whole area. This should be borne in mind for the further sections of this paper.

Deriving the regression parameter without historical mining data

In Krige's early work and in the illustration here, the database contains enough information to evaluate the 'actual' values that are being estimated. Witwatersrand-type gold has been mined since the 19th century and copious amounts of sampling data were available for a study such as this. In this author's early studies, around 50 stopes had already been mined before the correction factors were developed. With the advent of Matheron's theory of regionalized variables (1965) it became apparent that the regression parameters could be determined *before* half the deposit had been mined out.

Matheron showed that the semivariogram model – under certain assumptions – was mathematically equivalent to calculating the covariance model. That is, the covariance between two values a certain distance apart can be found from:

(Total sill on the semi-variogram model) –
(Semivariogram at that distance)

This relationship can also be used to derive dispersion variances for blocks, *viz*:

(Total sill on the semivariogram model) –
(Average semivariogram within the block)

In fact, the covariance between any two sets of entities – samples or blocks – can be derived from the semivariogram model for the samples. The development of the mathematics for the regression factors can be found in Clark (1983).

Krige (1996) uses the following notation:

- BV represents the dispersion variance of block values within the deposit or study area
- KV represents the kriging variance obtained during the estimation of the block.

In more traditional geostatistical notation:

- BV = total sill on the semivariogram – $\bar{\gamma}(A,A)$
- KV = $\Sigma\, w_i\, \gamma(S_i,A) + \lambda - \bar{\gamma}(A,A)$

where the total sill on the semivariogram is taken to be the best estimate for the dispersion variance of single samples within the study area. $\bar{\gamma}(A,A)$ represents the average semivariogram within the block, also known as the 'within block variance'. $\gamma(S_i,A)$ is the semivariogram between each sample and the block being estimated, and wi represents the weight given to that sample.

For each block in the model, the slope of the relevant LS regression line can be calculated as follows:

$$\text{Regression slope} = (BV - KV + \lambda)/(BV - KV + 2\lambda)$$

where λ represents the Lagrangian multiplier produced in the solution of the OK equations when using the semivariogram form. If the OK equations are solved using covariances instead of semivariograms, the sign should be reversed on the Lagrangian multiplier. In Snowden's (2001) notation, $\mu = -\lambda$.

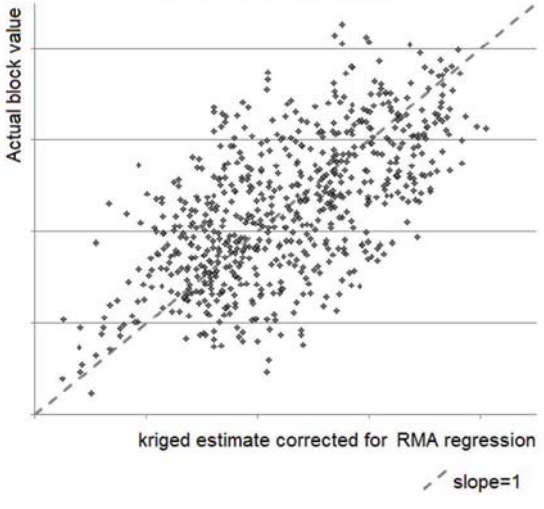

Figure 3—Comparison between actual block values and ordinary kriging estimates corrected for RMA regression from a sampling grid at six blocks (60% of range of influence)

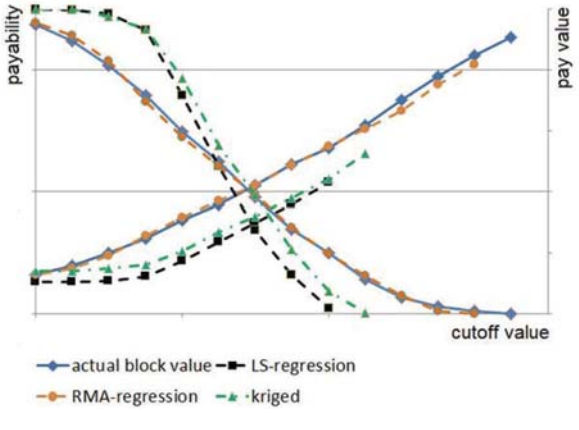

Figure 4—Grade/payability curves of actual block values and ordinary kriging estimates from a sampling grid at six blocks (60% of range of influence) compared to LS and RMA regression lines

Note that this formula is not actually quoted in Krige (1996). In more traditional geostatistical notation, this formula (*cf.* Clark 1983) would be written:

$$\{\text{Total sill} - \Sigma\, w_i\, \gamma(S_i,A)\} /$$
$$\{\text{Total sill} - \Sigma w_i\, \gamma(S_i,A) + \lambda\}$$

To calculate the RMA slope for each block, the formula becomes:

$$\{\text{Total sill} - \bar{\gamma}(A,A)\} /$$
$$\{\text{Total sill} - \Sigma\, w_i\, \gamma(S_i,A) + \lambda\}$$

Note also that the formula in Snowden (2001) uses the absolute value of μ. This would be correct if μ is negative, but not if μ is positive (*i.e.* λ is negative). It is possible for the λ value to be negative if the sampling layout is very dense or (at least) excessive to needs.

All of the parameters needed to generate the regression slope are available during the OK process, so that the calculation of the regression slope demands very little extra computation time during block estimation. In this way, the regression slope appropriate to each individual block estimate can be evaluated and included in the output for the block kriging exercise. In Figures 2, 3, and 4 the individual regression parameters were used to provide the 'corrected' estimate in each case.

Kriging efficiency

The major parameter proposed in Krige (1996) and documented in Snowden (2001) is the 'kriging efficiency'. This is a comparative measure of confidence in the individual block estimate. In Krige's (1996) notation, this parameter is calculated as:

$$\text{Kriging efficiency} = (BV - KV)/(BV)$$

and is usually expressed as a percentage rather than the proportion that would be given by the formula. Figure 5 shows the relationship between LS and RMA parameters and the kriging efficiency to the kriging variance for each block, using the sparse data grid.

It should be noted that kriging efficiency can take a negative value. As discussed in Krige (1996), the situation for which KV = BV is when the kriging estimate provides the same level of reliability as simply using the global average value as the block estimate. This author coined the term *ygiqgam*[1] for this phenomenon and uses this criterion to indicate when resources or reserves should be classified as Inferred. As a general rule, any block with negative kriging efficiency should never be included in a Measured resource category. The sampling grid chosen for this illustration – 60% of the range of influence of the semivariogram – equates very approximately to the spacing at which kriging efficiency tends to zero. It is also close to the distance which many practitioners use for 'Measured' resources.

Denser sampling grid

As a (possibly) more realistic exercise, a sampling grid at three-block spacing was also studied. Figure 6 shows the kriged estimates versus the actual block values, the 45° line, and the overall regression slope for the (almost) 700 blocks.

The closer sampling interval (three blocks) brings actual and kriged estimates corrected by the LS regression coefficient into much closer agreement, as shown in Figure 7.

Effect on the grade/payability curve

The effect of data spacing on the estimated block values is evident in the grade/payability curves of actual block values from sampling grids of different sizes. Figure 8 compares two restricted data-sets at three block and six block spacing with the exhaustive potential data-set. This graph indicates that more widely spaced sampling is unlikely to fully represent the high or low values that could be encountered during mining. According to this example, the limited data-sets give a similar general behaviour as regards value (pay grade) but seriously underestimate the likely payable tonnage.

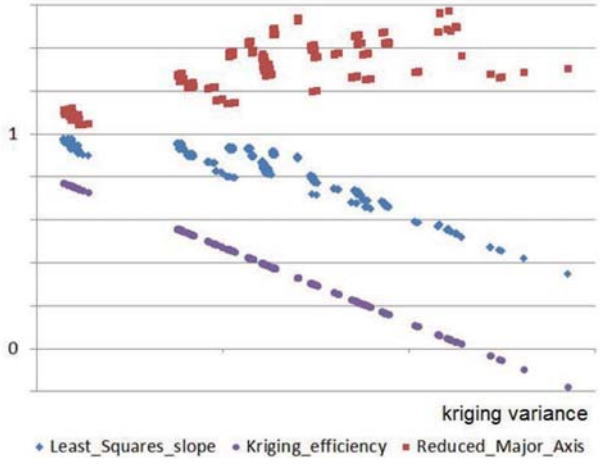

Figure 5—LS and RMA parameters from a sampling grid at six blocks (60% of range of influence) compared to OK variance

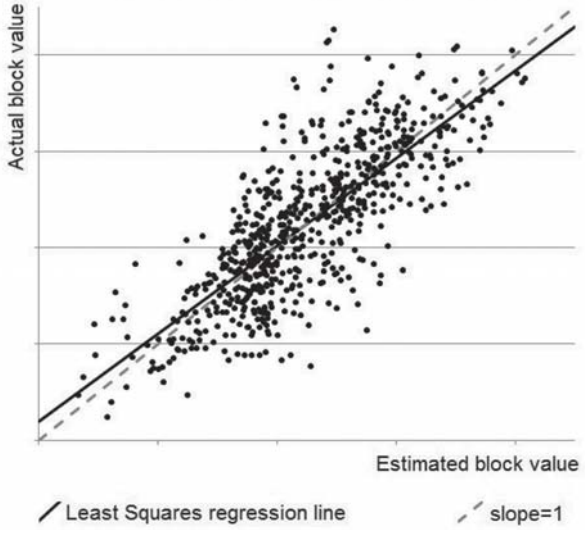

Figure 6—Comparison between actual block values and OK estimates from a sampling grid at three blocks (30% of the range of influence) showing the LS regression line

[1]Your guess is as good as mine'

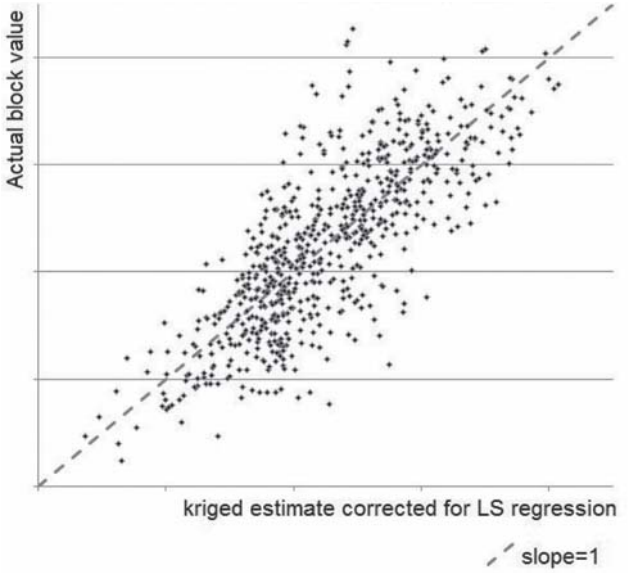

Figure 7—Comparison between actual block values and OK estimates corrected for LS regression from a sampling grid at three blocks (30% of the range of influence)

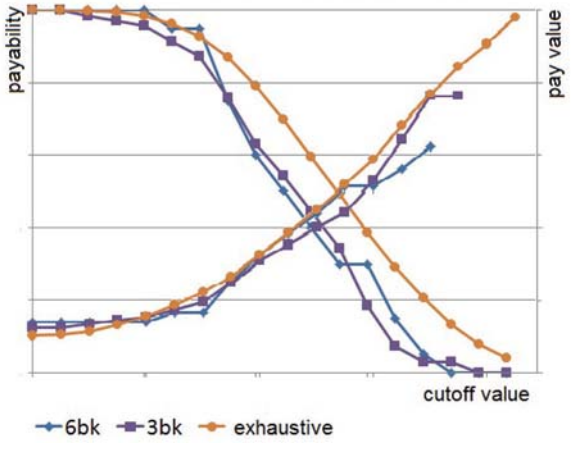

Figure 8—Grade/payability curves of actual block values from sampling grids at six blocks, three blocks, and an exhaustive data sampling grid (60%, 30%, and 1% of range of influence respectively)

Figure 9 compares the kriged block estimates based on the two sample spacings with the actual block values. The sparse data seriously over-estimates the payability for low grades and under-estimates the payability for higher cut-offs – as would be expected by the smoothing shown in previous sections. The grade estimated by kriging the six-block sparse grid seriously underestimates the recovered grade at any cut-off compared to the actual block values.

In contrast, the closer spaced sampling (three times block size) is almost identical to the pay grades in the actual blocks for every cut-off, but it seems to over-estimate payability at low cut-offs. A similar graph using the RMA corrected block grades for the six-block sampling and the LS corrected block grades from the three-block sampling would show almost identical grade/payability curves in this particular case.

Misclassification of ore and waste

The studies reported in this paper, in Clark (1983), and in Krige (1951, 1996) all illustrate how consideration of the regression effect – or conditional bias – can improve estimates for a mining block or stoping model. It is apparent, however, that emphasis on the potentially marginal improvements achieved by regression correction has masked a far more important consideration in mine planning based on estimated block models. Whatever the regression coefficient or the kriging efficiency, there still remains the fact that values allocated to potential mining blocks are still only *estimates*.

For any particular cut-off value, there will be blocks that are estimated as payable which will actually be waste. There will be blocks that are estimated to be below cut-off which will actually be payable. This problem is also discussed in detail in Krige's early work (1951) and many later papers. Figure 10 illustrates the problem of applying cut-off values to the estimated block values using our example with the three-block sampling, where the regression effect is minimal.

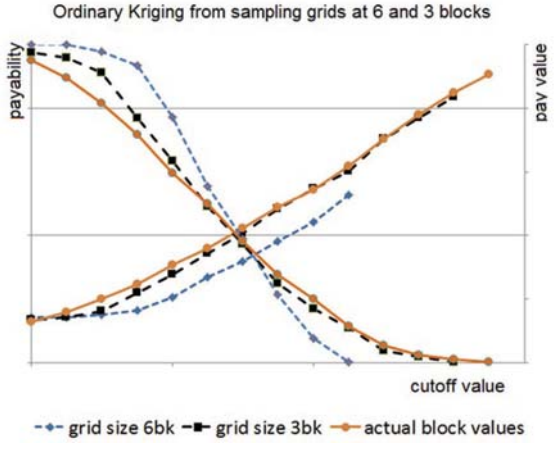

Figure 9—Grade/payability curves of actual block values compared to OK estimates from sampling grids at six blocks and three blocks (60% and 30% of range of influence)

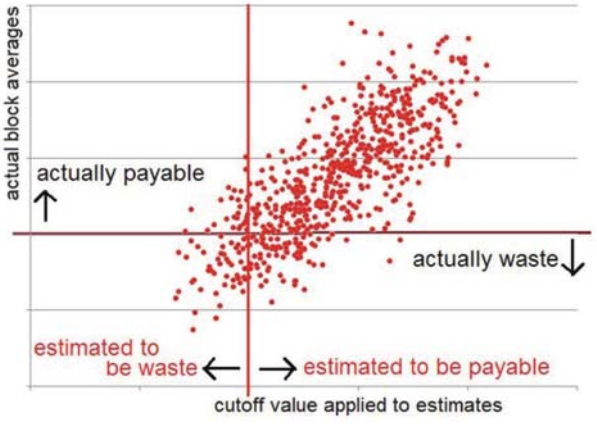

Figure 10—Block values estimated from samples at three-block grid spacing, applying the cut-off value to the estimates instead of the actual values

The majority of estimated block values are classified correctly as payable or waste. However, a significant number of blocks are misclassified. The practical implication of this is that blocks that are actually payable on average will be sent to the waste pile (or not mined), while waste material will be mined and delivered to the plant as payable. However much mathematics is applied to this situation, the result will be the same tonnage mined for a lower overall recovered value.

It should be emphasized that this is not a result of using a particular estimation technique, but is a fact of production. The only way to eliminate this effect is to instigate a grade control sampling plan that will narrow the scatter on the graph enough to achieve an absolute minimum of blocks in the two punitive quadrants. Or, in simpler language, to achieve a good enough grade control programme to be fully confident in the block values during production.

As a final illustration, a single cut-off was applied to the block estimates using the three-block sampling for OK. Those blocks estimated as above cut-off were separated from those classified as 'waste'. Grade/payability curves were produced from these two sets of blocks and are shown in Figure 11.

In this case, the payability curves are scaled to reflect how many blocks are classified as payable as opposed to waste. This example illustrates the proportion of 'payable' blocks that are actually non-payable and the values in the blocks that are classified as 'waste'.

Conclusions

Most of the above illustrations could equally well have been produced using theoretical methods. It is not necessary to have a vast database of previously mined areas to produce the regression factors or an assessment of the likely misclassification errors that will be incurred during production. This paper has used a case study where the database is exhaustive because it has been created from a conditional simulation based on a real-life case study.

It should be borne in mind that regression corrections, kriging efficiency, and misclassification assessments depend heavily on the sample values following a normal(-ish) behaviour. Statistics such as variance and covariance have little real meaning when applied to skewed sample data.

The example presented shows that least squares regression works well when the regression slope is less than (or not much greater than) 1. If a high degree of smoothing is present, an alternative approach such as RMA regression or affine corrections should be utilized, rather than least squares. Alternatively, simulation studies may be valuable when data is too sparse to achieve realistic results.

It cannot be emphasized strongly enough that a regression correction does not improve confidence in individual estimated block values. There will always be uncertainty in the true value of the block until it has been mined (and maybe afterwards). Misclassification of payable and non-payable blocks will inevitably lead to reconciliation problems during production – unless allowances are built into the mine plan for those recovery factors.

One puzzling factor is that many software packages now supply regression factors but do not seem to use them in adjusting the block estimates.

Kriging efficiency is simply a standardized form of the kriging variance. An advantage over simply considering the kriging variance is that it does provide an immediate indication of the *ygiagam* guideline as to where to stop trying to provide a local estimate for an individual block.

The main aim of this paper has been to show that approaches developed by Danie Krige 60 years ago are still vital in the production of mineral resource and reserve models and in ongoing mine planning.

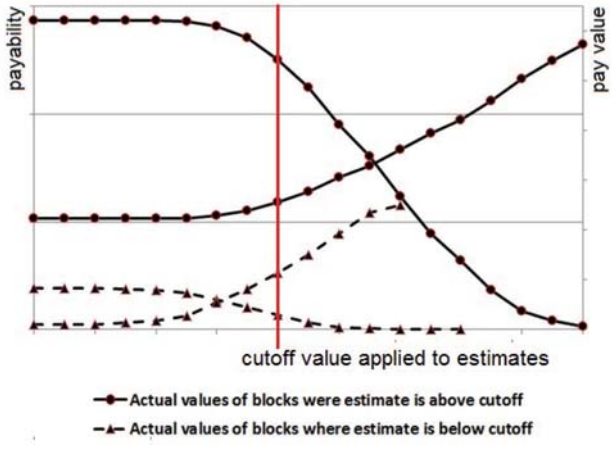

Figure 11—Block values estimated from samples at three-block grid spacing: grade/payability curves of actual block values mined as 'above cut-off'

References

Clark, I. 1983. Regression revisited. *Mathematical Geology*, vol. 15, no. 4. pp. 517–536.

Krige, D.G. 1951. A statistical approach to some basic mine valuation problems on the Witwatersrand. *Journal of the Chemical, Metallurgical and Mining Society of South Africa*, vol. 52. pp. 119–139.

Krige, D.G. 1996. A practical analysis of the effects of spatial structure and of data available and accessed, on conditional biases in ordinary kriging. *5th International Geostatistics Congress*, Wollongong, Australia 22–27 September 1996. Vol. 2. Baafi, E.Y. and Schofield, N.A. (eds.). Springer. pp. 799–810.

Matheron, G. 1965. La Theorie des Variables Regionalisees et ses Applications. Masson, Paris.

Snowden, D.V. 2001. Practical interpretation of mineral resource and ore reserve classification guidelines. *Mineral Resource and Ore Reserve Estimation - The AusIMM Guide to Good Practice*. Edwards. A.C. (ed.). Monograph 23. Australasian Intitute of Mining and Metallurgy, Melbourne. pp. 643–652.

Till, R. 1974. Statistical Methods for the Earth Scientist. Palgrave MacMillan. 168 pp. ◆

http://dx.doi.org/10.17159/2411-9717/2015/v115n1a6

The use of indirect distributions of selective mining units for assessment of recoverable mineral resources designed for mine planning at Gold Fields' Tarkwa Mine, Ghana

by W. Assibey-Bonsu*, J. Searra†, and M. Aboagye†

Synopsis

For new mining projects or for medium- to long-term areas of existing mines, drilling data is invariably on a relatively large grid. Direct estimates for selective mining units (SMUs), and also for much larger block units, will then be smoothed due to the information effects and the high error variance.

The difficulty is that ultimately, during mining, selection will be done on the basis of SMUs on the final close-spaced data grid (grade control), which will then be available, *i.e.* the actual selection will be more efficient, with fewer misclassifications. However, this ultimate mining position is unknown at the project feasibility stage and therefore has to be estimated. This estimation is required because any cash flow calculations made on the basis of the smoothed estimates will obviously misrepresent the overall economic value of the project, *i.e.* the average grade of blocks above cut-off will be underestimated and the tonnage overestimated for cut-off grades below the average grade of the orebody. Similarly, unsmoothed estimates will be conditionally biased and will give even worse results, particularly in local areas of short- and medium-term planning or mining.

This paper presents a case study of indirect post-processing and proportional modelling of recoverable resources designed for medium- and long-term mine planning at the Gold Fields' Tarkwa Mine in Ghana. The case study compares long-term indirect recoverable mineral resource estimates based on typical widely spaced feasibility data to the corresponding production grade control model as well as the mine production. The paper also proposes certain critical regression slope and kriging efficiency control limits to avoid inefficient medium- to long-term recoverable estimates, and highlights the danger of accepting block estimates that have a slope of regression less than 0.5.

Keywords

indirect conditioning, smoothing effect, conditional biases, post-processing, kriging efficiency, regression slope, information effect.

Introduction

At the exploration stage, kriged block estimates with a proper search routine will be conditionally unbiased and will have the lowest level of uncertainty, but will, unavoidably, be *smoothed* because of the level of data then available. This means they will have a lower dispersion variance than that of the final selective mining unit (SMU) distribution at the production stage, when more information will be available.

The smooth estimates will generally overestimate the tonnage above the economic cut-off and underestimate the corresponding grade, *i.e.* for cut-off grades below the mean grade of the orebody. The reason for this smoothing effect is that proper kriging is, in fact, a regression estimate and it is well known in classical statistics that regressed estimates have a variance equal to the variance of the dependent variable 'y' less the conditional variance of the 'y' values (or error variance of the regressed estimates). This error variance reduces as more data become available; at the same time, the smoothing effect will decrease, *i.e.*, the dispersion variance of the estimates will increase and the efficiency of the estimates will improve.

At the eventual production stage, more data will be available for acceptable estimation of large planning blocks as well as SMUs. However, this ultimate mining position is unknown at the project feasibility stage or for medium- to long-term planning, and therefore has to be estimated. This is because any decision to embark on capital-intensive projects, made on the basis of any of the smoothed estimates, will have obvious misrepresentations of the economic value of the project or the operation, *i.e.* the average grade of blocks above cut-off will be underestimated and the tonnage overestimated for cut-off grades below the mean grade of the orebody.

At the feasibility or early production stages, the problem is to estimate the tonnage and grade that will be recovered on the basis of information that will become available at the later production stage.

Various post-processing techniques have been proposed to correct for this smoothing feature, such as spectral postprocessor (Journel *et al.*, 2000). The alternative techniques of sequential Gaussian conditional simulation

* *Gold Fields Limited, Perth, Australia.*

† *Tarkwa Gold Mine, Gold Fields Limited, Ghana.*

(SGS) have also been suggested (Deutsch and Journel, 1992). Several post-processing techniques have been researched and published elsewhere (Assibey-Bonsu and Krige, 1999; Krige *et al.*, 2004, Deraisme and Assibey-Bonsu, 2011; 2012). The general indirect approach to the problem above is to derive the unknown SMU distribution from the observed distribution of relatively large kriged blocks (panels). The alternatives for the indirect approach as used in previous publications are uniform conditioning (Rivoirard, 1994, Assibey-Bonsu ,1998), multivariate uniform conditioning (Deraisme, Rivoirard, and Carrasco, 2008), and the assumed lognormal distribution of SMUs within large planning blocks (Assibey-Bonsu and Krige,1999; Marcotte and David, 1985). These techniques are indirect in the sense that the SMU distributions are inferred indirectly from initial estimated large kriged blocks/panels.

Regardless of the theoretical soundness, from a practical point of view, actual follow-up comparisons are absolutely essential. It is worth noting that geostatistics started on that approach, and for the benefit of the discipline this should continue. From the authors' perspective, such practical follow-up comparisons with real-world 'actual' production data for various post-processing techniques in the mining industry (at least in the gold mining context) are not readily found in the literature. It should be realized that whatever post-processing technique is used, the result will depend on the efficiency of the technique and parameters used in the execution of the process. Hence the estimate will always depend on how close the parameters are to the optimal choice, and thus the need for confirmation by comparisons with mined-out follow-up data.

The paper presents a case study, including production reconciliations, of an indirect post-processing and proportional modelling of recoverable mineral resources, developed for medium' and long-term mine planning at the Gold Fields Tarkwa Mine in Ghana. The case study compares long-term indirect recoverable mineral resource estimates based on typical widely spaced feasibility data to the corresponding production grade control model as well as the mine production. The paper also proposes certain critical regression slope and kriging efficiency control limits to avoid inefficient medium- to long-term recoverable estimates. In order to avoid potential conditional biases of the medium- to long-term indirect recoverable estimates, simple kriging with local means was used for the panel conditioning.

Indirect approach based on distribution of selective mining units within large planning blocks

The theoretical basis of the indirect approach used in this paper is summarized below (see also Figure 1).

Let us define:

L	Large planning block
S	SMU of interest
P	Entire population or global area being estimated
$B(^S/_L)$	Variance of actual SMU grades within large planning blocks
BV_s	Variance of actual SMU grades within P
BV_L	Variance of large planning block grades within P
σ^2_{se1}, σ^2_{se2}	Error variances of conditionally unbiased estimates at exploration and final production stages for SMUs respectively
σ^2_{LE1}, σ^2_{LE2}	Error variances of conditionally unbiased estimates at exploration and final production stages for the large planning blocks respectively (σ^2_{LE2} is assumed to be zero).

From Krige's relationship; variances of actual SMU grades:

$$BV_s = B(^S/_L) + BV_L$$

That is, $B(^S/_L) = BV_s - BV_L$

Dispersion variances of conditionally unbiased estimates within P for L ('$D(L/P)$')

$$D(^L/_P) = BV_L - \sigma^2_{LE1} \quad \text{(at exploration stage)} \qquad [1]$$
$$= BV_L - 0 \quad \text{(at final production stage)}$$

Similarly, dispersion variances of conditionally unbiased estimates within L for S ($D(^S/_L)$)

$$D(^S/_L) = B(^S/_L) - \sigma^2_{se1} \quad \text{(at exploration stage)}$$
$$= B(^S/_L) - \sigma^2_{se2} \quad \text{(at final production stage)}$$

Dispersion variance within P for S ($D(^S/_P)$) *i.e.*, the required variance for long-term estimates:

$$D(^S/_P) = BV_s - \sigma^2_{se1} \quad \text{(at exploration stage)}$$
$$= BV_s - \sigma^2_{se2} \quad \text{(at final production stage)}$$
$$= B(^S/_L) + BV_L - \sigma^2_{se2} \qquad [2]$$

To arrive at this required variance for long-term estimates (Equation [2]), the variance of L estimates at exploration (Equation [1]) must be adjusted or increased by:

$$B(^S/_L) + BV_L - \sigma^2_{se2} - (BV_L - \sigma^2_{LE1}) = B(^S/_L) - \sigma^2_{se2} + \sigma^2_{LE1}$$
$$= BV_s - BV_L - \sigma^2_{se2} + \sigma^2_{LE1}$$

In all cases, the large panels *must be conditionally unbiased* and are adjusted accordingly (as per above) to reflect the average grade improvements and tonnage reductions expected on the basis of the additional information that will become available at the later production stage. Although all analyses (including variograms and panel kriging) are done in the untransformed space, the required variance adjustments assume lognormal distribution of SMUs within the large planning blocks.

Case study

Geology

Gold Fields' Tarkwa operation exploits narrow auriferous conglomerates, similar to those mined in the Witwatersrand Basin of South Africa. Mining is currently conducted at four open pits – Pepe-Mantraim, Teberebie, Akontansi, and Kottraverchy.

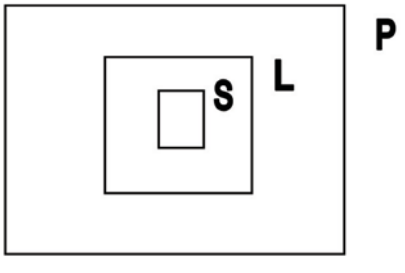

Figure 1—Diagram for methodology definition and illustration

The use of indirect distributions of selective mining units for assessment

The Tarkwa orebodies are located within the Tarkwaian System, which forms a significant portion of the stratigraphy of the Ashanti Belt in southwest Ghana. The Ashanti Belt is a north-easterly striking, broadly synclinal structure made up of Lower Proterozoic sediments and volcanics underlain by the metavolcanics and metasediments of the Birimian System. The contact between the Birimian and the Tarkwaian is commonly marked by zones of intense shearing and is host to a number of significant shear-hosted gold deposits.

The Tarkwaian unconformably overlies the Birimian and is characterized by lower intensity metamorphism and the predominance of coarse-grained, immature sedimentary units, which from oldest to youngest are shown in Figure 2.

The Banket Series, which hosts the Tarkwa orebody, varies in thickness from 32 m in the east at Pepe to 270 m in the west at Kottraverchy. Figure 3 shows the mineralized and potentially economic reefs in the Banket Series from the base upwards. Sedimentological studies of the detailed stratigraphy within individual footwall reef units have led to the recognition of both lateral and vertical facies variations. The potentially economic reefs are locally named the AFC, A, A1, A3, B2, CDE, F2, and G reefs.

The sedimentological data, gold accumulation, gold grade, and channel width data is further used to delineate geologically homogeneous local facies zones or geozones. These geozones or domains are used to constrain the statistical and geostatistical analyses on a soft domain basis. These homogeneous domains are particularly important for the simple kriging panel estimates, which are used for conditioning of the recoverable resource estimates.

Database and summary of mineral resources assessment process used on the mine

The data-set consists of reverse circulation (RC), grade control (GC), and diamond drilling (DD) information originating from exploration, resource, and grade control drilling data. For sample support requirements the gold data-set is composited on 1 m intervals.

Statistical and variographic analyses

Descriptive statistics are applied to develop an understanding of the statistical characteristics and sample population distribution relationships. Descriptive statistics in the form of histograms and probability plots (to evaluate the normality

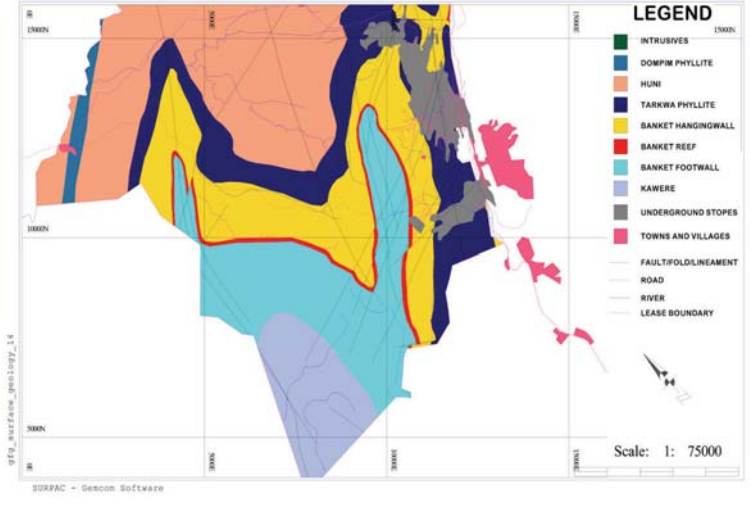

Figure 2—Surface geology

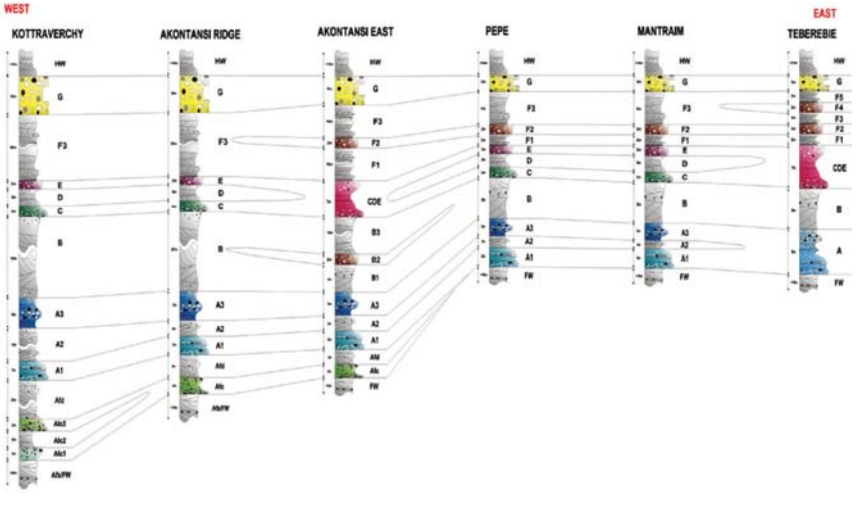

Figure 3—Stratigraphic profile of the Tarkwa oreody

and lognormality of the distribution) are used to develop an understanding of the statistical relationships within each domain. These also provide useful inputs with regard to selection of a post-processing technique, which is required for recoverable resource modelling. The statistical analysis also facilitates the application of top-cut values for kriging and variography processes. The top-cut values are derived from review and calculation from the normal and log probability plots.

Proportional block model derivation

The indirect post-processing methodology as developed for the mine requires the *in situ* modelling of mineralized tonnage proportions within respective panels. These are derived using Gold Fields' in-house software (Resource Evaluation System – 'RES'). The *in situ* mineralized proportions per panel are cross-checked against the physical wireframe volume as well as against the block model produced. The results are typically within 0.01% of each other and are considered accurate. Each panel is assigned a proportion of ore and waste (*in situ*), which are based essentially on the 3D geology wireframe of the orebody.

Selective mining units

All SMU sizes are as defined according to possible equipment, mining method, and mining selectivity, together with the geology of the orebody. At Tarkwa, the SMU size is 10 m x 5 m x 3 m with an assumed RC grade control drilling grid of 25 m x 25 m. During the early production period, certain areas were drilled on a 12.5 m x 12.5 m grid.

Panel estimation methods

Both ordinary kriging (OK) and simple kriging (SK) techniques are applied in developing the panel (50 m x 50 m x 3 m) resource estimation grade models. However, for post-processing of the recoverable resources, which are used for Whittle optimization, the SK panel grades are used. This is as a result of the relatively efficient SK estimates as reflected by higher kriging efficiencies observed for the SK panel estimates, especially in areas with limited data, as demonstrated in this paper (see section on analyses of kriging efficiency and slope of regression). In this regard, the SK panel estimates are conditionally unbiased. The simple kriging process uses a local or 'global' (*i.e.* domain) mean in the kriging process, depending on availability of data. If insufficient samples exist to support the local mean, then the 'global' mean of the respective domain or geozone is used in the SK process. In providing the mean value used for the SK estimation, historical mined-out information (when available) is taken into account for the respective reef horizons to ensure that the input SK mean values are efficient. It is critical that the SK input means are analysed for robustness, as inappropriate choice of this value may propagate biases, particularly in the presence of a drift. However, in Tarkwa's case, the geologically homogeneous domains provide practical stationary domains for this purpose.

Krige panel model checks

Various checks are performed on the krige block models to ensure that grades are assigned correctly to model cells. The first check involves viewing the composite data with block model cells to check that the grade values in the borehole correspond to block model cell values. Other checks performed include the number of samples used in estimation, kriging efficiency, regression slopes, block distance from samples, and search volumes. The estimation process also produces a log file to check average outputs, including average raw data *versus* average kriged values, minimum and maximum values, and SK *versus* OK values.

Analyses of kriging efficiency and slope of regression

Kriging efficiency

Kriging efficiency (KE) can be defined/measured as follows (Krige, 1996):

Kriging efficiency = $(BV\text{-}KV)/BV$ expressed as a percentage.

where

BV is the block variance (*i.e.* the variance of actual block values), and

KV is the kriging variance (*i.e.* the error variance of the respective block estimates).

For perfect valuations: $KV = 0$.

The dispersion variance (DV) of the estimates = BV, and then:

Kriging efficiency = $(BV\text{-}0)/BV = 100\%$.

Where only a global estimate of all blocks is practical, all blocks will be valued at the global or sub-domain mean, *i.e.*:

$DV = 0$, $KV = BV$, and kriging efficiency = $(BV\text{-}BV)/BV = 0\%$.

Usually blocks are valued imperfectly. With no conditional biases:

$DV = BV - KV$, and $KE = (BV\text{-}KV)/BV = DV/BV$.

However, with conditional biases present this relationship does not hold and then:

$DV > (BV\text{-}KV)$ because of insufficient smoothing, and kriging efficiency = $(BV\text{-}KV)/BV < DV/BV$

The kriging efficiency can even be negative if $KV>BV$. Such a situation is unacceptable and the block valuations will be worthless; yet the authors have encountered several such cases in the literature where the data accessed per block was inadequate and ordinary kriging efficiencies were negative (Krige, 1996). It should be noted that unlike ordinary kriging, the minimum kriging efficiency under simple kriging is zero.

Regression slope and critical control limits to avoid negative kriging efficiency estimates

Regression slope (slope) of actual block values on the estimates can be written as:

$$\text{Regression slope} = \frac{(BV - KV + |LM|)/}{(BV\text{-}KV + 2|LM|)} \quad [3]$$

where LM is the Lagrange multiplier and BV and KV are as defined above.

In order to avoid negative efficiency of block estimates, the following critical control limit test has been proposed for regression slopes (Assibey-Bonsu, 2014).

Where only a global estimate of all blocks is practical, all blocks will be valued at the global or sub-domain mean, *i.e.*

$KV = BV$
and
kriging efficiency =0
Substituting $KV=BV$ in Equation [3]:
Regression slope = $|LM|/2|LM| = 0.5$

Thus, a regression slope less than 0.5 will always lead to a negative block kriging efficiency estimate. This highlights the danger of accepting block estimates that have a slope of regression less than 0.5.

The critical regression slope limit of 0.5 should only be used to identify blocks that will result with negative kriging efficiencies. Ideal slopes of regression should be greater than 0.95, as proposed by Krige (1996).

Typical ordinary kriging efficiencies and slope of regression as observed at Tarkwa Mine

In providing kriged estimates on the mine, and particularly where limited data is available, significant conditional biases have been observed with OK, as demonstrated by the large negative kriging efficiencies and poor slopes of regression associated with a substantial number of the OK estimates as demonstrated in Figure 4. These significant conditional biases as observed with the OK estimates, particularly in areas with limited data, have adverse consequences on ore and waste selection for mine planning, as well as financial planning. As a result, relatively efficient local mean SK panel estimates, as reflected by higher kriging efficiencies, are used for resource panel conditioning, which forms the basis of the recoverable resource estimates at the mine.

Post-processing

The parent kriged blocks/panel (50 m x 50 m x 3 m) are subjected to post-processing as per the indirect recoverable resource methodology discussed in this paper (see also Assibey-Bonsu and Krige, 1999). The methodology incorporates the information effect and change of support correction for the relevant SMUs. A final production grade-control grid of 25 m x 25 m has been assumed in deriving the recoverable resources, which is based on the expected final production grade control drilling on the mine.

Table I shows the variances of different support sizes of respective geozones for the A Reef. The figure further provides the corresponding average error variances for the 50 m x 50 m x 3 m panels and the 5 m x 10 m x 3 m SMUs. As expected, the table demonstrates the reduction in variances from sample to SMU, and from SMU to the panels.

The post-process output provides recoverable tonnages, grades, and metal content estimates above respective cut-offs per block/panel. The probability recoverable post-processed tons, grades, and metal estimates for specific cut-offs derived for the respective panels are used for Whittle mine planning optimization. Thus, for the mine planning purposes, the base model provides recoverable grade-tonnage estimates based on 5 m x 10 m x 3 m SMUs derived, taking into account the production equipment on the mine.

Resource classification

The Mineral Resource classification is a function of the confidence of the whole process from drilling, sampling, geological understanding, and geostatistical relationships. The following aspects or parameters are considered for Mineral Resource classification:

- Sampling – quality assurance and quality control (QA/QC)
- Geological confidence
- Kriging efficiency and slope of regression
- Deviation based on the lower 90% confidence limit estimates.

Production reconciliation results

Table II illustrates typical results for comparisons of resource and grade control models within a common volume for one of

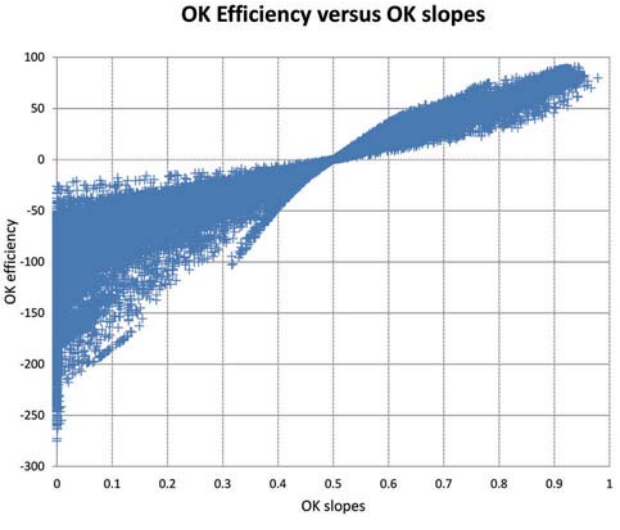

Figure 4—Typical ordinary kriging (OK) slopes of regression and OK efficiencies for panel estimates

Table I

Reduction of variances for different support sizes for A Reef (for sample, SMU and panels- Panel average error variances at exploration are for blocks with kriging block efficiency >20%)

Geozone	Sample variance	Block variance 5 x 10 x 3 m (SMU)	Block variance 50 x 50 x 3 m(panel)	Average error variance	
				50 x 50 x 3 m	5 x 10 x 3 m
1	1.052	0.335	0.083	0.051	0.142
2	0.745	0.247	0.059	0.035	0.090
3	1.722	0.577	0.166	0.091	0.236
4	3.205	0.812	0.232	0.129	0.440

the areas of the mine (the Pepe open pit area). The table shows good *in situ* reconciliation of the resource model, which is based on the SK indirect post-processing technique, when compared to the grade control models. Where differences are observed in the reef groupings they are due to geological re-zoning of the A Reef as A, A1, A2, and A3 for the resource model, which were subsequently combined as A Reef during mining at the Pepe area (*i.e.* for the grade control model, A Reef is equivalent to combined A, A1, A2, and A3 reefs for the resource model).

Table III further shows percentage errors of the reconciliations (as per Table II, for the resource model A, A1, A2, and A3 are combined as A, *i.e.*, on the same basis as the grade control model). The table shows individual reef percentage errors of -0.7%/3.9% and -5%/3.3% for tons and grade respectively. On a 'global' combined basis, percentage errors of -0.1%/-0.95% are observed for tons and grade respectively. These percentage errors indicate that the SK-based indirect recoverable resource models provide reliable grade, tonnage, and metal estimates inputs for mine planning and financial forecasts.

Figures 5 and 6 also show typical reconciliations of grade control models with production as observed on the mine. The figures also demonstrate good reconciliation between grade control models and that observed during production. As the resource models and the grade control models reconcile well (Tables II and III), this shows that a good reconciliation exists between the proportional post-processed recoverable resources estimates and production at the mine. The study further shows that in areas where adequate grade control data exists, good OK efficiencies/regression slopes are observed. Under these conditions, both ordinary and simple kriging estimates give similar production reconciliation results, *i.e.* within the grade control drilled areas (see also Figures 5 and 6). However, this is not the case for OK estimates for long-term areas of the mine, where drilling data is on a relatively large grid and significant conditional biases have been observed on OK panel estimates.

Conclusions

The study shows that appropriate application of an indirect post-processing technique provides efficient recoverable resource estimates for mine planning and financial forecast. The study further shows that it is critical that the conditioning panel estimates used for the post-processing are conditionally unbiased, if the corresponding recoverable resources estimates are to provide the lowest level of uncertainty for mine planning and financial forecasts. The study shows that kriging efficiency and slope of regression provide useful tools to measure the extent of conditional biases.

Acknowledgements

The authors are grateful to Gold Fields for permission to publish this paper based on a case study of the Group's Tarkwa Gold Mine.

Table II

Comparison of Indirect recoverable resource and grade control models (Pepe Area)

Reef	Resource model		Grade control model	
	Tons	Grade (g/t)	Tons	Grade (g/t)
A	9 321 811	1.38	10 385 781	1.39
A1	672 512	1.67		
A2	190 334	1.00		
A3	274 553	1.86		
C	1 569 111	0.91	1 566 705	0.94
E	1 081 803	0.79	1 123 823	0.80
F2	838 558	0.40	856 168	0.38
G	768 547	0.90	774 728	0.88
Total	14 717 229	1.22	14 707 205	1.21

Table III

Percentage errors, reconciliation of indirect recoverable resource (RM) and grade control models - Pepe Area (for RM, A Reef is: A, A1, A2, and A3 combined from Table II)

Reef	Tons (%)	Grade (%)
A	-0.70%	-1.02%
C	-0.15%	3.30%
E	3.88%	1.27%
F2	2.10%	-5.00%
G	0.80%	-2.22%
Total	-0.07%	-0.95%

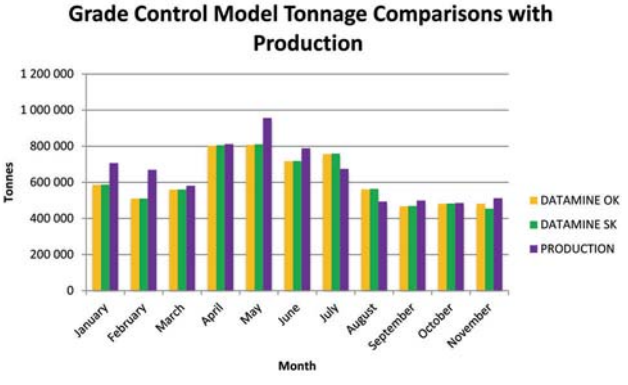

Figure 5—Typical reconciliation of grade control model vs production (tons)

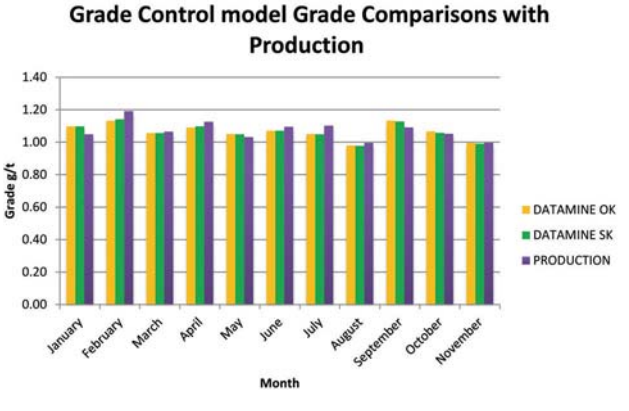

Figure 6—Typical reconciliation of grade control model vs production (grade)

References

Assibey-Bonsu, W. 2014. First Danie Krige Memorial Lecture. University of the Witwatersrand, May 2014. *Southern African Institute of Mining and Metallurgy*, Johannesburg.

Assibey-Bonsu, W. 1998. Use of uniform conditioning technique for recoverable resource/reserve estimation in a gold deposit. *Proceedings of Geocongress'98*, University of Pretoria, South Africa, July 1988. Geological Society of South Africa. pp. 68–74.

Assibey-Bonsu, W. and Krige, D.G. 1999. Use of direct and indirect distributions of selective mining units for estimation of recoverable resource/reserves for new mining projects. *APCOM'99 - 28th International Symposium on Computer Applications in the Minerals Industries*, Colorado School of Mines, Golden, CO, 20–22 October 1999. Colorado School of Mines.

Deraisme, J., Rivoirard, J., and Carrasco, P. 2008. Multivariate uniform conditioning and block simulations with discrete gaussian model : application to Chuquicamata deposit. *Proceedings of the 8th International Geostatistics Conference*, Santiago, Chile, 1–5 December 2008. Ortiz, J.M. and Emery, X. (eds.). pp. 69–78.

Deraisme, J., and Assibey-Bonsu, W. 2011. Localized uniform conditioning in the multivariate case, an application to a porphyry copper gold deposit. APCOM 2011. *Proceedings of the 35th International Symposium on Application of Computers and Operations Research in the Minerals Industry*, Wollongong, NSW, Australia 24–30 September 2011. Baffi, E.Y. (ed.). Australasian Institute of Mining and Metallurgy. pp. 131–140.

Deraisme, J. and Assibey-Bonsu, W. 2012. Comparative study of localized block simulations and localized uniform conditioning in the multivariate case. *Proceedings of the 13th International Geostatistics Conference*, 2012, Oslo, Norway. pp. 309–320.

Deutsch, C. V. and Journel, A.G. 1992. Geostatistical Software Library and User Guide. Oxford University Press. 340 pp.

Journel, A.G., Kyriadkidis, P.C., and Mao, S. 2000. Correcting the smoothing effect of estimators: a spectral postprocessor. *Mathematical Geology*, vol. 32, no. 7. pp. 787–813.

Krige, D.G. 1996. A practical analysis of the effects of spatial structure and data available and accessed, on conditional biases in ordinary kriging. *Proceedings of the Fifth International Geostatistics Congress*, Wolloongong, NSW, Australia. Baafi, E.Y. and Schofield, N.A. (eds). Kluwer, Dordrecht. vol. 2. pp. 799–810.

Krige, D.G., Assibey-Bonsu, W., and Tolmay, L. 2004. Post-processing of SK estimators and simulations for assessment of recoverable resources and reserves for South African Gold Mines. *Proceedings of the Seventh International Geostatistics Congress 2004*, Banff, Canada. Leuangthong, O. and Deutsch, C. V. (eds.). Springer, New York. pp. 375–386.

Marcotte, D. and David, M. 1985. The bigaussian approach: a simple method for recovery estimation. *Mathematical Geology*, vol. 17, no. 6. pp. 625–644.

Rivoirard, J. 1994. Introduction to Disjunctive Kriging and Non Linear Geostatistics. Clarendon Press, Oxford. 181 pp. ◆

5th Sulphur and Sulphuric Acid 2015 Conference

8–9 April 2015—CONFERENCE
10 April 2015—TECHNICAL VISIT

Southern Sun Elangeni Maharani
KwaZulu-Natal, South Africa

WHO SHOULD ATTEND

The Conference will be of value to:

- Metallurgical and chemical engineers working in the minerals and metals processing and chemical industries
- Metallurgical/Chemical/Plant Management
- Project Managers
- Research and development personnel
- Academic personnel and students
- Technology providers and engineering firms for engineering solutions
- Equipment and system providers
- Relevant legislators
- Environmentalists
- Consultants

SAIMM
THE SOUTHERN AFRICAN INSTITUTE OF MINING AND METALLURGY

For further information contact:

Conference Co-ordinator
Camielah Jardine, SAIMM
P O Box 61127, Marshalltown 2107
Tel: (011) 834-1273/7
Fax: (011) 833-8156 or (011) 838-5923
E-mail: camielah@saimm.co.za
Website: http://www.saimm.co.za

EXHIBITION/SPONSORSHIP

There are a number of sponsorship opportunities available. Companies wishing to sponsor or exhibit should contact the Conference Co-ordinator.

BACKGROUND

The production of SO_2 and Sulphuric acid remains a pertinent topic in the Southern African mining, minerals and metallurgical industry.

Due to significant growth in acid and SO_2 production as a fatal product, as well as increased requirement for acid and SO_2 to process Copper, Cobalt and Uranium, the Sub Saharan region has seen a dramatic increase in the number of new plants. The design capacity of each of the new plants is in excess of 1000 tons per day.

This event provides a forum for producers, technology suppliers, consumers, the legislator and other role players in the industry to discuss relevant issues on the topics related to acid and SO_2 production.

To ensure that you stay abreast of developments in the industry, The Southern African Institute of Mining and Metallurgy, invites you to participate in a conference on the production, utilization and conversion of Sulphur, Sulphuric acid and SO_2 abatement in metallurgical and other processes to be held April 2015 in KwaZulu-Natal.

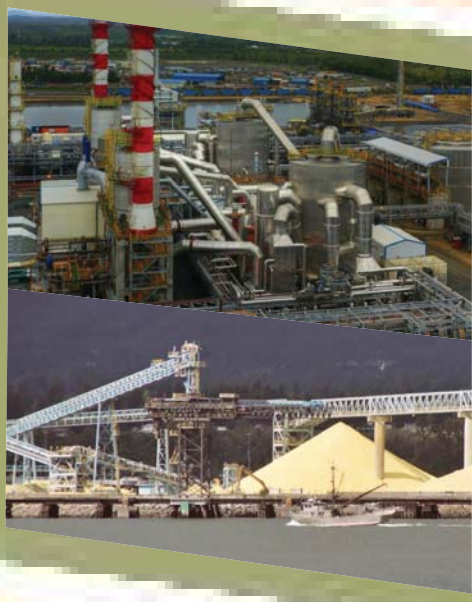

OBJECTIVES

- Expose SAIMM members to issues relating to the generation and handling of sulphur, sulphuric acid and SO_2 abatement in the metallurgical and other industries.
- Provide opportunity to producers and consumers of sulphur and sulphuric acid and related products to be exposed to new technologies and equipment in the field.
- Enable participants to share information and experience with application of such technologies.
- Provide opportunity to role players in the industry to discuss common problems and their solutions.

SPONSORS:

Begg Cousland World Class Filtration Solutions
DUPONT
MECS
BASF The Chemical Company
GORE Creative Technologies Worldwide
Spraying Systems Co.® Experts in Spray Technology
IAP INDUSTRIAL ACID PROOFING
HALDOR TOPSOE
CHEMETICS®
Outotec
STEULER KCH

Conference Announcement

http://dx.doi.org/10.17159/2411-9717/2015/v115n1a7

Cokriging of compositional balances including a dimension reduction and retrieval of original units

by V. Pawlowsky-Glahn*, J.J. Egozcue†, R.A. Olea§, and E. Pardo-Igúzquiza‡

Synopsis

Compositional data constitutes a special class of quantitative measurements involving parts of a whole. The sample space has an algebraic-geometric structure different from that of real-valued data. A subcomposition is a subset of all possible parts. When compositional data values include geographical locations, they are also regionalized variables. In the Earth sciences, geochemical analyses are a common form of regionalized compositional data. Ordinarily, there are measurements only at data locations. Geostatistics has proven to be the standard for spatial estimation of regionalized variables but, in general, the compositional character of the geochemical data has been ignored. This paper presents in detail an application of cokriging for the modelling of compositional data using a method that is consistent with the compositional character of the data. The uncertainty is evaluated by a Monte Carlo procedure. The method is illustrated for the contents of arsenic and iron in groundwaters in Bangladesh, which have the peculiarity of being measured in milligrams per litre, units for which the sum of all parts does not add to a constant. Practical results include maps of estimates of the geochemical elements in the original concentration units, as well as measures of uncertainty, such as the probability that the concentration may exceed a given threshold. Results indicate that probabilities of exceedance in previous studies of the same data are too low.

Keywords

geostatistics, linear coregionalization model, compositional data, equivalent class, geochemistry, detection limit, groundwater, Bangladesh.

Introduction

Compositional data consists of observations recording relative proportions in a system. The sample space is a simplex, which has an algebraic-geometric structure different from that of real space, known as Aitchison geometry of the simplex (Pawlowsky-Glahn and Egozcue, 2001; Pawlowsky-Glahn *et al.*, 2015). A subcomposition is a subset of all possible proportions. An example of compositional data is the percentages of different minerals in a rock specimen. For such a type of data, a first obvious property is that, when measured without error, the sum of the proportions of all components, known as *parts* in the compositional literature (in this case minerals), adds up to 100 per cent. In some other less frequent cases, such as the one of our interest, the sum of all proportions is not constant, requiring a slightly different approach. When several specimens have been collected and analysed over some geographical area, usually there is the interest of analyzing the fluctuations in composition both in variable and geographical space.

The exact nature and properties of compositional data have been a source of prolonged misunderstanding and neglect. Pearson (1897) published the first scientific study pointing to peculiar statistical properties when analysing ratio variables, not displayed by multiple variables varying in real space. However, his insights were mostly ignored for more than half a century until Chayes (1960, 1962, 1971, 1975, and 1983) devoted serious effort to advance the analysis of petrographic data. Compositional data analysis, however, would not take off until Aitchison (1982) introduced the logratio approach and published his monographs (1986).

Owing to the different properties from conventional multivariate data, the approach to compositional data analysis has been to convert the compositional variables to conventional real variables. The development of special statistics honoring the compositional peculiarities has proven to be a demanding endeavour showing no significant results. The strategy of representing compositions using logratio coordinates of the simplex (Mateu-Figueras *et al.*, 2011) makes possible the

* *Dept. Informàtica, Matemàtica Aplicada i Estadìstica, U. de Girona, Girona, Spain.*

† *Dept. Matemàtica Aplicada III, U. Politècnica de Catalunya, Barcelona, Spain.*

§ *United States Geological Survey, Reston, VA, USA.*

† *Instituto Geológico y Minero de España, Madrid, Spain.*

rigorous application of the standard methods of statistics, thus avoiding development of a parallel branch of statistics. The approach sometimes requires back-transforming the results of the analysis in coordinates to the original compositional proportions or concentrations. The literature sadly contains numerous examples in which compositional data is modelled implicitly under false assumptions, such that the parts vary between $-\infty$ to $+\infty$, and that they obey Euclidean geometry. The consequences of violating these assumptions are rarely evaluated and go unchecked. In our case, we are interested in applying the methods of geostatistics, which has become the prevalent approach to mapping when taking into account uncertainty. An early publication on the subject of spatial estimation of compositional data is that of Pawlowsky (1984), later expanded into a monograph (Pawlowsky-Glahn and Olea, 2004). Developments in recent years, such as the formulation of balances (Egozcue *et al.*, 2003: Egozcue and Pawlowsky-Glahn, 2005) (see Equation [3]), make it advisable to revisit the subject.

Geochemical surveys are one of the most common sources of compositional data in the Earth sciences. Survey results are reported as the chemical concentrations of several minerals, oxides, chemical elements, or combinations thereof, as measured in the laboratory. Analytical data that are collected and reported is selective, never including all the elements in the periodic table; therefore, the data available for study covers only a subcomposition of the entire system. For multiple reasons, the interest of the analysis concentrates even further on a detailed account of only a few of the compositional parts. This is the subject of our contribution. The modelling of subcompositions requires additional cautions not necessary for the modelling of whole systems (Pawlowsky, 1984). The first caution is that reduction of dimension implies some form of projection of the data-set preserving the original proportions, a topic not addressed in previous contributions, such as Tolosana-Delgado *et al.* (2011). Consistent with the compositional approach, the projection is preferred to be an orthogonal projection in the Aitchison geometry of the simplex (Egozcue and Pawlowsky-Glahn, 2005; Egozcue *et al.*, 2011; Pawlowsky-Glahn *et al.*, 2015). The second point concerns the presentation of results of cokriging. Interpolated maps of a single part, using the units in which the original composition was expressed, are a common interpretative tool that is not directly provided by a compositional analysis. The way to obtain these single-part maps from a compositional cokriging is also analysed for the first time in a spatial context, following an analysis in the nonspatial context (Pawlowsky-Glahn *et al.*, 2013).

We borrowed a public domain data-set to practically illustrate our methodology. We selected a survey of environmental importance conducted in the 1990s as a joint effort by the British Geological Survey and the Department of Public Health Engineering of Bangladesh (British Geological Survey, 2001a, b). Many authors have modelled this Bangladesh survey, none of whom took into account the compositional nature of the data, *e.g.* Anwar and Kawonine (2012), Chowdhury *et al.* (2010), Gaus *et al.* (2003), Hassan and Atkins (2011), Hossain and Piantanakulchai (2013), Hossain and Sivakumar (2006), Hossain *et al.* (2007), Pardo-Igúzquiza and Chica-Olmo (2005), Serre *et al.* (2003), Shamsudduha (2007), Shamsudduha *et al.* (2009), Yu *et al.* (2003). Moreover, the data-set has the peculiarity that instead of part per million, the concentrations are reported as milligrams per litre, a practice shown below to require a special final calibration to have the final results in the original units of measurement.

Following the original environmental interest of the survey, we selected arsenic and iron as the two chemical elements of interest. The main objectives of our paper are to (a) provide a summary review of cokriging for the stochastic mapping of compositional regionalized variables; (b) present and justify the multiple stages of preparation for compositional data required for a proper spatial estimation, in particular projection strategies for dimension reduction; (c) provide a novel back-transformations approach required for the display of results in the original units of concentration; and (d) model the uncertainty in the mapping.

Methodology

Aitchison geometry for compositional data

Compositional data comprises parts of some whole. Consequently, multiplication by a positive real constant does not change the knowledge that can be extracted from the data. Thus, the data can be modelled by equivalence classes of vectors whose components are proportional (Barceló-Vidal *et al.*, 2001). These equivalence classes contain a representative for which their components add to a given constant $\kappa > 0$, allowing a general approach independently if the sum of all parts is constant or not. All these representatives form the sample space of compositional data, the D-part simplex, S^D, defined as

$$S^D = \left\{ \mathbf{x} = [x_1, x_2, \dots, x_D] : x_1 > 0, x_2 > 0, \dots, x_D > 0; \sum_{i=1}^{D} x_i = \kappa \right\}$$

where κ is the closure constant, *e.g.* $\kappa = 10^6$ in the case of units of parts per million. All measurements done for the same specimen define a vector of values. In a tabulation, the standard practice is to have data registered row-wise and parts or variables column-wise.

The simplex, with the operations *perturbation* and *powering*, and the inner product, called the *Aitchison inner product*, is a $D-1$-dimensional Euclidean vector space (Billheimer *et al.*, 2001; Pawlowsky-Glahn and Egozcue, 2001). For $\mathcal{C}$ the closure operation,

$$\mathcal{C}(\mathbf{x}) = \left[\frac{\kappa x_1}{\sum_{i=1}^{D} x_i}, \frac{\kappa x_2}{\sum_{i=1}^{D} x_i}, \dots, \frac{\kappa x_D}{\sum_{i=1}^{D} x_i} \right], \ \mathbf{x} \in S^D, \quad [1]$$

and the perturbation is defined as

$$\mathbf{x} \oplus \mathbf{x}^* = \mathcal{C}[x_1 x_1^*, x_2 x_2^*, \dots, x_D x_D^*], \quad \mathbf{x}, \mathbf{x}^* \in S^D,$$

with inverse operation or subtraction

$$\mathbf{x} \ominus \mathbf{x}^* = \mathcal{C}\left[\frac{x_1}{x_1^*}, \frac{x_2}{x_2^*}, \dots, \frac{x_D}{x_D^*} \right];$$

powering is defined as

$$\alpha \odot \mathbf{x} = \mathcal{C}[x_1^\alpha, x_2^\alpha, \dots, x_D^\alpha], \quad \mathbf{x} \in S^D, \alpha \in \mathbb{R};$$

and the Aitchison inner product as

$$\langle \mathbf{x}, \mathbf{x}^* \rangle_a = \frac{1}{D} \sum_{i<j} \ln \frac{x_i}{x_j} \ln \frac{x_i^*}{x_j^*}, \quad \mathbf{x}, \mathbf{x}^* \in S^D. \quad [2]$$

The corresponding squared distance

$$d_a^2(\mathbf{x},\mathbf{x}^*) = \frac{1}{D}\sum_{i<j}\left(\ln\frac{x_i}{x_j} - \ln\frac{x_i^*}{x_j^*}\right)^2,$$

satisfies standard properties of a Euclidean distance (Martín-Fernández *et al.*, 1998), such as

$$d_a(\mathbf{x},\mathbf{x}^*) = d_a(\mathbf{a}\oplus\mathbf{x}, \mathbf{a}\oplus\mathbf{x}^*),$$
$$d_a(\alpha\odot\mathbf{x}, \alpha\odot\mathbf{x}^*) = |\alpha| d_a(\mathbf{x},\mathbf{x}^*).$$

The corresponding geometry is known as *Aitchison geometry*, and the subscript a is used accordingly (Pawlowsky-Glahn and Egozcue, 2001). The inner product (Equation [2]) and its norm, $\|\mathbf{x}\|_a = \sqrt{\langle \mathbf{x}, \mathbf{x}\rangle_a}$, ensure the existence of orthonormal bases. Orthonormal bases and their respective coordinates are important, as standard methods can be applied to the coordinates without restrictions or constraints. This implies that all compositional results and conclusions attained using coordinates do not depend on the specific basis of the simplex used to model compositions in coordinates. This is the core of the principle of working on coordinates (Mateu-Figueras *et al.*, 2011).

In practice, user-defined, simple, specific bases of the simplex can be used. The user defines a sequential binary partition (SBP) (Egozcue and Pawlowsky-Glahn, 2005, 2006) that assigns a set of D–1 coordinates, called balances, to each data location. Balances are normalized logratios of geometric means of groups of parts, and they belong to the family of *isometric logratio* (ilr) transformations (Egozcue *et al.*, 2003). Balances have expressions of the form

$$b = \sqrt{\frac{rs}{r+s}}\ln\frac{g_m(\mathbf{y})}{g_m(\mathbf{z})} \qquad [3]$$

where $g_m(.)$ is the geometric mean of the arguments; $\mathbf{y}$ and $\mathbf{z}$ are groups of parts determined in the SBP; and r and s are the number of parts in $\mathbf{y}$ and $\mathbf{z}$, respectively. Balances are scale-invariant quantities. They are also orthogonal log-contrasts (Aitchison, 2003, p. 85). As a consequence, computation of balances does not change with the units of the parts in the composition, or whether they are closed or not. This is important for applications, like the one presented in this contribution, where only some parts of the whole composition not exactly adding to a constant are modelled.

The ilr transformation and its inverse, plus a basis constructed using a SBP, have compact expressions useful for computation. Consider a $(D-1,D)$-matrix Θ, with entries θ_{ij}, which can take the values +1, –1, 0. Each row of Θ encodes one partition of the SBP. For the i-th row, $\theta_{ij} = +1$ points out that x_j belongs to the group of parts G_{i+}; similarly, $\theta_{ij} = -1$ indicates that x_j is in the group of parts G_{i-}; $\theta_{ij} = 0$, meaning that x_j is not involved in the i-th partition. From the SBP code Θ, the so-called contrast $(D-1,D)$-matrix Ψ is built up (Egozcue and Pawlowsky-Glahn, 2005, 2006; Tolosana-Delgado *et al.*, 2008; Egozcue *et al.*, 2011). If $\theta_{ij} = 0$, the corresponding entry of Ψ, ψ_{ij}, is also null. For $\theta_{ij} = +1$ and $\theta_{ij} = -1$ the values are, respectively:

$$\psi_{ij} = +\sqrt{\frac{s_i}{r_i(r_i+s_i)}}, \qquad \psi_{ij} = -\sqrt{\frac{r_i}{s_i(r_i+s_i)}}$$

where r_i, s_i are the number of +1 and –1 in the i-th row of Θ. The ilr transformation and its inverse are

$$\mathbf{b} = \mathrm{ilr}(\mathbf{x}) = \ln(\mathbf{x})\Psi^T, \qquad [4]$$
$$\mathbf{x} = \mathrm{ilr}^{-1}(\mathbf{b}) = \mathcal{C}\exp(\mathbf{b}\Psi)$$

where $\mathbf{x}$, $\mathbf{b}$ are row-vectors, with D –1 and D components, respectively; the logarithm, ln, and the exponential, exp, operate component-wise; and $(\cdot)^T$ denotes matrix transposition.

Orthogonal projections for compositions

Projections are the main tool of dimension reduction in data analysis. Dimension reduction of compositions is not an exception. Orthogonal projections make sure that distances between compositions are shorter in the projection than in the original D components. Therefore, projections for dimension reduction should be orthogonal (Egozcue and Pawlowsky-Glahn, 2005). The simplest case consists in using only some parts of a composition. This is an orthogonal projection on a subcomposition. However, there are other possible projections that do not correspond to this elementary case. In general, projections are better described in terms of coordinates and, particularly, using balances built up from a SBP.

The rationale of a generic, orthogonal, projection is as follows. A subspace of the simplex, $\mathcal{R} \subset S^D$, is defined by a set of d orthogonal, unitary, compositions $\mathbf{e}_1, \mathbf{e}_2,\ldots, \mathbf{e}_d$, $d \le D$–1, which constitute a basis of the subspace. The projection of $\mathbf{x} \in S^D$ into the d-dimensional subspace $\mathcal{R}$ is determined by the inner product $\langle \mathbf{x}, \mathbf{e}_i\rangle_a$, $i = 1,2,\ldots,d$. The orthogonal projection of $\mathbf{x}$ on the subspace is

$$\mathbf{x}_p = \bigoplus_{i=1}^{d} \langle \mathbf{x}, \mathbf{e}_i\rangle_a \odot \mathbf{e}_i .$$

The basis of the subspace $\mathcal{R}$, $\mathbf{e}_1, \mathbf{e}_2,\ldots, \mathbf{e}_d$, can be extended to a basis of S^D, by adding a set of unitary compositions, $\mathbf{e}_{d+1}, \mathbf{e}_{d+2},\ldots, \mathbf{e}_{D-1}$, such that they are mutually orthogonal, and orthogonal to the basis of the $\mathcal{R}$ subspace. The coordinates of $\mathbf{x}$ in this basis are $b_i = \langle \mathbf{x}, \mathbf{e}_i\rangle_a$, $i = 1,2,\ldots, D$–1. Evidently, projecting $\mathbf{x}$ on the subspace $\mathcal{R}$ reduces to making $b_i = 0$ for $i = d+1, d+2,\ldots, D$–1. In order to express the projection in the simplex, the ilr-inverse transformation (Equation [4]) is used. Denote the original ilr-coordinates, arranged in the D–1-vector by $\mathbf{b}$, and the ilr-coordinates after the projection, $\mathbf{b}_p$. If Ψ is the contrast matrix corresponding to the basis $\mathbf{e}_1, \mathbf{e}_2,\ldots, \mathbf{e}_{D-1}$, the projected composition $\mathbf{x}_p$ is obtained as

$$\mathbf{x}_p = \mathrm{ilr}^{-1}(\mathbf{b}_p) = \mathcal{C}\exp(\mathbf{b}_p\Psi). \qquad [5]$$

The assumption is that there is a reference subcomposition of interest and the projection to be carried out should retain all relative proportions contained in the reference subcomposition. The situation studied herein is a projection on a subspace including the reference subcomposition and other supplementary data. In general, any orthogonal projection of compositions suppresses the units in which the original composition was presented. There are scenarios in which it is worthwhile to have the projection using the original units. Consequently, it is worthwhile to study how to

recover original units after an orthogonal projection, which involves modelling some kind of total and the corresponding projection.

After expressing a composition $\mathbf{x} \in S^D$ in $D-1$ coordinates, ignoring the rest, is equivalent to an orthogonal projection of $\mathbf{x}$, thus reducing the dimensionality of the analysis. The choice of an orthogonal projection depends on the problem to be studied, and on the interpretability of the coordinates. The use of balances coming from a SBP is encouraged, as they can lead to easily interpretable coordinates.

Orthogonal projection on a subcomposition using balances

In practice, the most frequent orthogonal projection is on the subspace of a given reference subcomposition. Suppose that this subcomposition is $\mathbf{x}_s = \mathcal{C}[x_1,x_2,\ldots, x_{d+1}]$. The subcomposition is supposed to be made up of the first $d+1$ parts of $\mathbf{x}$. There is no loss of generality in this assumption, as the parts in $\mathbf{x}$ can always be reordered by a convenient permutation. An orthonormal basis for the subcomposition $\mathbf{x}_s$ is readily built up using a SBP. Let b_1 be the balance (coordinate) comparing the subcomposition $\mathbf{x}_s$ to the other parts in the composition, and b_i, $i = 2,\ldots,d$, be the balances (coordinates) corresponding to $\mathbf{x}_s$. The SBP of $\mathbf{x}_s$ can easily be extended to the original composition. Regardless of the extension of the SBP, balances b_i, $i = 2,\ldots,d$, of $\mathbf{x}$ are equal to those corresponding to $\mathbf{x}_s$ because balances are not affected by the closure applied to compute $\mathbf{x}_s$. Thus, projecting on a subcomposition is equivalent to keeping the balances $b_2,b_3,\ldots, b_d$ and setting the remaining balances to zero, *i.e.* $b_1, = 0$ and $b_{d+1} = 0 ,\ldots, b_{D-1} = 0$, to form the vector of $\mathbf{b}_p = 0$. Table I illustrates how this projection works for an example of $D = 6$ parts with $d = 1$, *i.e.* projection on a reference subcomposition of two parts. The projection on the reference subcomposition, $\mathcal{C}[x_1,x_2]$, is obtained by setting $b_1 = 0$ and $b_j = 0$ for $j = 3, 4, 5$. From $\mathbf{b}_p$ the projected composition is obtained using ilr-inverse in Equation [5] (Egozcue and Pawlowsky-Glahn, 2005).

The strategy of projecting the reference subcomposition may be not appropriate if some property from the complementary subcomposition is relevant and needs to be preserved. The obvious way of doing this consists in using the $D-1$ coordinates corresponding to the original composition $\mathbf{x}$ with no reduction of dimension at all. An intermediate possibility is considering both the coordinates of the reference subcomposition and one or more balances including parts in the complementary subcomposition. In the present example, we have taken only two balances, b_1 and b_2, to keep the presentation simple. Balance b_2 corresponds to the reference subcomposition $\mathcal{C}[x_1,x_2]$, and balance b_1 compares $[x_1,x_2]$ *vs.* $[x_3,x_4,\ldots, x_6]$; although filtering out details within each group, the balance b_1 is an interesting candidate to be preserved in the projection. Following the example in Table I, using only b_1 and b_2 is equivalent to an orthogonal projection from a five-dimensional space, ($\mathcal{S}^6$), into a subspace $\mathcal{R}$ of dimension 2, which is a substantial dimension reduction.

Table I

Sign code of a SBP in S^6 for a projection on the reference subcomposition $C[x_1,x_2]$. The balance b_2 compares x_1 and x_1; b_1 compares the subcomposition $C[x_1,x_2]$ with the complementary subcomposition. Further balances correspond to a SBP within the complementary subcomposition

Balance	x_1	x_2	x_3	x_4	x_5	x_6
b_1	+1	+1	−1	−1	−1	−1
b_2	+1	−1	0	0	0	0
b_3	0	0	+1	+1	−1	−1
b_4	0	0	+1	−1	0	0
b_5	0	0	0	0	+1	−1

The reference subcomposition is

$$\mathbf{x}_s = \mathcal{C}[x_1, x_2, \ldots, x_{d+1}].$$

Using an SBP within $\mathbf{x}_s$ the balances $b_2,b_3,\ldots, b_d$ are readily obtained. Also b_1 corresponds to the partition of $\mathbf{x}$ into the reference subcomposition and its complement, and its expression is

$$b_1 = \sqrt{\frac{(d+1)(D-d-1)}{D}} \ln \frac{(x_1 x_2 \cdots x_{d+1})^{1/(d+1)}}{(x_{d+2} x_{d+3} \cdots x_D)^{1/(D-d-1)}}. \quad [6]$$

The SBP of $\mathbf{x}$ is extended with an SBP of the complementary subcomposition, as illustrated with the example in Table I.

A useful projection is to preserve the values of the balances corresponding to the reference subcomposition $b_2,b_3,\ldots, b_d$ and b_1; other balances are set to zero. Denoting by $\mathbf{b}_p$ these projected balances, the ilr-inverse (Equation [5]) provides the projection (Egozcue and Pawlowsky-Glahn, 2005):

$$\mathbf{x}_p = \mathcal{C}[x_1, x_2, \ldots, x_{d+1}, g_c, g_c, \ldots, g_c]$$

where g_c is the geometric mean of parts within the complement of the reference sub-composition; this geometric mean is repeated $D-d-1$ times to have the D parts. The geometric mean g_c is a summary of the data within the complementary subcomposition. Moreover, $\mathbf{x}_p \in \mathcal{S}^D$, but it spans only a $(d+1)$-dimensional subspace. The vector $\mathbf{x}_p$ can be represented by its balances $\mathbf{b}_p = [b_1,b_2,\ldots, b_d,0,\ldots,0]$ where the reduction of dimension appears effective.

Other balances amongst $b_{d+1},b_{d+2},\ldots, b_{D-1}$ can also be preserved, producing orthogonal projections on subspaces of larger dimension. The choice of these projections should be related with the nature of the problem to be solved, and with the relevance of the balances preserved. The proposed selection of specific balances is here related to the characteristics of the orthogonal projection, but subsequent operations and modelling could be performed using any set of coordinates.

Results in the original units after a projection

Inverse transformed values are parts adding to 1. When the parts add to a different constant, such as concentrations adding to a million, the required scaling is trivial: all parts

need to be multiplied by the constant. In cases, such as molar concentrations or mg/ℓ, the backtransformation to the original units requires a more demanding scaling. Suppose that a D-part composition $\mathbf{x}$ is expressed in some meaningful units. For instance, in percentages, ppm, ppb, mg/ℓ or the like. Frequently, the fill-up component is omitted, and $\mathbf{x}$ appears as a non-closed vector. A closure of $\mathbf{x}$ causes the change of the original units. Also, after any orthogonal projection, these units are lost. In the simplest case, projection on a reference subcomposition, the result will be expressed as proportions within the subcomposition as an effect of the closure of the subcomposition. In some cases, the analyst can be interested in having the final results in the original units after projections such as those presented above. If the original composition is large, the interest might be in obtaining the parts in the reference subcomposition in the original units. However, such a demand cannot be satisfied in a strictly compositional framework. A kind of *total* needs to be known. Totals can be defined in a variety of ways (Pawlowsky-Glahn *et al.*, 2013 and 2014), but some of them are quite intuitive – for instance, the sum of parts in a given subcomposition, or even a single part, using the original units. In general, totals, denoted t, are positive quantities with sample space $\mathbb{R}_+$ or a two-part simplex $\mathcal{S}^2$. Following the principle of working in coordinates (Pawlowsky-Glahn and Egozcue, 2001; Mateu-Figueras *et al.*, 2011) the total is modelled by its only coordinate in $\mathbb{R}_+$, or in $\mathcal{S}^2$ closed to a constant κ_t. In the first case the coordinate is ln t; in the case of $\mathcal{S}^2$, the coordinate is proportional to ln $(t/(\kappa_t - t))$ (the *logit* transformation of t). Here, these coordinates are denoted generically by $\varphi(t)$.

The following procedure is aimed at obtaining the original units for the parts in the reference subcomposition. We assume that the projection is defined by the balances $b_2, b_3, \ldots, b_d$, of the subcomposition, plus b_1 as defined previously in Equation [6]. For this kind of projection, the total, $t = x_1 + \ldots + x_{d+1}$, expressed in the original units, is a useful choice, and will be used from now on. The total t can be obtained from its coordinate using φ^{-1}, *i.e.* if $\varphi(t) = \ln t$, φ^{-1} is the exponential function; if $\tau = \varphi(t) = \ln (t/((\kappa_t - t)))$, then $t = \varphi^{-1}(\tau) = \exp(\tau)/[1 + \exp(\tau)]$. The procedure to have the projected parts $\mathbf{x}_s \in \mathcal{S}^{d+1}$ in the original units has three steps, with the two first ones corresponding to the projection:

1. Find the balance-coordinates of $\mathbf{x}$. Set some of them to zero to perform the desired projection, thus obtaining the projected balances $\mathbf{b}_p$
2. Obtain $\mathbf{x}_p$, closed to some constant κ, applying the inverse ilr-transformation to the projected balances $\mathbf{b}_p$
3. Re-scale $\mathbf{x}_p$ to the original units, using the total t, to finally obtain the parts in $\mathbf{x}_s$ in the original units.

The two first steps have been described in the previous section. The third step is the calculation necessary to have the concentrations in the original units in $\mathbf{x}_p$. The vector containing the projected composition, scaled to the original units, is

$$\mathbf{x}_u = \mathbf{x}_p \cdot \frac{t}{x_{p1} + x_{p2} + \cdots + x_{p,d+1}}, \qquad [7]$$
$$t = x_1 + x_2 + \cdots + x_{d+1},$$

where the role of the total t appears clearly. The $\mathbf{x}_u$ is a closed composition when considering the original D-parts plus the fill-up value; but the first parts $x_{u1}, \ldots, x_{u,d+1}$, corresponding to the reference subcomposition do not appear closed as a subcomposition. On the other hand, the closure constant κ does not appear explicitly in the scaling, as it cancels out when dividing by $\sum_i x_{pi}$.

Cokriging

In our approach, the primary result of a spatial-compositional analysis is a set of interpolated maps of balances. The interpretation of these maps depends on the definition of the particular balances chosen by the analyst. However, the standard practice may require the analyst to generate a map of the concentration of a single part using the original units, *e.g.* in the following section, the illustrative example uses milligrams per litre. Then, a procedure to translate the results, expressed in balances, into a single element concentration is also required.

Cokriging is a multivariate method for the simultaneous interpolation of several regionalized variables. Obtaining interpolated maps of $D - 1$ balances using cokriging may be a hard task if D is a moderate to large number. To avoid such a challenging task, attention can be centered in a reference subcomposition containing $d + 1$ parts. Projections presented previously reduce the number of variables to be cokriged in a consistent way to $d + 1$ balances.

As pointed out in Myers (1983), cokriging should be performed before any projection or dimensional reduction of the data. Here we confront the tradeoff between the simplification of cokriging and the loss of measurement units – μg/ℓ in our case – caused by the projection of the compositional vector. In order to mitigate this loss, the alternative projection is preferred. For the sake of simplicity, only $d + 1$ balances will be cokriged. Additionally, interpolated values of the parts in the reference subcomposition in the original units are also required. As stated in the previous section, a total is also needed, and its coordinate $\varphi(t)$ should also be cokriged with the mentioned d +1 balances. Therefore, cokriging involves d + 2 variables.

The balances $b_1, b_2, \ldots, b_{d+1}$ and $\varphi(t)$ are transformed variables which have no support restrictions: they can span the whole real line, and they are no longer compositional or positive variables. Ratios of parts of compositions are frequently positively skewed, thus approximating lognormal distributions. These distributions approach normal distributions when log-transformed (Mateu-Figueras *et al.*, 2011). Hence, standard multivariate techniques can be applied to these log-transformations. In particular, cokriging can be applied, and the properties of cokriging properly hold: best (minimum variance) linear unbiased estimator.

To perform cokriging of the vector of these $d + 2$ variables, we use a matrix formulation of cokriging (Myers, 1982). Some advantages are:

- The components of the estimation vector are estimated simultaneously instead of repeating $d + 2$ times the undersampled formulation of cokriging, where the roles of primary and secondary variables are interchanged
- The full variance-covariance of the estimates is provided, while only the cokriging estimation variance is obtained when each variable is estimated separately
- Myers (1982) concludes that matrix formulation is computationally advantageous and the cross-semivariogram model is clearer.

For clarity of notation in the remainder of this section, non-random (column) vectors are denoted in lowercase and boldface, and matrices are presented in boldface capitals. Random variables are presented in capitals, and boldface if they form a random (column) vector. Let $\mathbf{Z} = (Z_1,Z_2,\ldots,Z_m)$ denote the vector of second order stationary random functions modelling the variables of concern; here they are $(b_1,b_2,\ldots,b_{d+1},\varphi(t))$. The random vector $\mathbf{Z}$ is observed in the set of n data locations $\mathbf{u}_k$, k =1, 2,...,n, normally expressed in coordinates as northing and easting in the case of a bidimensional spatial domain. The goal of cokriging is to estimate $\mathbf{Z}$ at a location $\mathbf{u}_0$, $\mathbf{Z}(\mathbf{u}_0)$, using the linear estimator

$$\mathbf{Z}^*(\mathbf{u}_0) = \sum_{k=1}^{n} \boldsymbol{\Gamma}_k \mathbf{Z}(\mathbf{u}_k), \quad [8]$$

where $\boldsymbol{\Gamma}_k$ is an (m, m)-matrix of weights. The weights $\boldsymbol{\Gamma}_k$ are obtained by minimizing an estimation variance, conditional to $\mathbf{Z}^*(\mathbf{u}_0)$ being an unbiased estimator of the mean value of $\mathbf{Z}(\mathbf{u}_0)$. A sufficient condition for $\mathbf{Z}^*(\mathbf{u}_0)$ to be unbiased is that

$$\sum_{k=1}^{n} \boldsymbol{\Gamma}_k = \mathbf{I}, \quad [9]$$

(Myers, 1982), where $\mathbf{I}$ is the (m, m)-identity matrix. Although there are different ways of defining the estimation variance in the multivariate estimation case, the form

$$\sum_{k=1}^{n} \mathrm{Var}\left(Z_i(\mathbf{u}_0) - Z_i^*(\mathbf{u}_0)\right), \quad [10]$$

is computationally advantageous. Minimization of the estimation variance (Equation [10]), subject to the unbiasedness condition [9], determines the weights, $\boldsymbol{\Gamma}_k$, by solving the cokriging system of equations

$$\mathbf{WG} = \mathbf{L}, \quad [11]$$

(Myers, 1982), where the number of equations is $m\cdot(n + +1)$ and

$$\mathbf{W} = \begin{bmatrix} \bar{\mathbf{C}}(\mathbf{u}_1,\mathbf{u}_1) & \cdots & \bar{\mathbf{C}}(\mathbf{u}_1,\mathbf{u}_n) & \mathbf{I} \\ \vdots & \ddots & \vdots & \vdots \\ \bar{\mathbf{C}}(\mathbf{u}_n,\mathbf{u}_1) & \cdots & \bar{\mathbf{C}}(\mathbf{u}_n,\mathbf{u}_n) & \mathbf{I} \\ \mathbf{I} & \cdots & \mathbf{I} & \mathbf{0} \end{bmatrix},$$

$$\mathbf{G} = \begin{bmatrix} \boldsymbol{\Gamma}_1 \\ \vdots \\ \boldsymbol{\Gamma}_n \\ \bar{\boldsymbol{\Lambda}} \end{bmatrix}, \qquad \mathbf{L} = \begin{bmatrix} \bar{\mathbf{C}}(\mathbf{u}_0,\mathbf{u}_1) \\ \vdots \\ \bar{\mathbf{C}}(\mathbf{u}_0,\mathbf{u}_n) \\ \mathbf{I} \end{bmatrix},$$

with $\bar{C}(\mathbf{u}_i\,\mathbf{u}_j)$ an estimator of the covariance matrix of $\mathbf{Z}(\mathbf{u}_i)$ and $\mathbf{Z}(\mathbf{u}_j)$, and $\bar{\boldsymbol{\Lambda}}$ an (m, m)-matrix of Lagrange multipliers.

The variance-covariance matrix of the estimator $\mathbf{Z}^*(\mathbf{u}_0)$ is

$$\mathbf{V} = \bar{\mathbf{C}}(0) - \sum_{i=1}^{n} \bar{\mathbf{C}}(\mathbf{u}_0,\mathbf{u}_i)\,\boldsymbol{\Gamma}_i - \bar{\boldsymbol{\Lambda}}, \quad [12]$$

(Myers, 1982), where $\bar{C}(0) = \bar{C}(\mathbf{u}_i\,\mathbf{u}_j)$ which does not depend on $\mathbf{u}_i$ under second order stationarity of $\mathbf{Z}$.

The cokriging estimator $\mathbf{Z}^*(\mathbf{u}_0)$ is a linear combination of the observations $\mathbf{Z}(\mathbf{u}_k)$ whenever the observed variables are real. However, if $\mathbf{Z}$ is taken as a raw composition, several disappointing consequences follow (Pawlowsky, 1984). The first one is that $\mathbf{Z}^*(\mathbf{u}_0)$ is no longer a linear estimator, as the linear combination in Equation [8] becomes nonlinear in the simplex, (see section on *Aitchison geometry for compositional data*) and ill-defined, as the non-convex combination of compositions is not assured to be a composition (Pawlowsky-Glahn *et al.*, 1993). A second issue of concern is that the unbiasedness property is lost because the centre of a random composition is not the mean when the composition is taken as a real vector (Aitchison, 1986; Pawlowsky-Glahn and Egozcue, 2001, 2002). A third pitfall is that all covariance matrices appearing in the cokriging equations ([11]–[12]) are spurious (Aitchison, 1986; Egozcue and Pawlowsky-Glahn, 2011; Pawlowsky, 1984).

Application: As and Fe in the groundwaters of Bangladesh

Available data

A well-known public-domain data-set is used to illustrate the above methodology: groundwater geochemical analysis conducted in the late 1990s in Bangladesh jointly by the local Department of Public Health Engineering and the British Geological Survey (2001a, b). The main objective of this exercise is to illustrate the adequate mapping of compositional data in general, not touching on other important and related subjects such as the genesis of the concentrations and the public health implications. The Bangladesh raw data require some pre-processing to address the following issues:

(a) There are indications in the British Geological Survey (2001a) report, supported also by Yu *et al.* (2003), that there is a systematic tendency of the As concentration to decrease with depth. This fact implies that proper modelling of the entire data-set requires a three-dimensional modelling. The simpler two-dimensional mapping of our interest thus requires the subdivision of the complex system of aquifers and aquitards into units without significant vertical fluctuations in concentration. Inspection of the data and the geology suggested that the aquifer between 7–41 m was sufficiently homogeneous for a two-dimensional modelling. This is the subject of the present application

(b) Another issue is that some of the values are below detection limit, that is, values greater than zero but small enough to be below the analytical precision of the laboratory. The detection limit for As is 0.5 μg/ℓ and 0.005 mg/ℓ for Fe. All data values below detection limits were replaced by an imputed value using the methodology described in Olea (2008)

(c) Four wells were discarded because all values were below detection limit, an unlikely situation in nature, which prompted the authors to suspect errors in the collection or processing of the specimens.

The original data-set consisted of 3416 records, each one containing the concentration of 20 solutes in water (parts) in milligrams per litre. Of the 20 parts analysed in the survey, Co, Cr, Li, V, Cu, and Zn were not considered, as they present serious problems related to values below detection limits and to rounding in the measurement process. The arsenic values were an exception in the sense that they were reported in micrograms per litre, but were changed to milligrams per litre for the purpose of modelling. The reader can visit the Internet to view maps posting the data (British Geological Survey, 2001a).

Here, only the set of solutes (As, Al, B, Ba, Ca, Fe, K, Mg, Mn, Na, P, Si, SO_4, Sr) is considered. A data-set consisting of 14 solutes and 2096 data locations was thus retained for further analysis.

Modelling

In the present development, available data corresponds to D = 14 parts of a larger composition in milligrams per litre. An analysis could be performed defining a fill-up value to the total given by the units of measurement. This method would require the analyst to know the density of water and the fill-up variable would essentially be water, for example, as done in Otero *et al.* (2005). Here, the fill-up part is ignored and only data in $\mathbf{x} \in S$ 14 is modelled. The subcomposition (As, Fe) is taken as the reference subcomposition. The available compositions at the observation points are projected following the approach developed previously, *i.e.* d = 1.

According to the emphasis by the British Geological Survey (2001a), interest is centred on As and Fe; therefore, the SBP was defined in a way that the first balance, b_1, reflects the relation of (As, Fe) *versus* the rest of parts, and the second balance, b_2, the relation of (As vs Fe). Following Equation [3], they are computed as:

$$b_1 = \sqrt{\frac{2 \cdot 12}{2+12}} \ln \frac{(\mathrm{As} \cdot \mathrm{Fe})^{1/2}}{(\mathrm{Al} \cdot \mathrm{B} \cdot \mathrm{Ba} \cdot \mathrm{Ca} \cdot \mathrm{K} \cdot \mathrm{Mg} \cdot \mathrm{Mn} \cdot \mathrm{Na} \cdot \mathrm{P} \cdot \mathrm{Si} \cdot \mathrm{SO_4} \cdot \mathrm{Sr})^{1/12}}, \quad [13]$$

$$b_2 = \sqrt{\frac{1 \cdot 1}{1+1}} \ln \frac{\mathrm{As}}{\mathrm{Fe}}. \quad [14]$$

The remaining $D - 2 = 12$ balances were defined without specific geological criteria. The following analysis does not depend on the choice of these balances. The SBP used is graphically displayed as the compositional dendrogram (Thió-Henestrosa *et al.*, 2008; Pawlowsky-Glahn and Egozcue, 2011) shown in Figure 1, obtained with the package CoDaPack (Comas-Cufí and Thió-Henestrosa, 2011).

The uppermost vertical bar, corresponding to the partition (As, Fe) *versus* the rest of parts, is the largest because the variance of b_1 is the largest one. It is, in fact, 5.4805, while b_2 has a variance of 1.7401, which is the second largest variance. Balances $b_3, b_4, \ldots, b_{13}$ are not necessary in the following analysis, and are not included in the cokriging system of equations.

Following the approach outlined previously, the total considered for having the results in the same original units is t = As + Fe (mg/ℓ). The number of variables to be cokriged is then d +2 = 3, *i.e.* b_1, b_2, $\varphi(t)$. The balances b_1 and b_2 are dimensionless, as in Equations [13] and [14] units disappear, while the units of t are the original milligrams per litre. The total variable t has compositional character because it is the ratio t over the total mass (solute and water) per litre. Frequently, the total mass, taken equal to $\kappa_t = 10^6$ mg/ℓ and $(t, 10^6 - t)$, is a composition in $\mathcal{S}^2$. In that case, the coordinate $\varphi(t)$ would be the logit transform of t, as mentioned previously. However, taking $\kappa_t = 10^6$ mg/ℓ is inadequate, as it

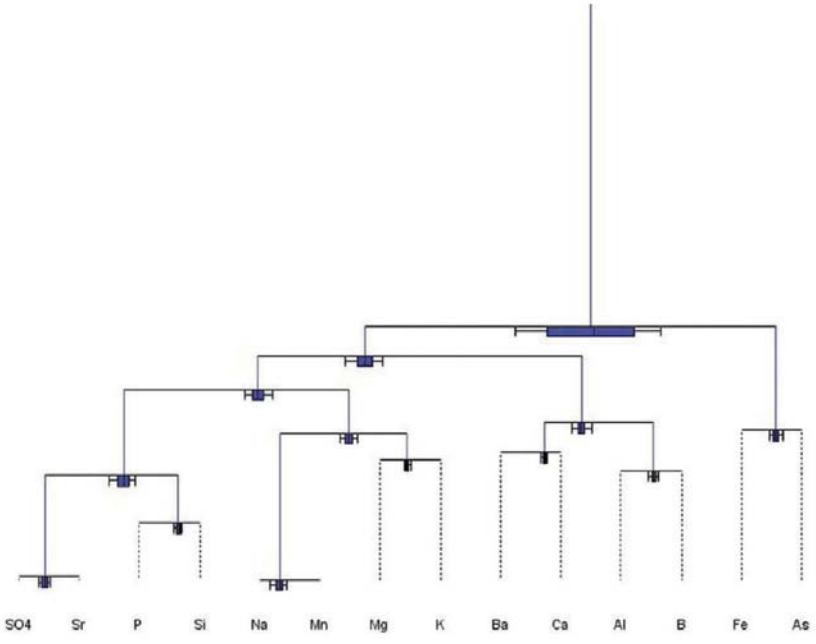

Figure 1—Compositional dendrogram corresponding to the sequential binary partition (SBP) of the 14 solutes in a Bangladesh survey (British Geological Survey, 2001a). Vertical bars are proportional to the variances of each balance. The fulcrum, or point of contact of vertical and horizontal bars, is the average balance. The horizontal box-plots correspond to the dispersion of each balance

ignores the mass of solute (Otero *et al.*, 2005). The alternative of considering t as a variable in $\mathcal{R}_+$ has been chosen and, consequently, $\varphi(t) = \ln(t)$ is considered as the corresponding coordinate to be used in the cokriging modeling.

The parameters of semivariograms and cross-semivariograms used for cokriging are given in Table II, and are displayed in Figure 2. Table III gives the eigenvalues for the coefficient matrices in the linear coregionalization model used in the inference of spatial correlation.

The study area was tessellated into a grid of locations with a spacing of 1 km comprising 460 columns and 660 rows with 123 079 of the locations within the borders of Bangladesh, covering the country with reasonable resolution. Cokriging was applied using the linear coregionalization models of Table II. The estimated maps of b_1, b_2, and ln (t) are shown in Figure 3. Maps (a) and (b) in Figure 3 contain the estimates balances after the projection of the whole composition and the corresponding cokriging. However, obtaining the results in the same original units (OU) of arsenic and iron is performed using Equations [5] and [7], which requires the cokriging results shown in map (c) of Figure 3 corresponding to natural logarithm of the sum of the two elements, both in the original units.

$$As_{OU} = \frac{As}{(As + Fe)} \exp(\ln(As_{OU} + Fe_{OU}))$$

$$Fe_{OU} = \frac{Fe}{(As + Fe)} \exp(\ln(As_{OU} + Fe_{OU})).$$

Figure 4 shows the interpolation of both elements in their original units (mg/ℓ). Despite its relevance, concentrations of arsenic are quite low relative to the other elements in the survey. So, for display, all values were multiplied by 1000 to change units to μg/ℓ, the standard form of reporting arsenic concentrations in hydrochemistry. These maps show that the compositional techniques are able to perform orthogonal projections to reduce the dimension of cokriging, and to express the results in the traditional form of maps of a single solute in the original units (mg/ℓ).

Table II

Model parameters of nested semivariograms and cross-semivariograms, all omnidirectional.

	Nugget	Spherical	Exponential
Range (km)	----	65	140
Semivariogram of balance b_1	3.5	0.90	3.5
Cross-semivariogram of and b_1 and b_2	0.75	0.35	0.77
Cross-semivariogram of and b_1 and ln(t)	2.02	0.75	1.50
Semivariogram of balance b_2	1.4	0.30	0.7
Cross-semivariogram of and b_2 and ln(t)	-0.57	0.13	0.45
Semivariogram of balance ln(t)	2.1	0.90	0.85

Table III

Eigenvalues of the matrices in the linear coregionalization model

	First	Second	Third
Nugget	0.05	1.98	4.96
Spherical model	0.34	1.73	2.9
Exponential model	0.15	0.51	4.39

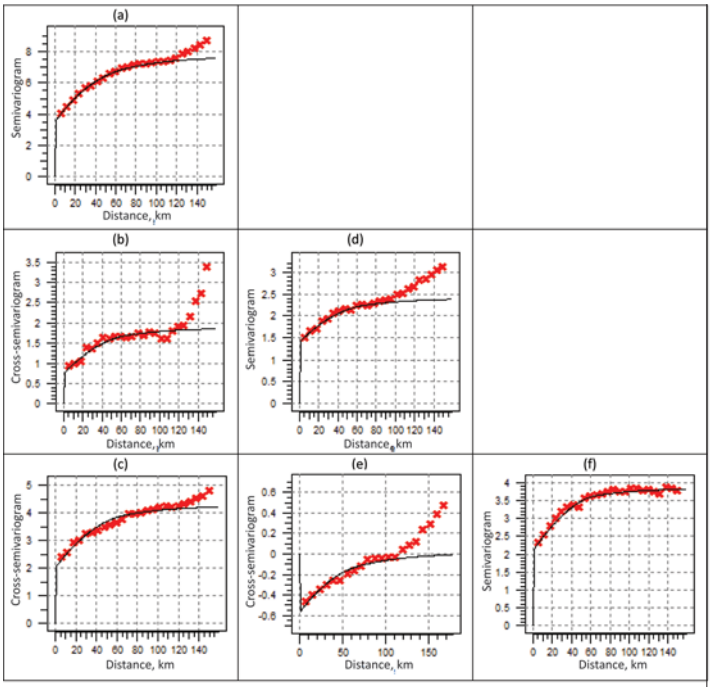

Figure 2—Spatial continuity for nested structures of semivariograms and cross-semivariograms: (a) b_1; (b) b_1 and b_2; (c) b_1 and ln t; (d) b_2; (e) b_{12} and ln t; (f) ln t. For distances greater than 100 km, a drift can be observed

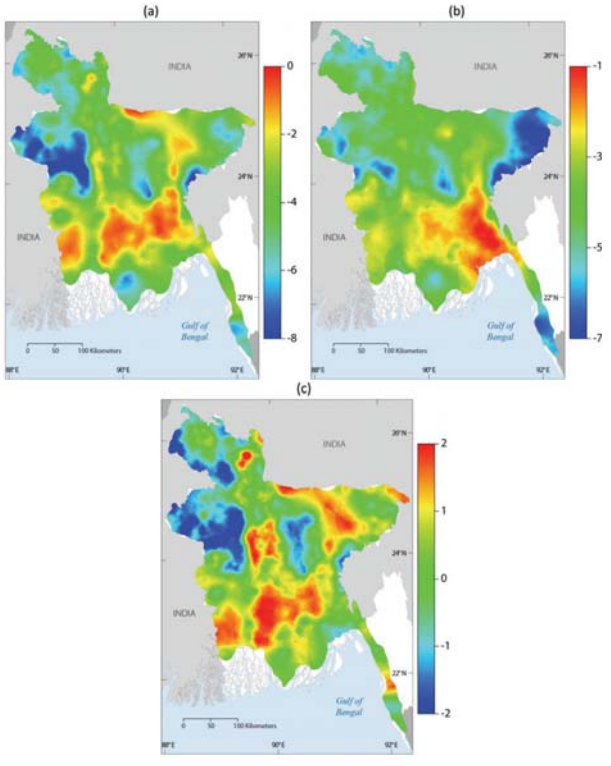

Figure 3—Maps of estimates for: (a) b_1; (b) b_2; (c) ln(As + Fe). In these maps and the maps in Figures 4, 6, 7, 8, and 9, the white denotes areas within Bangladesh without estimation; the small darker area in the northwest corner is in Nepal and the one in the extreme southeast corner is in Myanmar

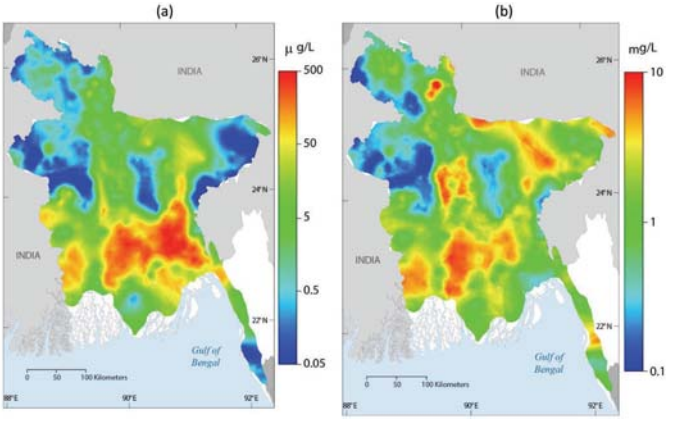

Figure 4—Map of estimated values in logarithmic scale (a) As; and (b) Fe

Uncertainty evaluation of As and Fe

Equation [12] is the variance-covariance matrix of the estimators. If the analyst is willing to assume multinormality of errors, the results can be used to assess uncertainty in the modelling. In particular, three measures have been computed: (a) the probability that As and Fe exceed a given threshold of concentration in milligrams per litre; (b) confidence intervals on As and Fe; and (c) validation of the coverage of the computed confidence intervals.

The scheme of the general procedure is shown in Figure 5. For each point in the interpolation grid, 1000 joint replications of (b_1, b_2, ln t) have been generated using the Cholesky method (Davis, 1987), following a multivariate normal distribution with a mean equal to the three estimated fields (Figure 3) and covariance $\mathbf{V}$ (see third step in the work-flow, Figure 5). The simulation step corresponds to the fourth step in Figure 5. The next step is the reconstruction of the concentrations of As and Fe from the simulated triplets (b_1, b_2, ln t). It consists of applying the ilr-inverse transformation to (b_1, b_2) (Equation [5]) to produce the closed reference subcomposition (As, Fe). Then (fifth step in the work-flow, Figure 5), using the simulated value of ln (t) = ln(As+Fe), Equation [7] allows the analyst to obtain the subcomposition in the original units (milligrams per litre).

The results from simulation are presented in several maps. Figure 6 shows the probability of the content of As exceeding 10, 50, and 100 µg/ℓ. The first limit of 10 µg/ℓ is

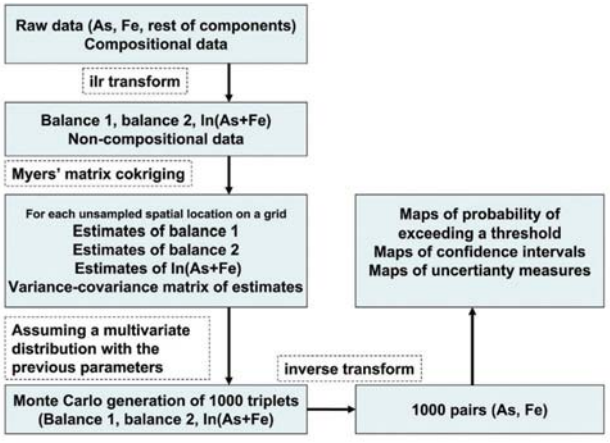

Figure 5—Methodology for assessing uncertainty evaluation by a Monte Carlo approach

the drinking water upper limit established by the World Health Service (WHS); the limit of 50 μg/ℓ is the limit used in Bangladesh, and 100 μg/ℓ is an arbitrary threshold that is 10 times the limit of the WHS and double the Bangladesh recommendation. The maps in Figure 6 show a large probability of exceeding the three limits of interest in more than the 50% of the area of Bangladesh. Other statistics that have been computed are the lower and upper limits of the 90% confidence interval on the mean value of As, the width of the interval (upper limit minus lower limit), as well as the median and standard deviation of the Monte Carlo distribution of As (Figures 7 and 8, respectively).

In order to proceed to a validation of the model, the dataset has been divided into two groups (Figure 9): a calibration set (519 values) and a validation set (1577 values). For each location in the validation set, the mean value of the triplet (b_1, b_2, ln t) is predicted from the points in the calibration set

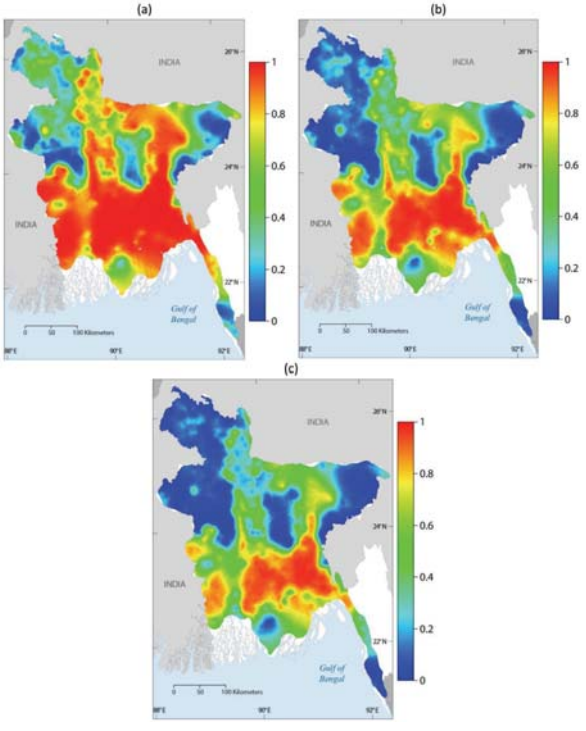

Figure 6—Map of the estimated probability that (a) As > 10 μg/ℓ; (b) As > 50 μg/ ℓ; and (c) As > 100 μg/ ℓ

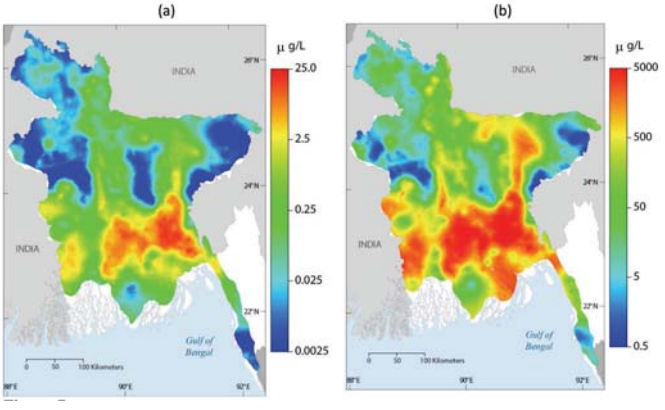

Figure 7—Limits of the 90% confidence interval on the estimated mean concentration of As, in logarithmic scale: (a) lower limit, and (b) upper limit

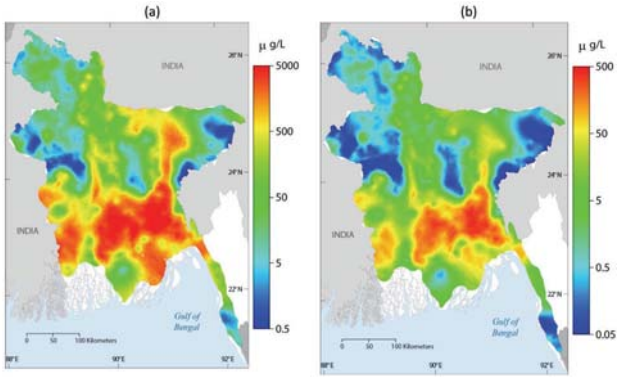

Figure 8—Maps of As concentrations, in logarithmic scale: (a) range of the 90% confidence interval, and (b) median of the estimated mean concentration

using the semivariograms (Table II); also the variance-covariance matrix **V** is taken from the global analysis. Then, a multivariate normal with these parameters is simulated 1000 times at each validation point. It produces triplets (b_1, b_2, ln t), which can be used to obtain simulated values of As and Fe. The probabilistic meaning of the α% Monte Carlo confidence intervals have been validated exhaustively by varying α from 0.01 to 0.99 and calculating the actual coverage by using the validation set from the previous validation exercise. The results are shown in Figure 10, where the nominal coverage is compared with the actual coverage. The results follow closely the 1:1 line, indicating the good agreement between nominal and actual coverage. The result confirms that, at least for the As concentration in Bangladesh, the combined use of balances and assumption of multinormality of errors is adequate. Considering that the modelling is independent from the physical nature of the analysed system, the modelling should work correctly for any other spatial compositional data.

Discussion in terms of practical results

In a strict sense, our practical results are not comparable to any of those from previous studies using the same Bangladesh data, because of our decision to limit our modelling within the depth range of 7–41 m below surface and our imputation of values below the detection limits. The original study set the cut-off at 150 m (British Geological Survey, 2001a; Gaus *et al.*, 2003), a practice followed by most other authors mentioned toward the end of the Introduction. Among the exceptions, Shamsudduha (2007) restricted his study to depths up to 25 m. Hossain *et al.* (2007) set the second shallowest cut-off behind ours at 75 m. On the less consequential issue of replacement of values below detection limit, again most authors followed the lead of the original British Geological Survey Report (2001a) of doing nothing – treating the detection limits as actual measurements – or replacing them by half the value of the detection limit. Instead, we used a method to extrapolate the probability distribution of values below detection limit (Olea, 2008). Hossain *et al.* (2007) unilaterally assigned the value 1 part per billion (ppb) to all values below detection limit, without noting or caring that 1 ppb is different from 1 μg/ℓ.

Despite working with different subsets of the same original data, maps of expected arsenic concentrations produced applying different methods are remarkably similar,

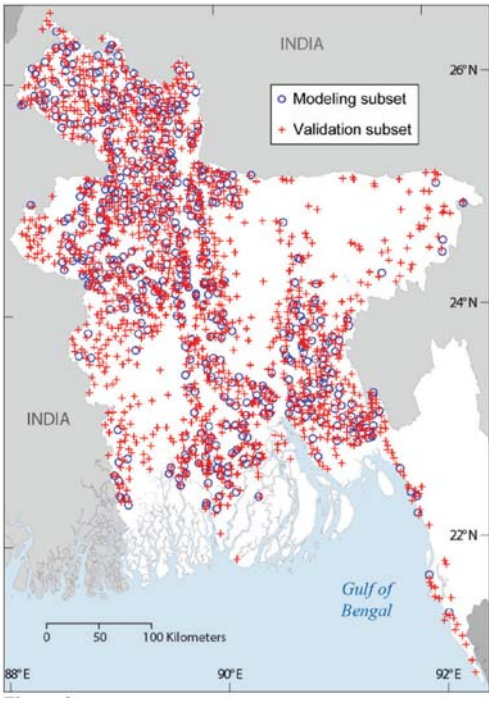

Figure 9—Map of data subsets used for calculations (blue circles) and validation (red crosses)

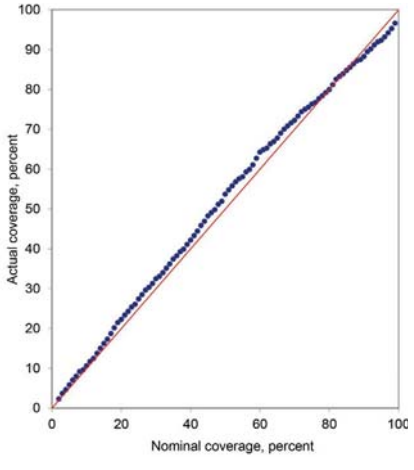

Figure 10—Nominal *versus* actual coverage of the confidence interval. The coverage of the confidence interval based on the Monte Carlo distribution follows closely the nominal value

as it is the case, for example, of our Figure 4a and the equivalent Figure 6.4 in the original study (British Geological Survey, 2001a, vol. 2, p. 83). Shamsudduha (2007) addresses the issue of lack of sensitivity to estimation methods by applying six different methods to the same data, including ordinary kriging without any transformation of the data, which has the potential of producing negative concentrations. This unacceptable inconsistency illustrates the potential danger of avoiding the use of compositional methods because, while non-compositional modelling appears to provide reasonable results most of the time, results may not always be coherent and optimal. At least at the present time, exact number and location of problematic estimates are impossible to predict. Unfortunately, there are no analytical expressions available to assess differences in results between compositional and noncompositional approaches. Discussion of methodological assumptions and comparison of numerical examples remain as the only approaches to evaluate alternative methods.

In addition to the desire to have optimal estimates, the main interest in applying stochastic methods to complex systems is to obtain measures of uncertainty associated with the modelling. There are several ways to display such uncertainty, ways that are not always easy to compare, for example, magnitude of potential errors or length of confidence intervals. Hossain *et al.* (2007), applying ordinary kriging to a logarithmic transformation of the data, made a cross-validation by evenly splitting at random the data into values used in the modelling and control points to compare results. For a 10 μg/ℓ threshold, they found that only 72.2% of the wells were correctly predicted to be safe. Serre *et al.* (2003) used a Bayesian maximum entropy approach to prepare two traditional maps: one for the estimate and another for their standard errors. Relative to our results, their standard errors, on average, are one order of magnitude smaller. Maps of probability of exceedance above selected thresholds are one of the most useful displays in geochemistry, a practice that had been abandoned by all authors of publications after the release of the British Geological Survey (2001a) report. The original study contains probabilities of exceedance for 5, 10, 50, and 150 μg/ℓ based on disjunctive kriging of logarithmic transformations (British Geological Survey, 2001a, vol. 2, p. 169). Our Figures 6a and 6b are the same type of maps for the second (As >10 μg/ℓ) and third thresholds (As >50 μg/ℓ). Our probabilities are significantly higher than those in the original report, suggesting that avoiding the balance approach to mapping compositional data seems to produce low probabilities of exceedance, which in cases of toxic elements in groundwater translates into false negatives – a dangerous situation in which the population is given assurance of safe drinking water when it may not, in fact, be safe. Our unique validation of confidence intervals (Figure 10) gives us assurance that our results are not an exaggerated claim about the possible existence of high concentrations, but a closer approximation to reality.

Conclusions

Compositions are a special type of data about relative proportions of variables in a system. All the parts of a composition, if present, are non-negative. Frequently, they are reported in such a way that they add to a constant to insure that data can be compared independently of the physical size of the specimens. In this case, the data values are in a simplex; they are thus constrained and do not vary over the whole real space. Consequently, statistical methods valid for data varying over the whole real space are not directly applicable to compositional data in a simplex, including cokriging.

Application of cokriging to compositional data requires as a minimum a different representation of the data, *i.e.* a representation in coordinates. This transformation moves the compositional data from the simplex to the whole real space. General purpose transformations, devised for other, unconstrained, regionalized variables, are unsatisfactory for compositional data because they do not properly handle the relative proportions carried by the data. The ilr transformation attains this goal, in particular because it is scale-invariant and subcompositionally coherent. Other transformations commonly used in compositional data analysis, such as the alr (additive logratio) and the clr (centered logratio), have not been considered. The alr leads to an oblique basis, distorting the measures of error like the kriging variance, when they are used as being orthonormal. The clr leads to a generating system with singular covariance matrices. Moreover, the use of ilr transformations to obtain coordinates makes the work with orthogonal projections easy, thus providing a way of supervised dimension reduction. Orthogonal projections in the simplex (*e.g.* on a subcomposition or defined through balances) allows generation of results in the same units as the input data, even if the sum of all parts do not add to a constant provided that some type of total in the original units is available.

Cokriging is the best multivariate method to use in producing estimates of compositional data at locations away for observation sites. In combination with Monte Carlo methods, under an assumption of multinormality of the balances, it is possible to assess the uncertainty of the estimators. Some theoretical advantages of the approach are:

(a) Scale-invariance and subcompositional coherence
(b) Controlled dimension reduction using orthogonal projections
(c) The possibility of having the results in the same original units
(d) Modelling using balances can result in estimation errors whose distribution can be assumed to be approximately multinormal in the transformed space
(e) Using Monte Carlo simulation to expand the cokriging results, it is possible to assess the uncertainty of the cokriging modelling.

Good conformance in confidence intervals indicates that the modelling in general, and the multinormality assumption in particular, are acceptable in this case. We have revisited the mapping of a hydrochemical survey from Bangladesh. We and the British Geological Survey applied different transformations and estimation methods. Indications are that the discrepancies are more significant in terms of assessing uncertainty than in terms of mapping expected values. At least in this comparative evaluation, the original study obtained lower probabilities of exceedance, more likely because of lack of adequacy of the transformations than because of the differences in estimation methods.

Acknowledgments

We are grateful to Raimon-Tolosana-Delgado (Helmholtz-Zentrum Dresden-Rossendorf, Germany), James Coleman (US Geological Survey), Michael Zientek (US Geological Survey) and an anonymous reviewer appointed by the journal for critically reviewing earlier versions of this paper. Eric Morrissey (US Geological Survey) and Christopher Garrity (US Geological Survey) helped us in the annotation of the maps.

This research has been partly supported by the Spanish Ministry of Economy and Competitiveness under the project METRICS (Ref. MTM2012-33236); and by the Agencia de Gestió d'Ajuts Universitaris i de Recerca of the Generalitat de Catalunya under project Ref: 2009SGR424.

Any use of trade, firm, or product names is for descriptive purposes only and does not imply endorsement by the US Government.

References

Aitchison, J. 1982. The statistical analysis of compositional data (with discussion). *Journal of the Royal Statistical Society, Series B* (Statistical Methodology) vol. 44, no. 2. pp. 139–177.

Aitchison, J. 1986. The Statistical Analysis of Compositional Data. *Monographs on Statistics and Applied Probability*. Chapman & Hall, London (UK). (Reprinted in 2003 with additional material by The Blackburn Press). 416 pp.

Aitchison, J. 2003. The Statistical Analysis of Compositional Data. The Blackburn Press, Caldwell, NJ. 435 pp.

Anwar, A. and Kawonine, N. 2012. Characterization of arsenic contamination in groundwater by statistical methods. *International Journal of Global Environmental Issues*, vol. 12, no. 2-4. pp. 302–317.

Barceló-Vidal, C., Martín-Fernández, J.A., and Pawlowsky-Glahn, V. 2001. Mathematical foundations of compositional data analysis. *Proceedings of IAMG'01 – The Sixth Annual Conference of the International Association for Mathematical Geology*. Ross, G. (ed.), pp. 1–20.

Billheimer, D., Guttorp, P., and Fagan, W. 2001. Statistical interpretation of species composition. *Journal of the American Statistical Association*, vol. 96, no. 456. pp. 1205–1214.

British Geological Survey. 2001a. Arsenic contamination of groundwater in Bangladesh. Technical report, BGS, Department of Public Health Engineering (Bangladesh). 630 pp. (Report WC/00/019). http://www.bgs.ac.uk/arsenic/Bangladesh/

British Geological Survey. 2001b. Arsenic contamination of groundwater in Bangladesh: data. Technical report, BGS, DPHE/BGS National Hydrochemical Survey, 1 Excel spreadsheet. http://www.bgs.ac.uk/research/groundwater/health/arsenic/Bangladesh/data.html)

Chayes, F. 1960. On correlation between variables of constant sum. *Journal of Geophysical Research*, vol. 65, no. 12. pp. 4185–4193.

Chayes, F. 1962. Numerical correlation and petrographic variation. *Journal of Geology*, vol. 70, no. 4. pp. 440–452.

Chayes, F. 1971. Ratio Correlation. University of Chicago Press, Chicago, IL. 99 pp.

Chayes, F. 1975. A priori and experimental approximation of simple ratio correlations. *Concepts in Geostatistics*. McCammon, R.B. (ed.). Springer Verlag, New York. pp. 106–137.

Chayes, F. 1983. Detecting nonrandom associations between proportions by tests of remaining-space variables. *Mathematical Geology*, vol. 15, no. 1. pp. 197–206.

Chowdhury, M., Alouani, A., and Hossain, F. 2010. Comparison of ordinary kriging and artificial neural network for spatial mapping of arsenic contamination of groundwater. *Stochastic Environmental Research and Risk Assessment*, vol. 24, no. 1. pp. 1–7.

Comas-Cufí, M. and Thio-Henestrosa, S. 2011. CoDaPack 2.0: a stand-alone, multi-platform compositional software. *CoDaWork'11: Proceedings of the 4th International Workshop on Compositional Data Analysis*, Sant Feliu de Guíxols, Girona, Spain. Egozcue, J.J., Tolosana-Delgado, R., and Ortego, M. (eds.). International Center for Numerical Methods in Engineering. Barcelona, Spain.

Davis, M. 1987. Production of conditional simulations via the LU triangular decomposition of the covariance matrix. *Mathematical Geology*, vol. 19, no. 2. pp. 91–98.

Egozcue, J.J., Barceló-Vidal, C., Martín-Fernández, J.A., Jarauta-Br Agulat, E., Díaz-Barrero, J.L., and Mateu-Figueras, G. 2011. Elements of simplicial linear algebra and geometry. *Compositional Data Analysis: Theory and Applications*. Pawlowsky-Glahn, V. and Buccianti A. (eds.). Wiley, Chichester, UK. 378 pp.

Egozcue, J. J. and Pawlowsky-Glahn, V. 2005. Groups of parts and their balances in compositional data analysis. *Mathematical Geology*, vol. 37, no. 7. pp. 795–828.

Egozcue, J. J. and Pawlowsky-Glahn, V. 2006. Simplicial geometry for compositional data. *Compositional Data Analysis in the Geosciences: From Theory to Practice*. Buccianti, A., Mateu-Figueras, G., and Pawlowsky-Glahn, V. (eds). Volume 264 of Special Publications. Geological Society, London. 212 pp.

Egozcue, J. J. and Pawlowsky-Glahn, V. 2011. Basic concepts and procedures. *Compositional Data Analysis: Theory and Applications*. Pawlowsky-Glahn, V. and Buccianti, A. (eds.). Wiley, Chichester, UK. 378 pp.

Gaus, I., Kinniburghi, D., Talbot, J., and Webster, R. 2003. Geostatistical analysis of arsenic concentration in groundwater in Bangladesh using disjunctive kriging. *Environmental Geology*, vol. 44, no. 8. pp. 939–948.

Hassan, M. and Atkins, P. 2011. Application of geostatistics with indicator kriging for analyzing spatial variability of groundwater arsenic concentrations in southwest Bangladesh. *Journal of Environmental Science and Health*, Part A, vol. 46, no. 11. pp. 1185–1196.

Hossain, F., Hill, J., and Bagtzoglou, A. 2007. Geostatistically based management of arsenic contaminated ground water in shallow wells of Bangladesh. *Water Resources Management*, vol. 21, no. 7. pp. 1245–1261.

Hossain, F. and Sivakumar, B. 2006. Spatial pattern of arsenic contamination in shallow wells of Bangladesh: regional geology and nonlinear dynamics. *Stochastic Environmental Research and Risk Assessment*, vol. 20, no. 1–2. pp. 66–76.

Hossain, M. and Piantanakulchai, M. 2013. Groundwater arsenic contamination risk prediction using GIS and classification tree method. *Engineering Geology*, vol. 156. pp. 37–45.

Martín-Fernández, J.A., Barceló-Vidal, C., and Pawlowsky-Glahn, V. 1998. Measures of difference for compositional data and hierarchical clustering methods. *Proceedings of IAMG'98 – The Fourth Annual Conference of the International Association for Mathematical Geology*. Buccianti, A., Nardi, G., and Potenza, R. (eds.). De Frede Editore, Naples. pp. 526–531.

Mateu-Figueras, G., Pawlowsky-Glahn, V., and Egozcue, J.J. 2011. The principle of working on coordinates. *Compositional Data Analysis: Theory and Applications*. Pawlowsky-Glahn, V. and Buccianti, A. (eds.). Wiley, Chichester, UK. pp. 31–42.

Myers, D.E. 1982. Matrix formulation of co-kriging. *Mathematical Geology*, vol. 14, no. 3. pp.249–257.

Myers, D.E. 1983. Estimation of linear combinations and co-kriging. *Mathematical Geology*, vol. 15, no. 5. pp. 633–637.

Olea, R. 2008. Inference of distributional parameters of compositional samples containing nondetects. *Proceedings of CoDaWork'08, The 3rd Compositional Data Analysis Workshop*, Universitat de Girona, Girona, Spain. Daunis-i Estadella, J. and Martín-Fernández, J.E. (eds.).http://dugi-doc.udg.edu/handle/10256/708 20 pp.

Otero, N., Tolosana-Delgado, R., Soler, A., Pawlowsky-Glahn V., and Canals, A. 2005. Relative *vs*. absolute statistical analysis of compositions: a comparative study of surface waters of a Mediterranean river. *Water Research*, vol. 39, no. 7. pp. 1404–1414.

Pardo-Igúzquiza, E. and Chica-Olmo, M. 2005. Interpolation and mapping of probabilities for geochemical variables exhibiting spatial intermittency. *Applied Geochemistry*, vol. 20, no. 1. pp. 157–168.

Pawlowsky, V. 1984. On spurious spatial covariance between variables of constant sum. Science de la Terre, Sér. *Informatique*, vol. 21. pp. 107–113.

Pawlowsky-Glahn, V. and Egozcue, J.J. 2001. Geometric approach to statistical analysis on the simplex. *Stochastic Environmental Research and Risk Assessment (SERRA)*, vol. 15, no. 5. pp. 384–398.

Pawlowsky-Glahn, V. and Egozcue, J.J. 2002. BLU estimators and compositional data. *Mathematical Geology*, vol. 34, no. 3. pp. 259–274.

Pawlowsky-Glahn, V. and Egozcue, J.J. 2011. Exploring compositional data with the coda-dendrogram. *Austrian Journal of Statistics*, vol. 40, no. 1–-2. pp. 103–113.

Pawlowsky-Glahn, V., Egozcue, J.J., and Lovell, D. 2013. The product space T (tools for compositional data with a total). *CoDaWork'2013. Compositional Data Analysis Workshop*. Filzmoser, P. and Hron, K. (eds.). [CD-ROM]. Technical University of Vienna.

Pawlowsky-Glahn, V., Egozcue, J.J., and Lovell, D. (2014). Tools for compositional data with a total. Statistical Modelling, prepublished November, 25, 2014, doi: 10.1177/1471082X14535526.

Pawlowsky-Glahn, V., Egozcue, J.J., and Tolosana-Delgado, R. 2015. Modeling and Analysis of Compositional Data. Wiley, Chichester, UK. 256 pp.

Pawlowsky-Glahn, V. and Olea R.A. 2004. Geostatistical Analysis of Compositional Data. No. 7 in *Studies in Mathematical Geology*. Oxford University Press. 181 pp.

Pawlowsky-Glahn, V., Olea, R.A., and Davis, J.C. 1993. Boundary assessment under uncertainty: a case study. *Mathematical Geology*, vol. 25. pp. 125–144.

Pearson, K. 1897. Mathematical contributions to the theory of evolution. on a form of spurious correlation which may arise when indices are used in the measurement of organs. *Proceedings of the Royal Society of London*, vol. LX. pp. 489–502.

Serre, M., Kolovos, A., Christakos, G., and Modis, K. 2003. An application of the holistochastic human exposure methodology to naturally occurring arsenic in Bangladesh drinking water. *Risk Analysis*, vol. 23, no. 3. pp. 515–528.

Shamsudduha, M. 2007. Spatial variability and prediction modelling of groundwater arsenic distributions in the shallowest alluvial aquifers in Bangladesh. *Journal of Spatial Hydrology*, vol. 7, no. 2. pp. 33–46.

Shamsudduha, M., Marzen, L., Uddin, A., Lee, M., and Saunders, J. 2009. Spatial relationship of groundwater arsenic distribution with regional topography and water-table fluctuations in the shallow aquifers of Bangladesh. *Environmental Geology*, vol. 57, no. 7. pp. 1521–1535.

Thio-Henestrosa, S., Egozcue, J.J., Pawlowsky-Glahn, V. Kov Acs, L.O., and Kov Acs, G.P. 2008. Balance-dendrogram. A new routine of CoDaPack. *Computers and Geosciences*, vol. 34. pp. 1682–1696.

Tolosana-Delgado, R., Pawlowsky-Glahn, V., and Egozcue, J.J. 2008. Indicator kriging without order relation violations. *Mathematical Geosciences*, vol. 40, no. 3. pp. 327–347.

Tolosana-Delgado, R., Van Den Boogaart, K.G., and Pawlowsky Glahn, V. 2011. Geostatistics for compositions. *Compositional Data Analysis: Theory and Applications*. Pawlowsky-Glahn, V. and Buccianti, A. (eds.). Wiley, Chichester, UK. pp. 73–86.

Yu, W., Harvey, C., and Harvey, C. 2003. Arsenic in groundwater in Bangladesh: a geostatistical and epidemiological framework for evaluating health effects and potential remedies. *Water Resources Research*, vol. 39, no. 6. pp. 1146–1162. ◆

http://dx.doi.org/10.17159/2411-9717/2015/v115n1a8

Application of Direct Sampling multi-point statistic and sequential gaussian simulation algorithms for modelling uncertainty in gold deposits

by Y. van der Grijp*† and R.C.A. Minnitt†

Synopsis

The applicability of a stochastic approach to the simulation of gold distribution to assess the uncertainty of the associated mineralization is examined. A practical workflow for similar problems is proposed. Two different techniques are explored in this research: a Direct Sampling multi-point simulation algorithm is used for generating realizations of lithologies hosting the gold mineralization, and sequential Gaussian simulation is applied to generate multiple realizations of gold distributions within the host lithologies. A range of parameters in the Direct Sampling algorithm is investigated to arrive at good reproducibility of the patterns found in the training image. These findings are aimed at assisting in the choice of appropriate parameters when undertaking the simulation step. The resulting realizations are analysed in order to assess the combined uncertainty associated with the lithology and gold mineralization.

Keywords

Direct Sampling, multi-point statistics, MPS simulation, training image, uncertainty in gold deposits.

Introduction

Traditionally, grade distribution in an orebody is modelled by creating a block model with a single version of geological domaining that in turn is populated with a single version of mineral grade distribution. Such a deterministic representation of reality conveys an impression that the size, geometry, and spatial position of geological units are perfectly known. If the density of the available data is such that the model can be inferred with high confidence, the approach is acceptable, but problems arise when data is widely spaced, interpretations are ambiguous, and multiple scenarios can be inferred with equal validity (Perez, 2011). Stochastic simulation, on the other hand, is used to generate multiple equiprobable realizations of a variable.

This study uses two approaches to stochastic modelling: namely, Direct Sampling (DS) for simulating lithology as geologically stationary domains, and sequential gaussian simulation (SGS) for simulating multiple realizations of grade distribution (Goovaerts, 1997) within the simulated lithologies. DS is one of many algorithms based on multiple-point statistics (MPS) and has as its basis a training image (TI). The training image is a conceptual representation of how random variables are jointly distributed in space, be they continuous or categorical variables. It portrays a model of geological heterogeneity on which further MPS simulation is based (Caers, 2011). While a two-point simulation aims at generating realizations that honour the data and the variogram model, an MPS simulation generates realizations that honour the data and the multi-point structures present in the TI (Remy, 2009).

A number of MPS algorithms have been developed in the last two decades, after the concept was first introduction by Guardiano and Srivastava in 1993 (Guardiano,1993). In 2002, Strebelle proposed the *snesim* algorithm for simulation of categorical variables. It utilized a 'search tree' structure to store conditional probabilities of data events which were extracted later during simulation. The *snesim* algorithm was computationally demanding, which made it prohibitive for simulation of large models. The *Filtersim* algorithm (Zhang *et al.*, 2006; Wu *et al.*, 2008) accommodated both continuous and categorical variables, as well as improved the computational demands by simulating batches of pixels rather than one pixel at a time. The *IMPALA* algorithm (Straubhaar *et al.*, 2011) used lists instead of trees, which reduced the memory requirements by allowing parallelization; however, it was still computationally demanding. In 2007, Arpat and Caers introduced the *SIMPAT* algorithm, which used distance functions to calculate similarity between the TI and conditioning data events.

* *Continental Africa – Geology Technical Services, AngloGold Ashanti. University of the Witwatersrand.*

† *School of Mining Engineering, University of the Witwatersrand.*

Multi-dimensional scaling, *MDS*, (Honarkhah and Caers, 2010) and the *CCSIM* method (Tahmasebi *et al.*, 2012) are other examples of MPS algorithms (Rezaee, 2013).

The DS algorithm is similar to other techniques in the way it uses the principle of sequential simulation. The difference lies in the way the conditional cumulative distribution function for the local data event is computed (Mariethoz *et al.*, 2013). Rather than storing the TI probabilities in a catalogue prior to simulation, the algorithm directly scans and samples the TI in a random fashion while conditioning to the data event d_n. It uses dissimilarity distances between the d_n and TI patterns. For each node x in the simulation grid, the TI is randomly scanned for matching patterns of nodes denoted y. A measure of satisfying the degree of 'matching' is determined by a user-defined distance threshold, which takes a range of values between 0 and 1. As soon as a TI pattern that matches the data event d_n exactly or within the defined threshold is found, the value of the central node of such TI pattern is pasted at location x.

The advantage of DS over other MPS algorithms is that it bypasses the step of explicit calculation of the conditional distribution function (cdf), and as a result avoids many technical difficulties encountered in other algorithms. Since the TI is scanned randomly, a strategy equal to drawing a random value from a cdf, the simulation speed is increased considerably (Mariethoz *et al.*, 2013). The DS algorithm can be applied to both categorical and continuous variables, as well as to multivariate cases. Another advantage, which has not been explored in the current study, is the possibility of using a very simple synthetic TI combined with a rotational field generated from structural readings of diamond-drill core, which would allow for more 'geologically-informed' simulations.

A detailed description of the DS algorithm, its parameters and their sensitivities, as well as practical considerations for different applications can be found in Mariethoz *et al.* (2012, 2013).

Practical application of the simulation algorithms

Geological setting

The algorithms have been applied to a data-set originating from Nyankanga deposit, Geita Gold Mine. The mine is located to the south of Lake Victoria in northwestern Tanzania. It is hosted within the Sukumaland Greenstone Belt of the Lake Victoria goldfields (Brayshaw, 2010). The local geology of the Nyankanga deposit comprises lens-shaped banded iron formation (BIF) packages with intercalations of intermediate and felsic intrusives termed 'diorites', and minor sedimentary rocks. The package is folded, faulted, sheared, and regularly cut by late-stage barren quartz porphyry (QP) dykes. Gold mineralization is localized along a distinct, shallowly dipping tabular shear zone. The highest grades are closely associated with BIFs, with sigmoidal or tabular orebodies. Within the diorite, the gold mineralization has a more erratic distribution and a lower average grade.

The local geology of the deposit lends itself well to the MPS simulation method. While the interface between BIF and diorite could be modelled successfully with conventional variogram-based techniques, they would have failed to reproduce continuous extensive sheets of barren dykes. The effect on the simulated mineral content was considered immaterial in the current case study; however, the issue was pursued to assist in future simulations.

Data description

The simulation was undertaken on a small portion of the deposit in the eastern part of the Nyankanga orebody. The location of the simulation volume in relation to the operating pit is shown in Figure 1.

The drill-hole data-set consists of 410 holes, 249 drilled by reverse circulation and 161 by diamond core drilling. The majority of the drill-holes are sampled at 1 m intervals. In the top portion of the deposit, dense grade-control drilling on a grid of 10 m (along easting) by 5 m (along northing) allowed for the definition of a well-informed TI (Figure 2).

Training image preparation

Choice of a TI for simulation of lithologies is of paramount importance in the application of MPS as it serves as the source of spatial patterns to be simulated.

A TI with 742 500 nodes evenly spaced at 2 m intervals was created. Three main lithologies – BIF, intrusive diorite complex, and barren QP dykes – were modelled and used for domaining the gold simulation. The boundary between BIF and diorite was modelled using a radial basis function method. QP dykes were modelled deterministically as tabular bodies. The resulting wireframes were used to code grid nodes in the TI (Figure 3).

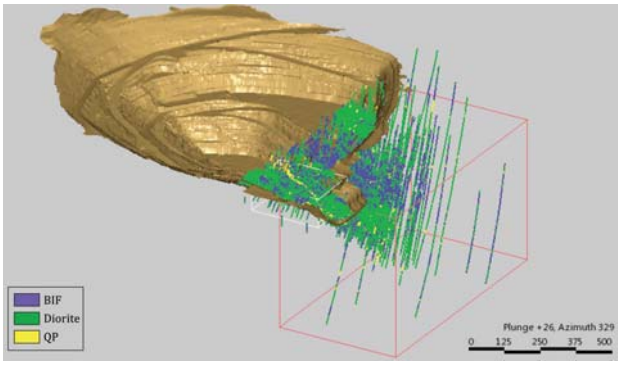

Figure 1—Isoclinal view of the Nyankanga pit showing drill-hole data-set used in the simulation. The white box represents the extent of the training image, the red box the main simulation volume

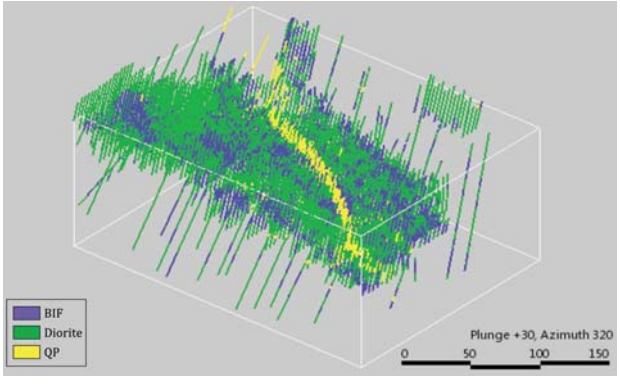

Figure 2—Drill-holes used in the creation of the training image

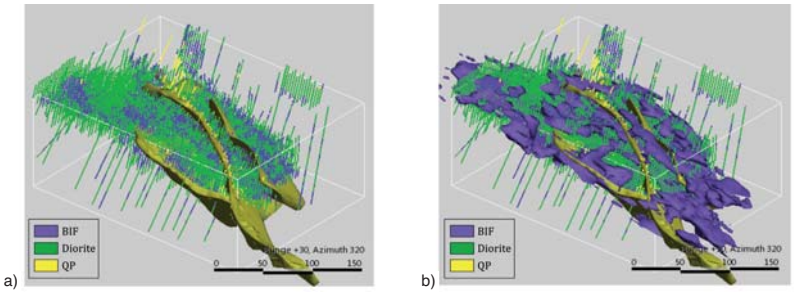

Figure 3—Wireframe models used to code the training image for: (a) dykes, (b) dykes and BIF

A ZX sectional view of the resulting TI is shown in Figure 4.

Training image trial simulation

A trial simulation was performed over the volume of the TI to ensure good overall reproducibility of the patterns contained in the image and to confirm the choice of simulation parameters before applying the TI to the main volume of interest.

In the unconditional simulation, the connectivity of dykes posed a major challenge, while simulated BIF and diorite shapes were reproduced quite reasonably. A number of parameters were tested, but none of them seemed to improve the connectivity dramatically. A comparison of the TI and the pattern derived by unconditional simulation is given in Figure 5.

Conditional simulation within the TI volume allowed for better connectivity of dykes, the high density of conditioning data being the main contributing factor. Honouring of the global lithology proportions was good, considering that no global proportions were specified in the simulation input. The comparison is presented in Table I.

Two realizations of the conditional simulation are displayed in Figure 6a and 6b.

The results of the gold simulation in all three lithology types were compared with the main statistics and gold distributions in the cumulative distribution plots of Figure 7. These diagrams illustrate the extent to which simulated output has honoured the conditioning data.

Indicator variograms for the simulated realizations of BIF and diorite lithologies from the TI in the principal directions of continuity (blue) compare well with the input variogram models for both lithologies (red), as shown in Figure 8.

The range and continuity of variograms created from the simulated gold values for each of the three lithologies were compared to the input gold variogram models, which although not perfect matches, were acceptably replicated in the simulation.

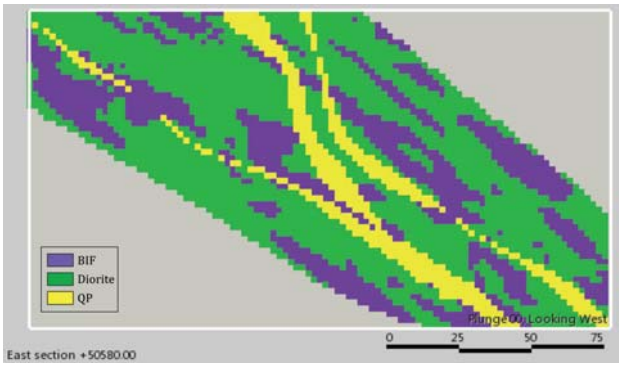

Figure 4—ZX sectional slice through Figure 3, showing the three main lithologies in the training image

Table I

Global proportions of the conditionally simulated lithologies within the training image

Lithology	Conditioning data within TI	Simulated proportions within TI
BIF	0.31	0.27
Diorite	0.61	0.66
QP	0.08	0.07

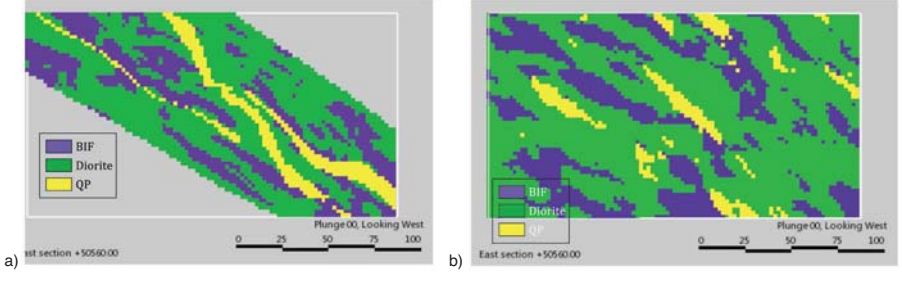

Figure 5—ZX sectional view of unconditional simulation of lithology: (a) training image with the three main lithologies, and (b) one realization by unconditional simulation within the training image volume

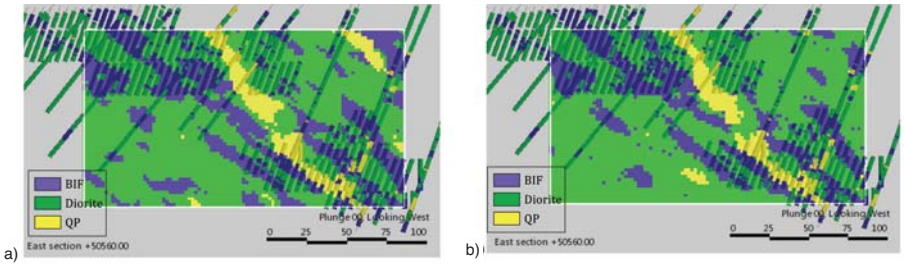

Figure 6—Two conditional realizations across the XZ sectional view within the volume of the training image

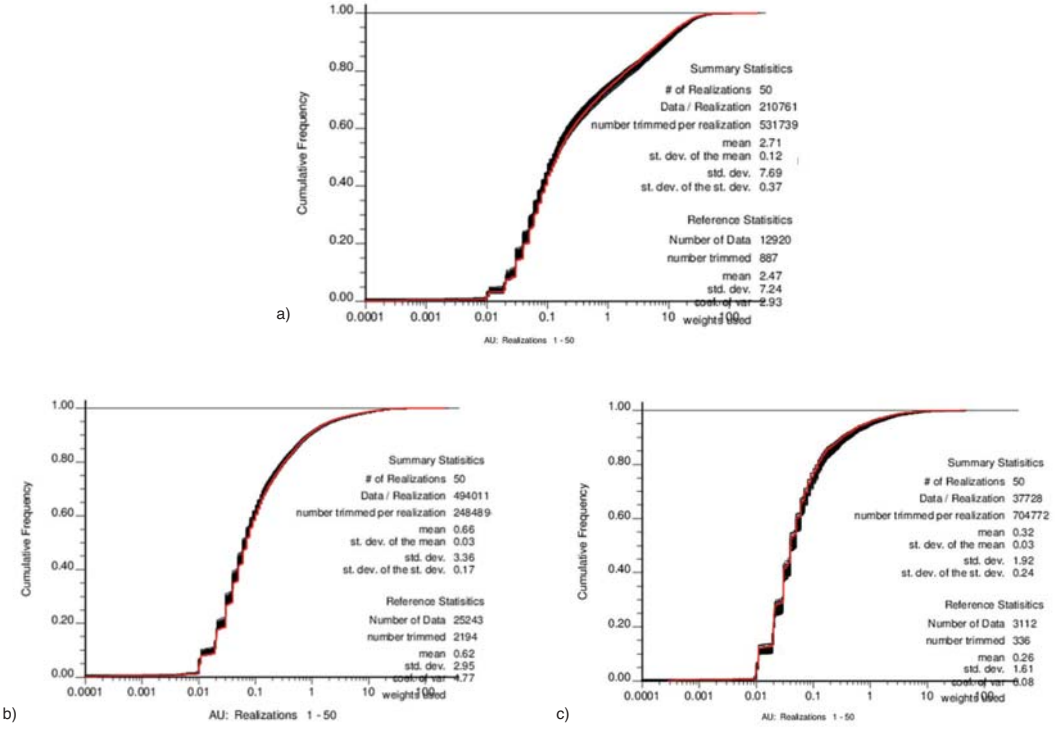

Figure 7—Cumulative distribution function reproduction of gold grades within the training image for: (a) BIF, (b) diorite, and (c) quartz porphyry

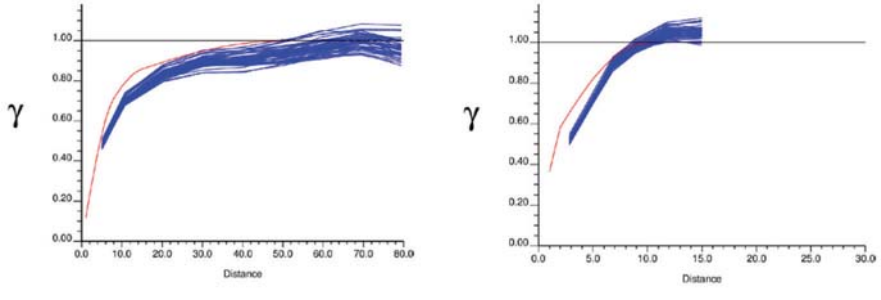

Figure 8—Indicator variogram reproduction for the simulated lithologies BIF and diorite (shown in blue), compared to an input variogram (shown in red): (a) for omnidirectional primary and secondary directions of anisotropy, and (b) comparison for the third direction of anisotropy

Simulation of the orebody

The main simulation for a more extensive volume was done for 50 realizations of both lithology and gold values. The best traditional approach in simulation is to generate 100–200 realizations (Deutsch, 2013) to stabilize the uncertainty and reduce 'uncertainty of the uncertainty' as much as possible. There are too many subjective decisions that might aggravate the uncertainty if a small number of realizations is produced.

The simulation grid consisted of 1 827 360 nodes evenly spaced at 5 m, and covering 470 m easting by 900 m northing by 540 m elevation. In order to reduce the computational demands, a mask object was used to block out the simulation grid nodes away from the mineralized shear zone.

Lithology simulation

Fifty realizations of lithology were performed. The results were subjected to the same tests as in the TI simulation. While reproduction of the BIF and diorite interface did not pose major problems, the issue of poor connectivity of the dykes re-emerged. The effect on the simulated mineral content was considered immaterial in the current case study; however, the issue was pursued to assist in future simulations.

The most satisfactory results were achieved by adding to the simulation input a conditioning grid object and a second TI.

The grid object had nodes flagged as QP if they fell within 20 m distance from the appropriate drill-hole intersections. The outcome of this approach was similar to a combination of hierarchical simulation and locally varying proportions. Figure 9 demonstrates this – the upper part of the simulation grid has higher content of nodes simulated as dykes than the portions down-plunge. This is explained by the higher density of drill coverage in the upper portions of the volume.

The second TI depicted large-scale repetitive morphology of the dykes, which was not captured in the first TI. Examples of the resulting simulation are shown in Figure 10.

Other DS parameters were tested to improve the continuity of the dykes, such as increasing the number of nodes and radii in the search neighbourhood, and increasing the distance threshold tolerance. None of these resulted in any significant improvement, while imposing higher computational demands.

Comparison of four realizations of lithology in the final simulation run in Figure 11 demonstrates the uniqueness of each realization; particularly, the further away it is from the conditioning data.

Drill-hole intersections through dykes in 3D display a radial attitude of the intrusions joining down-dip, with a plug-like intrusive body occurring in the top right corner of the simulation grid as seen in Figure 12. The plug-like volume would require defining another stationary domain and yet another TI; no further modelling of this feature is undertaken here. Future simulation work would benefit from the generation of synthetic TIs representing different lithological interfaces (BIF/diorite, host rock/QP dykes) and incorporation of structural readings of lithological contacts from diamond-drill core. Simple synthetic TIs with horizontal attitude of lithological boundaries, combined with a rotational field generated from the structural readings, would allow simulation of a more geologically truthful representation of the reality. Hierarchical simulation with different search parameters for different lithological interfaces would improve the result.

Validation was performed for honouring of lithology proportions. The global lithology proportions used as an

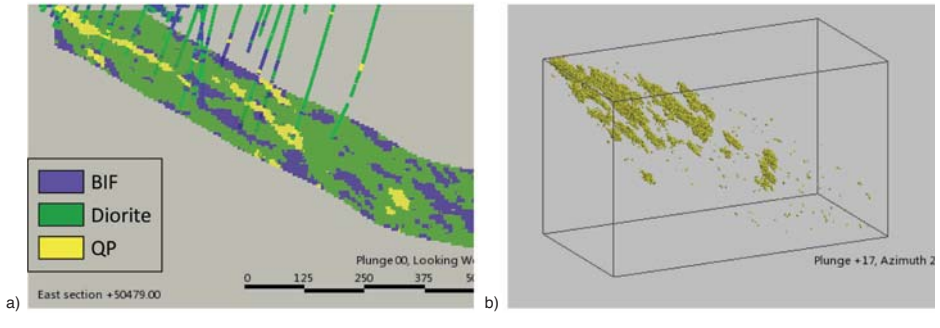

Figure 9—Conditional simulation of lithology over main grid, dykes conditioned by an additional grid object: (a) sectional view, (b) isoclinal view.

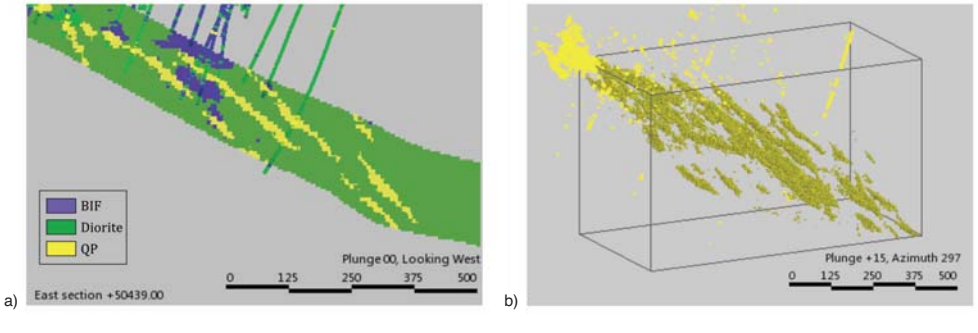

Figure 10—Lithology simulation using an additional training image depicting large-scale morphology of dykes: (a) sectional view, (b) isoclinal view. The drill-hole intervals logged for quartz porphyry dykes are displayed as yellow segments

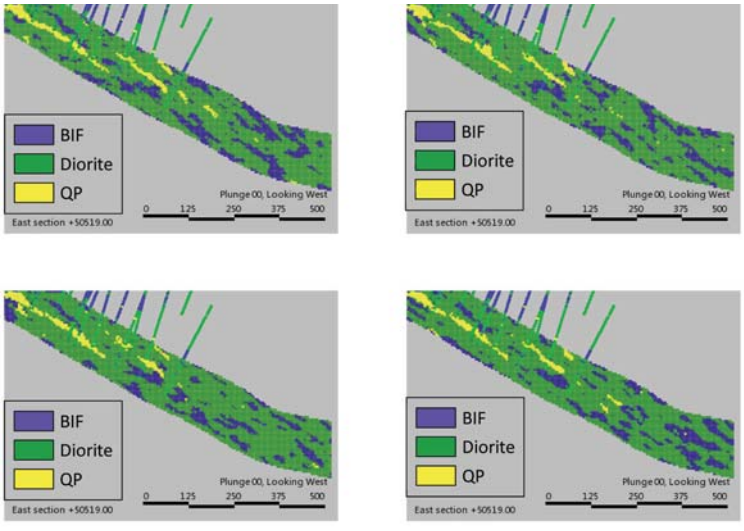

Figure 11—Four realizations of lithology for the final simulation run in XZ sectional views

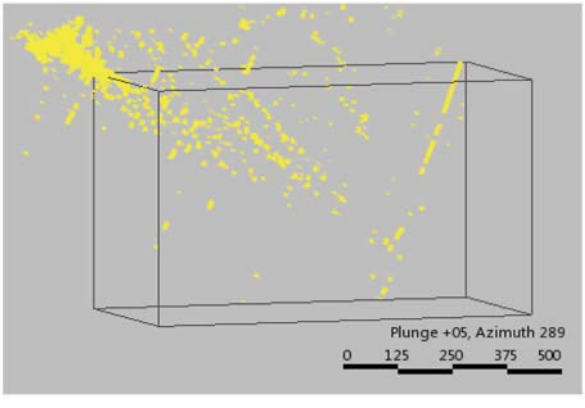

Figure 12 – Isoclinal view of dykes logged in the borehole core

additional input for the simulation were determined from the logging information of the conditioning drill-holes. Overall, the average values for the simulated global proportions are maintained. An overall fluctuation of a few per cent was observed across the 50 realizations, as shown in Table II. The effect was considered to be immaterial for the purpose of the study.

Figure 13 shows the histograms of the simulated proportions, the spread across the realizations being very narrow.

The variogram validation for the interface between the BIF and diorite was done for a portion of the simulation grid in the principal directions of continuity, and is shown in Figure 14. The simulation variograms between the BIF and diorite (blue) produced longer ranges of continuity than the input model (red). Further investigation into the reasons behind this would be beneficial.

A number of DS parameters have been tested to balance the simulation quality and processing time. The algorithm was run in multi-thread mode, using a 64-bit 8-core machine with 2.4 GHz processor. The average time required to produce a single realization of lithology for the main simulation grid was 20 minutes. Recommendations provided in Mariethoz *et al.* (2012, 2013) were followed to allow reasonable results in minimal time. The final parameters for the lithology simulation, conditioned with 44 780 drill-hole samples, were:

- Consistency of conditioning data: 0.05
- Number of conditioning nodes: 30
- Distance threshold: 0.05
- Distance tolerance for flagging nodes: 0.01
- Maximum fraction of training image to be scanned: 0.3.

Grade simulation

The 50 realizations of lithology were used for subsequent geostatistical domaining in the SGS simulation of 50 realizations for gold grade. Simulations were run for each lithology with the transformation of the gold values into Gaussian space and back being built-in to the SGS algorithm. The Gaussian variogram models based on the densely spaced grade control drilling were supplied as an input to the simulation of grade in each lithological domain.

The realizations of gold grade were validated in the same way as the TI, including visual checking, validation of the statistics, and variogram checking.

While the drill-hole samples are honoured in each of the realizations, it is also evident that each realization is unique, especially as we move away from the conditioning data. The four realizations in Figure 15 depict the short-range

Table II

Comparison of the simulated and global lithology input proportions in the conditioning drill-holes, the training image, and 50 simulated realizations

Lithology	Conditioning data within main simulation volume	Simulated proportions within TI	Simulated proportions within main simulation volume
BIF	0.29	0.27	0.26
Diorite	0.67	0.66	0.72
QP	0.04	0.07	0.02

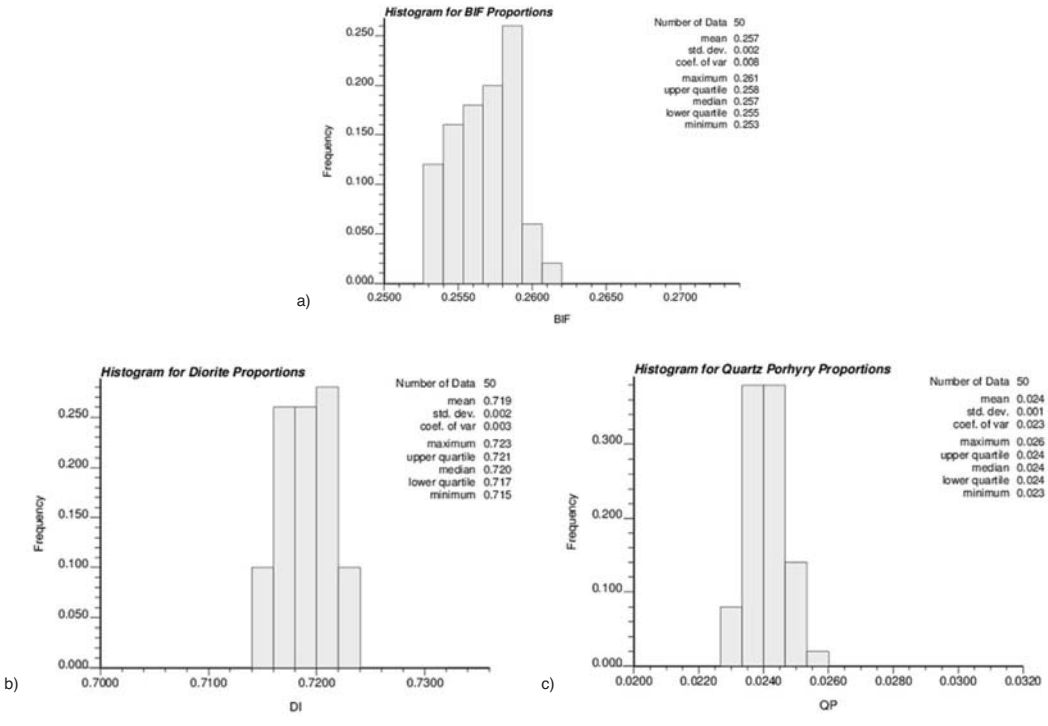

Figure 13—Histograms of the simulated lithology proportions across the 50 realizations: (a) proportions of banded iron formation, (b) proportions of diorite, (c) proportions of quartz porphyry

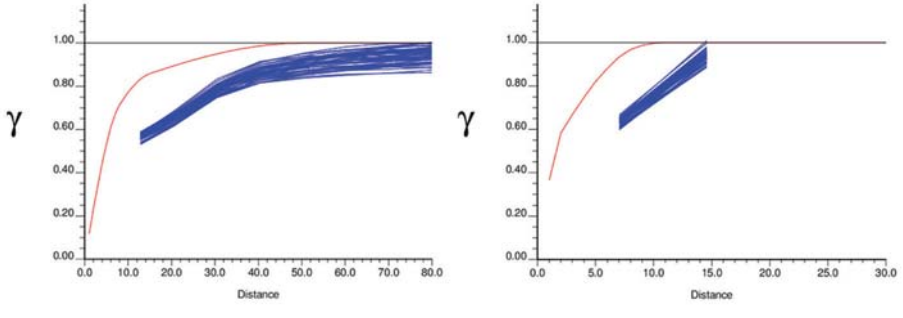

Figure 14—Variogram validation for the 50 simulated lithology realizations (shown in blue) compared to the input variogram model (shown in red): (a) omnidirectional variograms in the plane of continuity, (b) variograms in the third direction of continuity

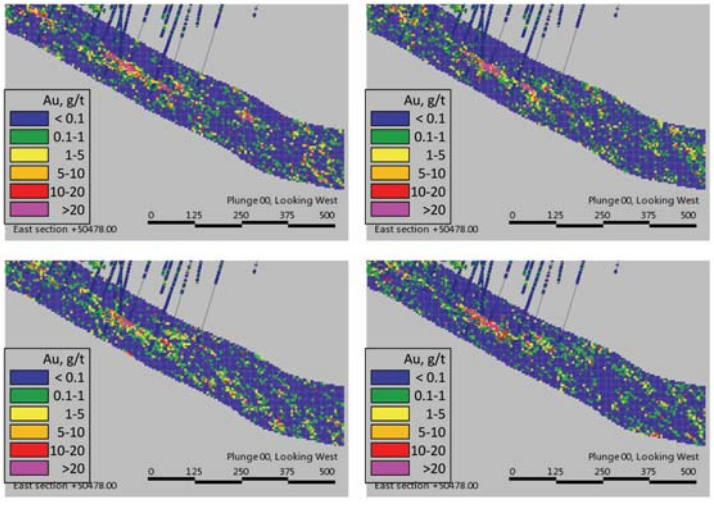

Figure 15—XZ sectional view for four realizations of gold grade simulation within main simulation volume

variability inherited from the variogram models of the densely spaced data in the TI. Differences between the realizations represent the joint uncertainty: from the lithology simulation and the grade realizations within it.

Cumulative distribution functions of gold grades for the simulated realizations and conditioning grades for the different lithology types are compared in Figure 16.

Gold variogram reproduction was checked within a small portion of the simulation grid, for BIF and diorite lithologies only. The comparison was done for the back-transformed data against the variogram models constructed in the original data units, and is shown in Figure 17 and Figure 18.

While the gold variograms within the BIF domain display a good fit with the input model, the diorite variograms are not as well-behaved and show a high degree of variance against the original model, as shown in Figure 18.

The noise in the variograms of the diorite at a short-scale distance is partially attributed to the fact that the model in the original space reaches 70% of variance within the range of 22–25 m for the main continuity plane. This distance, expressed in terms of the simulation grid nodes, represents separation of 2–3 nodes as the orientation of anisotropy is oblique to the geometry of the simulation grid, the smallest lag separation distance being about 7.5 m. An example realization of gold within diorite in Figure 19 shows sporadic mineralization down the plunge of the orebody. Another explanation is that insufficient care has been taken in deciding on the extents of the volume for variogram validation. The volume spanned the shear zone boundary and contained samples of high- and low-grade stationary domains, thereby introducing additional noise into the variograms. It would be beneficial to run the variogram

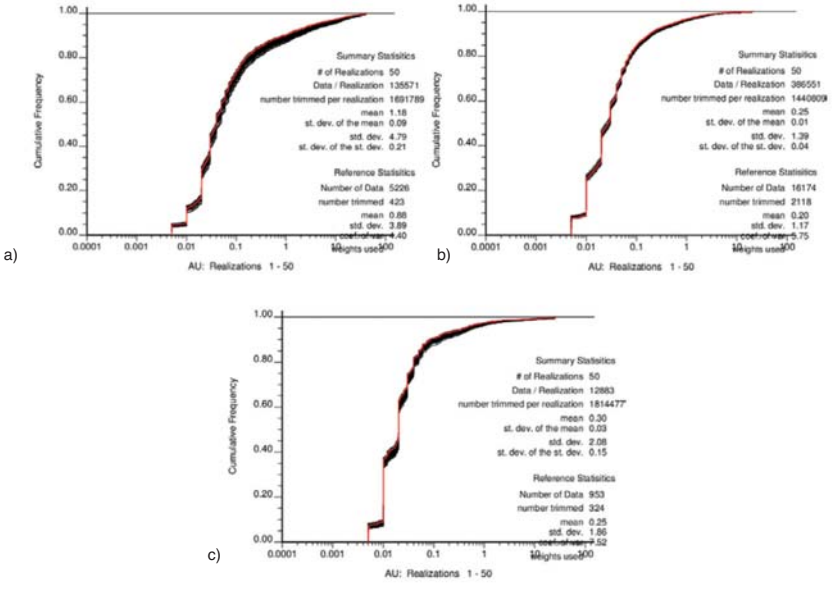

Figure 16—Cumulative distribution functions for the simulated gold values *versus* conditioning data for: (a) banded iron formation, (b) diorite, (c) quartz porphyry

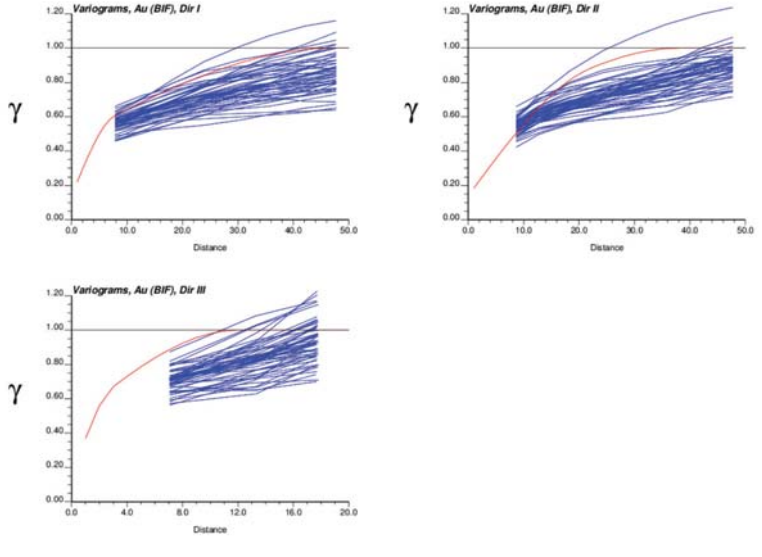

Figure 17—Variograms of the simulated gold realizations (shown in blue) in banded iron formation for the three principal directions of continuity compared to the input variogram model (shown in red)

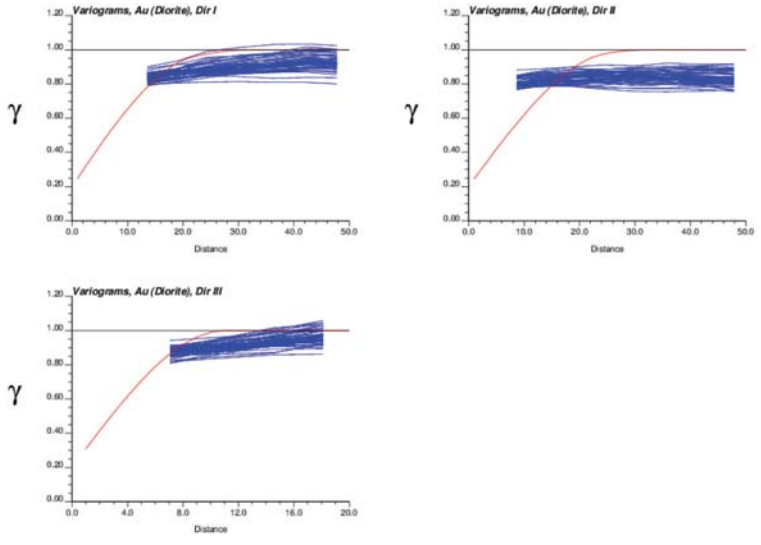

Figure 18—Variograms of the simulated gold realizations of diorite (shown in blue) for the three principal directions of continuity compared to the input variogram model (shown in red)

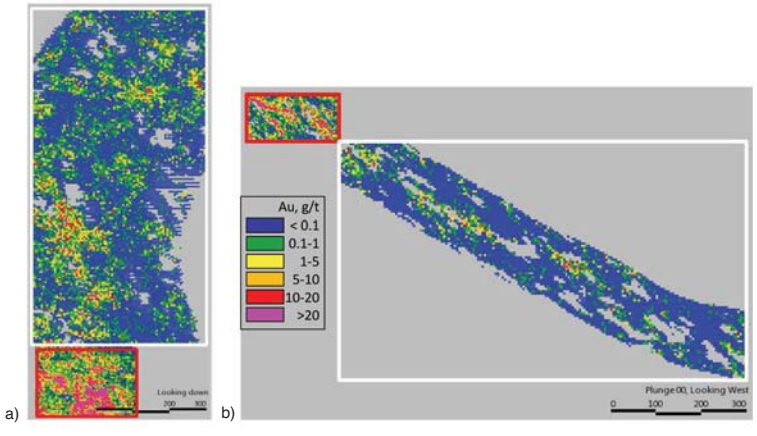

Figure 19—Diorite gold simulation. Banded iron formation and quartz porphyry lithologies have been 'cookie-cut' out: (a) plan view showing a slice of 20 m thickness, (b) sectional view. The red rectangle represents limits of the training image simulation grid, the white-limits of the main simulation volume

validation in Gaussian space. A simulation grid of finer resolution should be used to allow reproduction of short-scale continuity.

Analysing uncertainty

The geostatistical processing necessary for assimilating and interpreting the simulation outputs requires that the uncertainty be summarized to represent a joint uncertainty between lithology and grade. A number of options for summarizing both the lithology and grade realizations using GSLIB software (Deutsch and Journel, 1998) exist; the emphasis here is given to assessing uncertainty at a local level rather than on a global scale.

The weighted average summary of 50 realizations of the lithology created as an output a grid object with the probability of each lithology type, a most-likely-to-occur lithology and entropy, examples of which are shown in Figure 20. Post-processing for the most-likely-to-occur lithology would be similar to the results arising from indicator kriging.

The concept of entropy was propounded as far back as 1933 (Pauli, 1933; Shannon, 1948), and was introduced to geostatistics by Christakos in 1990. In the context of geostatistics, it is simply described as 'gain in knowledge'. Lower entropy values are observed in well-informed areas, where conditional probabilities are determined with high confidence. An example of this is shown in the cross-section of the orebody in Figure 21a and in the enlarged inset in Figure 21b. The highest entropy occurs along the peripheries of the most likely dykes, as this is the lithology with the highest uncertainty in the study.

The cross-sectional views of the conditional variance of the simulated gold values and the expected mean for 50 realizations are shown in Figure 22. Strong dependency or so-called 'proportional effect' between the local mean and the conditional variance is observed; a common feature in positively skewed distributions. It expresses itself as high-grade areas having greater variability, and hence greater uncertainty, than low-grade areas. For lognormal distributions, the local standard deviation is proportional to the local mean (Journel and Huijbregts, 1978).

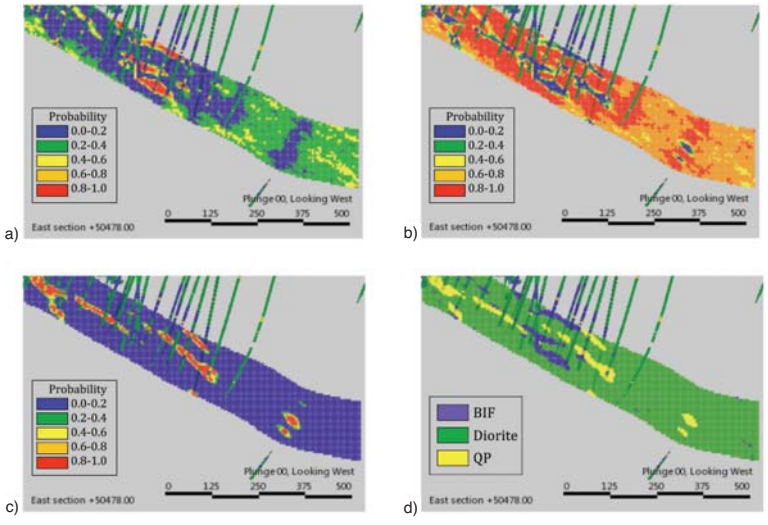

Figure 20—Summary output of lithology simulation: (a) probability of banded iron formation, (b) probability of diorite, (c) probability of quartz porphyry, and (d) the most likely-to-occur lithology type

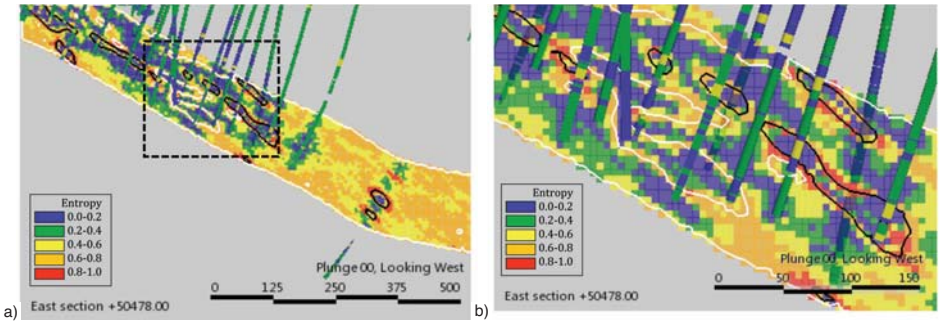

Figure 21—Entropy for lithology simulations along: (a) a ZX sectional view of the simulated grid, and (b) an enlarged area of the section. The solid outlines represent the most likely lithology types: black – interface between the quartz porphyry dykes and host rock, white – interface between the banded iron formation and diorite

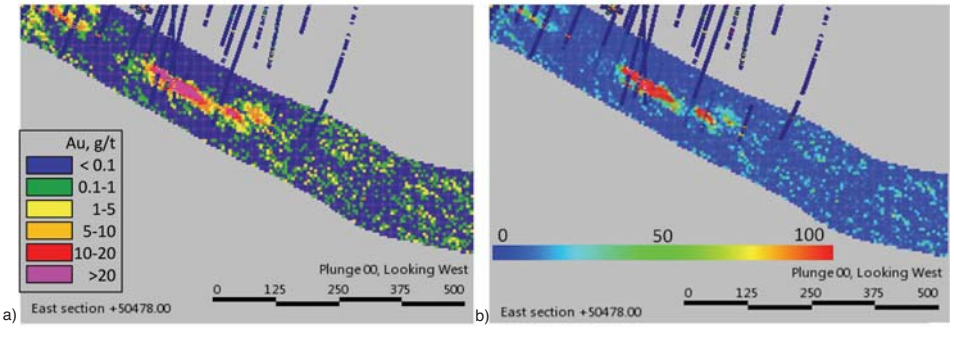

Figure 22—Sectional view showing results of E-type averaging of the gold simulation: (a) E-type mean of the 50 realizations, (b) conditional variance of the 50 realizations

The results of post-processing for a specific grade cut-off are shown in Figure 23, together with the outlines of the wireframes representing the most likely lithology, for ease of interpretation.

The tendency for high-grade values to be smeared across the simulation volume in the absence of conditioning data (Figure 23a and 23b) reflects a need to improve stationarity domaining. This had a material effect on the uncertainty assessment in the study. For future work, high-grade zones along the shear should be placed in a separate domain.

An example of post-processing for a specified probability interval to be within a relative error of the mean is shown in Figure 24. The short-scale variogram ranges induce a probability of 90% being observed in the vicinity of the drill-holes.

Different percentiles of probability intervals around the estimated E-type mean are displayed in Figure 25. The P10 percentile (Figure 25a) and P90 percentile (Figure 25c) are the symmetric 80% probability intervals around the E-type mean. The areas that are most certainly high in relation to

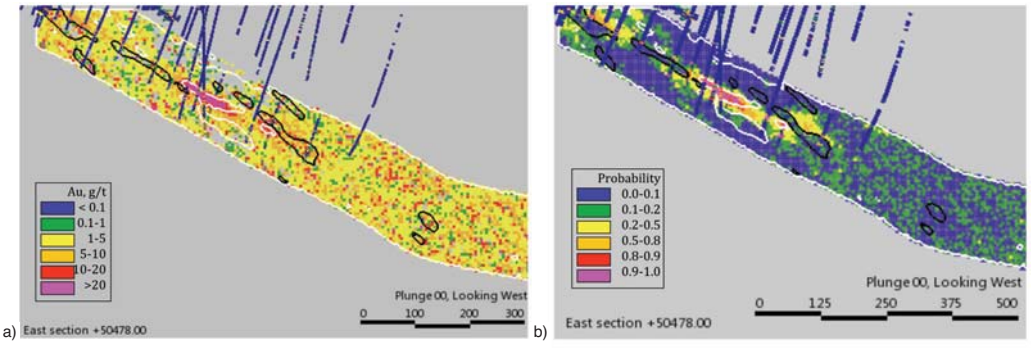

Figure 23—Sectional view of post-processing for a selected cut-off grade: (a) for the average grade above cut-off, and (b) probability of being above the cut-off grade; the solid outlines represent the most-likely lithology types: black for the interface between the quartz porphyry dykes and host rock, white for the interface between the banded iron formation and diorite

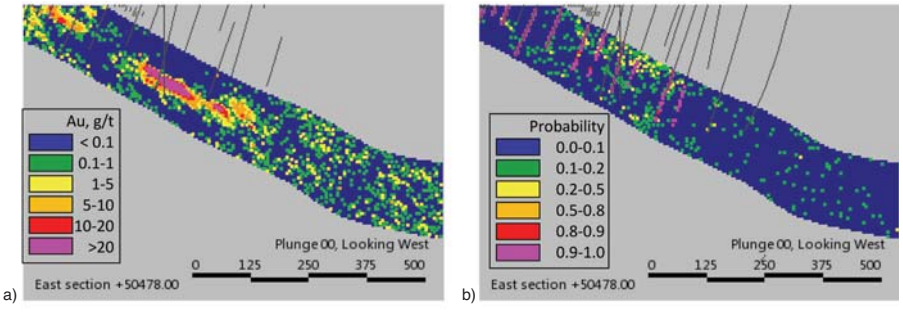

Figure 24—Sectional view of post-processing results of probability of being within 15% error of the Au E-type mean: (a) E-type mean of the 50 realizations, (b) probability of being within 15% error of the mean

the mean are shown as high-grade areas on the lower limit P10 percentile map. On the P90 percentile map, low grades are indicative of areas that are most certainly low grade. The P50 percentile map (Figure 25b) represents the most likely outcome.

Block averaging to recoverable resources

High-resolution simulation grids cannot be used efficiently. The advantage of simulating into a fine-resolution grid is that an upscaling to a different SMU size is possible, providing consistency of results. If the cell support is fine enough in comparison with the variogram model ranges, volume-variance relationships can be bypassed. Fine-resolution realizations upscaled to panel-size support can be used for further processing in the mine planning process; upscaling to SMU-size support can be used to assess uncertainty in the mine scheduling process.

For continuous variables involved in the estimation of the mineral resources, such as mineral concentrations and densities of rock types, averaging to a larger support size is linear. This means that for continuous variables the mean stays constant within the volume being upscaled. For categorical variables, the most probable lithology is assigned to larger size blocks by volume weighting.

Smoothing in the variables and uncertainty takes place during upscaling. This effect can be seen in Figure 26, which shows the fine-resolution simulation of 5 m nodes spacing (Figure 26a and 26b) and a version upscaled to a node spacing of 40 m easting x 40 m northing x 10 m elevation (Figure 26c and 26d). Large variability observed at a small scale is considerably smoothed in large-scale cells. Upscaled realizations can be processed to generate grade-tonnage curves that provide a representation of uncertainty in the recoverable metal.

The mining optimization should be performed for all upscaled realizations. It can also be done for a few selected realizations, which can be chosen based on different transfer functions or performance calculations (Deutsch, 2013), such as metal content or degree of 'connectivity' between panel blocks above a chosen cut-off grade. In this case, the scenarios could be a P50 percentile, which would represent a base case, with the P10 and P90 percentiles providing 80% confidence limits.

Discussion

In the current study, the MPS simulation approach for generating realizations of mineralized units has been combined with a traditional SGS simulation of grade. The Direct Sampling multi-point algorithm employed in the lithology simulation proved to be fast and flexible. Many parameters are available to ensure good reproduction of the patterns found in the training image, and good connectivity while maintaining global proportions of lithologies. Difficulties were encountered when simulating dykes. In terms of final uncertainty assessment, reproducing the continuity of dykes was of negligible importance; it was pursued in order to improve our understanding of the algorithm and for more effective use in future. Using an additional TI depicting large-scale morphology of dykes combined with distance-based conditioning for the grid nodes

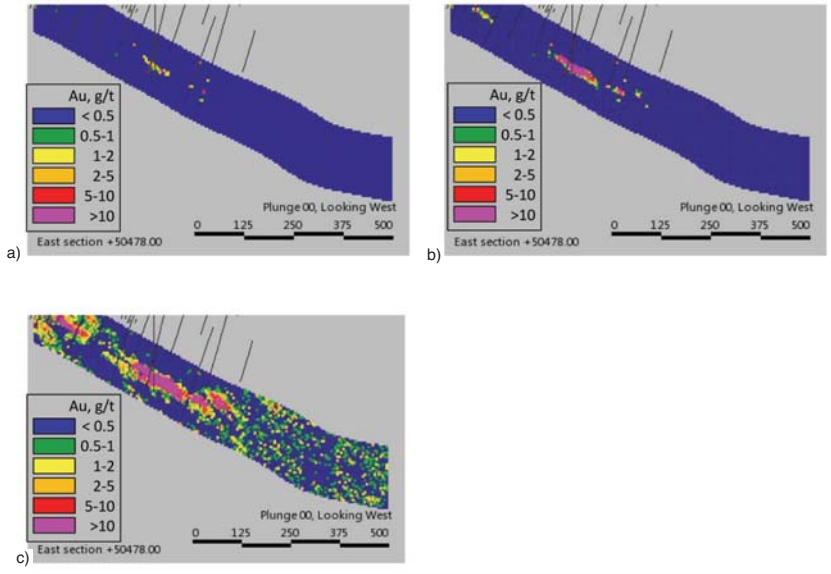

Figure 25—Sectional view showing probability intervals around the estimated E-type mean: (a) the P10 percentile, (b) the P50 percentile, and (c) the P90 percentile

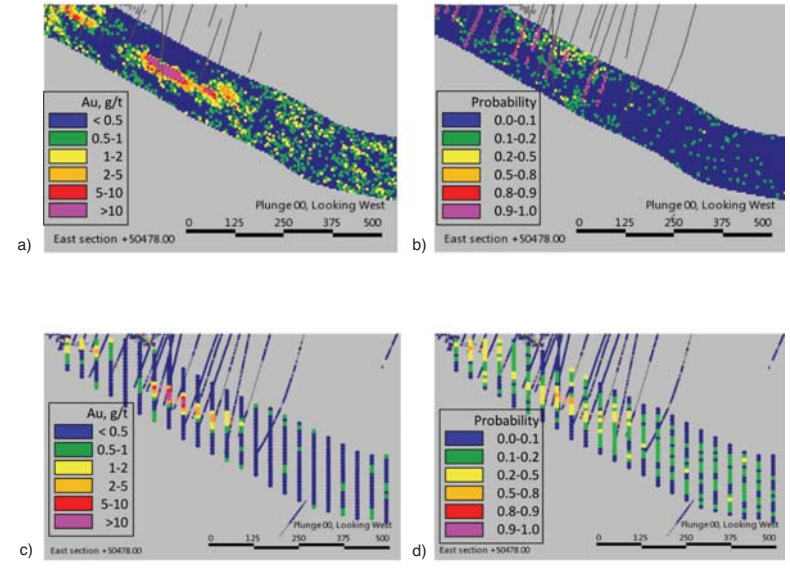

Figure 26—Sectional view of an up-scaled simulation model for the probability of being within 15% error of the E-type mean: (a) E-type mean of the 50 fine-scale realizations, (b) the probability of being within 15% error on a grid of 5 m x 5 m x 5 m node spacing, (c) the E-type mean of the 50 up-scaled realizations, and (d) the probability of being within 15% error on a grid of 40 m x 40 m x 10 m node spacing. In the coarse-resolution grid, points represent centroids of the up-scaled blocks

in the vicinity of the drill-holes, although not a holistically ideal approach, produced the most significant improvement. Implementing hierarchical simulation in the algorithm, as well as different search parameters for different lithological interfaces, would ease the task in future.

In the current case study, a traditional parametric algorithm such as sequential indicator simulation would have probably yielded sufficiently good and similar results for simulation of the BIF and diorite lithologies. It would, however, have failed at reproducing the morphology of dykes.

The possibility of running DS in multi-core mode makes it competitive with many other commercially available algorithms. This paper applies DS to a simple project, but the method can be implemented to more complex cases where variograms cannot be used to describe the continuity or to validate results.

The validation of the gold simulation results produced poorly-behaved variograms within the diorite domain. Probable reasons are insufficient resolution of the simulation grid to capture the short-scale variability, and non-stationarity.

Some practical considerations to be born in mind when performing simulation:

- Start with non-conditioned simulation until the pattern reproduction is good. The insufficiencies in parameters will come through in the main simulation where conditioning data is sparser

- Test parameters and keep track of both processing time and the quality of reproduction using a common reference location for easier comparison
- Full-scale features, such as boudin-like compartmentalizing of the host rock by dykes, must be present in the TI with sufficient repetition to avoid the effect of 'patching'
- Statistics for both continuous and categorical variables must be thoroughly checked in the early stages of simulation to enable reasonableness of the applied parameters and appropriate stationarity decisions to be validated
- Using trend as an additonal input into the SGS would assist in dealing with non-stationarity
- Performing a simulation exercise using exploration drill-holes only, within a production area, can allow reconciliation analysis to back-up the simulation results
- As anisotropy is borrowed from the TI, there will be short-scale continuity in the realizations and the simulation results might present noise
- Structural features logged in diamond-drill core could be used to impose better control on simulated geological boundaries
- Particular care needs to be taken when choosing a TI. It is the TI that carries the decision on stationarity and geological settings to be simulated over the entire volume of interest. The best approach is to have a stationary generic TI, and deal with any non-stationarity by the means of 'soft' conditioning: trends, local proportions, and potential fields for use on rotation and homothety.

The examples of uncertainty assessments demonstrate the value of information provided by stochastic simulations. The stochastic approach and uncertainty assessment are model-dependent and stationarity-dependent, and must rely on a robust quantitative validation of the model. Analysing the data and geological settings to make an appropriate decision on stationarity is crucial if statements about uncertainty are to be valid. Improper decisions about stationarity, as has been unintentionally demonstrated in the current study, result in higher uncertainty.

Realizations can be processed through a transfer function or performance calculation. In the context of mining it may be a grade-tonnage curve, the degree of connectivity between the ore/waste blocks, or mine scheduling. Realizations may be ranked in order to select a few for detailed processing.

The value of the stochastic approach to modelling is that it provides an appreciation of the extent of uncertainty when making an appropriate decision. On the other hand, it is also possible to average outcomes of many realizations and produce a smoothed result which is very close to that obtained by kriging.

Quantitative uncertainty, *e.g.* probability of being within ±15% with 90% confidence, can be used to support geometric criteria for classifying reserves and resources. In this way, probabilistic meaning will enhance classification and make it easier to understand for a non-specialist.

Uncertainty assessment is often not intuitive. Gold mineralization, for example, is characterized by skewed distributions and the proportional effect. This increased variability in the extreme values increases and spreads the uncertainty response, while larger proportions of low values tend to be associated with low uncertainty. Spatial correlation is relevant, since poor spatial correlation causes increase in uncertainty, and *vice versa*.

Stochastic modelling, and an MPS method in particular, increases the amount of technical work and computing power required. However, acceptance or rejection of a TI is more visual than a parametric model. It can be more inviting for involvement of specialist geological expertise, besides geostatisticians, and would provide more integration of different skills and ownership for field geologists.

References

Brayshaw, M., Nugus, M., and Robins, S. 2010. Reassessment of controls on the gold mineralisation in the Nyankanga deposit – Geita Gold Mines, North-Western Tanzania. *8th International Mining Geology Conference*, Queenstown, New Zealand, 21–24 August 2011. Australasian Institute of Mining and Metallurgy. pp. 153–168.

Caers, J. 2011 Modelling Uncertainty in the Earth Sciences. Wiley-Blackwell, Chichester, UK. pp. 90-106.

Christakos, G. 1990. A Bayesian/maximum-entropy view to the spatial estimation problem. *Mathematical Geology*, vol. 22, no. 7. pp. 763–777.

Deutsch, C. and Journel, A. 1998. GSLIB: Geostatistical Software Library and User's Guide. 2nd edn. Oxford University Press, Oxford.

Deutsch, C. 2013. Lectures on Citation Program in Applied Geostatistics, presented in Johannesburg, RSA. Centre for Computational Geostatistics. University of Alberta, Edmonton, Alberta, Canada.

Goovaerts, P. 1997. Geostatistics for Natural Resource Evaluation. Oxford University Press, New York.

Guardiano, F. and Srivastava, R. 1993. Multivariate geostatistics: beyond bivariate moments. *Quantitative Geology and Geostatistics*, vol. 5. pp. 133–144.

Honarkhah, M. and Caers, J. 2010 Stochastic simulation of patterns using distance-based pattern modelling. *Mathematical Geosciences*, vol. 42, no. 5. pp. 487–517.

Journel, A. and Huijbregts, C. 1978. Mining Geostatistics. Academic Press, p. 187.

Mariethoz, G., Meerschman, E., Pirot, G., Straubhaar, J., Van Meirvenne, M., and Renard, P. 2012. Guidelines to perform multiple-point statistical simulations with the Direct Sampling algorithm. *Ninth International Geostatistics Congress*, Oslo, Norway, 11–15 June 2012.

Mariethoz, G., Meerschman, E., Pirot, G., Straubhaar, J., Van Meirvenne, M., and Renard, P. 2013. A practical guide to performing multiple-point statistical simulations with the Direct Sampling algorithm. *Computers and Geosciences*, vol. 52. pp. 307–324.

Pauli, W. 1933. Die allgemeinen Prinzipien der Wellenmechanik. *Handbuch der Physik*. Geiger, H. and Scheel,K. (eds.). Springer, Berlin. 2nd edn, vol. 24, part 1. pp. 83–272.

Perez, C. and Ortiz, J. 2011. Mine-scale modeling of lithologies with multipoint geostatistical simulation. *IAMG*, 2011, University of Salzburg, 5–9 September 2011. pp. 123–132.

Remy, N., Boucher, A., and Wu, J. 2009. Applied Geostatistics with SGeMS.. Cambridge University Press.

Rezaee, H., Mariethoz, G., Koneshloo, M., and Asghari, O. 2013. Multiple-point geostatistical simulation using the bunch-pasting Direct Sampling method. *Computers and Geosciences*, vol. 54. pp. 293–308.

Shannon, C. 1948 A mathematical theory of communication. *Bell System Technical Journal*, vol. 27. pp. 379–423, 623–656.

Straubhaar, J., Renard, P., Mariethoz, G., Froidevaux, R., and Besson, O. 2011. An improved parallel multiple-point algorithm using a list approach. *Mathematical Geosciences*, vol. 43. pp. 305–328.

Tahmasebi, P., Hezarkhani, A., and Sahimi, M. 2012. Multiple-point geostatistical modelling based on the cross-correlation functions. *Computational Geosciences*, vol. 16, no. 3. pp. 779–797.

Wu, J., Boucher, A., and Zhang, T. 2008. A SGeMS code for pattern simulation of continuous and categorical variables: FILTERSIM. *Computers and Geosciences*, vol. 34, no. 12. pp. 1863–1876.

Zhang, T., Switzer, P., and Journel, A. 2006. Filter based classification of training image patterns for spatial simulation. *Mathematical Geology*, vol. 38, no. 1. pp. 63–80. ◆

List of papers published by Danie Krige from 1951–2008

1. A statistical approach to some mine valuation and allied problems on the Witwatersrand. *Unpublished Master's Thesis*, University of the Witwatersrand – 1951. (Separate)

2. A statistical approach to some basic mine valuation problems on the Witwatersrand - *J. of the Chem. Metall. and Min. Soc. of S.A.*, December, 1951 - discussions and replies March, May, July and August 1952. (Vol. 1….1). Also: *J. of the Institute of Mine Surveyors of S.A.* December 1952, March 1953. (Vol. 1…2)

3. A statistical analysis of some of the borehole values of the Orange Free State goldfield - *J. of the Chem. Metall. and Min. Soc. of S.A.*, September, 1952 - discussions and reply November 1952, and February 1953. (Vol. 1…3).

2/3*. Nos. 2 and 3 above were translated into French and republished in *Annales des Mines*, December 1955, - *under the title*: Travaux de M. D. G. Krige sur l'evaluation des gisements dans Les mines d'or Sub-Africaines. (Vol. 3…1)

4. 'n Statistiese analise van die vernaamste risiko verbonde aan kapitaal-belegging in nuwe goudmyne in Suid-Afrika - *Tegnikon*, Oktober 1955. English (Vol. 4…4) (Vol. 1…5)

5. A study of the relationship between development values and recovery grades on the South African goldfields - *J.S.A.I.M.M*, January 1959, - discussion and reply April and October 1959. (Vol. 1…6)

6. On the departure of ore value distributions from the lognormal model in South African gold mines. *J.S.A.I.M.M.*, November 1960, January and August 1961. (Vol. 1…8)

7. Developments in the valuation of gold mining properties from borehole results - *Seventh Commonwealth Mining and Metallurgical Congress*, 1961. (Vol. 1…9)

8. Effective pay limits for selective mining. *J.S.A.I.M.M.*, January and August 1962. (Vol. 1…10)

9. Economic aspects of stoping through unpayable ore. *J.S.A.I.M.M.*, January, March and August 1962. (Vol. 1…11)

10. Statistical Applications in Mine Valuation. Parts 1 and 2 - *Journal of Inst. of Mine Surveyors of S.A.*, June and September 1962. (Vol. 1…12)

11. The application of correlation and regression techniques in the selective mining of gold ores - *2nd APCOM Symposium*, University of Arizona, Tucson, April 1962. (Vol. 3…3)

12. The significance of a limited number of borehole results in the exploration of new South African gold fields - *2nd APCOM Symposium*, University of Arizona, Tucson, April 1962. (Vol. 3…2)

13. Value contours and improved regression techniques for ore reserve valuations (jointly with Ueckerman) - *J.S.A.I.M.M.*, May, July and October 1963. Republished in the *J. I. Mine Surveyors of S.A.*, September 1963, Vol. XII, No. 7. (Vol. 2…1)

14. A review of the impact of statistics on mine valuation in the gold mining industry - *J.S.A.I.M.M*, March 1964. (Vol. 2…2)

15. A brief review of the developments in the application of mathematical statistics to ore valuation in the South African gold mining industry - *4th APCOM Symposium*, Colorado School of Mines Quarterly Vol. 59, No. 4, October 1964. (Vol. 2…3)

16. Recent developments in South Africa in the application of trend surface and multiple regression techniques to gold ore valuation - *4th APCOM Symposium*, Colorado School of Mines Quarterly Vol. 59, No. 4, October 1964. (Vol. 2…4)

17. The use of mathematical statistics and computers for planning and control of gold mines of the Transvaal and Orange Free State, (jointly with P.C.Pirow) - *8th Commonwealth Mining and Met. Congress*, Australia, 1965. (Vol. 2…5)

18. Two-dimensional weighted moving average trend surfaces for ore valuation - *J.S.A.I.M.M.*, Special Symposium Vol., p.13, March 1966, also April 1967, pp. 472/4. (Vol. 2…7)

19. Applications of statistical and computer techniques for ore valuation in the Anglovaal Group (jointly with J.E. Heller) - *J.S.A.I.M.M*, Special Symposium Vol., March 1966. (Vol. 2…8)

20. Ore value trend surfaces for the South African gold mines based on a weighted moving average - *6th APCOM Symposium*, Penn. State University, April 1966. (Vol. 3…4)

21. A discussion on 20 by Matheron G: Kriging or Polynomial Interpolation Procedures. – *Canadian Min. and Met. Bulletin*, Sept 1967, pp 1041/1045. (Vol. 3…4)

22. A study of gold and uranium distribution patterns in the Klerksdorp goldfield - *Geoexploration 4*, pp. 43/53,1966. (Vol. 2…6)

23. A surveyor's approach to contour surfaces for gold ore values - *Proceedings of 3rd South African National Survey Conference*, January 1967. (Vol. 2…10)

24. The role of mathematical statistics in improved ore valuation techniques in South African gold mines - *Problems of Mathematical Geology* (in Russian), Vol. 1, 1968, Hayka, Moscow. (Vol. 2…13 + Vol. 4…9)

25. A review of some conceptual and practical implications of the use of valuation surfaces for gold ore reserve estimation, (jointly with Munro) -*Can. Inst. M.M.*, special Vol. 9, 1968. (Vol. 3…5)

26. The use of contour surfaces as predicitive models for ore values (jointly with Watson and others) - *A decade of Digital Computing in the Mineral Industry, SAIME*, Port City Press, Baltimore, 1969, pp. 127/161 (*8th APCOM Symposium*, Salt Lake City). (Vol. 2…18)

27. Some implications of the new assistance formula for South African gold mines, *J.S.A.I.M.M*, May and August 1968, and February 1969. (Vol. 2…14)

28. The development of statistical models for gold ore valuation in South Africa - *Sixth International Mining Congress*, Madrid, 1970. (Vol. 3…9)

29. The impact of taxation systems on mine economics - Can. I.M.M., Special Vol. 12, 1971, *9th APCOM Symposium*, Montreal, Canada, 1970. (Vol. 3…10)

30. Capital investment and risk analysis for a new mining project - *Journal of the Investment Analyst Society of South Africa*, November 1972. (Vol. 3…11)

31. Computer applications in investment analysis, ore valuation and planning for the Prieska Copper mine - *11th APCOM Symposium*, Tucson, Arizona, April 1973. (Vol. 3…12)

32. The fitting of contour surfaces to hanging and footwall data for an irregular ore body, (jointly with Rendu) - *13th APCOM Symposium*, Clausthal-Zellerfeld, West Germany, October 1975. (Vol. 2…19)

33. Some basic considerations in the application of geostatistics to gold ore valuation - *J.S.A.I.M.M*, April 1976, pp. 383/3. (Vol. 3…14).

34. A review of the development of geostatistics in South Africa - *Advanced Geostatistics in the Mining Industry*, Reidel Publishing Company, 1976, (Dordrecht, Holland). (Vol. 2…20)

35. A review of some geostatistical models for gold ore valuation in South Africa - *Problems of Mathematical Geology* (in Russian), Vol. 2, Hayka, Moscow, 1978 English (Vol. 3…13)…Russian (Vol. 4…18)

36. The evaluation of co-product uranium reserves on producing and potential new gold mines in South Africa - Evaluation of uranium resources, International Atomic Energy Advisory Group, December 1976, Rome. *Published in Evaluation of Uranium Resources*, *IAEA*, Vienna, (Vol. 3…15) and (Vol. 4…14)

37. The human element in APCOM's development - Keynote address for 15th APCOM Symposium, Brisbane, Australia, July 1977, *Proceedings published by the Australasian Inst. Min. Met.*, 1977. (Vol. 3…16)

38. South African Mine Valuation by C.D. Storrar - Chamber of Mines of S.A., 1977. *Assisted in preparation of Chapter 15, Statistical Mine Valuation*. (Vol. 6…1)

39. Grade Control and Geostatistics - *Grade Control Course, Dept. Geology*, Wits. Also *Chamber of Mines Workshop* -1979. (Vol. 6…2)

List of papers published by Danie Krige from 1951–2008

40. A review of some of the practical gains from geostatistical applications in South African ore valuation - *Future Trends in Geomathematics* – Pion Ltd., London, 1980. (Published version incomplete). (Vol. 4…16)

41. Long-term trends in domestic metal prices under international conditions of differential inflation rates and unstable currency exchange rates - *J.S.A.I.M.M*, September 1978. (Vol. 6…14)

42. Lognormal-de Wijsian Geostatistics for Ore Evaluation - *S.A.I.M.M Monograph No. 1*, 1978, 2nd edition, 1981. (Separate)

43. An analysis of the potential benefits to the State of realistic adjustments to the mining tax structure, *J.S.A.I.M.M*, July 1979. (Vol. 4…19)

44. Some novel features and implications of a general risk analysis model for new mining ventures - *S.A.I.M.M Colloqium*, 4 May 1979; *J.S.A.I.M.M*, October 1979. (Vol. 4…23)

45. Fiskale beleid vir die mynbou-bedryf - *AHI Kongres*, Mei, 1981. (Vol. 4…24)

46. Threshold rates of return on new mining projects as indicated by market investment results (jointly with J. Austin) - *S.A.I.M.M Colloquim*, 30 May 1980 - *J.S.A.I.M.M*, October 1980. (Vol. 6…4)

47. Some theoretical and practical aspects of geostatistics as practised in S. Africa - *Geostatistics Conference*, UNISA, Aug, 1981. (Vol. 6…6)

48. Studies of the effects of outliers and data transformation on variogram estimates for a base metal and gold ore body (jointly with E.J. Magri) - *Mathematical Geology*, Vol. 14, No. 6, 1982, pp. 557/563. (Vol. 6…7)

49. Geostatistical case studies of the advantages of lognormal-de Wijsian kriging with mean for a base metal mine and a gold mine (jointly with E.J. Magri) - *Mathematical Geology*, Vol. 14, No. 6, 1982. pp. 547/555. (Vol.6…8)

50. Gold mine productivity as affected by the average wet bulb temperature of the underground working places (jointly with C. P. Barnard) - *J.S.A.I.M.M*, May 1981, pp. 117/121. (Vol. 6…9)

51. A statistical analysis of the percentage of 'payable' ore stoped from payable ore reserves - *J.I.M.S.S.A*, March 1981, Vol. XXI, No. 1, pp. 129/135. (Vol. 6…10)

52. Geostatistics and the definition of uncertainly - (Sir Julius Wernher Memorial Lecture, I.M.M 26. 3.1984) - *Trans. Instn. Min. Metall.* (Sect. A), Vol. 93, 1984, pp. A41/47. (Vol. 6…11)

53. The use of geostatistics in defining and reducing the uncertainty of grade estimates - *Trans. Geol. Soc. S. Afr.*, 88 (1985), pp. 69/72. (Vol. 6…12)

54. Gold distribution patterns and grade valuation problems for deep mines - Proc. Int. Conf. on Gold, Johannesburg, *S.A.I.M.M.*, 1986. Vol. 1, pp. 3/14. (Vol. 6…13)

55. Factors affecting the long-term prospects of South Africa's gold production - *Long-term Prospects for Gold Mining*, Queen's Univ., Kingston, Canada. Proceedings No. 20 of Seminar, 1987. (Vol. 6…14)

56. Letter on 'Matheronian Geostatistics' - 1986. (Vol. 6…15)

57. Capital Investment in New Mining Projects-*Taipei*, 198. (Vol. 6…11a)

58. Taxation Implications of Capital Expenditure in Mining - *Capex in Mining Conference*, Johannesburg - 20/3/1986. (Vol. 7…1)

59. Elementary geostatistical models applied in forecasting South Africa's long-term gold production - *Jackling lecture, SME of AIME*, February, 1987 - *Mining Engineering,* June 1987. (Vol. 7…2)

60. Estimating grade differentials from drilling results on new gold properties. *20th APCOM Symposium*, Johannesburg, *S.A.I.M.M.*, October 1987. (Vol. 7…3)

61. A review of the development of geostatistics in South Africa - CSIR Colloquim, 24.9.1987. (Vol. 7…4)

62. Early South African geostatistical techniques in today's perspective. (Jointly with Guarascio and Camasani-Calzolari). *3rd International Geostatistical Congress*, Avignon, France, Sept, 1988. (Vol. 7...5)

63. A-priori parameter distribution patterns for gold grade in the Witwatersrand basin to be applied in borehole evaluations of potential new mines using Bayesian Geostatistical techniques. *22nd APCOM*, 1990, Berlin, pp. 715-726, - jointly with Kleingeld and Oosterveld. (Vol. 7…6)

64. Modelling of the underground patterns of gold concentrations in Witwatersrand reefs from surface borehole evidence. *First Geotechnica Congress*, Cologne, Sept.1991, Geo-Information-Systeme. Vol. 6, No. 3,1993. (Vol. 7…7)

65. New developments in borehole valuations of new gold mines and undeveloped sections of existing mines, (jointly with Assibey-Bonsu). *J.S.A.I.M.M.*, March 1992, Vol. 92, No. 3, pp. 71/77 - 65*. (Vol. 7…8)

66. Kriged variances fatally flawed – Sept. 1992, *The Northern Miner Magazine*

67. The relative rating of macro kriging and other techniques as applied to borehole valuations of new gold mines, (jointly with Assibey-Bonsu). *Proceedings 23rd APCOM*, Tucson, 1992, chapter 23 - 66. (Vol. 7…9)

68. Variability in gold grade and spatial structures of Witwatersrand reefs; the implications for geostatistical ore valuations. *J.S.A.I.M.M.*, March 1993, pp. 79/84. (Vol. 7…10)

69. The role of massive grade databases in geostatistical applications in South African gold mines, (jointly with C.E. Dohm). *Geostatistics for the Next Century*, (in honour of M.David). Kluwer Academic Publishers, Montreal, 1994. (Vol. 7…11)

70. An analysis of some essential basic tenets of geostatistics not always practised in ore valuations. Keynote address, *First Regional APCOM*, Slovenia, June, 1994. (Vol. 7…12)

71. A basic perspective on the roles of classical statistics, data search routines, conditional biases and information and smoothing effects in ore block valuations. *International Conference on Mining Geostatistics*, Kruger National Park, Sept. 1994. Unisa Publishers, 1996. (Vol. 7…13)

72. Some practical aspects of ore reserve estimation at Chuquicamata Copper Mine, Chile, (jointly with P.G. Dunn). 25th APCOM, Brisbane, Australia, July 1995. (Vol. 7…14)

73. *SAIMM Centenary republication of first paper* (1951). (Vol. 7…15)

74. A practical analysis of the effects of spatial structure and data available and used, on conditional biases in ordinary kriging - *5th International Geostatistics Congress*, Wollongong, Australia, 1996. (Vol. 7…16)

75. Block Kriging and the fallacy of endeavouring to reduce or eliminate smoothing. Keynote address, *2nd Regional APCOM Symposium*, Moscow State Mining University, August 1997. (Vol. 11…2)

76. Essential basic concepts in mining geostatistics and their links with geology and classical statistics. *Geo-Congress* 1998, Pretoria, South Africa, July 1998. South African Journal of the Geological Society of South Africa. Vol. 102 (2) 1999. pp 147–151. (Vol. 11...3)

77. Essential basic concepts and models in mining geostatistics and their geological context *Capricious Earth: Models and modelling of geological processes and objects*; Theophrastus Publications, St. Petersburg - Athens, Russia, 2000. (Vol. 11…4)

78. The use of the Principal Components technique to define anisotropy details for spatial structures. *APCOM '99 International Symposium*, Colorado School of Mines, Golden, October 1999. (Vol. 11…5)

79. Conditional Bias and Uncertainty of Estimation in Geostatistics. Keynote address for *APCOM'99 International Symposium*, Colorado School of Mines, Golden, October 1999. (Vol. 11…6)

80. Use of Direct and Indirect Distributions of Selective Mining Units for Estimation of Recoverable Resource/Reserves for New Mining Projects, (Co-author with W. Assibey-Bonsu). *APCOM'99 International Symposium*, Colorado School of Mines, Golden, October 1999. (Vol. 11….7)

List of papers published by Danie Krige from 1951–2008

81. Practical Problems in the estimation of recoverable reserves when using Kriging or Simulation Techniques (Jointly with co-author W.Assibey-Bonsu). *International Symposium on Geostatistical Simulation in Mining*, Perth Australia, October 1999. (Vol. 11…8)

82. The South African Code for reporting of mineral resources and mineral reserves and the geostatistical implications involved (as co-author with Camasani): *6th International Geostatistics Congress*, April, 2000, South Africa (Vol. 11…9)

83. Limitations in accepting repeated simulations to measure the uncertainties in recoverable resource estimates particularly for sections of an ore deposit (jointly with Assibey-Bonsu). *6th International Geostatistics Congress*, April 2000, South Africa. (Vol. 11…10)

84. Half a century of geostatistics from a South African perspective. Keynote address, *6th International Geostatistics Congress*, April 2000, South Africa. (Vol. 11…11)

85. The SAMREC code seen in a global context, jointly with Camasani *APCOM 2001*, Beijing, China, April, 2001. (Vol. 11…12)

86. Valuation of recoverable resources by kriging, direct conditioning or simulation, *APCOM 2001*, Beijing. April, 2001. (Vol. 11…13)

87. Comment on Journel's paper in *Mathematical Geology*, 2000, re a Spectral Postprocessor. (Vol. 11…14)

88. A classical statistical perspective on the birth and some critical developments of mining geostatistics. *UNISA conference in honour of Prof.F.Steffens*, May, 2002. (Vol. 13…1)

89. The genesis of geostatistics and some aspects of the valuation of diamond deposits (jointly with W.Kleingeld). *Fontainebleau publication*, 2002. (Vol. 13…2)

90. Mineral resource and reserve estimation. *AUSIMM Monograph No.23*. Critique February 2002. (Vol. 13.…3)

91. An analysis of the practical and economic implications of systematic underground drilling in deep South African gold mines, Co-author with Assibey-Bonsu W. *31st International Symposium on Computer Applications in the Mineral Industry*, Cape Town. Proceedings SAIMM, 2003, May 2003

92. Some practical aspects of the use of lognormal models for confidence limits and block distributions in South African gold mines. *31st International Symposium on Computer Applications in the Mineral Industry*, Cape Town. Proceedings SAIMM, 2003, May 2003.

93. Post-processing of SK estimators and simulations for assessment of recoverable resources and reserves for South African gold mines. *International Geostatistics Congress*, October 2004, Banff, Canada, Vol. 1 pp. 375–386, -jointly with W. Assibey-Bonsu and L. Tolmay

94. A practical review of some basic concepts and techniques for mining applications. Keynote Address, *33 APCOM*, April 2007, Santiago, Chile, pp. 11–15

95. Post-processing of estimators and simulations for assessment of recoverable resources and reserves for mining projects. *33 APCOM*, April 2007, Santiago, Chile, pp. 167–174, -jointly with W. Assibey-Bonsu and L. Tolmay

96. Uncertainty grade assessment for short and medium-term mine planning of underground mining operations. *International Geostatistics Congress*, December 2008, Santiago, Chile, pp. 739–748, -jointly with W. Assibey-Bonsu and L. Tolmay.

NOTES:

I. Certificates of merit were awarded by the S.A.I.M.M. for papers 2, 6,8, 9 and 13.

II. The gold medal of the S.A.I.M.M. was awarded in 1966 for No. 18 and for earlier research work, silver medals for No. 40 in 1979 and No. 63 in 1993, and a second gold medal in 1980 for No. 64.

III. The Daniel Cowan Jackling award was received from the SME of the AIME for No.58 and other contributions.

ARTICLES AND CONTRIBUTIONS NOT INCLUDED IN THE ABOVE LIST

Awards:

SAIMM gold medal: Dec. 1966	Vol. 2, no. 9, Vol. 8 no. 3
BSc, graduation, 1939	Vol. 5, no. 7
MSc. Graduation, 1951	Vol. 5, no. 12
DSc, graduation, 1963	Vol. 5, no. 14/15, vol. 8, no. 1
APCOM	Vol. 8 no. 2
SME of AIME	Vol. 8 no.2, vol. 9, no. 2
D.Eng. (HC), Pretoria 1981	Vol. 8, no. 5
S.A. Akademie 1982	Vol. 8, no. 4
State President 1982	Vol. 9, no. 3,5
DSc. (HC) UNISA 1996	Vol. 9, no. 6
DSc. (HC) Moscow State 1996	Vol. 12, No. 1, 7th article
Other	Vol. 9, no. 4, Vol. 12, no. 1

CONTRIBUTIONS TO DISCUSSIONS ON OTHER PAPERS:

Fleming D.R. On pay limits, 3/1968	Vol. 2, no. 12
McGillivray R.B. On computer mapping	Vol. 12, no. 16
Cook, N.G. On rock cutting	Vol. 2, no. 17

ARTICLES AND PRESS CUTTINGS:

Mathematical Statistical Techniques	3/1969, Vol. 3, no. 6
Trend Surface Analysis	4/1969, Vol. 3 no. 7
Evaluating Mining Ventures	7/1970, Vol. 3, no. 8
Diverse	Vol. 4, nos. 3, 5/8, 10, 24 Vol. 5, nos. 18/23, 26/44, 48/49, 51 Vol. 6, no. 2b

ECONOMIC TOPICS:

Book review: Frankel, H.S. – S.A. Gold Mining Industry --	Vol. 2, No. 11
Mining Taxation	Vol. 4, Nos. 1/2, 11/13, 15, 20/21 Vol. 6, no. 5
Risk Analysis	Vol. 4, no. 23
General	Vol. 5, no. 17, 24/25, 45/46

BOOK REVIEWS:

David M, 4/1978	Vol. 4, no. 22
McKenzie B.W. on mineral exploration, 1982	Vol. 6, no. 2c
Diverse	Vol. 10, no. 2

INTERNATIONAL ACTIVITIES

2015

11 – 12 March 2015 — **Mining Business Optimisation Conference 2015**
Mintek, Randburg, Johannesburg
Contact: Camielah Jardine
Tel: +27 11 834-1273/7, Fax: +27 11 838-5923/833-8156
E-mail: camielah@saimm.co.za, Website: http://www.saimm.co.za

8–10 April 2015 — **5th Sulphur and Sulphuric Acid 2015 Conference**
Southern Sun Elangeni Maharani KwaZulu-Natal, South Africa
Contact: Camielah Jardine
Tel: +27 11 834-1273/7, Fax: +27 11 838-5923/833-8156
E-mail: camielah@saimm.co.za, Website: http://www.saimm.co.za

23–25 April 2015 — **SANCOT Conference 2015**
Mechanised Underground Excavation
Elangeni Maharani, Durban
Contact: Yolanda Ramokgadi
Tel: +27 11 834-1273/7, Fax: +27 11 838-5923/833-8156
E-mail: yolanda@saimm.co.za, Website: http://www.saimm.co.za

12–13 May 2015 — **Mining, Environment and Society Conference: *Beyond sustainability—Building resilience***
Mintek, Randburg, South Africa
Contact: Yolanda Ramokgadi
Tel: +27 11 834-1273/7, Fax: +27 11 838-5923/833-8156
E-mail: yolanda@saimm.co.za, Website: http://www.saimm.co.za

10-11 June 2015 — **Risks in Mining 2015 Conference**
Johannesburg
Contact: Camielah Jardine
Tel: +27 11 834-1273/7, Fax: +27 11 838-5923/833-8156
E-mail: camielah@saimm.co.za, Website: http://www.saimm.co.za

14–17 June 2015 — **European Metallurgical Conference**
Dusseldorf, Germany, Website: http://www.emc.gdmb.de

14–17 June 2015 — **Lead Zinc Symposium 2015**
Dusseldorf, Germany, Website: http://www.pb-zn.gdmb.de

16–20 June 2015 — **International Trade Fair for Metallurgical Technology 2015**
Dusseldorf, Germany, Website: http://www.metec-tradefair.com

24–25 June 2015 — **Mine to Market Conference 2015**
Emperors Palace
Contact: Yolanda Ramokgadi
Tel: +27 11 834-1273/7, Fax: +27 11 838-5923/833-8156
E-mail: yolanda@saimm.co.za, Website: http://www.saimm.co.za

6–8 July 2015 — **Copper Cobalt Africa Incorporating The 8th Southern African Base Metals Conference**
Zambezi Sun Hotel, Victoria Falls, Livingstone, Zambia
Contact: Raymond van der Berg
Tel: +27 11 834-1273/7, Fax: +27 11 838-5923/833-8156
E-mail: raymond@saimm.co.za, Website: http://www.saimm.co.za

13–14 July 2015 — **School production of Clean Steel**
Emperors Palace, Johannesburg
Contact: Yolanda Ramokgadi
Tel: +27 11 834-1273/7, Fax: +27 11 838-5923/833-8156
E-mail: yolanda@saimm.co.za, Website: http://www.saimm.co.za

15–17 July 2015 — **Virtual Reality and spatial information applications in the mining industry Conference 2015**
University of Pretoria
Contact: Camielah Jardine
Tel: +27 11 834-1273/7, Fax: +27 11 838-5923/833-8156
E-mail: camielah@saimm.co.za, Website: http://www.saimm.co.za

11–14 August 2015 — **The Tenth International Heavy Minerals Conference 'Expanding the horizon'**
Sun City, South Africa
Contact: Camielah Jardine,
Tel: +27 11 834-1273/7, Fax: +27 11 838-5923/833-8156
E-mail: camielah@saimm.co.za, Website: http://www.saimm.co.z

19–20 August 2015 — **The Danie Krige Geostatistical Conference**
Geostatistical geovalue —rewards and returns for spatial modelling
Johannesburg
Contact: Yolanda Ramokgadi
Tel: +27 11 834-1273/7, Fax: +27 11 838-5923/833-8156
E-mail: yolanda@saimm.co.za, Website: http://www.saimm.co.za

15–17 September 2015 — **Formability, microstructure and texture in metal alloys Conference**
Contact: Yolanda Ramokgadi
Tel: +27 11 834-1273/7, Fax: +27 11 838-5923/833-8156
E-mail: yolanda@saimm.co.za, Website: http://www.saimm.co.za

28 September-2 October 2015 — **WorldGold Conference 2015**
Misty Hills Country Hotel and Conference Centre,
Cradle of Humankind
Gauteng, South Africa
Contact: Camielah Jardine,
Tel: +27 11 834-1273/7, Fax: +27 11 838-5923/833-8156
E-mail: camielah@saimm.co.za, Website: http://www.saimm.co.z

12–14 October 2015 — **Slope Stability 2015: International Symposium on slope stability in open pit mining and civil engineering**
In association with the
Surface Blasting School
15–16 October 2015
Cape Town Convention Centre, Cape Town
Contact: Raymond van der Berg
Tel: +27 11 834-1273/7, Fax: +27 11 838-5923/833-8156
E-mail: raymond@saimm.co.za, Website: http://www.saimm.co.za

21–22 October 2015 — **Young Professionals 2015 Conference**
Making your own way in the minerals industry
Mintek, Randburg, Johannesburg
Contact: Camielah Jardine
Tel: +27 11 834-1273/7, Fax: +27 11 838-5923/833-8156
E-mail: camielah@saimm.co.za, Website: http://www.saimm.co.za

28–30 October 2015 — **AMI: Nuclear Materials Development Network Conference**
Nelson Mandela Metropolitan University, North Campus
Conference Centre, Port Elizabeth
Contact: Raymond van der Berg
Tel: +27 11 834-1273/7, Fax: +27 11 838-5923/833-8156
E-mail: raymond@saimm.co.za, Website: http://www.saimm.co.za

8–13 November 2015 — **MPES 2015: Twenty Third International Symposium on Mine Planning & Equipment Selection**
Sandton Convention Centre, Johannesburg, South Africa
Contact: Raj Singhal, E-mail: singhal@shaw.ca or
E-mail: raymond@saimm.co.za, Website: http://www.saimm.co.za

Company Affiliates

The following organizations have been admitted to the Institute as Company Affiliates

AECOM SA (Pty) Ltd
AEL Mining Services Limited
Air Liquide (PTY) Ltd
AMEC Mining and Metals
AMIRA International Africa (Pty) Ltd
ANDRITZ Delkor(Pty) Ltd
Anglo Platinum Management Services (Pty) Ltd
Anglo Operations Ltd
Anglogold Ashanti Ltd
Atlas Copco Holdings South Africa (Pty) Limited
Aurecon South Africa (Pty) Ltd
Aveng Moolmans (Pty) Ltd
Axis House (Pty) Ltd
Bafokeng Rasimone Platinum Mine
Barloworld Equipment -Mining
BASF Holdings SA (Pty) Ltd
Bateman Minerals and Metals (Pty) Ltd
BCL Limited
Becker Mining (Pty) Ltd
BedRock Mining Support (Pty) Ltd
Bell Equipment Company (Pty) Ltd
BHP Billiton Energy Coal SA Ltd
Blue Cube Systems (Pty) Ltd
Bluhm Burton Engineering (Pty) Ltd
Blyvooruitzicht Gold Mining Company Ltd
BSC Resources
CAE Mining (Pty) Limited
Caledonia Mining Corporation
CDM Group
CGG Services SA
Chamber of Mines
Concor Mining
Concor Technicrete
Council for Geoscience Library
CSIR-Natural Resources and the Environment
Department of Water Affairs and Forestry
Deutsche Securities (Pty) Ltd
Digby Wells and Associates
Downer EDI Mining
DRA Mineral Projects (Pty) Ltd
Duraset
Elbroc Mining Products (Pty) Ltd
Engineering and Project Company Ltd
eThekwini Municipality
Evraz Highveld Steel and Vanadium Corp Ltd
Exxaro Coal (Pty) Ltd
Exxaro Resources Limited
Fasken Martineau
FLSmidth Minerals (Pty) Ltd
Fluor Daniel SA (Pty) Ltd
Franki Africa (Pty) Ltd Johannesburg
Fraser Alexander Group
Glencore
Goba (Pty) Ltd
Hall Core Drilling (Pty) Ltd
Hatch (Pty) Ltd
Herrenknecht AG
HPE Hydro Power Equipment (Pty) Ltd
Impala Platinum Limited
IMS Engineering (Pty) Ltd
JENNMAR South Africa
Joy Global Inc. (Africa)
Leco Africa (Pty) Limited
Longyear South Africa (Pty) Ltd
Lonmin Plc
Ludowici Africa
Lull Storm Trading (PTY)Ltd T/A Wekaba Engineering
Magnetech (Pty) Ltd
Magotteaux(PTY) LTD
MBE Minerals SA Pty Ltd
MCC Contracts (Pty) Ltd
MDM Technical Africa (Pty) Ltd
Metalock Industrial Services Africa (Pty)Ltd
Metorex Limited
Metso Minerals (South Africa) (Pty) Ltd
Minerals Operations Executive (Pty) Ltd
MineRP Holding (Pty) Ltd
Mintek
MIP Process Technologies
Modular Mining Systems Africa (Pty) Ltd
Runge Pincock Minarco Limited
MSA Group (Pty) Ltd
Multotec (Pty) Ltd
Murray and Roberts Cementation
Nalco Africa (Pty) Ltd
Namakwa Sands (Pty) Ltd
New Concept Mining (Pty) Limited
Northam Platinum Ltd - Zondereinde
Osborn Engineered Products SA (Pty) Ltd
Outotec (RSA) (Proprietary) Limited
PANalytical (Pty) Ltd
Paterson and Cooke Consulting Engineers (Pty) Ltd
Polysius A Division Of Thyssenkrupp Industrial Solutions (Pty) Ltd
Precious Metals Refiners
Rand Refinery Limited
Redpath Mining (South Africa) (Pty) Ltd
Rosond (Pty) Ltd
Royal Bafokeng Platinum
Roymec Tecvhnologies (Pty) Ltd
RSV Misym Engineering Services (Pty) Ltd
Rustenburg Platinum Mines Limited
SAIEG
Salene Mining (Pty) Ltd
Sandvik Mining and Construction Delmas (Pty) Ltd
Sandvik Mining and Construction RSA(Pty) Ltd
SANIRE
Sasol Mining(Pty) Ltd
Scanmin Africa (Pty) Ltd
Sebilo Resources (Pty) Ltd
SENET
Senmin International (Pty) Ltd
Shaft Sinkers (Pty) Limited
Sibanye Gold (Pty) Ltd
Smec SA
SMS Siemag South Africa (Pty) Ltd
SNC Lavalin (Pty) Ltd
Sound Mining Solutions (Pty) Ltd
SRK Consulting SA (Pty) Ltd
Time Mining and Processing (Pty) Ltd
Tomra Sorting Solutions Mining (Pty) Ltd
TWP Projects (Pty) Ltd
Ukwazi Mining Solutions (Pty) Ltd
Umgeni Water
VBKOM Consulting Engineers
Webber Wentzel
Weir Minerals Africa

Forthcoming SAIMM events...

EXHIBITS/SPONSORSHIP

Companies wishing to sponsor and/or exhibit at any of these events should contact the conference co-ordinator as soon as possible

For the past 120 years, the Southern African Institute of Mining and Metallurgy, has promoted technical excellence in the minerals industry. We strive to continuously stay at the cutting edge of new developments in the mining and metallurgy industry. The SAIMM acts as the corporate voice for the mining and metallurgy industry in the South African economy. We actively encourage contact and networking between members and the strengthening of ties. The SAIMM offers a variety of conferences that are designed to bring you technical knowledge and information of interest for the good of the industry. Here is a glimpse of the events we have lined up for 2015. Visit our website for more information.

SAIMM
THE SOUTHERN AFRICAN INSTITUTE OF MINING AND METALLURGY

For further information contact:
Conferencing, SAIMM
P O Box 61127, Marshalltown 2107
Tel: (011) 834-1273/7
Fax: (011) 833-8156 or (011) 838-5923
E-mail: raymond@saimm.co.za

Website: http://www.saimm.co.za

SAIMM DIARY

2015

- **CONFERENCE**
  Mining Business Optimisation Conference 2015
  11–12 March 2015, Mintek, Randburg, Johannesburg
- **CONFERENCE**
  5th Sulphur and Sulphuric Acid 2015 Conference
  8–10 April 2015, Southern Sun Elangeni Maharani KwaZulu-Natal
- **CONFERENCE**
  SANCOT Conference 2015 Mechanised Underground Excavation
  23–25 April 2015, Elangeni Maharani, Durban
- **CONFERENCE**
  Mining, Environment and Society Conference
  12–13 May 2015, Mintek, Randburg, Johannesburg
- **CONFERENCE**
  Risks in Mining 2015 Conference
  10–11 June 2015, Johannesburg
- **CONFERENCE**
  Mine to Market Conference 2015
  24–25 June 2015, Emperors Palace, Johannesburg
- **CONFERENCE**
  Copper Cobalt Africa Incorporating The 8th Southern African Base Metals Conference
  6–8 July 2015, Zambezi Sun Hotel, Victoria Falls, Livingstone, Zambia
- **SCHOOL**
  Production of Clean Steel
  13–14 July 2015, Emperors Palace, Johannesburg
- **CONFERENCE**
  Virtual Reality and spatial information applications in the mining industry Conference 2015
  15–17 July 2015, University of Pretoria, Pretoria
- **CONFERENCE**
  The Tenth International Heavy Minerals Conference
  11–14 August 2015, Sun City, South Africa
- **CONFERENCE**
  The Danie Krige Geostatistical Conference 2015
  19–20 August 2015, Johannesburg
- **CONFERENCE**
  Formability, microstructure and texture in metal alloys Conference 2015
  15–17 September 2015
- **CONFERENCE**
  World Gold Conference 2015
  28 September–2 October 2015, Misty Hills Country Hotel and Conference Centre, Cradle of Humankind, Muldersdrift
- **SYMPOSIUM**
  International Symposium on slope stability in open pit mining and civil engineering
  12–14– October 2015
  In association with the
  Surface Blasting School 15–16 October 2015, Cape Town Convention Centre, Cape Town

MINING WITH

ELBROC
MINING PRODUCTS (PTY) LTD

OMNI 150

AVAILABLE IN 20 TON, 40 TON AND 55 TON

The 'Sacrificial' hydraulic prop that performs in accordance with the COMRO guidelines for rockburst and rockfall conditions.

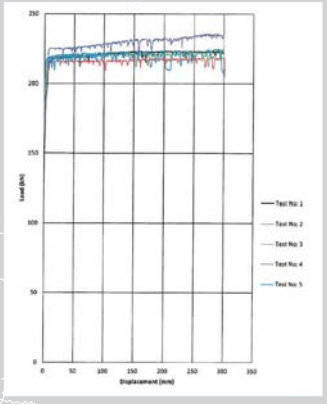

Omni 150 CSIR Graph
20 Ton Props

- 150mm diameter
- Covers stoping widths up to 6m
- Controlled yielding
- Safe remote installation
- Superb energy absorption
- Light, easy and quick to install
- Constant support resistance
- Cannot be over extended
- Resilient in rockburst conditions
- Standard attachments
- Can accommodate numerous seismic events
- Reusable for specific applications (20 Ton prop – only)
- Longer lengths available on request

The Omni 150 prop range has been extended from the current 20 ton unit and now includes 40 and 55 ton props.

Testing at CSIR has been completed and the results show that these props are able to handle areas where more load is required than a normal 20 ton unit.

The 40 ton prop is used in special areas where a higher load than normal is required – haulages, x/cuts, sets.

The 55 ton props are installed in areas where removal of stability pillars is undertaken. Props in excess of 5.5m have been installed which has enabled the successful mining of pillars to take place. Access ways are not restricted by bulk pack construction and material storage. This assists egress into and out of the site.

Standard equipment is used throughout the Omni range and no additional equipment is needed.

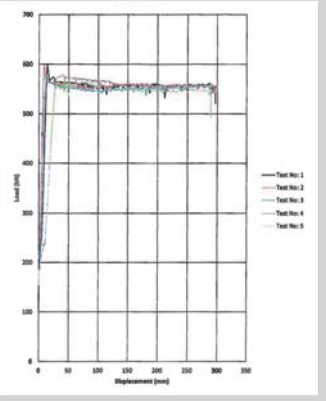

Omni 150 CSIR Graph
55 Ton Props

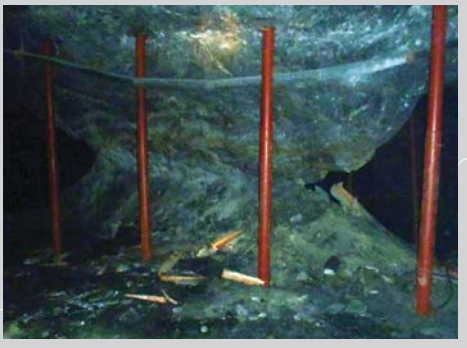

a member of the rbh royal bafokeng holdings

FOR OUR FULL PRODUCT RANGE
PLEASE VISIT OUR WEBPAGE

SABS ISO 9001

Errol Wilson
Sales Director
Cell: 083 451 3424
errolw@elbroc.co.za

Alec Adamson
Business Development Manager
Cell: 082 520 7372
aleca@elbroc.co.za

Jan van Jaarsveld
Internal Sales
Cell: 082 320 9069
janvj@elbroc.co.za

Herman Wilken
Coal
Cell: 082 524 7057
hermanw@elbroc.co.za

Sias West
Carltonville
Cell: 072 469 9037
siasw@elbroc.co.za

www.elbroc.co.za

Elbroc Sales Tel: 011 974 8013 • Fax: 011 974 2019 • sales@elbroc.co.za